BACTERIAL OUTER MEMBRANE VESICLES AS MEDIATORS OF COLIBACTIN TOXICITY

A Thesis

Submitted to the Faculty

of

University of Puerto Rico

Rio Piedras Campus

by

Yermary Morales Lozada

In partial Fulfillments of the

Requirements for the Degree

of

Doctor in Philosophy

September 27, 2021

University of Puerto Rico

Rio Piedras Campus

San Juan, Puerto Rico

ACCEPTED BY THE FACULTY OF THE DEPARTMENT OF CHEMISTRY
OF THE UNIVERSITY OF PUERTO RICO AT RIO PIEDRAS
IN PARTIAL FULFILLMENT OF THE REQUIREMENTS
FOR THE DEGREE OF

Doctor of Philosophy

_____

Abel Baerga Ortiz, Ph.D
Directos of Disertation

_____

Carlos R. Cabrera, Ph.D
Committee Member

_____

Ingrid Montes Gozáles, Ph.D
Committee Member

_____

Marvin J. Bayro, Ph.D
Committee Member

_____

Liz M. Díaz, Ph.D
Chairperson
Department of Chemistry

September 2021

Table of Contents

List of Tables

List of Figures

Figure S5.1b Giemsa staining of HeLa cells treated with OMV isolation “Process Blank”.

Figure S5.1c Giemsa staining of HeLa cells treated with OMVs isolated from *pks*$^{+}$ *E. coli* IHE3034 strain.

Figure S5.1d Giemsa staining of HeLa cells treated with OMVs isolated from *E. coli* IHE3034 ∆*clbP* mutant strain.

Figure S5.1e Giemsa staining of HeLa cells treated with OMVs isolated from *E. coli* DH10B control strain.

Figure S5.2 OMVs from IHE3034 Δ*clbP* mutant *E. coli* are internalized in significant higher amount than OMVs from WT strain by HeLa cells after 4 hrs of treatment.

Figure S5.3 OMVs from IHE3034 Δ*clbP* mutant *E. coli* are localized in the nucleus in significant higher amount than OMVs from WT strain in HeLa cell after 4 hrs of treatment.

List of Abbreviations

°C: Celsius

ACC: amino cyclopropane-carboxylic acid

A_{FA} : Area of fatty acids

A_{IS}: Area of internal standard

ANOVA: Analyses of variance

***B. fragilis*:** *Bacteroides fragilis*

BAC: Bacterial artificial chromosome

BCA: Bicinchoninic acid

BFT: *B. fragilis* toxin

bp: Base pair

BSA: Bovine serum albumin

C994: 994 m/z

CA: California

***cagA*:** cytotoxin-associated gene A

CBA: Cytometric bead array

CD: Crohn's Disease

CDK: cyclin dependent kinase

CDK: Cyclin-dependent kinases

CDT: Cytolethal Distending Toxin

Cif: Cycle inhibitory factor

C_{IS} : Concentration of internal standard

CNFs: Cytotoxic Necrotizing Factors

CO_2: Carbon dioxide

CRC: Colorectal cancer

D-PBS: Dulbecco's phosphate-buffered saline

Da: Dalton

DAPI: 4′,6-diamidino-2-phenylindole

DBS: Double strand-breaks

ddH_2O: Deionized and distilled water

DDR: DNA damage response

DiO: 3,3′-dioctadecyloxacarbocya-nine perchlorate

DLS: Dynamic light scattering

DMEM: Dulbecco's Modified Eagle's Medium

DMSO: Dimethyl sulfoxide

DNA: Deoxyribonucleic acid

DSBs: Double-strand breaks

dsDNA: Double-strand DNA

E-cadherin: epithelial cadherins

E. coli **:** *Escherichia coli*

EDTA: Ethylenediaminetetraacetic acid

EI-MS: Electro ionization mass spectrometry

EtBf: Enterotoxigenic *Bacteroides fragilis*

ExPEC: Extraintestinal pathogenic

F. nucleatum**:** *Fusobacterium nucleatum*

F. prausnitzii: *Faecalibacterium prausnitzii*

FA: Fatty acid

FA: Fatty acid

FAME: Fatty acids methyl esters

FBS: Fetal Bovine Serum

g: Grams

GADPH: Glyceraldehyde 3-phosphate dehydrogenase

GC-MS: Gas chromatography mass spectrometry

GC/MS: Gas Chromatography

GI: Gastrointestinal

***H. pylori*:** *Helicobacter pylori*

HCl: Hydrochloric acid

hr: hour

hrs: Hours

IBD: Inflammatory bowel diseases

ICL: Interstrand crosslinks

IFNγ : Interferon gamma

IL: Interleukin

IS: Internal standard

kDa: Kilodaltons

kV: Kilovolts

LB: Lysogenic broth

LC-MS: Liquid chromatography mass spectrometry

LCFA: Long-chain fatty acids

LPS: Lipopolysaccharide

LPS: Lipopolysaccharide

MALDI: Matrix-assisted laser desorption/ionization

MATE: Multidrug efflux transporters

MCP-1: monocyte chemoattractant protein-1

mg: Milligrams

min.: Minutes

mL: Milliliters

mM: millimolar

MS-MS: Tandem mass spectrometry

mW: Miliwatts

MW: Molecular weight

N: Nitrogen

NEB: New England Biolab

NF-kB: Nuclear factor kappa-light-chain-enhancer of activated B cells

ngs: Nanograms

nrps: Non-ribosomal peptide synthase

NIST: National Institute of Standards and Technology

OD: Optical density

OMVs: Outer membrane vesicles

OMVs: Outer membrane vesicles

PAGE: Polyacrylamide gel electrophoresis

PCR: Polymerase chain reaction

PDI: Polydispersity index

SDS: Sodium dodecyl sulfate

PFA: Paraformaldehyde

PK/NRP: Polyketide/non-ribosomal peptide

pks: Polyketide synthase

PVDF: Polyvinylidene fluoride

rpm: Revolutions per minutes

SCFs: Small-chain fatty acids

sec.: seconds

SEM: Scanning electron microscopy

TAE: Tris-acetate-EDTA

TBE: Tris-Borate-EDTA

TE: Thioesterase

TFA: Trifluoro acetic acid

TNF-α : Tumor necrosis factor alpha

TOF: Time-of-flight

TRITC: Tetramethylrhodamine

U: Units

UC: Ulcerative Colitis

UPLC-MS: Ultra-performance liquid chromatography mass spectrometry

USA: United State of America

V: Volts

Vol: Volumen

WT: wild-type

α-CHCA: α-Cyano-4-hydroxycinnamic acid

µg: Micrograms

µL: Microliters

Abstract of the Dissertation

Colibactin is the product of a hybrid non-ribosomal peptide/polyketide synthase complex (*pks island*) found in some strains of *Escherichia coli*. Bacterial strains harboring the *pks island* show peculiar toxicity toward mammalian cells in culture with a distinctive phenotype that includes DNA damage, cell cycle arrest, and megalocytosis of the infected cells. It has been shown by our group that the *pks island* can be found in the normal gut microflora and its presence is positively correlated with colorectal cancer (CRC). Despite the notable interest in elucidating the mode of action of colibactin, its structure, the detailed mechanism of action, and the mechanism by which colibactin is transported to host cells remains unknown. The broad objective of this investigation was to develop molecular strategies towards the isolation of colibactin in pursuance of its structure and eventually, its mode of action. To do so, we first made a variant strain of the *pks*$^{+}$ *E. coli* IHE3034 deficient of *clbP* gene, a key enzyme involved in the activation of colibactin. In our strain, removal of clbP did not cause a complete decrease in the megalocytosis phenotype (toxicity) on infected cells as expected but caused the accumulation of an unknown product of 994 Da. In addition, since the production of colibactin takes place in the space between the inner and outer membranes, we explored the involvement of bacterial outer membrane vesicles (OMVs) in colibactin toxicity. In all cases, we compared a natural producer of colibactin, strain IHE3034 with the mutant Δ*clbP*. We further found that (1) colibactin production does not have any detectable effects on the chemical composition, size, and amount of bacterial OMVs, (2) OMVs were sufficient to elicit the colibactin hallmarks of genotoxicity, including megalocytosis and DNA Damages on treated cells. However, we also found that (3) OMVs from both the *pks*+ strain and the

Δ*clbP* mutant did not cause interstrand crosslinks, contrary to what was expected based on the proposed genotoxic mode of action of colibactin. Interestingly and an unforeseen outcome, we found that OMVs from the strain incapable to produce the active colibactin Δ*clbP* mutant, caused a substantial amount of toxicity towards cells. From these efforts, we conclude that OMVs vesicles are involved in the genotoxicity of colibactin although we have yet to find the compound in these vesicles.

Author Biography

Yermary Morales Lozada was born in San Juan Puerto Rico, on September 9, 1986. She is the fourth child and the only daughter of her parents, Edelmira Lozada and Luis A. Morales. Her older brothers are Luis a. Morales, Jose L. Morales, and Antonio L. Morales. Yermary grew up with her family in Naranjito, PR, where she completed her education until high school. She graduated with honors from the Francisco Morales High School and immediately received early admission to the Chemistry Department of the University of Puerto Rico, Rio Piedras Campus. Yermary began her undergraduate research felowship following her first year in college as she became convinced that scientific research was her professional goal. Yermary worked as a research assistant for a period of 5 years in the Biochemistry Laboratory of Dr. Reginald Morales. Under the guidance of Dr. Morales and Dr. Quesada, Yermary measured the activity of the enzyme phospholipase A2 (PLA2) on the membrane of human red blood cells. Through this experience, she developed her expertise in protein purification, biological sample management, enzyme activity assays, and other biochemical techniques. Also, during her undergraduate studies, Yermary complemented her Chemistry background with substantial coursework in Biology, earning a spot in the prestigious MBRS-RISE research program.

In 2007, in the midst of her undergraduate studies, Yermary gave birth to a child, Edmary V. Matos-Morales. Being a full-time student in a demanding science career while simultaneously being the head of household and a single mother, has been Yermary's most consequential achievement.

In 2012, Yermary was admitted to the Chemistry Graduate Department Program at the University of Puerto Rico, Rio Piedras Campus. She approved her qualifying exams in 2013 with outstanding grades. After that, she joined the Biochemistry and Enzymology Laboratory under the mentorship of Dr. Abel Baerga-Ortiz at Molecular Sciences Research Center (MSRC). The focus of this laboratory is to study the mechanisms by which the human microbiome influences human disease. Yermary's work centered in deciphering the molecular mechanism by which colibactin, a toxin produced by a bacterium the naturally resides in the human gut, causes tissue damage. With her vast knowledge in both Chemistry and Biology, Yermary was able to implement new experimental designs and original methodologies that elevated the scope of work within the research group to new heights.

Yermary also participated in numerous conferences in Puerto Rico and the United States. She also lead numerous outreach events where she brought science to kids and was a tutor for students who struggled with Maths and Sciences.

Vita

2012	B.S. Chemistry, University of Puerto Rico
2021	Ph. D. Biochemistry, University of Puerto Rico

Publications

Morales-Lozada, Y.; Báez-Bravo, G.; Soto-Berrios, O.; Gómez-Moreno, R.; Perkins, G. M. and Baerga-Ortiz, A. Bacterial outer membrane vesicles mediate genotoxic effects of the *pks* genomic island. **2021** (manuscript in preparation)

Field of Study

Major Field: Chemistry

Studies in Biochemistry

Professor Abel Baerga-Ortiz, Ph.D.

Dedication

To my beloved daughter, **Edmary,** whose very existence encourages me day by day to passionately complete all my goals. The moment I realized that each of my achievements meant a grander scope for the life you will one day make for yourself, my goals became duties. This is for you!

To my older brother, **Luisito,** for showing me the enrapturing beauty of science when I was a child. Thanks to you, that same child has and will continue to dedicate herself to sharing and uncovering the elegance of science.

To my parents, **Mirita** and **Wiso,** who supported me lovingly throughout graduate school. Thank you both for believing in me, this would not have possible without you. I just wanted to make you proud! I hope that someday I might return even the smallest portion of the I owe you both.

To my family, friends, and mentee who generously provided their encouragement and support.

Acknowledgements

Earning a doctoral degree requires more than personal dedication, passion, and constancy. It requires a team of people to help and guide you in its accomplishment. In my journey as a graduate student, there were delightful moments and trying times. Fortunately, throughout this journey I have been surrounded by outstanding individuals who I owe a debt of gratitude.

I am extremely grateful to my thesis advisor Dr. Abel Baerga-Ortiz, who encouraged me and believed that I would complete my work. Thank you for your trust, guidance in shaping my experimental methods, critiquing my results, and for the feedback throughout my project. But, above all, thank you for being present and understanding of all the difficult and unanticipated situations life brought. You were, unquestionably, the advisor I needed to guide me during this process.

My gratitude is extended to the RISE Program. I am honored for the opportunity to have been part of the RISE Fellowship and for their financial and professional support. I am very grateful for the funding opportunity to undertake my doctoral studies for these last years under the NIGMS-RISE 5R25GM061151-19 grant from the National Institutes on Minority Health and Disparities, National Institutes of Health (NIH). Especially to Dr. Orestes Quesada and Dr. Reginal Morales for their mentorship, not only during my doctoral studies and as a RISE student fellow, but also since the very beginning as an undergraduate student. The strong background preparation in research, the confidence, and the motivation that you both gave me were definitely crucial in my professional development to become a scientist.

To my thesis committee: Dr. Ingrid Montes, Dr. Carlos Cabrera, Dr. Reginal Morales, and Dr. Marvin Bayro. Thank you all for your advice, objective evaluation, and dedication to help me grow academically and professionally. You all treated me with the respect and gave me the recognition that I strived for. These allowed my sense of responsibility to develop and blossom, providing me with the confidence needed for a career in the

sciences. I am thankful for Dr. Ingrid Montes, a professor whom I have admired since we first met during my undergraduate studies. Because beyond being my professor, you taught me the importance of communicating, mentoring, and teaching others to help them grow. You have been a role model for me in so many ways. Dr. Reginal Morales, you are not physically in this world but I have plenty of memories of our conversations about "culture", science and life. I will never forget your last word to me in my Thesis Proposal Presentation- "I have seen you growing scientifically and you will go far if you continue like this. This degree and knowledge are yours and no one can take it away from you, you have to finish it". Those words will remain in my heart forever, rest in peace "Reggie."

Also, I want to acknowledge the past and current members of our "ABO Lab" research team. Vilmarie Mercado, I have no words to express my gratitude and appreciation for your help, caring, friendship, support in the academic as in the professional and personal way. Thank you for the continuous encouragement through all these years in all my processes. You became family. To past lab-mates, Melissa Ortiz, Dr. Ramon Gomez, Dr. Carlos Rúllan, and Dr. Uldaeliz Trujillo thanks for patiently passing me all your knowledge when I started in the laboratory. To the current lab-mates, Rachell Martinez, Yesenia Acevedo and, Jeremy Colon. To all of you, thanks for a cherished time spent together in the lab, and social settings. I really enjoy those days. To all my mentees, but especially to Dr. Gabriela Baez and Ohel Soto-Berrios. Gabriela, you was my first mentee when I started graduate school, you teach me how to become a mentor but you end becoming my friends. Ohel, it is for me an honor to be a part of your professional development, you contributed to complete my project. Thank you for your loyalty, your help to achieve my last experiments, and all our interesting conversations.

I want to thank the people who helped me to understand a lot about different instrumentation and laboratory techniques throughout these years. First, Neuroimaging and Electrophysiology Facility (NIEF), especially to Bismark Madera for all his help, support, and availability not only to perform my microscopy confocal experiments but also for training me on the methodologies for image analysis. To the Material Characterization Center, Inc. (MCC), especially to Cristina Diaz-Borrero and Mildret Rivera-Isaac for their

help in surface analysis and mass spectrometry experiments respectively. Also thank Dr. Dina P. Bracho-Rincon and Dr. Jose A. Gonzalez-Feliciano for their mentoring, advising, and teaching in many aspects of cell culture and molecular techniques. Thanks also to Dr. Yancy Ferrer-Acosta all her help in tissue culture.

Arriving at my dissertation required more than academic support, and I have many, many people to thank for listening, helping, advising, and supporting me during all this journey of graduate school. Sara Delgado, Bianca Valdéz, Freisa Joaquín, Michelle Hernández, Wilma Cintrón, Diana Díaz, Irivette Dominguez, and Dina Bracho. You all have been unwavering in your personal and professional support and for many memorable days.

Lastly, I want to extend my gratitude for the support in several aspects I received from the UPR-RP Department of Chemistry, the UPR-RP Dean of Graduate Studies and Research (DEGI), and to the Molecular Science Research Center (MSRC).

To all of you,

Thanks!

BACTERIAL OUTER MEMBRANE VESICLES AS MEDIATORS OF COLIBACTIN TOXICITY

Chapter 1. Introduction

1.1 THE GUT MICROBIOTA IN HEALTH AND DISEASE

The human body houses important communities of microorganisms acquired since birth.[1] These communities (known collectively as the microbiota) are composed mostly of bacteria but also include viruses, fungi, and archaea.[2,3] These microorganisms bring with them an extensive collection of genes (termed microbiome) which in combination, outnumber those found in the human genome.[3,4] Microbes in the human body are distributed mainly in communities or "niches" in which local diversity depends on the specific environment or needs in a particular body site (Skin, Oral, Vaginal, Gastrointestinal tract).[3,5–11] For example, vaginal microbiota is rich in *Lactobacillus*, whose major function is to protect and to prevent infection from other pathogens by producing antimicrobial and antifungal compounds[12,13]; whereas intestinal microbiota is rich in *Firmicutes* and *Bacteroidetes*, whose major functions include nutrients acquisition and metabolism[12,14]. With its implications and importance in human health, the microbiota has been categorized as the "forgotten organ"[15]. However, despite all the recent advances in uncovering the functions harbored in the microbiota, exactly how it influences health and disease is still under intense investigation.

The gastrointestinal (GI) tract harbors the largest portion of the microbial community and the broadest diversity, thus most of the studies are focused on the importance and involvement of the gut microbiota in health or disease. The GI alone is composed of approximately ten times more microbial cells than human cells[12,14]. There is not a specific recipe for a healthy microbial composition, but a common thought in the field is

that a balanced microbial composition is one that can resist or easily return to equilibrium following a stress-related perturbation[16]. It has been found that gut microbiota is highly variable among healthy individuals although there is a shared core of functionalities and conserved metabolic pathways[16–19]. Nevertheless, studies aimed at determining the microbial population in healthy individuals agree on the fact that a "normal" gut microbiota is rich in the *Firmicutes* and *Bacteroidetes* phyla[20,21] (about 90% of the total community) with a low abundance of *Proteobacteria* (including *E. coli*), *Actinobacteria*, *Fusobacteria*, and *Verrucomicrobia* phyla[17,22]. *Firmicutes* are related with the production of butyrate, which among its benefits include anti-inflammatory activity, activation of the production of mucin (intestinal epithelial defense barrier) and as the principal energy source of colonic epithelial cells[23–25]. On the other hand *Bacteroidetes* are more associated with the production of propionate and acetate, which naturally decrease appetite (stimulating satiety) and inhibit fatty acids production and storage[24,26].

One of the main benefits of the gut microbiota is its role in training the host immune system. For instance, the host's innate and acquired immune response is constantly challenged by the continuous exposure to specific molecules made by commensal microbes[27]. This interaction creates a tolerance toward commensal microbes and at the same time enhances the host sensitivity to detect and respond effectively against other invading pathogens[28,29]. In fact, a comparative study between germ-free mice vs microbe-colonized mice, reveals that germ-free mice were more susceptible to pathogenic infection and that the re-colonization of the germ-free mice with intestinal

microbiota is enough to re-establish normal inmmunity[15,30,31]. In addition to helping to train the host immune system, the microbiota also exerts a direct protective mechanism against infection by foreign pathogens, by producing antimicrobial substances and by competing for nutrients, rendering their environment resistant to pathogen colonization[32,33].

The microbiota also plays a fundamental role in obtaining dietary nutrients from food, as well as in the metabolism of drug and other foreign substances that the human body alone cannot metabolize. Gut microbes contribute to human metabolism with the production of enzymes that are not encoded in the human genome, but help to break down polysaccharides, polyphenols, and unabsorbed sugars, which are degraded into small-chain fatty acids (SCFs) such as butyrate, acetate, and propionate[30,34,35]. This source of SCFs is then used by colon epithelial cells to maintain the healthy functionality of the intestinal barrier and the immunological host response[35,36]. In addition, certain gut microbes from the *Bacteroidetes* phylum also have the capacity to metabolize drugs and xenobiotic compounds either for excretion or for activation[37]. For example, Sulfasalazine (also known as Azulfidine®), used to treat bowel inflammation, is barely absorbed by upper intestine when orally ingested, but once it reaches the colon bacterial enzymes transform it into the 5-aminosalicylic acid absorbable form.[37,38]. These and other numerous benefits, make the human microbiota and its microbiome a functional, integral, and essential component of human health.

On other hand, the alteration of the normal microbial symbiosis, also called dysbiosis,

has been associated with the development of diseases like inflammatory bowel diseases (IBD), obesity, allergic disorders, Type 1 diabetes mellitus, autism and, even cancer[16,39]. For example, among IBD patients, specifically those suffering from Crohn's Disease (CD), it is common to see a decrease in commensal bacteria (*Firmicutes* and *Bacteroides, thus decreasing SCFs*) with a relative increment in *Enterobacteriaceae (Escherichia/Shigella),* causing a prolonged intestine inflammatory response and eventually, tissue damage[40,41]. Similarly, obesity has also been associated with the alteration in the ratio of *Firmicutes*:*Bacteroidetes,* the most abundant phyla in healthy individuals[21]*.* This dysbiotic microbial composition consequently alters the SCF production, favoring fat absorption and accumulation, thus, contributing to obesity[21,39,42]. Interestingly, a recent study where germ-free mice were transplanted with fecal material from a pair of twins: one obese and the other one non-obese, revealed that the mouse receiving fecal material from the obese twin, increased its body fat. On the other hand, the mouse that received the fecal material from the non-obese twin did not gain as much weight[43]. Dysbiosis also causes a decrease in the protective and immunomodulatory effects that maintain homeostasis in the human gut. Thus, resulting in the prolonged inflammatory response and the damage of intestinal tissue and barrier integrity, allowing virulent pathogens to take advance to colonize, leading to deleterious effects on human health (Figure 1.1).

One persistent question in the field of microbiome studies, is whether changes in the microbiota are a cause of the disease or an outcome of it. However, an evident shift in microbial composition is constantly observed between healthy and non-healthy

individuals, but these alterations will more likely be reflected on the microbial functions than in the composition of bacteria[16]. Thus, since microbial effects on human health are likely to be driven by microbial functions and mechanisms, it is more important to study and delineate those functions, rather than catalog the microbial composition.

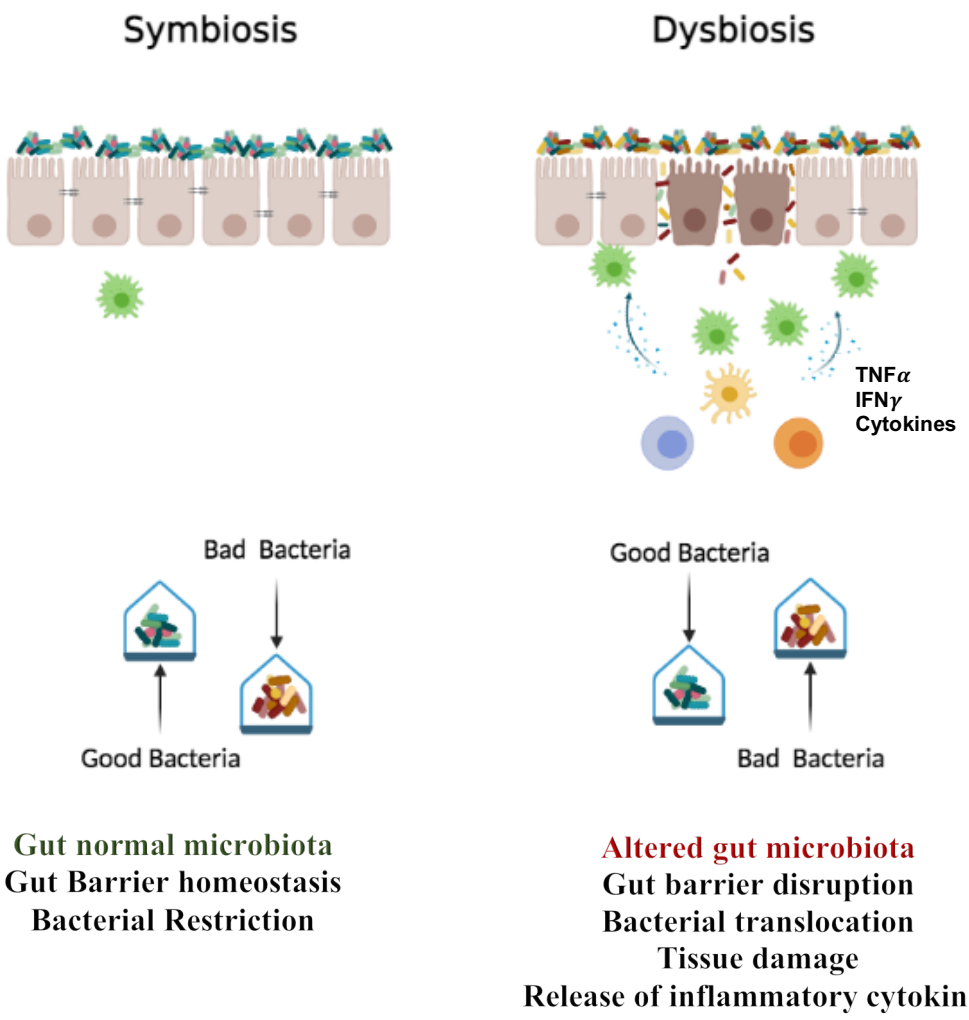

Figure 1.1 Schematic representation of symbiosis vs dysbiosis. Symbiosis (left side) is defined by the balanced combination between beneficial and pathogenic bacteria. “Good” bacteria shape the immune system, produce compound like SCFA to maintain the integrity of the intestine barrier, create the environment to resist colonization of harmful pathogens, and metabolize complex compounds that the human body cannot. Dysbiosis (right side) resulted by the alteration of the healthy microbes composition where pathogenic bacteria become more abundant. “Bad” bacteria are related with prolonged inflammation, tissue damage, intestine barrier disruption among other damages leading to IBD, Cancer development, and among other unhealthy outcomes. Figure were adapted from Celardo et. al 2020, Torr et. al 2019

1.2 THE GUT MICROBIOTA AND COLORECTAL CANCER

Colorectal cancer (CRC) is the third (2021 estimation; Figure 1.2) most common type of cancer detected in both men and women in the USA[44]. Remarkably, in Puerto Rico, CRC is the second (2018 statistics) most common death cause cancer in both men and women (Figure 1.3). The epidemiology of CRC is complex and cases can be grouped into "familial CRC" which accounts for 30% of cases and "sporadic CRC" which accounts for the other 70%[45,46]. Among the environmental risk factors for CRC are smoking, alcohol consumption, nutrition, and the gut microbiota[47,48]. In fact, several species of bacteria have been implicated in either the promotion of CRC or in the protection against it and based on these criteria they have been classified as "good" or "bad" for human health[49,50].

Estimated New Cases

Males				Females		
Prostate	248,530	26%		Breast	281,550	30%
Lung & bronchus	119,100	12%		Lung & bronchus	116,660	13%
Colon & rectum	79,520	8%		Colon & rectum	69,980	8%
Urinary bladder	64,280	7%		Uterine corpus	66,570	7%
Melanoma of the skin	62,260	6%		Melanoma of the skin	43,850	5%
Kidney & renal pelvis	48,780	5%		Non-Hodgkin lymphoma	35,930	4%
Non-Hodgkin lymphoma	45,630	5%		Thyroid	32,130	3%
Oral cavity & pharynx	38,800	4%		Pancreas	28,480	3%
Leukemia	35,530	4%		Kidney & renal pelvis	27,300	3%
Pancreas	31,950	3%		Leukemia	25,560	3%
All Sites	**970,250**	**100%**		**All Sites**	**927,910**	**100%**

Estimated Deaths

Males				Females		
Lung & bronchus	69,410	22%		Lung & bronchus	62,470	22%
Prostate	34,130	11%		Breast	43,600	15%
Colon & rectum	28,520	9%		Colon & rectum	24,460	8%
Pancreas	25,270	8%		Pancreas	22,950	8%
Liver & intrahepatic bile duct	20,300	6%		Ovary	22,950	5%
Leukemia	13,900	4%		Uterine corpus	12,940	4%
Esophagus	12,410	4%		Liver & intrahepatic bile duct	9,930	3%
Urinary bladder	12,260	4%		Leukemia	9,760	3%
Non-Hodgkin lymphoma	12,170	4%		Non-Hodgkin lymphoma	8,550	3%
Brain & other nervous system	10,500	3%		Brain & other nervous system	8,100	3%
All Sites	**319,420**	**100%**		**All Sites**	**289,150**	**100%**

Figure 1.2 Ten leading cancer types for the estimated new cancer cases and deaths by sex, United States, 2021. Colorectal cancer (CRC) is positioned as the third most common cause of cancer death. Ranking is based on modeled projections and may differ from the most recent observed data. Imagen taken from *Cancer statistics, 2021*; American Cancer Society.

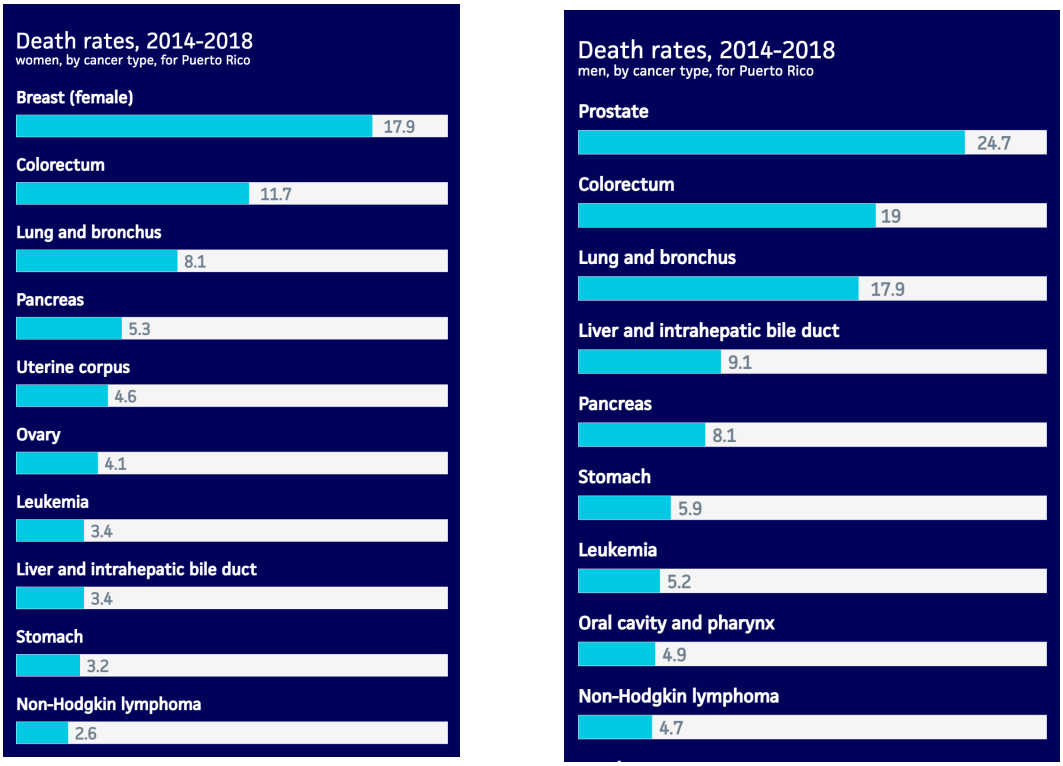

Figure 1.3 Ten leading cancer type causing deaths by sex, Puerto Rico, 2014-2018. CRC is the second cancer related death cause in both women and men in Puerto Rico. Images taken from *Cancer statistics, 2021*; American Cancer Society.

Among the "good" bacteria, we can start by naming *Faecalibacterium prausnitzii* (*F. prausnitzii*), an endogenous bacterium of the commensal microbiota which is considered to be a biomarker for healthy individuals[51]. In fact, *F. prausnitzii* is found in low abundance in IBD and Colitis patients[52]. One of the benefits of *F. prausnitzii* is its capacity to produce butyrate and salicylic acid[53], both metabolites that play roles in stimulating a protective immune responses in the gut[54]. It has been also reported that *F. prausnitzii* has anti-inflammatory activity by the secretion of several metabolites capable of reducing chemically-induced inflammation in mouse model by blocking NF-kB (Nuclear factor kappa-light-chain-enhancer of activated B cells) activation, IL-8 (Interleukine-8) production and the up-regulation of T cell production[51,55–57]. In addition, there are studies indicating that metabolites secreted by *F. prausnitzii* play a role in enhancing intestinal barrier[58,59]. In fact, a colitis-induced mouse model treated with *F. prausnitzii* results in a decrease in intestinal permeability, the mouse weight recovery, and the higher expression of the tight junction protein claudin-1, thus, attenuating the detrimental effects of colitis in the mice[59]. Due to all the beneficial effects of *F. prausnitzii* in human health, have placed this bacteria as a promising candidate as a probiotic to treat inflammatory bowel diseases such as Ulcerative Colitis (UC) and Chron's Disease[56,58].

Then there are the "bad bacteria". A well-known example of a "bad bacteria" is *Helicobacter pylori* (*H. pylori*) which as has been linked with gastric cancer [60,61]. *H. pylori* produces a toxin encoded by the *cagA* gene (cytotoxin-associated gene A) which

alters important signaling pathways on stomach cells allowing the bacteria an easy attachment, resulting in chronic inflammation and carcinogenesis[61]. Another "bad bacteria" is *Fusobacterium nucleatum* (*F. nucleatum*), a commensal bacterium normally found in the oral cavity, but also an opportunistic pathogen at other body sites[62]. For instance, several reports implicate *F. nucleatum* in cancer development due to its high abundance in tumor specimens of CRC patients when compared with normal contols[63–67]. A third example is the Enterotoxigenic *Bacteroides fragilis* (EtBf), which has been shown to be correlated with CRC development by the production of *B. fragilis* toxin (BFT)[68]. BFT is a metalloprotease which triggers the cleavage of E-cadherin, a tumor suppressor protein in charge of cell grow and regulate cellular differentiation. Thus, causing intestinal barrier permeability and NF-kB signaling activation leading to mucosal inflammation[68,69].

1.3 *ESCHERICHIA COLI* AS A CANCER RISK FACTOR

Escherichia coli is a member of the normal gut microbiota, but some strains may contain factors that increase the likelihood of developing cancer[70]. One of these factors are the *cyclomodulins*, which alter the normal cellular cycle of the infected cell by inhibiting or promoting proliferation[71]. The first bacterial toxin involved in blocking a eukaryote cell cycle, is the Cytolethal Distending Toxin (CDT)[71,72]. CDT-producing *E. coli* provoke cytopathic effects on cultured cells by cell cycle arrest specifically in G2/M transition, which lead the infected cell to cell enlargement, DNA double strand-breaks (DBS) and re-organization of actin network into stress fibres[72]. Similarly, others *E. coli* strains: the enteropathogenic and the enterohemorrhagic, specifically, those that harbor the *cif*

genes, produce the Cycle inhibitory factor (Cif)[71,73]. Cif cause cells cycle arrest by inhibit the cyclin dependent kinase (CDK) 1-CyclinB on infected cells, which play a role in specifically the G2/M cell cycle transition[71,73]. Interesting, the effect of Cif on cell cycle are not related to DNA damage canonical repair pathway, as it has been observed in other similar cyclomodulatory toxins[73]. As well, Cytotoxic Necrotizing Factors (CNFs) is another toxin related with *E. coli* cancer promotion. CNFs provoke on infected cell the constitutive activation of the Rho GTPase, a biomolecular "on-off" switch of important cellular process. Consequently, the irregular activation of Rho GTPase lead to cytoskeleton alterations, NF-kB activation and the production of anti-apoptotic factors as well as pro-inflammatory cytokines. A recently discovered cyclomodulin is the genotoxic compound Colibactin, a polyketide-non ribosomal peptide hybrid compound produced by *E. coli* strains harboring the *pks island* gene cluster[74] which will be discussed in detail in next section (section 1.4 PKS ISLAND). Taking together these finding imply that commensal *E. coli* can acquire the potential to exert or promote carcinogenesis.

1.4 *PKS ISLAND*

The *pks island* is a cluster of genes present in some strains of commensal *E. coli* (specifically the B2 phylogenic group) and in other proteobacteria commonly found in the human gut, that elicit a variety of effects on the mammalian cells that it contacts[74,75]. These genes encode a group of proteins that control the synthesis of a putative polyketide/non-ribosomal peptide (PK/NRP) compound termed Colibactin. The mechanism of action and structural characterization of colibactin are yet to be completely elucidated (Figure 1.4 A) [74,76].

The *pks island* was discovered in 2006 for its ability to elicit a rare cellular phenotype known as megalocytosis (Figure 1.4 B). Megalocytic phenotype has been observed in the liver cells of bovine cattle after ingestion of toxic compounds[77,78]. These megalocytic cells are easily identified by their enlarged nuclei that can be readily seen in a microscope[74,79]. It was described that strains of *E. coli* harboring the *pks* genes are also capable of provoking such damage in which the mammalian cell is arrested during division (specifically G2/M transition), and become senescent[80,81], as a result of the DNA damage via double strand-breaks[82,83] induced by colibactin[74]. When cells exhibit this phenotype, a number of markers of DNA damage become significantly activated: γH2AX, ATM, CHK1, and CHK2. All these genotoxic damages associated with colibactin are characteristic hallmarks of cells likely to become carcinogenic[84,85]. Thus, the presence of the *pks island* can cause extensive damage to the cellular genome and to its capacity to control division.

The presence of colibactin-producing *E. coli* in the human gut has been associated with sporadic colorectal cancer development and progression[80,81,86,87]. Studies have reported that colonic *E. coli* from biopsies obtained from CRC patients were four times more likely to contain *pks island* than *E. coli* from non-CRC biopsies[83,88]. Bacteria harboring these genes induce tumor growth, both in chronic intestinal inflammation mouse models and in intestinal biopsies from CRC patients[80], further supporting the link between colibactin and CRC.

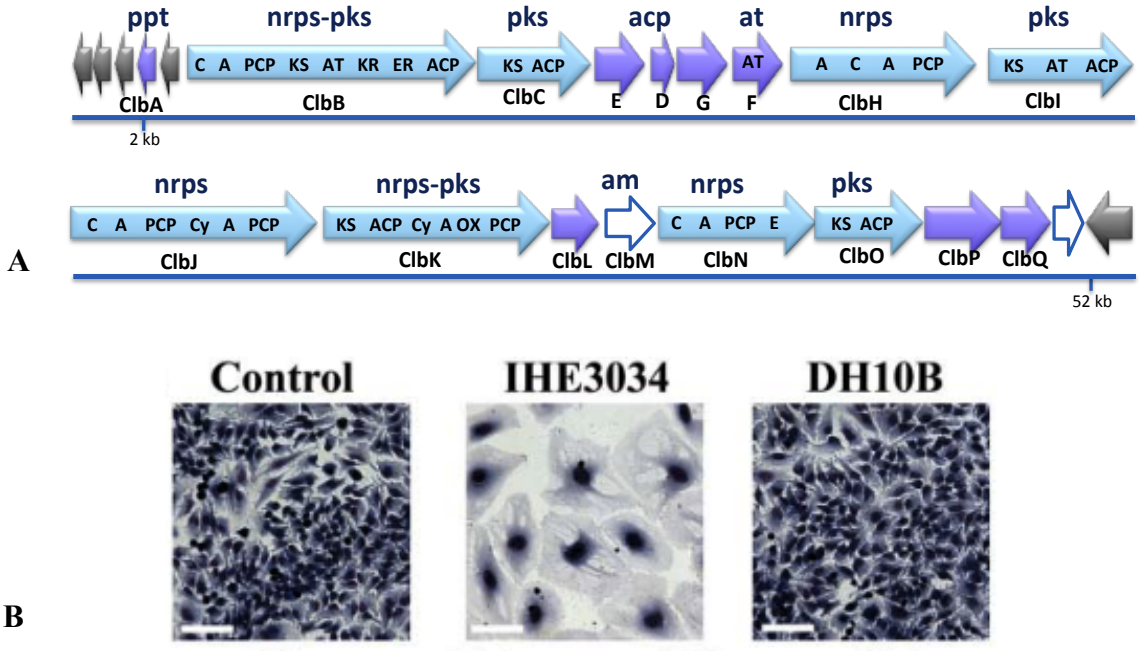

Figure 1.4: The *pks* genes encodes for colibactin biosynthesis. A) The *pks* genomic island which encodes for the synthetases necessary for colibactin biosynthesis. (*ppt*, phosphopantetheinyl transferase; *nrps*, nonribosomal peptide synthetase; *pks*, polyketide synthase; *hcdh*, hydroxyl acyl coA dehydrogenase; *acp*, acyl carrier protein; *dhg*, ab dehydrogenase; *at*, acyl-transferase; *am*, amidase; *te*, thioesterase; *A*, adenylation; *ACP/PCP*, phosphopantetheine/acyl carrier; *AT*, acyltransferase; *C*, condensation; *Cy*, cyclization; *ER*, enoyl reductase; *KR*, ketoacyl reductase; *KS*, ketoacyl synthase; *OX*, oxidation. **B)** Giemsa staining of HeLa cells after 72 hours of infection at 37°C and 5% CO_2 with *E. coli* IHE3034 (*pks*+) and DH10B (*pks*-) bacterial strains. Cells were co-incubated with HeLa cells for 4 hrs, then washed and re-incubated with gentamycin up to 72 hrs. HeLa cells without any bacterial infection was used as negative control. Scale bars, 100 uM. *E. coli* IHE3034 (*pks*+) cause a toxic effect which result in a detectable cell body and nucleus enlargement phenotype called megalocytosis. (Nougayrède et. al, 2006)

Colibactin is made as the final product of a series of Claisen-like condensation reactions catalyzed by a PKS/NRPS hybrid multienzymes[89]. Its synthetic pathway starts in the bacterial cytosol where is made as the inactive precursor, pre-colibactin[90]. Pre-colibactin is then activated by the peptidase clbP by a hydrolytic de-acylation which provokes an intramolecular re-arrangement and consequently its activation (reactive version)[91]. A number of different versions and intermediates of colibactin have been isolated and their structures determined.

The isolation of active colibactin directly from its producer bacteria has been impossible so far. Since the production of colibactin intermediates has been very low and sometimes undetectable, strategies have been developed to increase yield by genetically modifying the *pks genes,* disabling several enzymes to promote the accumulation of intermediates. Early attempts to determine the complete colibactin structure involved the elimination of the peptidase clbP, which as mentioned before, is essential for the maturation of pre-colibactin into the de-acylated active compound during the final steps of its biosynthesis[92–94]. This ***Δ****clbP* mutant was capable of accumulating sufficient amounts of colibactin intermediates to be isolated and characterized structurally [93–101]. Various groups are making great efforts to decipher the *colibactin* structure, however, most structures show intermediates with no biological activity (Figure 1.5) [74,91,92,95].

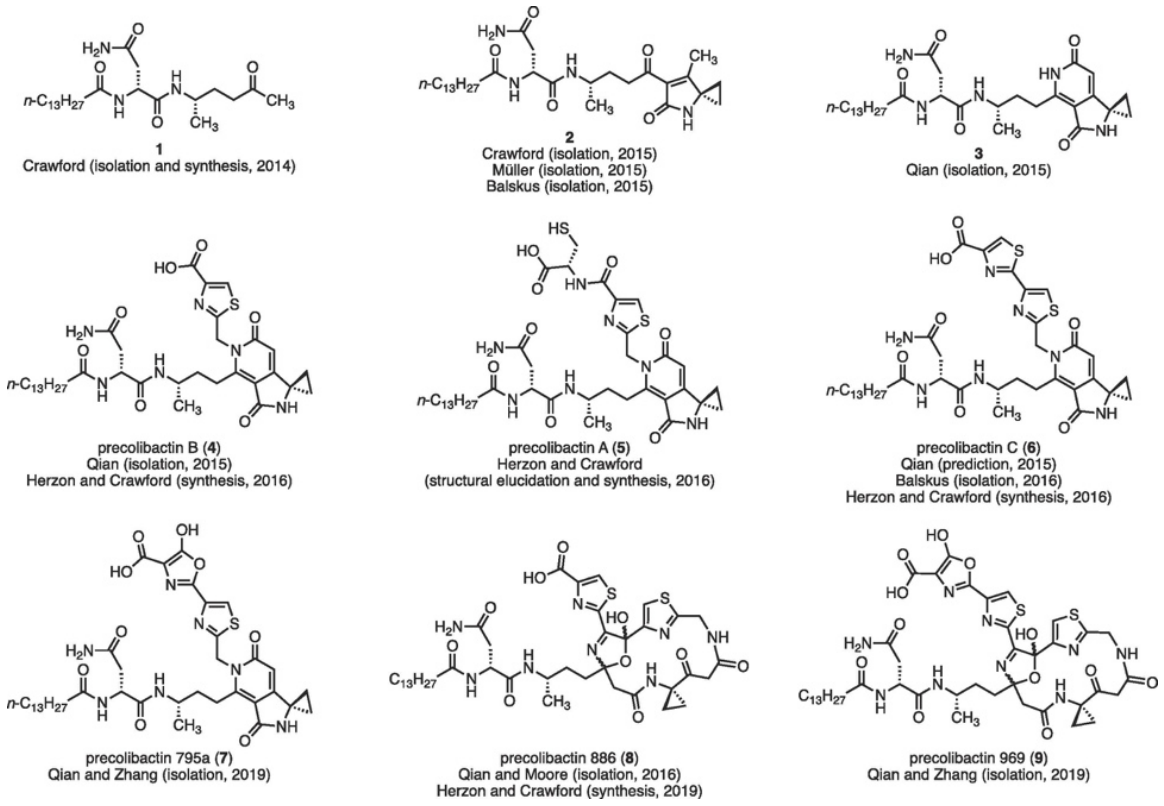

Figure 1.5 Isolated, synthetized and predicted pre-colibactins. (Image originally published in Wernke *et al*., 2020). All of these structures were obtained through the deletion of *clbP* gene as evidenced by the presence of the *N*-myristoyl moiety. Throughout these efforts it has been clear that colibactin contains a cyclopropyl moiety with a pair of thioazole functional groups. None of these compounds, however, have genotoxic activity.

Exactly how colibactin can mount a thorough attack on the cell has been a subject of intense study over the last couple of years[102]. The initial questions on the activity of colibactin, emphasize on its chemical structure and possible modes of action. Since, an efficient method to isolate colibactin directly from its producer bacterial culture is lacking, researchers have devised other molecular strategies to isolate and characterize intermediates of this genotoxin. The strategy commonly implemented by various research groups was inspired by the pro-drug resistance mechanism described for colibactin activation[93,94,103,104]. This mechanism relies on the peptidase clbP activity, which catalyzes the transformation of the colibactin precursor compound (pre-colibactin) into its active version (colibactin). A colibactin-producing bacteria with an inactivated clbP peptidase, was found to accumulate enough pre-colibactin intermediates in sufficient amounts to be characterized chemically [93,103]. From these efforts, it was determined that the colibactin structure contains: (1) the asparagine-acyl moiety (Myristoyl-*D*-Asn), which confers colibactin the pro-drug resistance activity and target site for clbP peptidase[93,94]; (2) the a electrophilic cyclopropyl moiety, which is considered the DNA reactive site of colibactin and thus termed as the colibactin 'warhead" [95,96,100]. This reactive cyclopropyl reacts specifically with adenine residues causing the formation of interstrand crosslinks which then result in double-stranded breaks of mammalian DNA[105].

While most of the efforts into elucidating the colibactin mechanism of action have centered on the structure and reactivity of the molecule, there are many unanswered questions how colibactin is transported from the bacteria to the mammalian cell: How

does colibactin get to the nucleus of an infected cell? The most likely route of transport is diffusion. Like many bacterial antibiotics and toxins, colibactin could be made and expelled by *E. coli* and then passively diffuse through the mammalian cell membrane. Early observations suggested that this model was not right since most efforts to isolate and characterize colibactin from bacterial cultures were unsuccessful. Clearly, there is a route by which colibactin is transferred from the producing bacteria into the nucleus of the infected cell and our laboratory proposed that this route could involve bacterial vesicles from its outer membrane.

1.5 OUTER MEMBRANE VESICLES

Outer membrane vesicles (OMVs) are sphere-like nanoscale particles spontaneously shed by gram-negative bacteria[106,107]. These vesicles have several functions, among them is the delivery of proteins, virulence factors, bacterial survival factors, horizontal genes transfer, and immunomodulation[108–110]. OMVs are responsible for the release of the outer membrane and periplasm content out of the cell while protecting the content from proteases and other hydrolytic cells protective factors[111]. Additionally, OMVs give bacteria the advantage to reach host cells located deep into a tissue that cannot be reached by the whole bacteria itself[112]. Some of the components transported in these vesicles can be either functional substances with a particular target and/or purpose or can be also just waste material such as misfolded proteins[113]. Therefore, these vesicles are an essential, dynamic, and multifunctional tool for bacteria survival and bioactivity.

OMVs from certain *E. coli* strains, including non-pathogenic bacteria, can cause DNA damage and promote an inflammatory response in mammalian cells by themselves[114,115]. Interestingly, these outcomes are similar to those attributed to *pks island* and colibactin.

1.6 ARE COLIBACTIN EFFECTS MEDIATED BY OUTER MEMBRANE VESICLES?

While much has been learned about the colibactin structure and its biochemical function, exactly how it is delivered to the infected cells is not known. Initial studies showed that the damage caused by colibactin to the mammalian cell is dependent on direct physical contact with the bacterial producer[74]. An attractive hypothesis on the delivery of colibactin to mammalian cells involves bacterial OMVs (Figure 1.6).

It has been a goal in our research group to elucidate the structure and transfer of colibactin into infected cells. However, during the course of this work, other groups, notably Crawford[101] in Yale and Balskus[105] in Harvard were very quick to determine the structure of active colibactins and their reactivity with DNA[91]. Our group concentrated on developing the hypothesis that bacterial OMVs are the vehicle by which colibactin is transferred to cause infection. We isolated OMVs from clinical strain IHE3034 and found that OMVs on their own were capable of causing megalocytosis in HeLa cells.

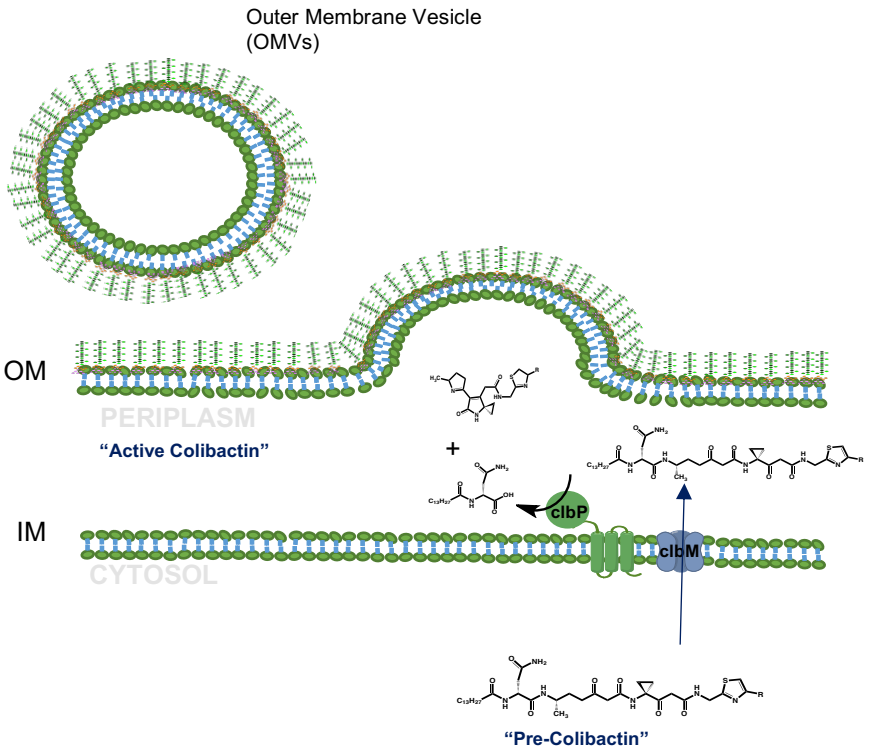

Figure 1.6 Schematic representation of the suggested biosynthetic route for colibactin and its possible interaction with the OMVs of its producer bacteria. Pks/nrps enzymes synthesize pre-colibactin inside the bacterial cell. The pre-colibactin is subsequently translocated to the periplasmic space by a transporter protein (ClbM). We suggest that after its activation by the peptidase (ClbP), colibactin interact with the bacterial outer membrane and may use them as vehicle to reach target cells and exert its toxicity. (Nougayrède *et al*., 2006; Cougnoux *et al*., 2012; Bian *et al*., 2013 and 2015; Brotherton *et al*., 2013; Mousa *et al*., 2016; Vizcaino *et al*., 2015; Wernke *et al*., 2020).

1.7 AIMS

Aim 1: To develop a molecular strategy to increase the yield of colibactin for structural studies.

Specific aim 1: To delete the *clbP* peptidase gene to cause the accumulation of pre-colibactin.

Specific aim 2: To assess deleterious effects of accumulated pre-colibactin intermediate. (this includes both growth and morphology)

Aim 2: To determine biological activity of OMVs secreted by *E. coli* strain harboring *pks* genes.

Specific aim 3: To characterize the OMVs extracted from *E. coli* harboring the *pks* genes in terms of size distribution and fatty acid composition.

Specific aim 4: To assess the biological activity of OMVs extracted from *E. coli* harboring the *pks* genes.

1.8 REFERENCES

(1) Robertson, R. C.; Manges, A. R.; Finlay, B. B.; Prendergast, A. J. The Human Microbiome and Child Growth – First 1000 Days and Beyond. *Trends Microbiol.* **2019**, *27* (2), 131–147. https://doi.org/10.1016/j.tim.2018.09.008.

(2) Gill, S. R.; Pop, M.; DeBoy, R. T.; Eckburg, P. B.; Turnbaugh, P. J.; Samuel, B. S.; Gordon, J. I.; Relman, D. A.; Fraser-Liggett, C. M.; Nelson, K. E. Metagenomic Analysis of the Human Distal Gut Microbiome. *Science.* **2006**, *312* (5778), 1355–1359.

(3) Thursby, E.; Juge, N. Introduction to the Human Gut Microbiota. *Biochem. J.* **2017**, *474* (11), 1823–1836. https://doi.org/10.1042/BCJ20160510.

(4) Bäckhed, F.; Ley, R. E.; Sonnenburg, J. L.; Peterson, D. A.; Gordon, J. I. Host-

Bacterial Mutualism in the Human Intestine. *Science.* **2005**, *307* (5717), 1915–1920. https://doi.org/10.1126/science.1104816.

(5) Lloyd-Price, J.; Mahurkar, A.; Rahnavard, G.; Crabtree, J.; Orvis, J.; Hall, A. B.; Brady, A.; Creasy, H. H.; McCracken, C.; Giglio, M. G.; McDonald, D.; Franzosa, E. A.; Knight, R.; White, O.; Huttenhower, C. Strains, Functions and Dynamics in the Expanded Human Microbiome Project. *Nature* **2017**, *550* (7674), 61–66. https://doi.org/10.1038/nature23889.

(6) Aas, J. A.; Paster, B. J.; Stokes, L. N.; Olsen, I.; Dewhirst, F. E. Defining the Normal Bacterial Flora of the Oral Cavity. *J. Clin. Microbiol.* **2005**, *43* (11), 5721–5732. https://doi.org/10.1128/JCM.43.11.5721-5732.2005.

(7) Nimish Deo, P.; Deshmukh, R. Oral Microbiome: Unveiling the Fundamentals. *J. oral Maxillofac. Pathol.* **2019**, *23* (1), 122–128. https://doi.org/10.4103/jomfp.JOMFP.

(8) Costello, E. K.; Lauber, C. L.; Hamady, M.; Fierer, N.; Gordon, J. I.; Knight, R. Bacterial Community Variation in Human Body Habitats Across Space and Time. *Science.* **2009**, *326* (5960), 1694–1697. https://doi.org/10.1126/science.1177486.Bacterial.

(9) Greenbaum, S.; Greenbaum, G.; Moran-Gilad, J.; Weintruab, A. Y. Ecological Dynamics of the Vaginal Microbiome in Relation to Health and Disease. *Am. J. Obstet. Gynecol.* **2019**, *220* (4), 324–335. https://doi.org/10.1016/j.ajog.2018.11.1089.

(10) Dieterich, W.; Schink, M.; Zopf, Y. Microbiota in the Gastrointestinal Tract. *Med. Sci.* **2018**, *6* (4), 116. https://doi.org/10.3390/medsci6040116.

(11) Chu, D. M.; Ma, J.; Prince, A. L.; Antony, K. M.; Seferovic, M. D.; Aagaard, K. M. Maturation of the Infant Microbiome Community Structure and Function across Multiple Body Sites and in Relation to Mode of Delivery. *Nat. Med.* **2017**, *23* (3), 314–326. https://doi.org/10.1038/nm.4272.

(12) Dekaboruah, E.; Suryavanshi, M. V.; Chettri, D.; Verma, A. K. Human Microbiome: An Academic Update on Human Body Site Specific Surveillance and Its Possible Role. *Arch. Microbiol.* **2020**, *202* (8), 2147–2167. https://doi.org/10.1007/s00203-020-01931-x.

(13) Dover, S. E.; Aroutcheva, A. A.; Faro, S.; Chikindas, M. L. Natural Antimicrobials and Their Role in Vaginal Health: A Short Review. *Int. J. Probiotics Prebiotics* **2008**, *3* (4), 219–230.

(14) Hillman, E. T.; Lu, H.; Yao, T.; Nakatsu, C. H. Microbial Ecology along the Gastrointestinal Tract. *Microbes Environ.* **2017**, *32* (4), 300–313. https://doi.org/10.1264/jsme2.ME17017.

(15) O'Hara, A. M.; Shanahan, F. The Gut Flora as a Forgotten Organ. *EMBO Rep.* **2006**, *7* (7), 688–693. https://doi.org/10.1038/sj.embor.7400731.

(16) Bäckhed, F.; Fraser, C. M.; Ringel, Y.; Sanders, M. E.; Sartor, R. B.; Sherman, P. M.; Versalovic, J.; Young, V.; Finlay, B. B. Defining a Healthy Human Gut Microbiome: Current Concepts, Future Directions, and Clinical Applications. *Cell Host Microbe* **2012**, *12* (5), 611–622. https://doi.org/10.1016/j.chom.2012.10.012.

(17) Clemente, J. C.; Ursell, L. K.; Parfrey, L. W.; Knight, R. The Impact of the Gut Microbiota on Human Health: An Integrative View. *Cell* **2012**, *148* (6), 1258–1270. https://doi.org/10.1016/j.cell.2012.01.035.

(18) Burke, C.; Steinberg, P.; Rusch, D.; Kjelleberg, S.; Thomas, T. Bacterial Community Assembly Based on Functional Genes Rather than Species. *Proc. Natl. Acad. Sci. U. S. A.* **2011**, *108* (34), 14288–14293. https://doi.org/10.1073/pnas.1101591108.

(19) Turnbaugh, P. J.; Hamady, M.; Yatsunenko, T.; Cantarel, B. L.; Ley, R. E.; Sogin, M. L.; Jones, W. J.; Roe, B. a; Jason, P.; Egholm, M.; Henrissat, B.; Heath, A. C.; Knight, R.; Gordon, J. I.; Rey, F. E.; Manary, M. J.; Trehan, I.; Dominguez-Bello, M. G.; Contreras, M.; Magris, M.; Hidalgo, G.; Baldassano, R. N.; Anokhin, A. P.; Heath, A. C.; Warner, B.; Reeder, J.; Kuczynski, J.; Caporaso, J. G.; Lozupone, C. a.; Lauber, C.; Clemente, J. C.; Knights, D.; Knight, R.; Gordon, J. I. A Core Gut Microbiome between Lean and Obesity Twins. *Nature* **2009**, *457* (7228), 480–484. https://doi.org/10.1038/nature07540.A.

(20) Mahowald, M. A.; Rey, F. E.; Seedorf, H.; Turnbaugh, P. J.; Fulton, R. S.; Wollam, A.; Shah, N.; Wang, C.; Magrini, V.; Wilson, R. K.; Cantarel, B. L.; Coutinho, P. M.; Henrissat, B.; Crock, L. W.; Russell, A.; Verberkmoes, N. C.; Hettich, R. L.; Gordon, J. I. Characterizing a Model Human Gut Microbiota Composed of

Members of Its Two Dominant Bacterial Phyla. *Proc. Natl. Acad. Sci. U. S. A.* **2009**, *106* (14), 5859–5864. https://doi.org/10.1073/pnas.0901529106.

(21) Magne, F.; Gotteland, M.; Gauthier, L.; Zazueta, A.; Pesoa, S.; Navarrete, P.; Balamurugan, R. The Firmicutes/Bacteroidetes Ratio: A Relevant Marker of Gut Dysbiosis in Obese Patients? *Nutrients* **2020**, *12* (5). https://doi.org/10.3390/nu12051474.

(22) Eckburg, P. B.; Bik, E. M.; Bernstein, C. N.; Purdom, E.; Dethlefsen, L.; Sargent, M.; Gill, S. R.; Nelson, K. E.; Relman, D. A. Diversity of the Human Intestinal Microbial Flora. *Science.* **2005**, *308* (5728), 1635–1638.

(23) Canani, R. B.; Costanzo, M. Di; Leone, L.; Pedata, M.; Meli, R.; Calignano, A. Potential Beneficial Effects of Butyrate in Intestinal and Extraintestinal Diseases. *World J. Gastroenterol.* **2011**, *17* (12), 1519–1528. https://doi.org/10.3748/wjg.v17.i12.1519.

(24) Venegas, D. P.; De La Fuente, M. K.; Landskron, G.; González, M. J.; Quera, R.; Dijkstra, G.; Harmsen, H. J. M.; Faber, K. N.; Hermoso, M. A. Short Chain Fatty Acids (SCFAs)Mediated Gut Epithelial and Immune Regulation and Its Relevance for Inflammatory Bowel Diseases. *Front. Immunol.* **2019**, *10*. https://doi.org/10.3389/fimmu.2019.00277.

(25) Louis, P.; Flint, H. J. Diversity, Metabolism and Microbial Ecology of Butyrate-Producing Bacteria from the Human Large Intestine. *FEMS Microbiol. Lett.* **2009**, *294* (1), 1–8. https://doi.org/10.1111/j.1574-6968.2009.01514.x.

(26) Louis, P.; Flint, H. J. Formation of Propionate and Butyrate by the Human Colonic Microbiota. *Environ. Microbiol.* **2017**, *19* (1), 29–41. https://doi.org/10.1111/1462-2920.13589.

(27) Kogut, M. H.; Lee, A.; Santin, E. Microbiome and Pathogen Interaction with the Immune System. *Poult. Sci.* **2020**, *99* (4), 1906–1913. https://doi.org/10.1016/j.psj.2019.12.011.

(28) Bene, K.; Varga, Z.; Petrov, V. O.; Boyko, N.; Rajnavolgyi, E. Gut Microbiota Species Can Provoke Both Inflammatory and Tolerogenic Immune Responses in Human Dendritic Cells Mediated by Retinoic Acid Receptor Alpha Ligation. *Front. Immunol.* **2017**, *8* (APR). https://doi.org/10.3389/fimmu.2017.00427.

(29) Shi, N.; Li, N.; Duan, X.; Niu, H. Interaction between the Gut Microbiome and Mucosal Immune System. *Mil. Med. Res.* **2017**, *4* (1), 1–7. https://doi.org/10.1186/s40779-017-0122-9.

(30) Shanahan, F. The Host-Microbe Interface within the Gut. *Bailliere's Best Pract. Res. Clin. Gastroenterol.* **2002**, *16* (6), 915–931. https://doi.org/10.1053/bega.2002.0342.

(31) Hooper, L. V.; MacPherson, A. J. Immune Adaptations That Maintain Homeostasis with the Intestinal Microbiota. *Nat. Rev. Immunol.* **2010**, *10* (3), 159–169. https://doi.org/10.1038/nri2710.

(32) Sassone-Corsi, M.; Raffatellu, M. No Vacancy: How Beneficial Microbes Cooperate with Immunity to Provide Colonization Resistance to Pathogens. *J. Immunol.* **2015**, *194* (9), 4081–4087. https://doi.org/10.4049/jimmunol.1403169.No.

(33) Maltby, R.; Leatham-Jensen, M. P.; Gibson, T.; Cohen, P. S.; Conway, T. Nutritional Basis for Colonization Resistance by Human Commensal Escherichia Coli Strains HS and Nissle 1917 against E. Coli O157:H7 in the Mouse Intestine. *PLoS One* **2013**, *8* (1), 1–10. https://doi.org/10.1371/journal.pone.0053957.

(34) Rowland, I.; Gibson, G.; Heinken, A.; Scott, K.; Swann, J.; Thiele, I.; Tuohy, K. Gut Microbiota Functions: Metabolism of Nutrients and Other Food Components. *Eur. J. Nutr.* **2018**, *57* (1), 1–24. https://doi.org/10.1007/s00394-017-1445-8.

(35) Silva, Y. P.; Bernardi, A.; Frozza, R. L. The Role of Short-Chain Fatty Acids From Gut Microbiota in Gut-Brain Communication. *Front. Endocrinol. (Lausanne).* **2020**, *11* (January), 1–14. https://doi.org/10.3389/fendo.2020.00025.

(36) Morrison, D. J.; Preston, T. Formation of Short Chain Fatty Acids by the Gut Microbiota and Their Impact on Human Metabolism. *Gut Microbes* **2016**, *7* (3), 189–200. https://doi.org/10.1080/19490976.2015.1134082.

(37) Sun, C.; Chen, L.; Shen, Z. Mechanisms of Gastrointestinal Microflora on Drug Metabolism in Clinical Practice. *Saudi Pharm. J.* **2019**, *27* (8), 1146–1156. https://doi.org/10.1016/j.jsps.2019.09.011.

(38) Crouwel, F.; Buiter, H. J. C.; De Boer, N. K. Gut Microbiota-Driven Drug Metabolism in Inflammatory Bowel Disease. *J. Crohn's Colitis* **2021**, *15* (2), 307–

315. https://doi.org/10.1093/ecco-jcc/jjaa143.

(39) Degruttola, A. K.; Low, D.; Mizoguchi, A.; Mizoguchi, E. Current Understanding of Dysbiosis in Disease in Human and Animal Models. *Inflamm. Bowel Dis.* **2016**, *22* (5), 1137–1150. https://doi.org/10.1097/MIB.0000000000000750.

(40) Baldelli, V.; Scaldaferri, F.; Putignani, L.; Del Chierico, F. The Role of Enterobacteriaceae in Gut Microbiota Dysbiosis in Inflammatory Bowel Diseases. *Microorganisms* **2021**, *9* (4), 1–15. https://doi.org/10.3390/microorganisms9040697.

(41) Morgan, X. C.; Tickle, T. L.; Sokol, H.; Gevers, D.; Devaney, K. L.; Ward, D. V.; Reyes, J. A.; Shah, S. A.; LeLeiko, N.; Snapper, S. B.; Bousvaros, A.; Korzenik, J.; Sands, B. E.; Xavier, R. J.; Huttenhower, C. Dysfunction of the Intestinal Microbiome in Inflammatory Bowel Disease and Treatment. *Genome Biol.* **2012**, *13* (9). https://doi.org/10.1186/gb-2012-13-9-r79.

(42) Tilg, H.; Moschen, A. R. Microbiota and Diabetes: An Evolving Relationship. *Gut* **2014**, *63* (9), 1513–1521. https://doi.org/10.1136/gutjnl-2014-306928.

(43) Ridaura, V. K.; Faith, J. J.; Rey, F. E.; Cheng, J.; Alexis, E.; Kau, A. L.; Griffin, N. W.; Lombard, V.; Henrissat, B.; Bain, J. R.; Muehlbauer, M. J.; Ilkayeva, O.; Semenkovich, C. F.; Funai, K.; Hayashi, D. K.; Lyle, B. J.; Martini, M. C.; Luke, K.; Clemente, J. C.; Treuren, W. Van; Walters, W. A. Cultured Gut Microbiota from Twins Discordant for Obesity Modulate Adiposity and Metabolic Phenotypes in Mice. *Science.* **2014**, *341* (6150), 1–22. https://doi.org/10.1126/science.1241214.Cultured.

(44) Siegel, R. L.; Miller, K. D.; Fuchs, H. E.; Jemal, A. Cancer Statistics, 2021. *CA. Cancer J. Clin.* **2021**, *71* (1), 7–33. https://doi.org/10.3322/caac.21654.

(45) Lichtenstein, P.; Holm, N. V.; Verkasalo, P. K.; Iliadou, A.; Kaprio, J.; Koskenvuo, M.; Pukkala, E.; Skytthe, A.; Hemminki, K. Environmental and Heritable Factors in the Causation of Cancer — Analyses of Cohorts of Twins from Sweden, Denmark, and Finland. *N. Engl. J. Med.* **2000**, *343* (2), 78–85.

(46) Jasperson, K. W.; Tuohy, T. M.; Neklason, D. W.; Burt, R. W. Hereditary and Familial Colon Cancer. *Gastroenterology* **2010**, *138* (6), 2044–2058. https://doi.org/10.1053/j.gastro.2010.01.054.

(47) Haggar, F. A.; Boushey, R. P. Colorectal Cancer Epidemiology: Incidence, Mortality, Survival, and Risk Factors. *Clin. Colon Rectal Surg.* **2009**, *22* (4), 191–197. https://doi.org/10.1055/s-0029-1242458.

(48) Song, M.; Chan, A. T. Environmental Factors, Gut Microbiota, and Colorectal Cancer Prevention. *Clin. Gastroenterol. Hepatol.* **2018**, *17* (2), 275–289. https://doi.org/10.1016/j.cgh.2018.07.012.

(49) Wang, H.; Wei, C. X.; Min, L.; Zhu, L. Y. Good or Bad: Gut Bacteria in Human Health and Diseases. *Biotechnol. Biotechnol. Equip.* **2018**, *32* (5), 1075–1080. https://doi.org/10.1080/13102818.2018.1481350.

(50) Górska, A.; Przystupski, D.; Niemczura, M. J.; Kulbacka, J. Probiotic Bacteria: A Promising Tool in Cancer Prevention and Therapy. *Curr. Microbiol.* **2019**, *76* (8), 939–949. https://doi.org/10.1007/s00284-019-01679-8.

(51) Lopez-Siles, M.; Duncan, S. H.; Garcia-Gil, L. J.; Martinez-Medina, M. Faecalibacterium Prausnitzii: From Microbiology to Diagnostics and Prognostics. *ISME J.* **2017**, *11* (4), 841–852. https://doi.org/10.1038/ismej.2016.176.

(52) Sokol, H.; Pigneur, B.; Watterlot, L.; Lakhdari, O.; Bermudez-Humaran, L. G.; Gratadoux, J.-J.; Blugeon, S.; Bridonneau, C.; Furet, J.-P.; Corthier, G.; Grangette, C.; Vasquez, N.; Pochart, P.; Trugnan, G.; Thomas, G.; Blottiere, H. M.; Dore, J.; Marteau, P.; Seksik, P.; Langella, P. Faecalibacterium Prausnitzii Is an Anti-Inflammatory Commensal Bacterium Identified by Gut Microbiota Analysis of Crohn Disease Patients. *PNAS* **2008**, *105* (43), 16731–16736. https://doi.org/10.1002/path.1711620408.

(53) Miquel, S.; Leclerc, M.; Martin, R.; Chain, F.; Lenoir, M.; Raguideau, S.; Hudault, S.; Bridonneau, C.; Northene, T.; Bowene, B.; Bermúdez-Humarán, L. G.; Sokol, H.; Thomas, M.; Langella, P. Identification of Metabolic Signatures Linked to Anti-Inflammatory Effects of Faecalibacterium Prausnitzii. *MBio* **2015**, *6* (2), 1–10. https://doi.org/10.1128/mBio.00300-15.

(54) Ferreira-Halder, C. V.; Faria, A. V. de S.; Andrade, S. S. Action and Function of Faecalibacterium Prausnitzii in Health and Disease. *Best Pract. Res. Clin. Gastroenterol.* **2017**, *31*, 643–648. https://doi.org/10.1016/j.bpg.2017.09.011.

(55) Martín, R.; Chain, F.; Miquel, S.; Lu, J.; Gratadoux, J. J.; Sokol, H.; Verdu, E. F.;

Bercik, P.; Bermúdez-Humarán, L. G.; Langella, P. The Commensal Bacterium Faecalibacterium Prausnitzii Is Protective in DNBS-Induced Chronic Moderate and Severe Colitis Models. *Inflamm. Bowel Dis.* **2014**, *20* (3), 417–430. https://doi.org/10.1097/01.MIB.0000440815.76627.64.

(56) Qiu, X.; Zhang, M.; Yang, X.; Hong, N.; Yu, C. Faecalibacterium Prausnitzii Upregulates Regulatory T Cells and Anti-Inflammatory Cytokines in Treating TNBS-Induced Colitis. *J. Crohn's Colitis* **2013**, *7* (11), e558–e568. https://doi.org/10.1016/j.crohns.2013.04.002.

(57) Quévrain, E.; Maubert, M. A.; Michon, C.; Chain, F.; Marquant, R.; Miquel, S.; Carlier, L.; Pigneur, B.; Kharrat, P.; Thomas, G.; Rainteau, D.; Aubry, C.; Breyner, N.; Lavielle, S.; Chassaing, G.; Chatel, J. M.; Trugnan, G.; Xavier, R.; Langella, P.; Sokol, H.; Seksik, P. Identification of an Anti-Inflammatory Protein from Faecalibacterium Prausnitzii, a Commensal Bacterium Deficient in Crohn's Disease. *Gut* **6AD**, *65* (3), 415–425. https://doi.org/10.1136/gutjnl-2014-307649.Identification.

(58) Martín, R.; Miquel, S.; Chain, F.; Natividad, J. M.; Jury, J.; Lu, J.; Sokol, H.; Theodorou, V.; Bercik, P.; Verdu, E. F.; Langella, P.; Bermúdez-Humarán, L. G. Faecalibacterium Prausnitzii Prevents Physiological Damages in a Chronic Low-Grade Inflammation Murine Model. *BMC Microbiol.* **2015**, *15* (1), 1–12. https://doi.org/10.1186/s12866-015-0400-1.

(59) Carlsson, A. H.; Yakymenko, O.; Olivier, I.; Håkansson, F.; Postma, E.; Keita, Å. V.; Söderholm, J. D. Faecalibacterium Prausnitzii Supernatant Improves Intestinal Barrier Function in Mice DSS Colitis. *Scand. J. Gastroenterol.* **2013**, *48* (10), 1136–1144. https://doi.org/10.3109/00365521.2013.828773.

(60) Forman, D.; Newell, D. G.; Fullerton, F.; Yarnell, J. W.; Stacey, A. R.; Wald, N.; Sitas, F. Association between Infection with Helicobacter Pylori and Risk of Gastric Cancer: Evidence from a Prospective Investigation. *BMJ* **1991**, *302* (6788), 1302–1305.

(61) Amieva, M.; Peek, R. M. Pathobiology of Helicobacter Pylori-Induced Gastric Cancer Manuel. *Gastroenterology* **2016**, *150* (1), 64–78. https://doi.org/10.1053/j.gastro.2015.09.004.Pathobiology.

(62) Han, Y. W. Fusobacterium Nucleatum: A Commensal-Turned Pathogen. *Curr. Opin. Microbiol.* **2015**, 141–147. https://doi.org/10.1016/j.mib.2014.11.013.Fusobacterium.

(63) Shang, F. M.; Liu, H. L. Fusobacterium Nucleatum and Colorectal Cancer: A Review. *World J. Gastrointest. Oncol.* **2018**, *10* (3), 71–81. https://doi.org/10.4251/wjgo.v10.i3.71.

(64) M., C.; R.L., W.; J.D., F.; L., D.; M., K.; J., S.; R., B.; P., W.; E., A.-V.; R.A., M.; R.A., H. Fusobacterium Nucleatum Infection Is Prevalent in Human Colorectal Carcinoma. *Genome Res.* **2012**, *22*, 299–306. https://doi.org/10.1101/gr.126516.111.Freely.

(65) McCoy, A. N.; Araújo-Pérez, F.; Azcárate-Peril, A.; Yeh, J. J.; Sandler, R. S.; Keku, T. O. Fusobacterium Is Associated with Colorectal Adenomas. *PLoS One* **2013**, *8* (1). https://doi.org/10.1371/journal.pone.0053653.

(66) Wong, S. H.; Kwong, T. N. Y.; Chow, T. C.; Luk, A. K. C.; Dai, R. Z. W.; Nakatsu, G.; Lam, T. Y. T.; Zhang, L.; Wu, J. C. Y.; Chan, F. K. L.; Ng, S. S. M.; Wong, M. C. S.; Ng, S. C.; Wu, W. K. K.; Yu, J.; Sung, J. J. Y. Quantitation of Faecal Fusobacterium Improves Faecal Immunochemical Test in Detecting Advanced Colorectal Neoplasia. *Gut* **2017**, *66*, 1441–1448. https://doi.org/10.1136/gutjnl-2016-312766.

(67) Yang, Y.; Weng, W.; Peng, J.; Hong, L.; Yang, L.; Toiyama, Y.; Gao, R.; Liu, M.; Yin, M.; Pan, C. Fusobacterium Nucleatum Increases Proliferation of Colorectal Cancer Cells and Tumor Development in Mice by Activating TLR4 Signaling to NFκB, Upregulating Expression of MicroRNA-21. **2014**, *15* (1), 34–48. https://doi.org/10.1053/j.gastro.2016.11.018.Fusobacterium.

(68) Housseau, F.; Sears, C. L. Enterotoxigenic Bacteroides Fragilis (ETBF)-Mediated Colitis in Min (Apc+/-) Mice: A Human Commensal-Based Murine Model of Colon Carcinogenesis. *Cell Cycle* **2010**, *9* (1), 3–5. https://doi.org/10.4161/cc.9.1.10352.

(69) Sears, C. L.; Garrett, W. S. Microbes, Microbiota and Colon Cancer. *Cell Host Microbe* **2014**, *15* (3), 317–328. https://doi.org/10.1016/j.chom.2014.02.007.Microbes.

(70) Bonnet, M.; Buc, E.; Sauvanet, P.; Darcha, C.; Dubois, D.; Pereira, B.;

Dechelotte, P.; Bonnet, R.; Pezet, D.; Darfeuille-Michaud, A. Colonization of the Human Gut by E. Coli and Colorectal Cancer Risk. *Clin. Cancer Res.* **2014**, *20* (4), 859–867. https://doi.org/10.1158/1078-0432.CCR-13-1343.

(71) Nougayrède, J. P.; Taieb, F.; De Rycke, J.; Oswald, E. Cyclomodulins: Bacterial Effectors That Modulate the Eukaryotic Cell Cycle. *Trends Microbiol.* **2005**, *13* (3), 103–110. https://doi.org/10.1016/j.tim.2005.01.002.

(72) Pérès, S. Y.; Marchès, O.; Daigle, F.; Nougayrède, J. P.; Hérault, F.; Tasca, C.; De Rycke, J.; Oswald, E. A New Cytolethal Distending Toxin (CDT) from Escherichia Coli Producing CNF2 Blocks HeLa Cell Division in G2/M Phase. *Mol. Microbiol.* **1997**, *24* (5), 1095–1107. https://doi.org/10.1046/j.1365-2958.1997.4181785.x.

(73) Taieb, F.; Nougayrède, J. P.; Oswald, E. Cycle Inhibiting Factors (Cifs): Cyclomodulins That Usurp the Ubiquitin-Dependent Degradation Pathway of Host Cells. *Toxins (Basel).* **2011**, *3* (4), 356–368. https://doi.org/10.3390/toxins3040356.

(74) Nougayrède, J.-P.; Homburg, S.; Taieb, F.; Boury, M.; Brzuszkiewicz, E.; Gottschalk, G.; Buchrieser, C.; Hacker, J.; Dobrindt, U.; Oswald, E. Escherichia Coli Induces DNA Double-Strand Breaks in Eukaryotic Cells. *Science.* **2006**, *313* (5788), 848–851. https://doi.org/10.1126/science.1127059.

(75) Putze, J.; Hennequin, C.; Nougayrède, J. P.; Zhang, W.; Homburg, S.; Karch, H.; Bringer, M. A.; Fayolle, C.; Carniel, E.; Rabsch, W.; Oelschlaeger, T. A.; Oswald, E.; Forestier, C.; Hacker, J.; Dobrindt, U. Genetic Structure and Distribution of the Colibactin Genomic Island among Members of the Family Enterobacteriaceae. *Infect. Immun.* **2009**, *77* (11), 4696–4703. https://doi.org/10.1128/IAI.00522-09.

(76) Homburg, S.; Oswald, E.; Hacker, J.; Dobrindt, U. Expression Analysis of the Colibactin Gene Cluster Coding for a Novel Polyketide in Escherichia Coli. *FEMS Microbiol. Lett.* **2007**, *275* (2), 255–262. https://doi.org/10.1111/j.1574-6968.2007.00889.x.

(77) Bull, L. B. The Histological Evidence of Liver Damage from Pyrrolizidine Alkaloids. *Aust. Vet. J.* **1955**, *31*, 33–40. https://doi.org/10.1111/j.1751-0813.1955.tb05488.x.

(78) Jago, M. V. The Development of the Hepatic Megalocytosis of Chronic Pyrrolizidine Alkaloid Poisoning. *Am. J. Pathol.* **1969**, *56* (3), 405–421.

(79) Buc, E.; Dubois, D.; Sauvanet, P.; Raisch, J.; Delmas, J.; Darfeuille-Michaud, A.; Pezet, D.; Bonnet, R. High Prevalence of Mucosa-Associated E. Coli Producing Cyclomodulin and Genotoxin in Colon Cancer. *PLoS One* **2013**, *8* (2). https://doi.org/10.1371/journal.pone.0056964.

(80) Cougnoux, A.; Dalmasso, G.; Martinez, R.; Buc, E.; Delmas, J.; Gibold, L.; Sauvanet, P.; Darcha, C.; Déchelotte, P.; Bonnet, M.; Pezet, D.; Wodrich, H.; Darfeuille-Michaud, A.; Bonnet, R. Bacterial Genotoxin Colibactin Promotes Colon Tumour Growth by Inducing a Senescence-Associated Secretory Phenotype. *Gut* **2014**, *63* (12), 1932–1942. https://doi.org/10.1136/gutjnl-2013-305257.

(81) Dalmasso, G.; Cougnoux, A.; Delmas, J.; Darfeuille-Michaud, A.; Bonnet, R. Bacterial Genotoxin Colibactin Promotes Colon Tumour Growth by Inducing a Senescence-Associated Secretory Phenotype. *Gut* **2014**, *5* (5), 675–680. https://doi.org/10.4161/19490976.2014.969989.

(82) Cuevas-Ramos, G.; Petit, C. R.; Marcq, I.; Boury, M.; Oswald, E.; Nougayrède, J.-P. Escherichia Coli Induces DNA Damage in Vivo and Triggers Genomic Instability in Mammalian Cells. *Proc. Natl. Acad. Sci. U. S. A.* **2010**, *107* (25), 11537–11542. https://doi.org/10.1073/pnas.1001261107.

(83) Arthur, J. C.; Perez-Chanona, E.; Mühlbauer, M.; Tomkovich, S.; Uronis, J. M.; Fan, T.-J.; Campbell, B. J.; Abujamel, T.; Dogan, B.; Rogers, A. B.; Rhodes, J. M.; Stintzi, A.; Simpson, K. W.; Hansen, J. J.; Keku, T. O.; Fodor, A. A.; Jobin, C. Intestinal Inflammation Targets Cancer-Inducing Activity of the Microbiota. *Science.* **2012**, *338* (6103), 120–123. https://doi.org/10.1126/science.1224820.

(84) Shay, J. W.; Roninson, I. B. Hallmarks of Senescence in Carcinogenesis and Cancer Therapy. *Oncogene* **2004**, *23* (16 REV. ISS. 2), 2919–2933. https://doi.org/10.1038/sj.onc.1207518.

(85) Khanna, K. K.; Jackson, S. P. DNA Double-Strand Breaks: Signaling, Repair and the Cancer Connection. *Nat. Genet.* **2001**, *27* (3), 247–254. https://doi.org/10.1038/85798.

(86) Arthur, J. C.; Perez-Chanona, E.; Mühlbauer, M.; Tomkovich, S.; Uronis, J. M.;

Fan, T.; Campbell, B. J.; Abujamel, T.; Dogan, B.; Rogers, A. B.; Rhodes, J. M.; Stintzi, A.; Simpson, K. W.; Hansen, J. J.; Keku, T. O.; Fodor, A. A.; Jobin, C. Intestinal Inflammation Targets Cancer-Inducing Activity of the Microbiota. *Science.* **2012**, *338* (6103), 120–123. https://doi.org/10.1126/science.1224820.Intestinal.

(87) Tomkovich, S.; Yang, Y.; Winglee, K.; Gauthier, J.; Mühlbauer, M.; Sun, X.; Mohamadzadeh, M.; Liu, X.; Martin, P.; Wang, G. P.; Oswald, E.; Fodor, A. A.; Jobin, C. Locoregional Effects of Microbiota in a Preclinical Model of Colon Carcinogenesis. *Cancer Res.* **2017**, *77* (10), 2620–2632. https://doi.org/10.1158/0008-5472.CAN-16-3472.

(88) Shimpoh, T.; Hirata, Y.; Ihara, S.; Suzuki, N.; Kinoshita, H.; Hayakawa, Y. Prevalence of Pks - Positive Escherichia Coli in Japanese Patients with or without Colorectal Cancer. *Gut Pathog.* **2017**, *9*. https://doi.org/10.1186/s13099-017-0185-x.

(89) Li, Z.; Li, J.; Cai, W.; Lai, J. Y. H.; Mckinnie, S. M. K.; Zhang, P.; Moore, B. S.; Zhang, W.; Qian, P. Macrocyclic Colibactin Induces DNA Double-Strand Breaks via Copper-Mediated Oxidative Cleavage. *Nat. Chem.* **2019**, *11* (10), 880–889. https://doi.org/10.1038/s41557-019-0317-7.

(90) Faïs, T.; Delmas, J.; Barnich, N.; Bonnet, R.; Dalmasso, G. Colibactin: More than a New Bacterial Toxin. *Toxins (Basel).* **2018**, *10* (4), 16–18. https://doi.org/10.3390/toxins10040151.

(91) Wernke, K. M.; Xue, M.; Tirla, A.; Kim, C. S.; Herzon, S. B.; Crawford, J. M. Structure and Bioactivity of Colibactin. *Bioorg. Med. Chem. Lett.* **2020**, *30* (15), 127280. https://doi.org/10.1016/j.bmcl.2020.127280.

(92) Vizcaino, M. I.; Engel, P.; Trautman, E.; Crawford, J. M. Comparative Metabolomics and Structural Characterizations Illuminate Colibactin Pathway-Dependent Small Molecules. *J. Am. Chem. Sociaty* **2014**, *136* (26), 9244–9247. https://doi.org/10.1021/ja503450q.

(93) Bian, X.; Fu, J.; Plaza, A.; Herrmann, J.; Pistorius, D.; Stewart, A. F.; Zhang, Y.; Müller, R. In Vivo Evidence for a Prodrug Activation Mechanism during Colibactin Maturation. *ChemBioChem* **2013**, *14* (10), 1194–1197.

https://doi.org/10.1002/cbic.201300208.

(94) Brotherton, C. A.; Balskus, E. P. A Prodrug Resistance Mechanism Is Involved in Colibactin. *J. Am. Chem. Sociaty* **2013**, *135*, 3359–3362. https://doi.org/10.1021/ja312154m.

(95) Bian, X.; Plaza, A.; Zhang, Y.; Müller, R. Two More Pieces of the Colibactin Genotoxin Puzzle from Escherichia Coli Show Incorporation of an Unusual 1-Aminocyclopropanecarboxylic Acid Moiety. *Chem. Sci.* **2015**, *6* (5), 3154–3160. https://doi.org/10.1039/C5SC00101C.

(96) Brotherton, C. A.; Wilson, M.; Byrd, G.; Balskus, E. P. Isolation of a Metabolite from the Pks Island Provides Insights into Colibactin Biosynthesis and Activity. *Org. Lett.* **2015**, *17* (6), 1545–1548. https://doi.org/10.1021/acs.orglett.5b00432.

(97) Healy, A. R.; Nikolayevskiy, H.; Patel, J. R.; Crawford, J. M.; Herzon, S. B. A Mechanistic Model for Colibactin-Induced Genotoxicity. *J. Am. Chem. Soc.* **2016**, *138* (48), 15563–15570. https://doi.org/10.1021/jacs.6b10354.

(98) Li, Z. R.; Li, Y.; Lai, J. Y. H.; Tang, J.; Wang, B.; Lu, L.; Zhu, G.; Wu, X.; Xu, Y.; Qian, P. Y. Critical Intermediates Reveal New Biosynthetic Events in the Enigmatic Colibactin Pathway. *ChemBioChem* **2015**, *16* (12), 1715–1719. https://doi.org/10.1002/cbic.201500239.

(99) Zha, L.; Wilson, M. R.; Brotherton, C. A.; Balskus, E. P. Characterization of Polyketide Synthase Machinery from the Pks Island Facilitates Isolation of a Candidate Precolibactin. *ACS Chem. Biol.* **2016**, *11* (5), 1287–1295. https://doi.org/10.1021/acschembio.6b00014.

(100) Vizcaino, M. I.; Crawford, J. M. The Colibactin Warhead Crosslinks DNA. *Nat. Chem.* **2015**, *7* (5), 411–417. https://doi.org/10.1038/nchem.2221.

(101) Xue, M.; Kim, C. S.; Healy, A. R.; Wernke, K. M.; Wang, Z.; Frischling, M. C.; Shine, E. E.; Wang, W.; Herzon, S. B.; Crawford, J. M. Structure Elucidation of Colibactin and Its DNA Cross-Links. *Science.* **2019**, *365* (6457). https://doi.org/.1037//0033-2909.I26.1.78.

(102) Dougherty, M. W.; Jobin, C. Shining a Light on Colibactin Biology. *Toxins (Basel).* **2021**, *13* (5), 1–15. https://doi.org/10.3390/toxins13050346.

(103) Cougnoux, A.; Gibold, L.; Robin, F.; Dubois, D.; Pradel, N.; Darfeuille-Michaud,

A.; Dalmasso, G.; Delmas, J.; Bonnet, R. Analysis of Structure-Function Relationships in the Colibactin-Maturating Enzyme ClbP. *J. Mol. Biol.* **2012**, *424* (3–4), 203–214. https://doi.org/10.1016/j.jmb.2012.09.017.

(104) Dubois, D.; Baron, O.; Cougnoux, A.; Delmas, J.; Pradel, N.; Boury, M.; Bouchon, B.; Bringer, M. A.; Nougayrède, J. P.; Oswald, E.; Bonnet, R. ClbP Is a Prototype of a Peptidase Subgroup Involved in Biosynthesis of Nonribosomal Peptides. *J. Biol. Chem.* **2011**, *286* (41), 35562–35570. https://doi.org/10.1074/jbc.M111.221960.

(105) Wilson, M. R.; Jiang, Y.; Villalta, P. W.; Stornetta, A.; Boudreau, P. D.; Carrá, A.; Brennan, C. A.; Chun, E.; Ngo, L.; Samson, L. D.; Engelward, B. P.; Garrett, W. S.; Balbo, S.; Balskus, E. P. The Human Gut Bacterial Genotoxin Colibactin Alkylates DNA. *Science.* **2019**, *363* (709). https://doi.org/10.1126/science.aar7785.

(106) Schwechheimer, C.; Kuehn, M. J.; Rodriguez, D. L. Outer-Membrane Vesicles from Gram-Negative Bacteria: Biogenesis and Functions. *Nat. Rev. Microbiol.* **2015**, *13* (10), 605–619. https://doi.org/10.1038/nrmicro3525.Outer-membrane.

(107) Guerrero-Mandujano, A.; Hernández-Cortez, C.; Ibarra, J. A.; Castro-Escarpulli, G. The Outer Membrane Vesicles: Secretion System Type Zero. *Traffic* **2017**, *18* (7), 425–432. https://doi.org/10.1111/tra.12488.

(108) Parker, H.; Keenan, J. I. Composition and Function of Helicobacter Pylori Outer Membrane Vesicles. *Microbes Infect.* **2012**, *14* (1), 9–16. https://doi.org/10.1016/j.micinf.2011.08.007.

(109) Manning, A. J.; Kuehn, M. J. Contribution of Bacterial Outer Membrane Vesicles to Innate Bacterial Defense. *BMC Microbiol* **2011**, *11* (1), 258. https://doi.org/10.1186/1471-2180-11-258.

(110) Ellis, T. N.; Kuehn, M. J. Virulence and Immunomodulatory Roles of Bacterial Outer Membrane Vesicles. *Microbiol. Mol. Biol. Rev.* **2010**, *74* (1), 81–94. https://doi.org/10.1128/mmbr.00031-09.

(111) Kulp, A.; Kuehn, M. J. Biological Functions and Biogenesis of Secreted Bacterial Outer Membrane Vesicles. *Annu Rev Microbiol.* **2010**, *64*, 163–184. https://doi.org/10.1146/annurev.micro.091208.073413.Biological.

(112) Kuehn, M. J.; Kesty, N. C. Bacterial Outer Membrane Vesicles and the Host-Pathogen Interaction. *Genes Dev.* **2005**, *19* (22), 2645–2655. https://doi.org/10.1101/gad.1299905.

(113) McBroom, A. J.; Kuehn, M. J. Release of Outer Membrane Vesicles by Gram-Negative Bacteria Is a Novel Envelope Stress Response. *Mol. Microbiol.* **2007**, *63* (2), 545–558. https://doi.org/10.1111/j.1365-2958.2006.05522.x.

(114) Tyrer, P. C.; Frizelle, F. A.; Keenan, J. I. Escherichia Coli-Derived Outer Membrane Vesicles Are Genotoxic to Human Enterocyte-like Cells. *Infect. Agent. Cancer* **2014**, *9* (1), 2. https://doi.org/10.1186/1750-9378-9-2.

(115) Park, K.; Choi, K.; Kim, Y.; Hong, B. S.; Kim, O. Y.; Kim, J. H.; Yoon, M.; Koh, G.; Kim, Y.; Gho, Y. S. Outer Membrane Vesicles Derived from Escherichia Coli Induce Systemic Inflammatory Response Syndrome. **2010**, *5* (6), 1–6. https://doi.org/10.1371/journal.pone.0011334.

Chapter 2: Efforts to Isolate Colibactin and Elucidate its Structure.

Abstract

Colibactin is a secondary metabolite made by bacterial strains that harbor the *pks* genomic island. Its chemical structure has eluded chemical biologists since the very discovery of the *pks* gene cluster in 2006. The isolation of colibactin from bacterial cultures, as well as its characterization, has proven to be extremely challenging and difficult under standard conditions of chemical extraction and analysis. Its difficulty is thought to be because it is produced in low quantities and it is not secreted into the media, as its activity is thought to proceed by a contact-dependent mechanism. Molecular strategies to isolate intermediates of colibactin have been implemented to determinate its biosynthesis route. In this chapter, we report attempts from our laboratory to detect colibactin intermediates in the naturally producing bacteria *E. coli* IHE3034 with the final goal of contributing to the elucidation of colibactin structure. We also review the efforts from the last fifteen years by other groups, aimed at elucidating the colibactin structure.

2.1 Introduction

Colibactin is the name given to the natural product made by some strains of *Escherichia coli* and other gram-negative bacteria that harbor the *pks* genomic island[1,2]. Contact with *pks*+ strains will cause megalocytosis, which is a cellular phenotype marked by cell arrest and DNA damage[2]. Colibactin has been associated with increased risk of colorectal cancer, especially in individuals with a concurrent diagnosis of inflammatory bowel disease (IBD)[3,4].

The biosynthesis of colibactin is carried out by a mixed PKS/NRPS enzyme system encoded in the *pks island* which builds the compound through repeated Claisen-like condensation reactions of acyl and aminoacyl units[5]. Although the chemical structure a great number of precursors and intermediates have been elucidated, the structure of the final colibactin product remains unsolved[6].

Colibactin is initially synthesized as an inactive precursor, called pre-colibactin, inside the bacterial cell [7–9]. Pre-colibactin is subsequently translocated to the periplasmic space through a transporter (ClbM)[9], activated by a peptidase (ClbP) [7,8,10,11], and finally exported out of the bacterial cell (Figure 2.1). The mechanism by which active colibactin is exported to the target cell is yet to be discovered.

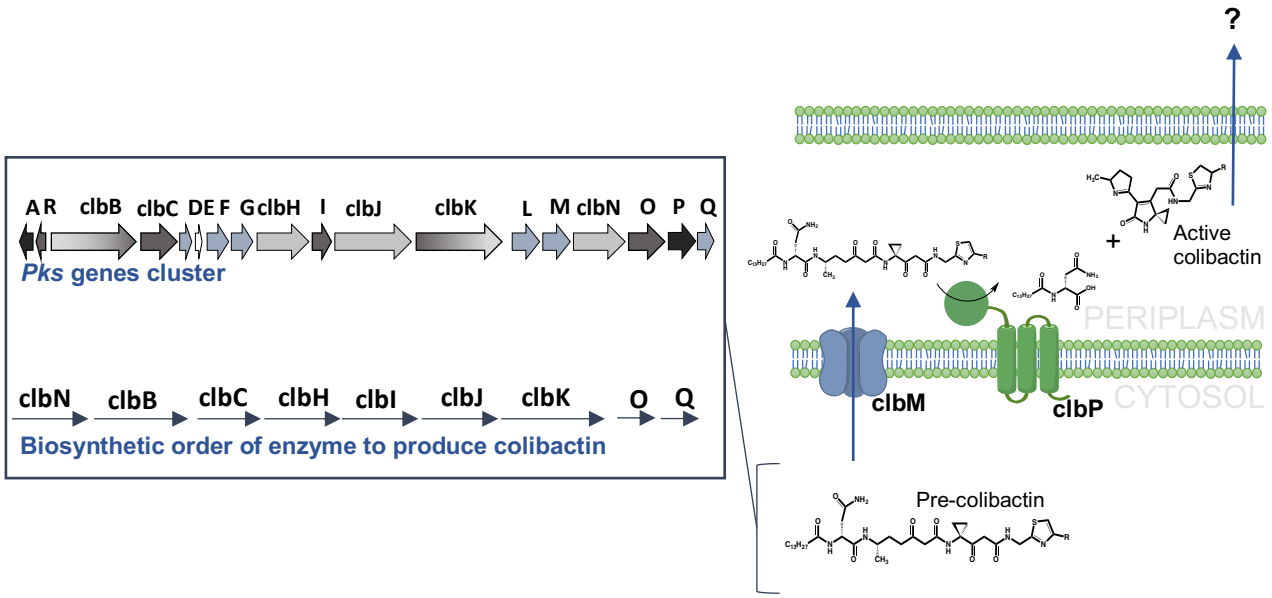

Figure 2.1 Schematic representation of the production and the pro-drug mechanism activation for colibactin. PKS/NRPS enzymes synthesize pre-colibactin inside the bacterial cell. The pre-colibactin is subsequently translocated to the periplasmic space by transporter (ClbM), activated by a peptidase (ClbP), and finally exported out of the bacterial cell toward the target cell by an unknown mechanism. (Nougayrède *et al*., 2006; Cougnoux *et al*., 2012; Bian *et al*., 2013 and 2015; Brotherton *et al*., 2013; Mousa *et al*., 2016; Vizcaino *et al*., 2015; Wernke *et al*., 2020).

The lack of an efficient method for the isolation of the active version of colibactin directly from its producer bacterial culture, has prompted researchers to devise other molecular strategies to isolate and characterize intermediates of this genotoxin. The first strategy exploited the pro-drug resistance mechanism of colibactin synthesis described by Balskus and co-workers[8]. This mechanism involves the peptidase clbP whose function is to process the pre-colibactin into its active version, colibactin[7,10,11]. ClbP is an extra-cytoplasmic and trans-membrane enzyme localized specifically in the bacterial inner membrane[7] (Figure 2.1). This peptidase hydrolyzes an amide bond in the pre-colibactin intermediate resulting in the *N*-myristoyl asparagine by-product and presumably, in active colibactin toxin.[8,10] The production of adequate amounts of pre-colibactin, and other intermediates for chemical elucidation has required the deletion of genes along the biosynthesis and processing route, one of them is the clbP gene[12,13]. Its deletion had been shown not only to promote the accumulation of numerous colibactin biosynthesis intermediates (which will be discussed later on this chapter) in the periplasmic space, but also its absence abolishes the megalocytic phenotype in the infected mammalian cell[12,13]. Thus, clbP is an important target for the study of colibactin structure and activity.

2.2 Colibactin intermediate isolation attempt using the natural colibactin-producing *E. coli* strain IHE3034.

In this work, we report the deletion of *clbP* gene from clinical strain IHE3034, which is a known *pks*+ isolate from a case of neonatal meningitis.[14] We expected that the lack of *clbP* would cause an interruption in the normal production of colibactin, thus causing the

accumulation of incomplete intermediates inside the cell, which would enable their eventual characterization and structure determination (Figure 2.2). We analyzed organic extracts of the IHE3034 Δ*clbP* and found a characteristic signal by mass spectrometry that was consistent with what we know about colibactin. This signal, however, was not always detected and its presence depended on a number of factors that were not identified. We place this finding in the context of other efforts that were taking place simultaneously in the US, Hong Kong and Germany for the elucidation of colibactin.

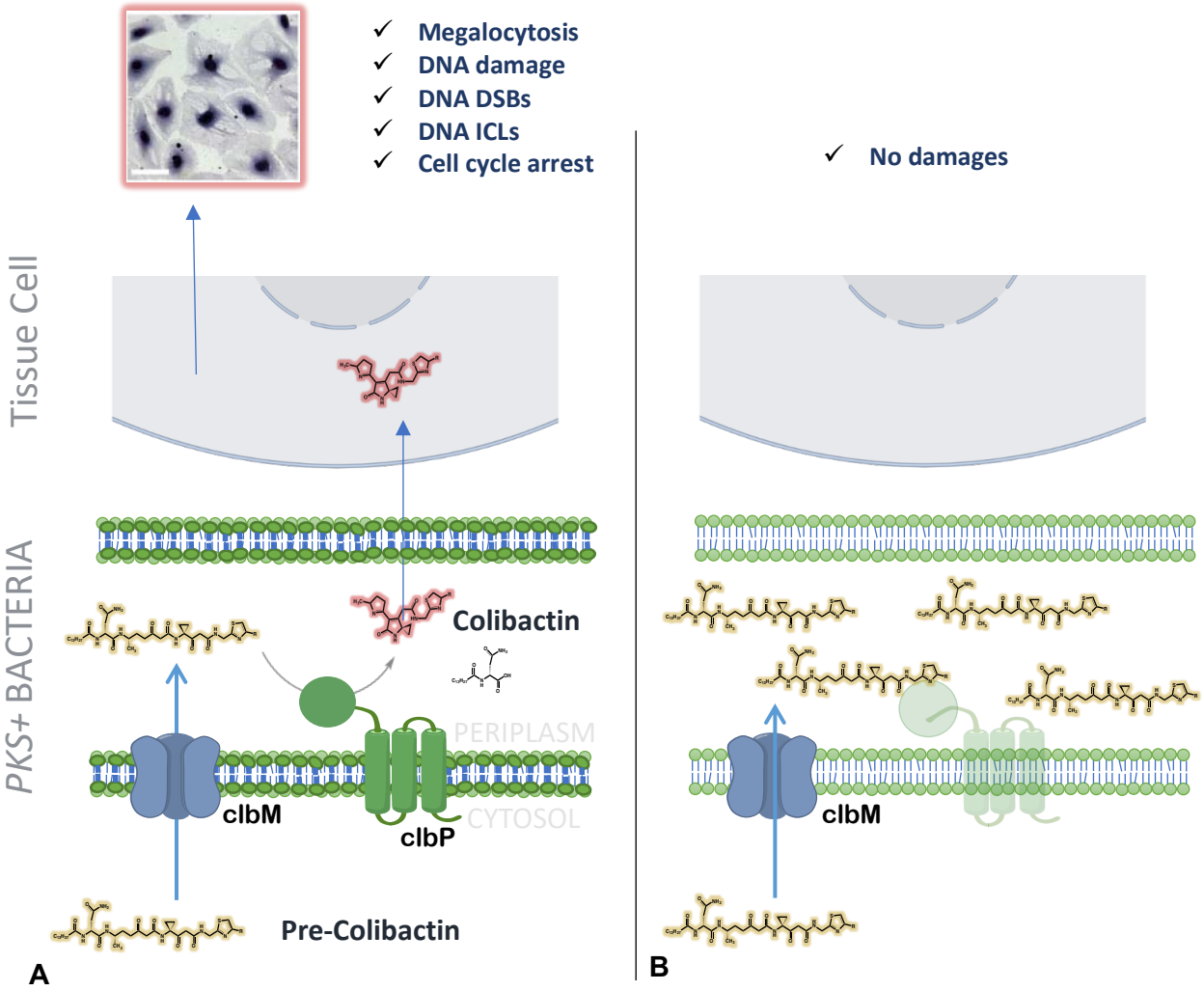

Figure 2.2: ClbP peptidase removal promote colibactin intermediate accumulation. Schematic representation of: A) the colibactin activation by the pro-drug mechanism of the peptidase *clbP* and B) the expected accumulation to occur when the *clbP* gene is knockout on *pks*$^{+}$ *E. coli* strains.

2.2.1 Materials and Methods.

2.2.1.1 Bacterial strains. *E. coli* IHE3034 *pks*$^{+}$ was kindly donated by Dr. Eric Oswald from the University of Toulouse, France. The *E. coli* DH10B *pks*$^{-}$ (non-genotoxic) was used in all the experiments as a control strain. All strains, including the Δ*clbP* mutant detailed, later on, were "re-animated" from cryogenic storage in lysogenic broth (LB) medium (Sigma-Aldrich) agar for 24 hrs at 37 °C. Colonies were then selected and grown in liquid LB for 16-18 hrs (unless specified otherwise) at 37 °C. Followed by the corresponding experiments.

2.2.1.2 Deletion of the *ClbP* gene. Deletion of the *clbP* gene was performed using Red/ET recombination following the Quick & Easy *E. coli* Gene Deletion Kit from Gene Bridges (Cat. No. K006). The procedure is described in details by Dr. Gomez-Moreno in his thesis dissertation (UPR-Medical Sciences Campus 2018). Briefly, primers with a 5'-overhang of the first 50 bp of the *clbP* gene (homology arms) were used to amplify a lineal cassette encoding the kanamycin resistance gene (supplementary material section 2.6, Table S2.1). Overnight cultures of *E. coli* were prepared for electroporation. *E. coli* cells were centrifuged for 30 seconds at 11,000 rpm, the supernatant was removed, and the pellet was resuspended in sterile ultra-pure water (EMD Milllipore). This step was repeated two times. Then, cells were incubated with the pRed/ET plasmid encoding the recombinase for 1 minute. This plasmid contains the enzymes to perform the recombination between the *clbP*-homology arms of the lineal cassette and the *clbP* gene. This was followed by electroporation with 5 ms pulses of 1,350 V using the MicroPulserTM (BioRad). Cells were then resuspended in LB liquid (Sigma-Aldrich)

medium for 70 minutes, at 30 °C, and shaken at 100 rpm. The transformed *E. coli* cells were then plated in LB agar (Sigma-Aldrich) with ampicillin (Sigma-Aldrich) overnight. Lastly, pRed/ET+ *E. coli* colonies were selected and incubated in LB with ampicillin and 10 % *L*-Arabinose for 60 min. at 37 °C to induce the expression of proteins necessary for recombination. The recovered cells were prepared for electroporation, incubated with the *clbP* homology arm-lineal cassette, and electroporated as described above. Cells were then incubated in LB for 3 hrs at 37 °C and plated in LB agar with Kanamycin (Sigma-Aldrich) for 24 hrs at 37 °C. Colonies were selected and transfer to liquid LB, with 50 µg/mL of Kanamycin, for 24 hours at 37 °C and shaking at 250 rpm. The overnight culture was stored in glycerol at -80 °C.

2.2.1.3 Confirmation of *ClbP* deletion by PCR. To validate that the *clbP* gene was successfully removed from the *E. coli* IHE3034 *pks*$^{+}$ strain, PCR was employed using genomic DNA from the Δ*clbP* strain. For DNA extraction, 1.5 mL o overnight culture of each strain was centrifugated at 13,000 rpms for 15 minutes. Resultant bacterial pellets were resuspended with 500 uL of ddH_2O and cell lysis was induced by heating at 95-100 ^{o}C for 10 min. Then, cellular debris was removed by centrifugation and supernatant was uses as a template for PCR amplification. Specific primers that were used are summarized section 2.6 (supplementary material); Table S2.2. Briefly, using Phusion® High DNA polymerase (NEB), an initial denaturation step of 1 minute at 98 °C was performed followed by 30 cycles of 10 seconds at 98 °C, 30 seconds at the corresponding annealing temperature (section 2.6, Table S2.2), and 2 min. at 72 °C. All reactions were finalized with a final extension step of 10 min. at 72 ^{o}C. *E. coli* DH10B

pks$^-$ was used as a negative control, *E. coli* IHE3034 *pks*$^+$ as a positive control, and water as a PCR blank. All PCR products were visualized by running a 1 % agarose gel electrophoresis stained with GelRed™(Biotium).

2.2.1.4 Growth curves for IHE3034 and IHE3034 Δ*clbP*. Overnight culture of *E. coli* IHE3034 *pks*$^+$, *E. coli* IHE3034 Δ*clbP*, and *E. coli* DH10B *pks*$^-$ were seeded in a 96-well plate in LB liquid medium (Sigma-Aldrich). The optical density (OD) was measured using the Synergy H1 hybrid reader (BioTek) at 600 nm for 24 hrs at 37 °C under constant movement.

Values were reported as means of biological replicates and statistical analysis was performed by two-way analyses of variance (ANOVA) with "Tukey's Multiple Comparison" test for multiple comparisons. All statistical analyses were conducted using Prism 6 software (GraphPad, La Jolla, CA, United States).

2.2.1.5 HeLa cells culture. HeLa cells (ATCC CCL-2) were cultured in Dulbecco's Modified Eagle's Medium (DMEM; SIGMA Cat No. D5796) supplemented with 10 % fetal bovine serum (FBS) (SIGMA Cat. No. F2442) and Penicillin/Streptomycin (100 U:100 µg/mL) (CORNING Cat. No. 30-002CI). The cells were grown in a 24 wells culture plate with a total volume of 1 mL and with a sterile round coverslip in each well. They were then incubated at 37 °C, in 5 % CO_2, until 50% confluence was achieved to further infection.

Values were reported as means of biological replicates and statistical was performed by one-way analyses of variance (ANOVA) with “Tukey’s Multiple Comparison” test for multiple comparisons. All statistical analyses were conducted using Prism 6 software (GraphPad, La Jolla, CA, United States).

2.2.1.6 Confirmation of *ClbP* deletion by HeLa infection. Approximately, 7.5 x 10^5 bacterial cells were inoculated in 1 mL of DMEM with 10 % FBS and without antibiotic, this was then added to the HeLa cells and co-incubated for 4 hrs. Following infection time, cell media was removed carefully and fresh media containing gentamycin was added. Then, after 72 hrs incubated at 37 °C and 5 % CO_2, the HeLa cells morphology was analyzed under a light microscope (Nikon ECLIPSE LV100N POL) using Giemsa staining, following the manufacturer's instructions (SIGMA Cat. No. GS500). Briefly, cells attached to the round coverslip were fixed using methanol, followed by three consecutive washes with ddH_2O. Then, cells were incubated at room temperature with 1 mL of 1:20 solution of Giemsa stain:water for 30 min. Coverslips were transferred upside down in an optical microscope slide with a minimal amount of Xylene-based mounting media (Cat. # LC-A).

2.2.1.7 Extraction of colibactin intermediates. After culturing the *E. coli* strains overnight, cells were harvested by centrifugation at 5,000 rpm and 4 °C. Then, cell pellets were lysed by sonication. Protease inhibitor and DNases were added for compounds preservation. Lysate solutions were centrifuged for 45 min. at 4 °C and 12,000 rpm for lysis pellet formation. The resultant lysis supernatant was collected for

further extraction with ethyl acetate with two consecutive extractions of 20 mL. The organic phase was dried with magnesium sulfate, filtered and evaporated with nitrogen (N_2 (g)) for solvent elimination.

2.2.1.8 MALDI Mass Spectrometry characterization of extracts[15]**.** The dried extracts were re-suspended in 5 µL of acetonitrile and mixed in a 1:1 ratio with a solution of α-cyano-4-hydroxy-cinnamic acid methyl ester (10 µg/mL) in 0.01 % TFA (trifluoro acetic acid). Spectra was recorded on a MALDI-TOF-TOF mass spectrometer in the linear and positive ion mode.

2.2.1.9 Bacterial organic extract assay on HeLa cells. HeLa cells were maintained by serial passages in DMEM supplemented with 10 % FBS, non-essential amino acids, 1.5 g/L sodium bicarbonate, and 50 µg/mL of Penicillin/Streptomycin. Cells seed of 10 x 10^3 cells /mL was incubated in a 24 wells plate with a sterile glass coverslip (12 mm, round). Extracts from *E. coli* IHE3034, IHE3034-Δ*clbP* mutant, DH10B negative control, and process blank were dissolved in a minimal known amount of DMSO up to a final concentration of no more than 0.01 %. Extracts were applied to HeLa cell cultures when they reach 50 % of confluency. Cells without extracts addition and with 0.01 % DMSO were used as experimental negative controls. Cells were co-incubated with extracts for 4 hrs, washed with PBS buffer and re-incubated with DMEM media up to 72 hrs at 37 °C and 5 % CO_2.

2.2.1.10 LPS extraction. Lipopolysaccharide (LPS) was extracted from *E. coli* strains using a protocol adapted from the University of California San Diego Glycobiology Research and Training Center (Section 2.6, Supplemental procedure S1: LPS Extraction). Briefly, harvested bacterial cells (2-3 g) were resuspended in 20 mL of autoclaved and filtered ddH_2O. Resuspended cells were then heated at 68 °C under constant agitation for 10 min, followed by the slow addition of 20 mL of 90 % phenol solution. The 1:1 (bacteria : phenol) solution was incubated for 30 min. under the same conditions. After the incubation period, the milky-white resulted solution was transferred into ice and centrifugated for 45 min. at 3500 rpm for phase separation. The LPSs containing the upper layer were collected and dialyzed by 1 kDa dialysis tubing. The resulted LPSs extracts were lyophilized and stored at – 20 °C until further analysis.

2.2.1.11 Membrane analysis by trans-esterification and GC-MS. Acidic methanolysis was used to esterify fatty acids or other membrane-anchored compounds associated to pks island from extracted LPS, followed by liquid-liquid extraction with ethyl acetate for further analysis by gas chromatography mass spectrometry (GC-MS). Briefly, for LPS analysis, ~50 mg of lyophilized LPS were incubated under reflux with 4 mL of methanol and 2 drops of HCl for 2 hrs at 50 °C. Liquid-liquid extraction was then performed with two steps of 10 mL of ethyl acetate. The enriched organic phase was dried with magnesium sulfate and the solvent was eliminated by evaporation with nitrogen (N_2 (gas)). Once dry, all samples were stored at -20 °C under a nitrogen atmosphere for preservation until further analysis. For analysis by GC-MS (Agilent; DB-5 COLUMN), first dried lipids were resuspended in 1 mL of ethyl acetate. LPS samples for GC-MS

were prepared by mixing 85.5 µL of ethyl acetate a, 84.5 µL of methyl heneicosanoate (0.322 m*M*) internal standard and, 30 µL of the resuspended extract for a final volume of 200 µL.

The relative composition of fatty acids was calculated as follows: First, the millimoles of each fatty acid was determined using the formula (1) and (2) where (A_{FA}/A_{IS}) is the ratio between the peak areas for each fatty acid and the peak area for the internal standard obtained from the gas chromatogram, C_{IS} is the known concentration of the internal standard (in m*M*) and $\frac{Vol_{total\ dilution}}{Vol_{FA\ aliquote}}$ (sample dilution for GC analysis) is the dilution factor used to resuspend the concentrated fatty acids (in µL). From here the millimoles of each fatty acid per gram of LPS extracted were calculated and graphed using equation (3).

$$C_{FA} = \left(\frac{A_{FA}}{A_{IS}}\right) C_{IS} \quad (1)$$

$$mmol_{FA} = \frac{C_{FA}\left(\frac{Vol_{total\ dilution}}{Vol_{FA\ aliquote}}\right)}{1000} \quad (2)$$

$$\frac{mmol_{FA}}{g_{extrated\ LPS}} \quad (3)$$

Values were reported as one time event and statistical was performed by two-way analyses of variance (ANOVA) with “Tukey’s Multiple Comparison” test for multiple comparisons. All statistical analyses were conducted using Prism 6 software (GraphPad, La Jolla, CA, United States).

2.2.1.12 Quantification of proinflammatory cytokine release by LPS. The cytometric bead array (CBA) mouse inflammation kit (BD Biosciences; San Diego, CA) was used to measure the concentrations of tumor necrosis factor (TNF-α), monocyte chemoattractant protein-1 (MCP-1), interleukin-10 (IL-10), IL-6, and IL-12 from mouse bone marrow-derived neutrophils according to the manufacturer's instructions using flow cytometer and the BD CBA software (BD Biosciences). These experiments were performed in collaboration with Dr. Anthony V. Washington and Dr. Jessica Morales.

Values were reported as means of technical replicates and statistical was performed by two-way analyses of variance (ANOVA) with “Tukey’s Multiple Comparison” test for multiple comparisons. All statistical analyses were conducted using Prism 6 software (GraphPad, La Jolla, CA, United States).

2.2.2 Results

2.2.2.1 *E. coli* IHE3034 clbP peptidase deletion confirmation by PCR.

To cause the accumulation of colibactin intermediates, we deleted the *clbP* gene in the pathogenic strain IHE3034 by homologous recombination and confirmed by polymerase chain reaction (PCR). First, we used two genes to confirm the presence or absence of the *pks genes* in the strains used in this study, *clbN* and *clbQ*. *ClbN* gene codes for an NRP synthase involved in the initial step of colibactin biosynthesis (colibactin biosynthetic route will be discussed in details in section 2.3) . *ClbQ* gene codes for the thioesterase (TE) presumably involved in the final steps of colibactin biosynthesis. Qualitative analysis of our results confirms the presence of *clbN* and *clbQ* in *E. coli*

IHE3034 and its isogenic mutant strain IHE3034 (Δ*clbP*) by the bands observed at around 700 bp (section 2.6; Table S2.2 for expected amplicon size of each gene; clbN 733bp; clbQ 723 bp). The laboratory strain used as *pks* negative control DH10B shows no presence of neither *clbN* nor *clbQ* as expected (Figure 2.3 a and c). Figure 2.3 b shows a band around 1500 bp (expected amplicon size for clbP 1515 bp) for *E. coli* IHE3034 WT but not for IHE3034 Δ*clbP*-mutant nor DH10B, confirming the absence of the *clbP* gene in the produced IHE3034 mutant.

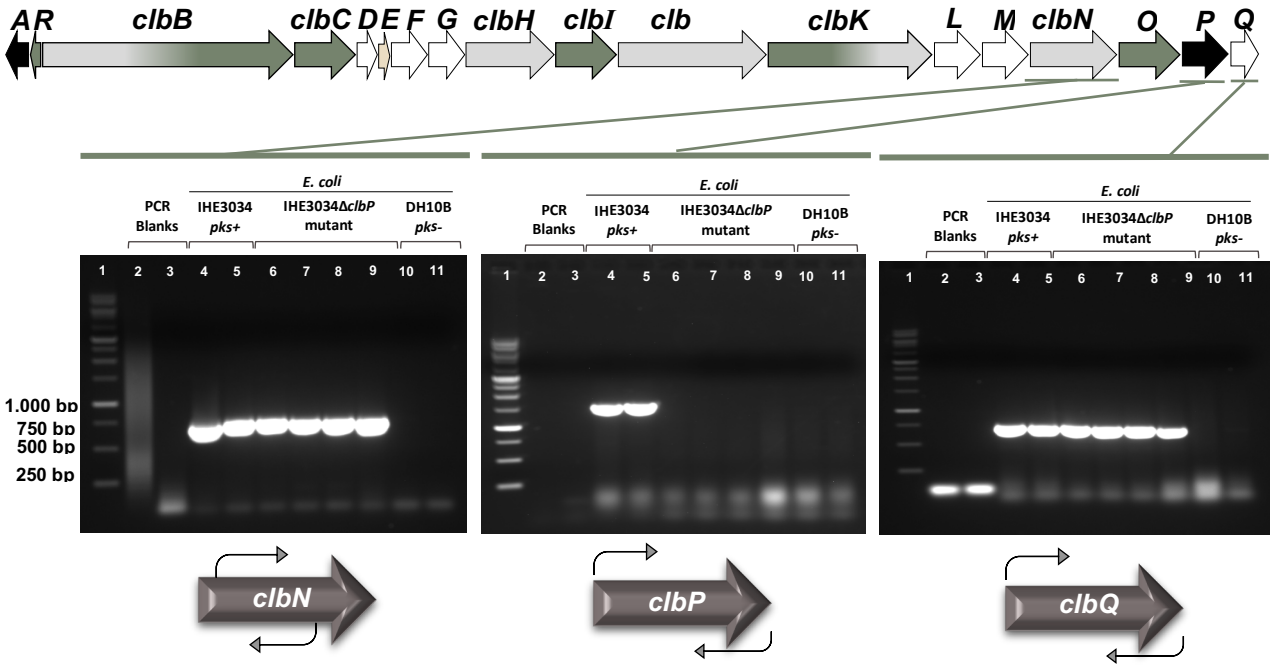

Figure 2.3 *ClbP* gene deletion on *pks*$^{+}$ *E. coli* strain IHE3034. Agarose gel electrophoresis of the PCR results of the amplification of (a) *clbN* gene, (b) *clbP* gene, and (c) *clbQ* gene for each *E. coli* samples. Lanes correspond to: (1) 1kb DNA standards, (2 and 3) PCR Blank (4 and 5) *E. coli* IHE3034 *pks*$^{+}$ (6 to 9) *E. coli* IHE3034 Δ*clbP* (10 and 11) *E. coli* DH10B *pks*$^{-}$. Electrophoresis were carried out in TAE running buffer for 1 hr at 100 V using a 1 % agarose gel.

2.2.2.2 Effect of *clbP* deletion on bacterial growth.

Genomic modification in the bacterial genome can trigger unintended effects which could affect the viability of the modified bacteria. To rule out any generalized effect on bacterial growth caused by the lack of the *clbP* gene, we compared the growth curves of IHE3034 and IHE3034 (Δ*clbP*) mutant. No significant differences were observed between wild-type and mutant strains with a *p*-value of 0.0851 (Figure 2.4). The deletion of *clbP* did not impair, nor did it enhance, the growth rate of IHE3034 *E. coli*.

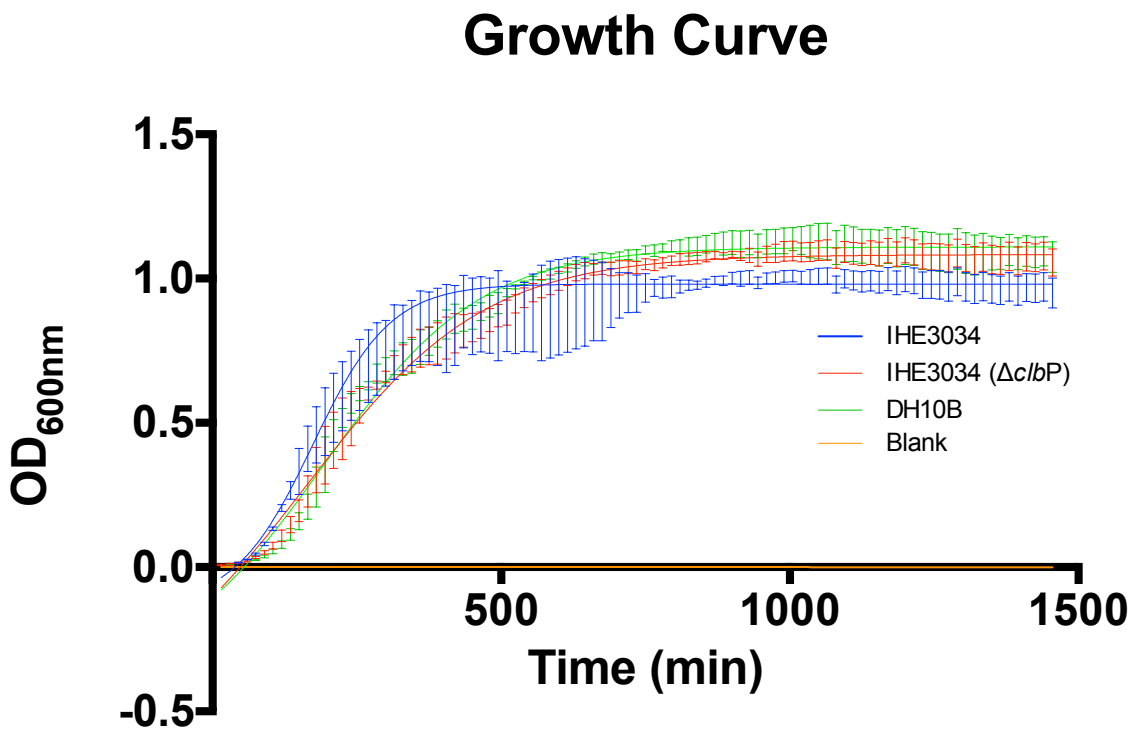

Figure 2.4. *ClbP* gene deletion on *pks+ E. coli* strain IHE3034 does not affect cell growth. *E. coli* IHE3034 *pks+, E. coli* IHE3034 Δ*clbP*, *E. coli* DH10B *pks-,* and control blank samples were incubated at 37 ºC under constant shaking for 24 hrs. Growth control "Blank" is lysogenic bacterial broth (LB) with any bacteria inoculation. Two-way ANOVA analysis show no significant difference between growth or viability caused by the *clbP* deletion (p-value = 0.0851).

2.2.2.3 Effect of *clbP* deletion on HeLa cells.

Megalocytosis is a visible phenotype associated with colibactin toxicity on mammalian cells[2]. An enlargement of the cell body and the nucleus are the qualitative characteristics of megalocytosis[2,16,17]. To evaluate whether the deletion of *clbP* gene in the IHE3034 strain causes the expected decrease in megalocytosis, HeLa cells were infected with either wild type IHE3034 (colibactin producer) or Δ*clbP* IHE3034 (mutant) and compared with negative controls. Infected cells were stained with Giemsa stain to visually detect cell morphology and the nucleus area was used to indirectly measure the degree of megalocytosis on infected cells. *E. coli* IHE3034 *pks*+ (wild-type) showed the expected megalocytosis phenotype when compare with *E. coli* laboratory strain DH10B or cells without any bacterial addition. Statistical analysis shows significant differences in the nuclear size between wild-type IHE3034 and either the DH10B strain or cells without treatment with a *p*-value in both cases of < 0.0001. This confirms the capacity of IHE3034 *E. coli* to induce megalocytosis on mammalian cells. Both, uninfected cells and cells infected with the *pks* negative control *E. coli* DH10B strain show no megalocytosis (Figure 2.5 A; images of triplicates are in section 2.6, Figures S2.2 a, b, c, and d).

Surprisingly the *E. coli* IHE3034 ∆*clbP* also induced megalocytosis, although its colibactin production is impaired. Qualitative analysis of Giemsa-stained infected cells shows a slight reduction in megalocytosis on cells infected with the IHE3034 Δ*clbP* (mutant). On the other hand, when the nuclear areas of infected cells were quantitatively measured, no significant difference was observed ($p > 0.05$; Figure 2.5 B).

These results suggest that the lack of the *clbP* gene alone is not sufficient to eradicate magalocytosis in the pathogenic *E. coli* IHE3034.

Another notable observation was that cells infected with either pathogenic or non-pathogenic bacterial strain, had a decrease in cell viability (qualitatively) when compared with cells without any bacterial infection, thus suggesting a an effect on cell viability by the presence of either infectious or non-infectious *E. coli* strains, which is independent of the presence of *pks* genes.

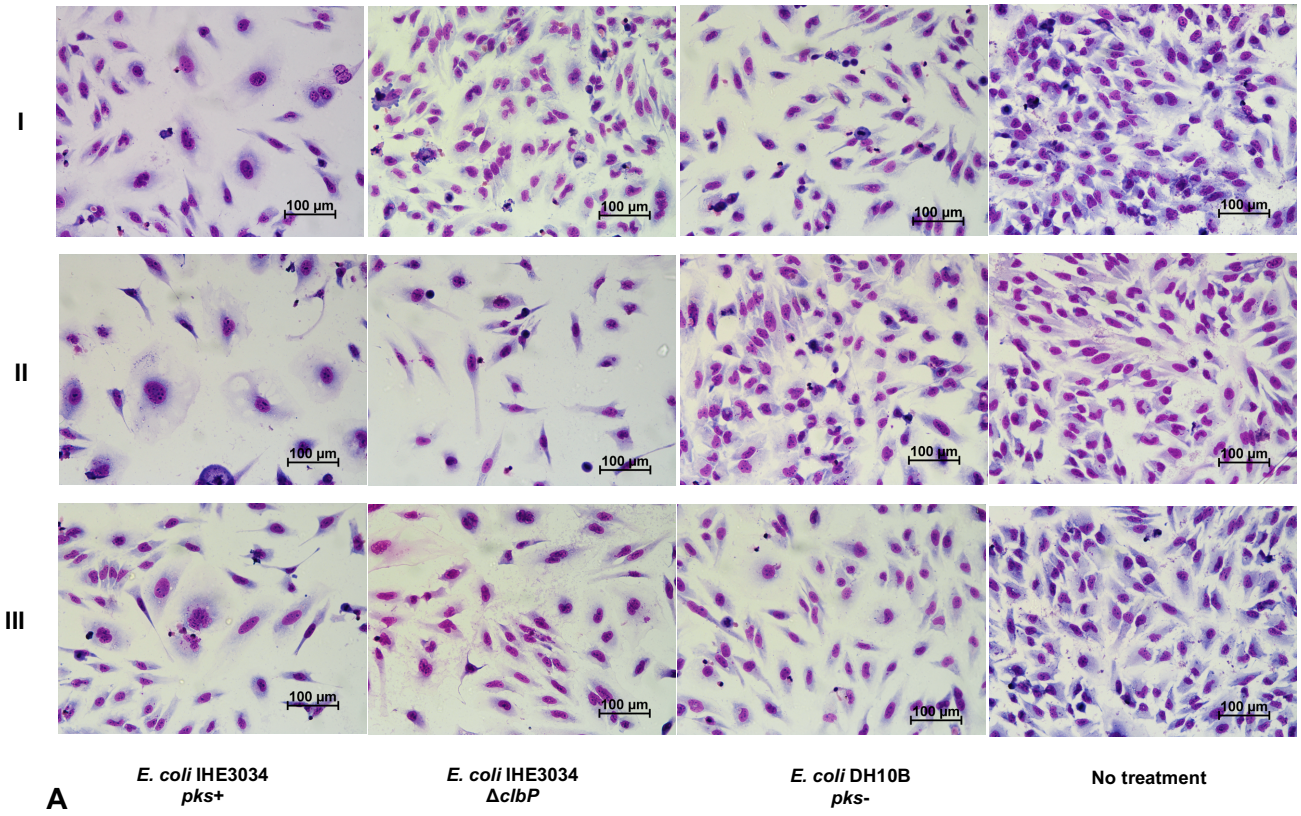

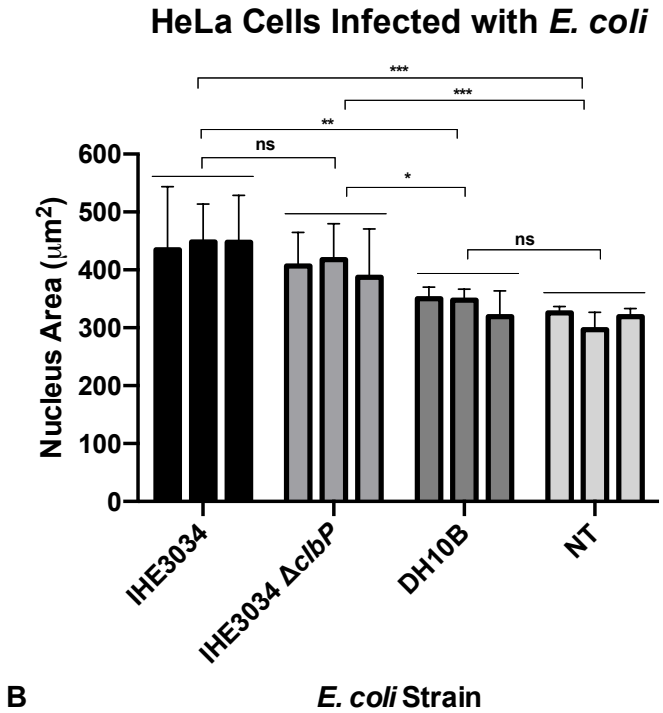

Figure 2.5. *ClbP* gene deletion on *pks*$^{+}$ *E. coli* strain IHE3034 does not cause a measurable decrease in megalocytosis on HeLa cells. A) I, II, and III are representative images of each triplicate. All images were taken at 40 X of magnification. HeLa cells were analyzed after 72 hrs post a bacterial infection period of 4 hrs. **B**) One-way ANOVA analysis show no significant difference between cells infected neither wild type nor *clbP* deficient IHE3034 *E. coli* strain. *P*-values: ns $P > 0.05$; * $P \leq 0.05$; ** $P \leq 0.01$; *** $P \leq 0.001$ and **** $P \leq 0.0001$.

2.2.2.4 *ClbP* deletion in the colibactin-producer IHE3034 *E. coli* strain promotes the accumulations of a 994 m/z compound.

Organic extracts of cultured bacteria were prepared and analyzed to assess whether *clbP* deletion in the IHE3034 strain causes the accumulation of any colibactin intermediate. MALDI-ToF-ToF spectra of these extracts were obtained using α-Cyano-4-hydroxycinnamic acid (α-CHCA) as the matrix, and they revealed a peak around 994 m/z (C994) in extracts where the *clbP* gene was deleted, thus suggesting the accumulation of a colibactin intermediate (Figure 2.6). To our knowledge, this was the first report of the detection of a biosynthetic intermediate compound of this molecular weight in any colibactin-producing strain. Comparison of the MS-MS fragmentation peaks of C994 found no similarities with the already published pre-colibactin intermediate structures[13,18,19]. Analysis of MS-MS fragmentation peaks of C994 found reveals a methyl loss (peak 979.5618 m/z; Figure 2.6 E). Furthermore, it can be seen that the base peak (peak 854.5244 m/z; Figure 2.6 E) agrees with the fragmentation of the loss of the second peak corresponding to 140.1920 m/z molecular weight. We attempted to scale up the production of this intermediate to yield enough material for structural elucidation. However, these attempts did not yield the desired signal by MALDI-ToF-ToF, suggesting that colibactin production is due to specific conditions that we were unable to identify.

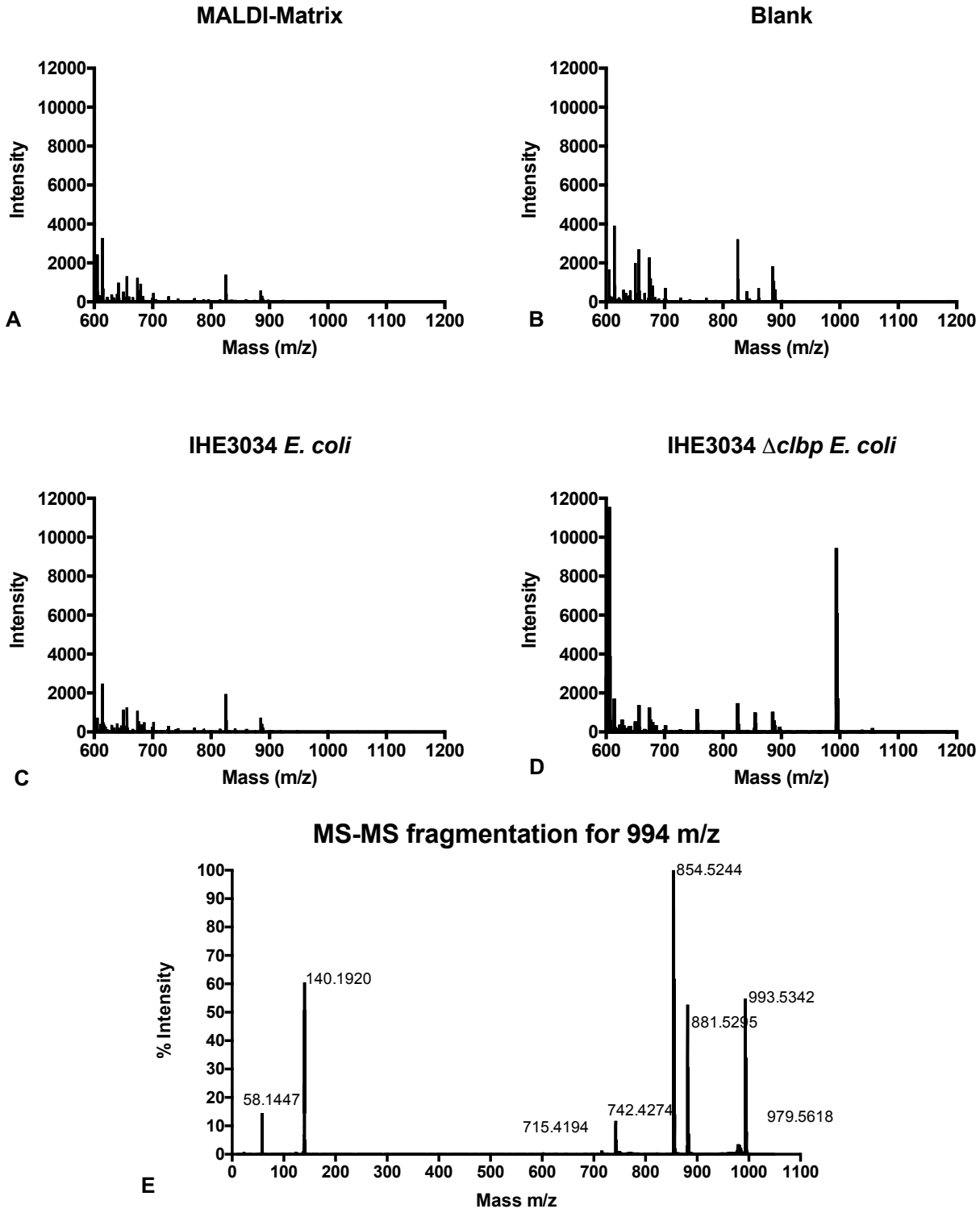

Figure 2.6. *ClbP* deletion cause an accumulation of a compound of 994 m/z. A-D) Ethyl acetate extract from the soluble portion of cell lysate from the wild type IHE3034 and the IHE3034 (Δ*clbP) E. coli* strains by MALDI TOF-TOF mass spectrometry analysis. Sample with only matrix added and from bacterial culture media (blank) without any bacterial inoculation was used as background control. **E)** MS-MS fragmentation spectra of C994 compound.

2.2.2.5 The organic extract of *E. coli* IHE3034 Δ*clbP* failed to promote megalocytosis in HeLa cells

In order to assess the biological activity of the bacterial extracts, we prepared ethyl acetate extracts from *E. coli* IHE3034, both wild type and Δ*clbP* as described previously, and assayed on HeLa cells. Extracts were made from both the lysate supernatant (water-soluble compounds) and the lysis pellet (insoluble compounds), and subsequently assayed for signs of megalocytosis of treated cells. Megalocytosis was barely detected qualitatively in several of the HeLa cultures. However, cell morphology phenotypes above basal levels could not be associated with a specific bacterial extract. (Figure 2.7). No significant qualitative differences in megalocytosis when experimental samples were compared with negative controls (Figure 2.7). IHE3034 *clbP* mutant strain was cultured in different culture media with variation in carbon source supplementation (Figure 2.7; *Δclb*P A-lysogenic broth , *Δclb*P B-terrific broth, *Δclb*P C-0.4% Glycerol, Δ*clbP* D-0.4% Acetate) in order to enhance colibactin production, but none of them resulted in any biological activity increment in term of megalocytosis. Intriguingly, cells treated with extracts from bacterial pellets (insoluble compounds) impaired cell viability in comparison with bacterial supernatants (section 2.6, Figure S2.2). Unfortunately, this toxicity cannot be attributed to C994 as this compound was neither detected nor characterized (as explained in section 2.2.2.4).

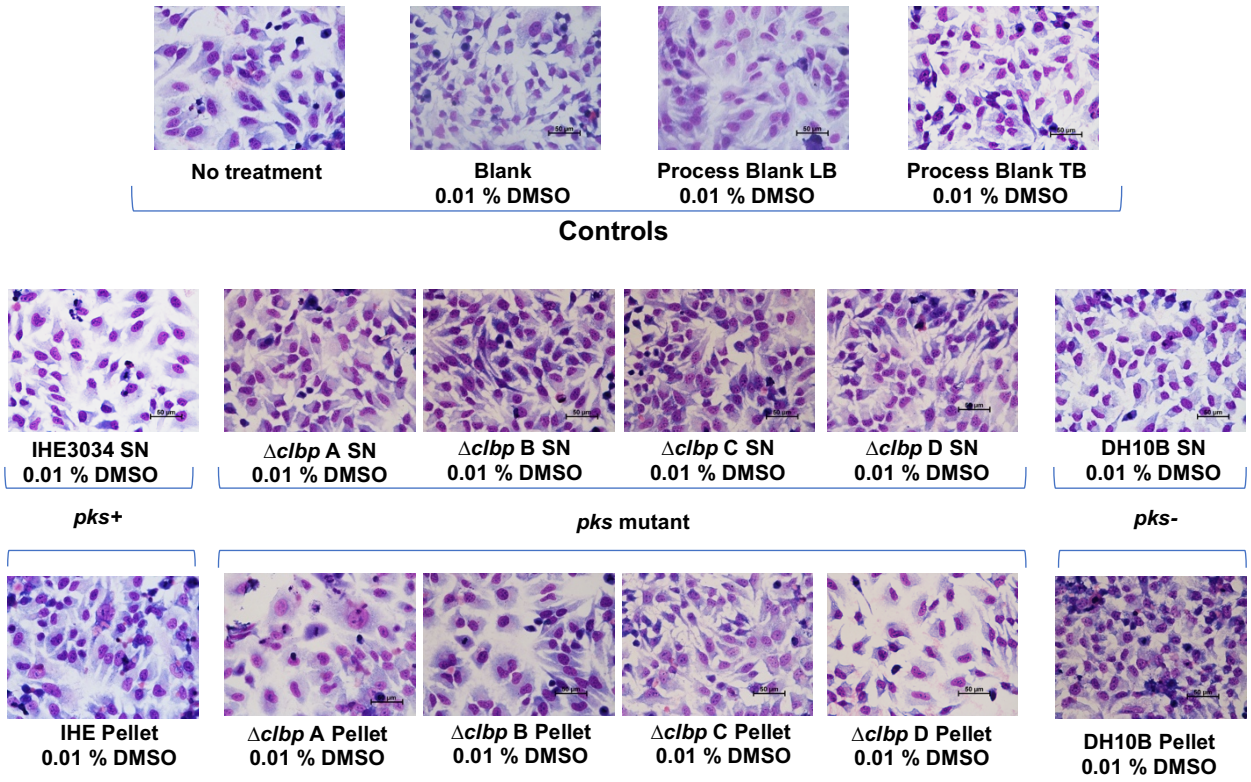

Figure 2.7. Giemsa staining of HeLa cells treated with organic extracts from *pks+* and *pks- E. coli* strains. Cells were treated with extract by a co-incubation of 4 hours at 37 ºC and 5 % CO_2 in DMEM media. After co-incubation, cells were washed and re-incubated with fresh media under the same conditions. Photos were taken after 72 hrs post treatment at 40X of magnification. Three images of each sample were taken, but just one representative image was used in this figure. All extracts were re-suspended in DMSO. IHE3034 mutant strains were culture in different culture media as follow: *ΔclbP* A-lysogenic broth , *ΔclbP* B-terrific broth, *ΔclbP* C-0.4% Glycerol, Δ*clbP* D-0.4% Acetate. SN – lysis supernatant

2.2.2.6 Investigating the presence of colibactin as a component of the lipopolysaccharide (LPS) of the bacterial outer membrane.

Gram-negative bacteria possess an outer membrane composed primarily of proteins and phospholipids, and its outermost membrane is covered with lipopolysaccharides (LPS). LPS are glycolipids composed of three structural domains: Lipid A, the core oligosaccharides, and the O-antigen. Lipid A is the hydrophobic portion of the molecule. This latter part is mostly conserved between species levels but can be modified in response to environmental stress or condition[20]. They are considered endotoxins due to their involvement in stimulating the human immune system, provoking systemic inflammation and septic shock[21].

The fact that colibactin toxicity was found to be contact-dependent[2] and the fact that free colibactin had proved to be nearly impossible to solvent-extract or isolate, suggested that colibactin could be covalently linked to the membrane of its producer bacteria.

To explore this hypothesis we isolated LPS from the membrane of both IHE3034 and IHE3034 Δ*clbP* using a standard phenol extraction protocol. This extracted LPS was then subjected to the trans-esterification technique, a commonly used method to evaluate the lipids profile of cell membranes. It was expected that the trans-esterification could facilitate the detachment of the compound as it does with fatty acids, thus rendering it amenable to analysis by GC/MS. The pro-inflammatory activity of the extracted LPS was also evaluated in bone marrow-derived neutrophils from mouse.

2.2.2.6.1 GC-MS Analysis of Compounds Extracted from LPS

The trans-esterified phenol extracts of LPS obtained from the IHE3034, IHE30304 Δ*clbP* and DH10B *E. coli* strains were analyzed by GC/MS. We searched in the GC/MS spectra for the presence of unexpected signals (those not corresponding to the typical components of LPS) but found that signals were mostly contaminants unrelated to colibactin production.

The fatty acids composition of the lipid A (lipidic moiety of LPS) were also evaluated in all the strains. The LPS fatty acids methyl esters (FAME) profiles were similar between strains under these experimental conditions. Two-Way ANOVA analysis show small differences in 12:0 and 14:0 FA ratio between *E. coli* IHE3034 strains and the negative control DH10B LPS samples (Figure 2.8). This can be attributed to the fact that DH10B is a different *E.coli* strain (non-pathogenic) but it cannot be associated with the production of colibactin. Thus, there is no association in LPS production/ composition associated with the *pks* genes.

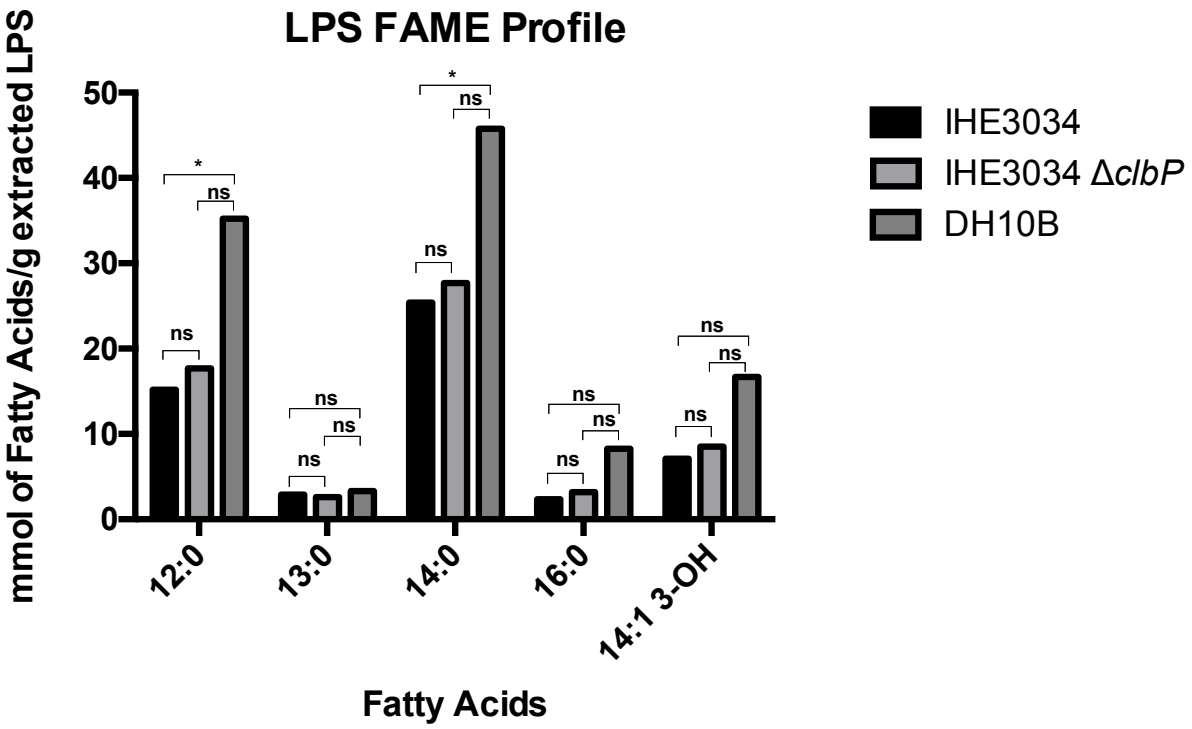

Figure 2.8. Resulted compounds after trans-esterification of extracted LPS from the colibactin-producing *E. coli* IHE3034 by GC mass spectrometry. LPS from IHE3034 (WT, *pks*+), IHE3034 Δ*clbP* (isogenic mutant) and DH10B (negative control, *pks*-) *E. coli* strains were extracted by standard phenol extraction method. Lyophilized LPSs were trans-esterified by acidic methanolysis and extracted with ethyl acetate. Two-Way ANOVA analysis show no significant difference between wild type and mutant strains. *p*-values: ns $p > 0.05$; * $p \leq 0.05$; ** $p \leq 0.01$; *** $p \leq 0.001$ and **** $p \leq 0.0001$.

2.2.2.6.2 The pro-inflammatory activity of the LPS extracted from the colibactin-producing *E. coli* IHE3034.

The pro-inflammatory response towards LPS extracted from the *pks*$^{+}$ *E. coli* IHE3034 strain was evaluated by measuring cytokine release from bone marrow-derived mouse neutrophils. The concentrations of IL6, IL10, MCP1, IFNγ and TNFα were significantly lower than those elicited by the immunogenic commercial LPS, suggesting poor immunogenic activity of the LPS extracted from IHE3034 strain (Figure 2.9). Since the pro-inflammatory activity of IHE3034 LPS was considerably lower than expected, this line of inquiry was abandoned, as it was cost-prohibitive.

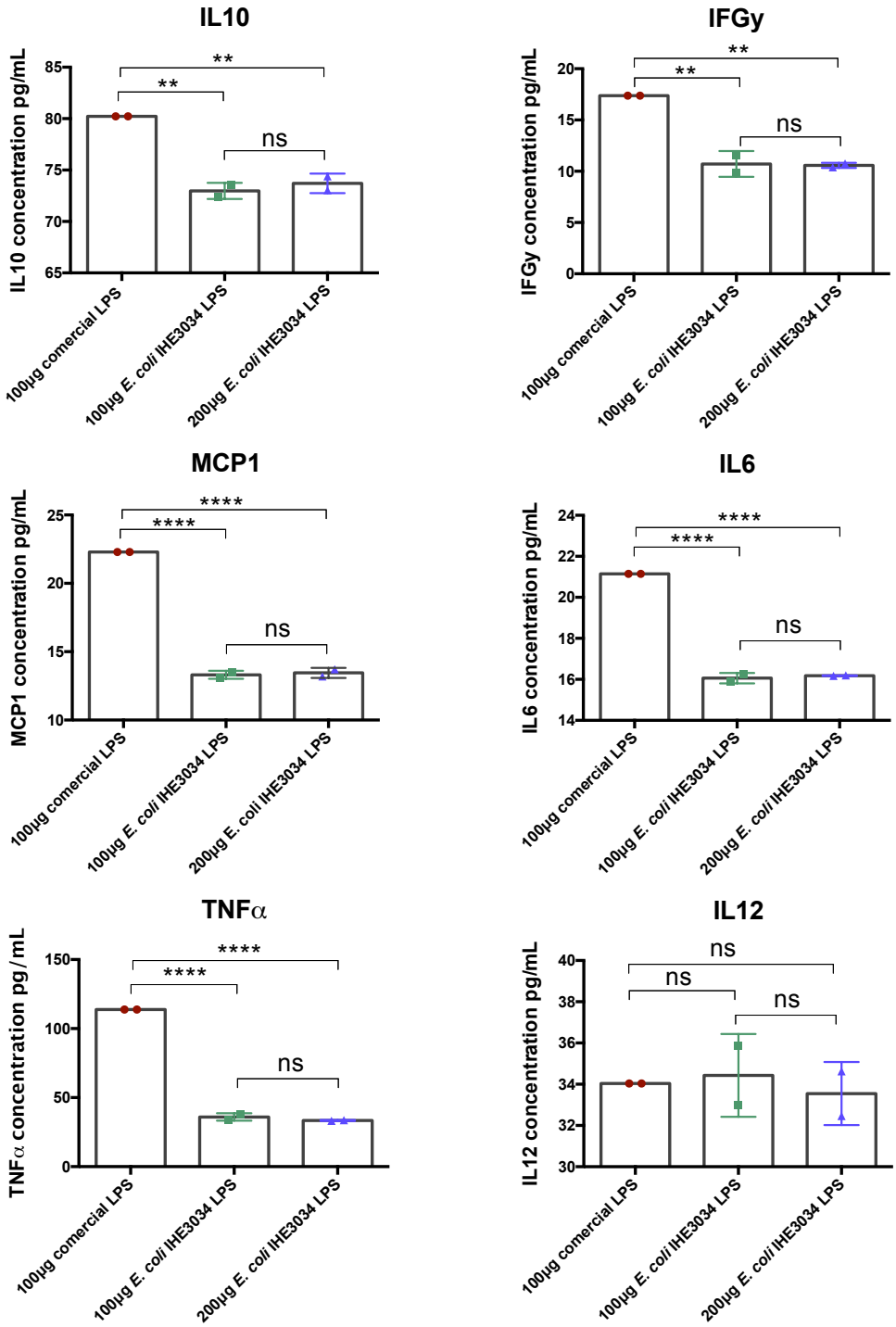

Figure 2.9. Pro-inflammatory activity of LPS from the *pks* positive *E. coli* strain IHE3034 on mouse derived neutrophils. Production of several cytokines were quantified after neutrophils exposition to LPS extracted from the colibactin-producing bacterial strain IHE3034 and compared with commercial LPS. LPS from IHE3034 have the same potential to activate IL12 production as commercial LPS does. All other cytokines (IL6, IFGy, MCP1 assayed show no activity towards to LPS from the IHE3034 strain. Statistical analysis was carried out with One-Way ANOVA. *p* -values: ns $p > 0.05$; * $p \leq 0.05$; ** $p \leq 0.01$; *** $p \leq 0.001$ and **** $p \leq 0.0001$. LPS-lipopolysaccharide; IL6-Interleukin-6; IL10-Interleukin-10; IL12-Interleukin-12; TNFα-tumor necrosis factor alpha; IFNγ-interferon gamma; MCP1-monocyte chemoattractant protein 1.

2.2.3 Discussion

Since its discovery reported in 2006, the *pks* genomic island and its resulting product colibactin have generated great interest [2]. The postulated role of colibactin in colorectal carcinogenesis through DNA damage provides a direct mechanistic connection between specific genes from the gut microbiota and cancer [3,4,22,23]. Not surprisingly, there have been numerous attempts to elucidate its biosynthesis [7,8,10,11,24–29], its chemical structure[10,12,13,18,19,30], and its mechanism of genotoxicity [30–32]. In many of these reports, there is a common observation of accumulation of colibactin intermediates in *E. coli* cells as a result of the *clbP* gene deletion, enough to characterize chemically. These intermediates have been the basis of efforts to elucidate the structure of active colibactin [33]. In this work we also aimed to contribute in shed light about colibactin structure. The principal goal of this work was to produce a clinically relevant *E. coli* strain (not a laboratory strain as other groups have done) capable to produce colibactin but deficient in its capacity to produce it in its active version. Thus, we will be able to isolate colibactin intermediates for structural characterization.

Other groups have also used the *clbP* gene deletion as a strategy to isolate colibactin intermediates, but usually, most of them use artificial plasmids containing the *pks genes* inserted into a laboratory *E. coli* strain which contains no additional virulence factors[11,12,19,25,26,30,34]. In this work, we have chosen to use a more clinically relevant and technically challenging *E. coli* strain: the IHE3034. This strain is a well-studied extraintestinal pathogenic (ExPEC) strain originally isolated from a newborn that developed meningitis[35]. Moreover, this strain was the study system in which the *pks*

island was discovered for the first time, thus converting IHE3034 into a relevant and comparable study system for our experiments[2].

The successful production and validation of the Δ*clbP* mutant of *E. coli* IHE3034 has been presented. However, infection of HeLa cells with IHE3034 Δ*clbP* did not result in the abolishment of megalocytosis that was expected[12,36]. Other groups had made the Δ*clbP* in *Nissle* 1917 and in a bacterial artificial chromosome (BAC) containing the *pks* genes (for further heterologous expression in a non-virulent strain) but never in the IHE3034 *E. coli* strain[11,12]. Interestingly, the degree of megalocytosis caused by the *clbP* mutant, suggests that other virulence factors harbored in the IHE3034[37] strain could be also sharing similar toxicity as colibactin or that there is another peptidase rescuing the clbP activity[11]. Additionally, a decrease in cellular abundance was observed in all samples treated with *E. coli,* even with the non-pathogenic DH10B strain. These results indicate that both pathogenic and non-pathogenic bacterial strains used in this experiment have a background toxicity toward HeLa cells that is not related to the pathogenicity associated with colibactin.

The deletion of *clbP* gene also resulted in the accumulation of a 994 m/z compound in organic extracts. All MS structural analyses of pre-colibactin intermediates reported in the literature were performed by LC-MS or UPLC-MS. This project explored the use of MALDI-ToF-ToF mass spectrometry to analyze bacterial extracts, and this was expected to be a more suitable method involving the quick preparation of a dry crystallized sample. Additionally, the matrix-assisted ionization and evaporation of the

sample is gentler than the electrospray ionization. Still, we were unable to consistently detect the C994 compound in our extracts, suggesting that C994 is unstable and that its production takes place under specific conditions that we were unable to identify. This lack of stability has been also observed by other groups in colibactin intermediates of high molecular weight (>600 kDa)[13]. Despite our initial interest in the C994 compound, there were signs that this compound may not be related to colibactin after all, as its MS/MS fragmentation failed to show the characteristic peaks corresponding to some signature pre-colibactin intermediates fragments in other reports.

Colibactin extraction has been notoriously difficult. The task of deciphering its structure has been limited to incomplete intermediate characterization without getting the structure of the active compound. In efforts to seek active colibactin, we attempted atypical extraction protocol on the bacterial membrane, specifically we searched within bacterial LPS. The GC/MS chromatogram of the trans-esterified LPS extracted from *E. coli* IHE3034 shows that the LPS extracted from all strains have a similar lipid composition, with no signals attributable to new compounds such as colibactin. There are reports of some pathogenic strains of *E. coli* with the capacity to modify the acylation of lipid A moiety of its LPS, as a defense mechanism[20]. However, this was not the case of strain IHE3034.

The immunogenic activity of this extracted LPS was also evaluated against bone marrow-derived mouse neutrophils. The LPS extracted from the *pks*$^{+}$ IHE3034 stimulated the production of IL-12 as commercial LPS does. However, the same

extracted LPS failed to stimulate the production of the other cytokines in the panel, namely, IL6, IL10, MCP1, IFNγ, and TNFα. Cytokines are part of the first line of defense in the human body against pathogen-derived or endogenous signals and their release is typically stimulated by LPS[38]. In this particular case, no dramatic pro-inflammatory effects were attributable to the LPS extracted from this clinical strain IHE3034. It has been observed that some pathogenic strains of *E. coli* have adapted to suppress their pro-inflammatory signals, thus evading the immune system[39].

In conclusion, a variant strain of the *E. coli* IHE3034 deficient of *clbP* gene was made to promote the accumulation of colibactin intermediates. Our results showed that this deletion did not abolish any of the typical phenotypes of colibactin exposure. This could be a function of the degree of complexity involved in working with a clinical strain of *E. coli*.

While we attempted to shed light on the then unknown colibactin structure, other groups were making amazing efforts to uncover the structure and mechanism of colibactin. Here we mention some of these efforts from other research groups, which have resulted in the near elucidation of colibactin structure and mode of action.

2.3 Colibactin biosynthesis, structure, and mechanism of action discovered by other groups.

The structure of the active colibactin natural product is still unknown. However, during the past decade, many efforts have been directed at elucidating its structure and mechanism of action.

An atypical feature of the colibactin biosynthesis is that *pks genes* do not follow the sequential PKS/NRPS biosynthetic logic, in which the enzymes are used in the same order in which they are encoded in the genome. Based on the structures of isolated pre-colibactin intermediates that have been published, it is clear that colibactin biosynthesis does not use its PKS/NRPS enzymes in the same order they appear in the gene cluster (Figure 2.10). Accumulated evidence supports the idea that colibactin biosynthesis starts with clbN synthase, which initiates colibactin formation by the insertion of an *L*-asparagine residue followed by its acylation by the incorporation of the C_{14} *N*-acyl subunit. Then, the compound continues its elongation by clbB enzyme and so on with the others *pks island* encoded enzymes (Figure 2.10). This apparent violation of the "co-linearity rules" made it difficult to establish predictions about its structure.

One of the most important findings on colibactin's structure was the discovery of a highly reactive spiro-cyclopropane moiety [18,30]. The exact mechanism by which the 1-aminocyclopropane-carboxylic acid (ACC) residue is incorporated in the colibactin formation is not completely clear. What is known, is that it is a derivative from a methionine residue that undergoes intramolecular rearrangements and its incorporation

is mediated by the nrps clbH[18,30] (Figure 2.11). The ACC moiety is commonly found in plant-based metabolites but rarely found in bacterial secondary metabolites[18,40]. This ring-strained spiro-cyclopropyl moiety is labile to electrophilic ring-opening reactions resulting in an irreversible covalent attachment with the target. Thus, the cyclopropyl moiety is the structural "warhead" of Colibactin[30] responsible for its mechanism of action and genotoxicity.

Recent work by the groups of Nougayréde, Balskus, and Crawford, has shed light on both the structure and the mechanism of action of colibactin. The direct exposure of purified DNA to colibactin-producing bacteria resulted in DNA damage consisting of interstrand crosslinks, revealing and confirming the mechanism by which Colibactin inflicts its toxicity[30,41]. This is further supported by the results of an *in vivo* experiment in which DNA adducts were formed in the genomic material of cells extracted from a mouse infected with a *pks* positive bacteria; moreover, their data suggests that colibactin reacts specifically with adenine residues causing the interstrand crosslinks which then result in double-stranded breaks of mammalian DNA[32]. The most plausible structure that would explain the interstrand DNA crosslinks is that of a suggested dimer with two highly reactive cyclopropyl moieties that react with the DNA of the infected cells[33], causing as consequence the formation of double-stranded breaks (Figure 2.11). If the mode of action of colibactin is through highly reactive cyclopropyl moieties, then the molecule is expected to be highly unstable and difficult to isolate. A strategy to circumvent the lack of stability of the natural product is through the synthesis of known intermediates and likely candidates. In fact, the group of Jason Crawford at

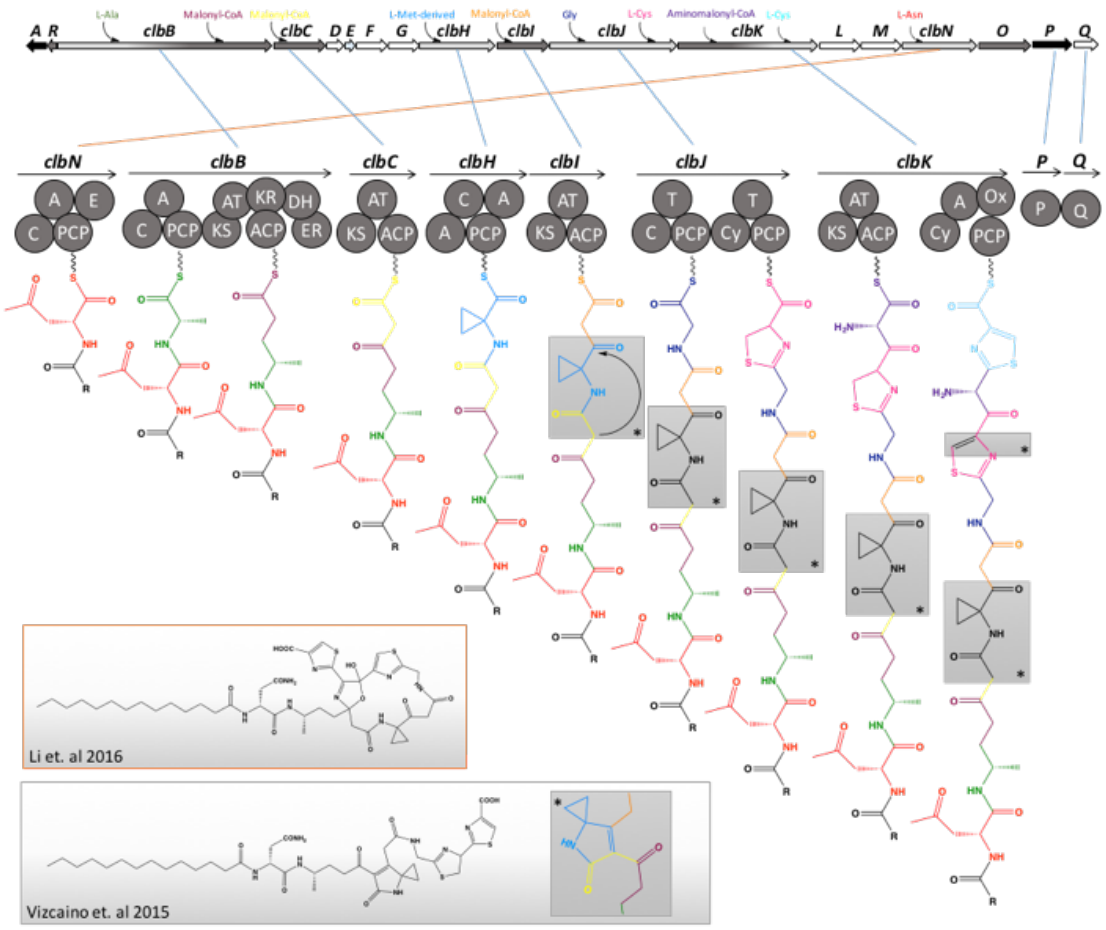

Figure 2.10. Initial proposed biosynthesis of pre-colibactin. Abreviattions: C, condensation; A, adenylation; E, epimerization; KS, ketosynthase; KR, ketoreductase; DH, dehydratase; ER enoylreductase; AT*, inactivated acyltransferase (AT); Cy, dual condensation/cyclization; Ox, oxidase.

Yale, synthesized a dimeric colibactin-inspired molecule which showed the capacity for interstrand crosslinks with DNA and the formation of adenine adducts. However, this unusually active analog of colibactin, has never been isolated from a naturally producing bacteria.

Despite many efforts to ascertain the colibactin structure and mode of action, there are still outstanding questions about the structure of active colibactin. The deletion of key genes along the colibactin pathway has resulted in the identification of important intermediates which have taken us closer to the complete structure. Clearly, if colibactin is highly reactive towards DNA and other biomolecules, it is likely to be unstable and thus hard to isolate. To increase the likelihood of obtaining an active compound, the chemical isolation efforts have been complemented with elegant synthetic schemes aimed at identifying plausible candidate molecules. However, the search for the active colibactin is far from over and is an on-going endeavor with clear relevance to microbiome-induced colorectal cancer and inflammation.

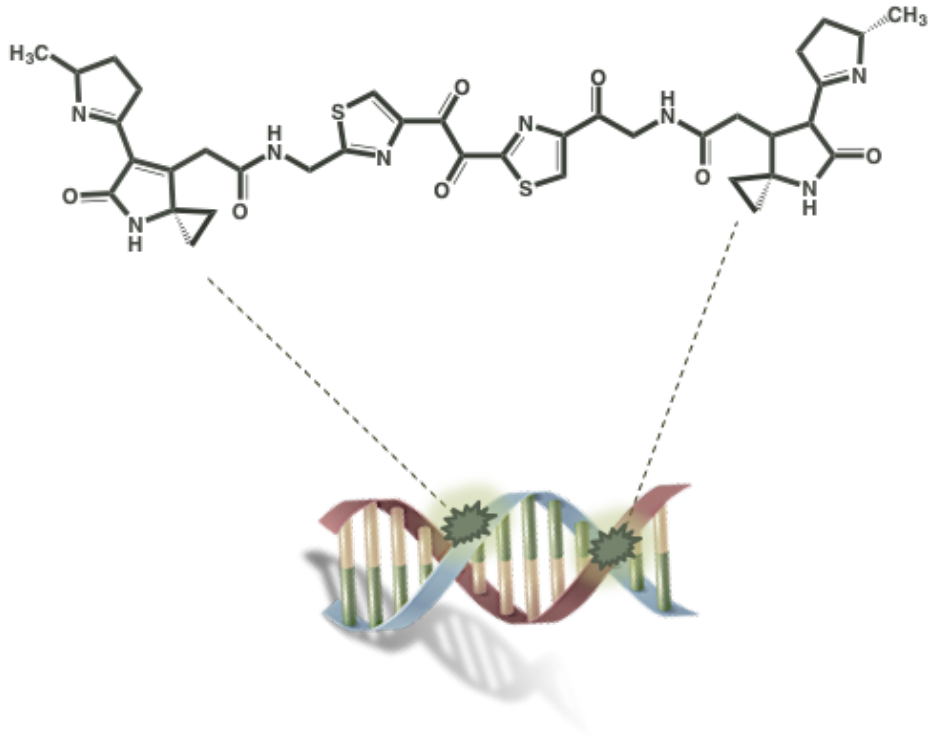

Figure 2.11. Colibactin dimer proposed by Crawford *et al.* Colibactin dimer proposed by Crawford and co-workers, based on characterization of DNA adduct resulted by infection assay with a colibactin-producing *E. coli* strain and its crosslinking bioactivity. The electrophilic cyclopropyl moiety undergo a ring-opening reaction by the nucleophilic attack from an adenine residue resulting in and irreversible covalent bond. (Xue et al. 2019).

2.5 References

(1) Putze, J.; Hennequin, C.; Nougayrède, J. P.; Zhang, W.; Homburg, S.; Karch, H.; Bringer, M. A.; Fayolle, C.; Carniel, E.; Rabsch, W.; Oelschlaeger, T. A.; Oswald, E.; Forestier, C.; Hacker, J.; Dobrindt, U. Genetic Structure and Distribution of the Colibactin Genomic Island among Members of the Family Enterobacteriaceae. *Infect. Immun.* **2009**, *77* (11), 4696–4703. https://doi.org/10.1128/IAI.00522-09.

(2) Nougayrède, J.-P.; Homburg, S.; Taieb, F.; Boury, M.; Brzuszkiewicz, E.; Gottschalk, G.; Buchrieser, C.; Hacker, J.; Dobrindt, U.; Oswald, E. Escherichia Coli Induces DNA Double-Strand Breaks in Eukaryotic Cells. *Science.* **2006**, *313* (5788), 848–851. https://doi.org/10.1126/science.1127059.

(3) Cuevas-Ramos, G.; Petit, C. R.; Marcq, I.; Boury, M.; Oswald, E.; Nougayrède, J.-P. Escherichia Coli Induces DNA Damage in Vivo and Triggers Genomic Instability in Mammalian Cells. *Proc. Natl. Acad. Sci. U. S. A.* **2010**, *107* (25), 11537–11542. https://doi.org/10.1073/pnas.1001261107.

(4) Arthur, J. C.; Perez-Chanona, E.; Mühlbauer, M.; Tomkovich, S.; Uronis, J. M.; Fan, T.-J.; Campbell, B. J.; Abujamel, T.; Dogan, B.; Rogers, A. B.; Rhodes, J. M.; Stintzi, A.; Simpson, K. W.; Hansen, J. J.; Keku, T. O.; Fodor, A. A.; Jobin, C. Intestinal Inflammation Targets Cancer-Inducing Activity of the Microbiota. *Science.* **2012**, *338* (6103), 120–123. https://doi.org/10.1126/science.1224820.

(5) Li, Z.; Li, J.; Cai, W.; Lai, J. Y. H.; Mckinnie, S. M. K.; Zhang, P.; Moore, B. S.; Zhang, W.; Qian, P. Macrocyclic Colibactin Induces DNA Double-Strand Breaks via Copper-Mediated Oxidative Cleavage. *Nat. Chem.* **2019**, *11* (10), 880–889. https://doi.org/10.1038/s41557-019-0317-7.

(6) Wernke, K. M.; Xue, M.; Tirla, A.; Kim, C. S.; Herzon, S. B.; Crawford, J. M. Structure and Bioactivity of Colibactin. *Bioorg. Med. Chem. Lett.* **2020**, *30* (15), 127280. https://doi.org/10.1016/j.bmcl.2020.127280.

(7) Cougnoux, A.; Gibold, L.; Robin, F.; Dubois, D.; Pradel, N.; Darfeuille-Michaud, A.; Dalmasso, G.; Delmas, J.; Bonnet, R. Analysis of Structure-Function Relationships in the Colibactin-Maturating Enzyme ClbP. *J. Mol. Biol.* **2012**, *424* (3–4), 203–214. https://doi.org/10.1016/j.jmb.2012.09.017.

(8) Brotherton, C. A.; Balskus, E. P. A Prodrug Resistance Mechanism Is Involved in Colibactin. *J. Am. Chem. Sociaty* **2013**, *135*, 3359–3362. https://doi.org/10.1021/ja312154m.

(9) Mousa, J. J.; Yang, Y.; Tomkovich, S.; Shima, A.; Newsome, R. C.; Tripathi, P.; Oswald, E.; Bruner, S. D.; Jobin, C. MATE Transport of the E. Coli-Derived Genotoxin Colibactin. *Nat. Microbiol.* **2016**, *1* (1), 15009. https://doi.org/10.1038/nmicrobiol.2015.9.

(10) Bian, X.; Fu, J.; Plaza, A.; Herrmann, J.; Pistorius, D.; Stewart, A. F.; Zhang, Y.; Müller, R. In Vivo Evidence for a Prodrug Activation Mechanism during Colibactin Maturation. *ChemBioChem* **2013**, *14* (10), 1194–1197. https://doi.org/10.1002/cbic.201300208.

(11) Dubois, D.; Baron, O.; Cougnoux, A.; Delmas, J.; Pradel, N.; Boury, M.; Bouchon, B.; Bringer, M. A.; Nougayrède, J. P.; Oswald, E.; Bonnet, R. ClbP Is a Prototype of a Peptidase Subgroup Involved in Biosynthesis of Nonribosomal Peptides. *J. Biol. Chem.* **2011**, *286* (41), 35562–35570. https://doi.org/10.1074/jbc.M111.221960.

(12) Vizcaino, M. I.; Engel, P.; Trautman, E.; Crawford, J. M. Comparative Metabolomics and Structural Characterizations Illuminate Colibactin Pathway-Dependent Small Molecules. *J. Am. Chem. Sociaty* **2014**, *136* (26), 9244–9247. https://doi.org/10.1021/ja503450q.

(13) Li, Z. R.; Li, Y.; Lai, J. Y. H.; Tang, J.; Wang, B.; Lu, L.; Zhu, G.; Wu, X.; Xu, Y.; Qian, P. Y. Critical Intermediates Reveal New Biosynthetic Events in the Enigmatic Colibactin Pathway. *ChemBioChem* **2015**, *16* (12), 1715–1719. https://doi.org/10.1002/cbic.201500239.

(14) Meier, C.; Oelschlaeger, T. A.; Merkert, H.; Korhonen, T. K.; Hacker, J. Ability of Escherichia Coli Isolates That Cause Meningitis in Newborns to Invade Epithelial and Endothelial Cells. *Infect. Immun.* **1996**, *64* (7), 2391–2399. https://doi.org/10.1128/iai.64.7.2391-2399.1996.

(15) Hioki, Y.; Kuyama, H.; Hamana, C.; Takeyama, K.; Tanaka, K. An Improved Sample Preparation Method for the Sensitive Detection of Peptides by MALDI-MS. *J. Mass Spectrom.* **2013**, *48*, 1217–1223. https://doi.org/10.1002/jms.3283.

(16) Bull, L. B. The Histological Evidence of Liver Damage from Pyrrolizidine Alkaloids. *Aust. Vet. J.* **1955**, *31*, 33–40. https://doi.org/10.1111/j.1751-0813.1955.tb05488.x.

(17) Jago, M. V. The Development of the Hepatic Megalocytosis of Chronic Pyrrolizidine Alkaloid Poisoning. *Am. J. Pathol.* **1969**, *56* (3), 405–421.

(18) Bian, X.; Plaza, A.; Zhang, Y.; Müller, R. Two More Pieces of the Colibactin Genotoxin Puzzle from Escherichia Coli Show Incorporation of an Unusual 1-Aminocyclopropanecarboxylic Acid Moiety. *Chem. Sci.* **2015**, *6* (5), 3154–3160.

https://doi.org/10.1039/C5SC00101C.

(19) Brotherton, C. A.; Wilson, M.; Byrd, G.; Balskus, E. P. Isolation of a Metabolite from the Pks Island Provides Insights into Colibactin Biosynthesis and Activity. *Org. Lett.* **2015**, *17* (6), 1545–1548. https://doi.org/10.1021/acs.orglett.5b00432.

(20) Steimle, A.; Autenrieth, I. B.; Frick, J. S. Structure and Function: Lipid A Modifications in Commensals and Pathogens. *Int. J. Med. Microbiol.* **2016**, *306* (5), 290–301. https://doi.org/10.1016/j.ijmm.2016.03.001.

(21) Opal, S. M. Endotoxins and Other Sepsis Triggers. *Contrib. Nephrol.* **2010**, *167*, 14–24. https://doi.org/10.1159/000315915.

(22) Cougnoux, A.; Dalmasso, G.; Martinez, R.; Buc, E.; Delmas, J.; Gibold, L.; Sauvanet, P.; Darcha, C.; Déchelotte, P.; Bonnet, M.; Pezet, D.; Wodrich, H.; Darfeuille-Michaud, A.; Bonnet, R. Bacterial Genotoxin Colibactin Promotes Colon Tumour Growth by Inducing a Senescence-Associated Secretory Phenotype. *Gut* **2014**, *63* (12), 1932–1942. https://doi.org/10.1136/gutjnl-2013-305257.

(23) Healy, A. R.; Herzon, S. B. Molecular Basis of Gut Microbiome-Associated Colorectal Cancer: A Synthetic Perspective. *J. Am. Chem. Soc.* **2017**, *139* (42), 14817–14824. https://doi.org/10.1021/jacs.7b07807.

(24) Brachmann, A. O.; Garcie, C.; Wu, V.; Martin, P.; Ueoka, R.; Oswald, E.; Piel, J. Colibactin Biosynthesis and Biological Activity Depend on the Rare Aminomalonyl Polyketide Precursor. *Chem. Commun.* **2015**, *51* (66), 13138–13141. https://doi.org/10.1039/c5cc02718g.

(25) Li, Z.-R.; Li, J.; Gu, J.-P.; Lai, J. Y. H.; Duggan, B. M.; Zhang, W.-P.; Li, Z.-L.; Li, Y.-X.; Tong, R.-B.; Xu, Y.; Lin, D.-H.; Moore, B. S.; Qian, P.-Y. Divergent

Biosynthesis Yields a Cytotoxic Aminomalonate-Containing Precolibactin. *Nat. Chem. Biol.* **2016**, *12* (10), 773–775. https://doi.org/10.1038/nchembio.2157.

(26) Zha, L.; Wilson, M. R.; Brotherton, C. A.; Balskus, E. P. Characterization of Polyketide Synthase Machinery from the Pks Island Facilitates Isolation of a Candidate Precolibactin. *ACS Chem. Biol.* **2016**, *11* (5), 1287–1295. https://doi.org/10.1021/acschembio.6b00014.

(27) Zha, L.; Jiang, Y.; Henke, M. T.; Wilson, M. R.; Wang, J. X.; Kelleher, N. L.; Balskus, E. P. Colibactin Assembly Line Enzymes Use S-Adenosylmethionine to Build a Cyclopropane Ring. *Nat. Chem. Biol.* **2017**, *13* (10), 1063–1065. https://doi.org/10.1038/nchembio.2448.Colibactin.

(28) Trautman, E. P.; Healy, A. R.; Shine, E. E.; Herzon, S. B.; Crawford, J. M. Domain-Targeted Metabolomics Delineates the Heterocycle Assembly Steps of Colibactin Biosynthesis. *J. Am. Chem. Soc.* **2017**, *139* (11), 4195–4201. https://doi.org/10.1021/jacs.7b00659.Experimental.

(29) Guntaka, N. S.; Healy, A. R.; Crawford, J. M.; Herzon, S. B.; Bruner, S. D. Structure and Functional Analysis of ClbQ, an Unusual Intermediate-Releasing Thioesterase from the Colibactin Biosynthetic Pathway. *ACS Chem. Biol.* **2017**, *12* (10), 2598–2608. https://doi.org/10.1021/acschem-bio.7b00479.Primers.

(30) Vizcaino, M. I.; Crawford, J. M. The Colibactin Warhead Crosslinks DNA. *Nat. Chem.* **2015**, *7* (5), 411–417. https://doi.org/10.1038/nchem.2221.

(31) Bossuet-greif, N.; Vignard, J.; Taieb, F.; Mirey, G.; Dubois, D.; Petit, C.; Oswald, E.; Nougayrède, J.-P. The Colibactin Genotoxin Generates DNA Interstrand Cross- Links in Infected Cells. *MBio* **2018**, *9* (2).

https://doi.org/10.1128/mBio.02393-17.

(32) Wilson, M. R.; Jiang, Y.; Villalta, P. W.; Stornetta, A.; Boudreau, P. D.; Carrá, A.; Brennan, C. A.; Chun, E.; Ngo, L.; Samson, L. D.; Engelward, B. P.; Garrett, W. S.; Balbo, S.; Balskus, E. P. The Human Gut Bacterial Genotoxin Colibactin Alkylates DNA. *Science.* **2019**, *363* (709). https://doi.org/10.1126/science.aar7785.

(33) Xue, M.; Kim, C. S.; Healy, A. R.; Wernke, K. M.; Wang, Z.; Frischling, M. C.; Shine, E. E.; Wang, W.; Herzon, S. B.; Crawford, J. M. Structure Elucidation of Colibactin and Its DNA Cross-Links. *Science.* **2019**, *365* (6457). https://doi.org/.1037//0033-2909.I26.1.78.

(34) Healy, A. R.; Nikolayevskiy, H.; Patel, J. R.; Crawford, J. M.; Herzon, S. B. A Mechanistic Model for Colibactin-Induced Genotoxicity. *J. Am. Chem. Soc.* **2016**, *138* (48), 15563–15570. https://doi.org/10.1021/jacs.6b10354.

(35) Korhonen, T. K.; Valtonen, M. V; Parkkinen, J.; Vaisanen-rhen, V.; Finne, J.; Svenson, S. B.; Makela, P. H. Serotypes , Hemolysin Production , and Receptor Recognition of Escherichia Coli Strains Associated with Neonatal Sepsis and Meningitis. *Infect. Immun.* **1985**, *48* (2), 486–491. https://doi.org/10.1128/IAI.48.2.

(36) Id, M.; Id, P. B.; Bossuet-greif, N. Deciphering the Interplay between the Genotoxic and Probiotic Activities of Escherichia Coli Nissle 1917. **2019**, 1–24.

(37) Bauchart, P.; Germon, P.; Brée, A.; Oswald, E.; Hacker, J.; Dobrindt, U. Pathogenomic Comparison of Human Extraintestinal and Avian Pathogenic Escherichia Coli - Search for Factors Involved in Host Specificity or Zoonotic Potential. *Microb. Pathog.* **2010**, *49* (3), 105–115.

https://doi.org/10.1016/j.micpath.2010.05.004.

(38) Kany, S.; Vollrath, J. T.; Relja, B. Cytokines in Inflammatory Disease. *Int. J. Mol. Sci.* **2019**, *20* (6008), 1–31.

(39) Kawahara, K. Variation, Modification and Engineering of Lipid a in Endotoxin of Gram-negative Bacteria. *Int. J. Mol. Sci.* **2021**, *22* (5), 1–15. https://doi.org/10.3390/ijms22052281.

(40) Wang, K. L. C.; Li, H.; Ecker, J. R. Ethylene Biosynthesis and Signaling Networks. *Plant Cell* **2002**, *14*, 131–151. https://doi.org/10.1105/tpc.001768.

(41) Bossuet-greif, N.; Vignard, J.; Taieb, F.; Mirey, G.; Dubois, D.; Petit, C.; Oswald, E. The Colibactin Genotoxin Generates DNA Interstrand Cross- Links in Infected Cells. **2018**, *9* (2), 1–15.

2.6 Supplementary Material

Table S2.1 Summary of PCR conditions for amplification of the *clbP* flanked-lineal cassette and validation of the mutant strain (*ΔclbP)*

Bacterial Gene	Annealing Temp (°C)	Sequence (5' to 3')	Amplicon Size (bp)
clbP	63	*clbP*_F: CACCATGACAATAATGGAACACGTT *clbP*_R: TTACTCATCGTCCCACTCCTTGTTG	1514
clbP	63	*clbP*_F: ACCGTGACTGATGTAAGGGC *clbP*_R: AAACCCGTTCTGTTTCATGC	252
*clbP*_ Homology arms	62	*clbP*_F: TTACTCATCGTCCCACTCCTTGTTGTGTAATAGA ATTCGTTTAATTTGATAATTAACCCTCACTAAAGG GCGG *clbP*_R: ATGACAATAATGGAACACGTTAGCATTAAAACAT TATATCATCTCCTGTGTACGACTCACTATAGGGC TCG	1737

Table S2.2 Primers used to confirm the deletion was solely of the *clbP* gene

Bacterial Gene	Annealing Temp (°C)	Sequence (5' to 3')	Amplicon Size (bp)
clbN	63	clbN_F: GTTTTGCTCGCCAGATAGTCATTC clbN_R: CAGTTCG GGTATGTGTGGAAGG	733
clbP	57	clbP_F: TTACTCATCGTCCCACTCCTTG clbP_R: ATGACAATAATGGAACACGTTAG	1515
clbQ	57	clbQ_F: CACCATGAGTAATATCAGTTTGTAT clbQ_R: CTACCCTACTATTTCGAGTGA	723

Supplemental procedure S1:

Extraction of smooth or semi-rough Lipopolysaccharides (LPS) from gram-negative bacteria (e.g. *Escherichia coli*)
Adapted from the University of California San Diego Glycobiology Research and Training Center

Materials:

E. coli cells
LB
Phenol redistilled
Dialysis tubing (1000 MWCO)
Oil Bath (Mineral oil and heating pan)
Water bath with
Heating and Stirring plate
Chemical Hood
Cold Centrifuge
15mL Falcon tubes
50mL Falcon Tubes
Filter and Autoclaved ddH_2O
100mL autoclaved crystal bottles
Stirrer
Autoclaved 1L Flask
Autoclaved Centrifuge Plastic Bottles
Autoclaved spatulas
Scale
Small round-bottom flask
Acetone (to wash)
Methanol
Ethyl acetate
Reflux condenser
Magnesium Sulfate
Dry ice
Roto-evaporador

Preparation of 90% Phenol solution:

1) Phenol at room temperature is crystalized. The entire phenol bottle should be pre-heated at 68ºC in the water bath to solubilize the phenol.

2) Mix 2mL of autoclaved and filter water with 18mL of pre-heated Phenol solution to obtain a 90% Phenol Solution.

Preparation of the Bacteria Pellet:

1) A pre-culture of gram-negative bacteria is required, overnight growth in 20mL of LB in a 50mL Falcon Tube.

2) The following day the 20mL pre-culture is added to LB in a 1L Flask. The gram-negative bacteria should be grown to their log late phase (measured by OD600).

3) Harvest the LB containing the bacteria in a centrifuge plastic bottle.

4) Using a scale balance each centrifuge plastic bottle.

5) Centrifuge at 10,000rpm for 5min at 4ºC.

6) Remove the supernatant and wash the pellet with autoclaved and filter milliQ and centrifuge at 10,000rpm for 5min at 4ºC.

6) The pellet should weight 2-3g.

Extraction of smooth or semi-rough LPS:

1) Pre-heat the oil bath at 68ºC.

2) Re-suspend the pellet form in the centrifuge plastic bottle by adding 20mL of autoclave and filter milliQ water.

3) Transfer the 20mL to a 100mL crystal bottle (autoclaved). The crystal bottle is then heated in the oil bath for 10min with continuous stirring for 10min at 68ºC.

4) Add 20mL of the 90% Phenol solution, slowly, to the heated cell suspension in 20mL of water. **NOTE:** A milky-white appearance will appear after adding the Phenol.

5) The 1:1 solution of Phenol and water should stir vigorously for 30min.

6) Immediately transfer the solution to ice or water bath (<10ºC).

7) Transfer the solution to a 50mL Falcon tube and centrifuge the extract for 45min at 3500rpm for 45min. Then, transfer the upper layer to a new 50mL Falcon tube, this is the phenol saturated water layer, smooth and semi-rough LPS extracts are in this layer . The middle layer is insoluble cellular components and bottom layer is residual phenol phase.

8) Meanwhile, 20mL of autoclaved and filter milliQ water should be heated to 68ºC in the oil bath. Transfer this pre-heated water solution to the remaining middle and bottom layers, and mix.

9) Transfer this entire solution to a new autoclave 100mL crystal bottle and stir vigorously from 30min and cool down as in step 6.

10) Then, centrifuge for 45min at 3500rpm at 10ºC and extract the upper layer to the same 50mL Falcon tube as in step 7.

Dialysis with 1,000 MWCO (or 1kDa) dialysis tubing:

1) The extracted LPS then are transferred to 1kDa dialysis tubing. Using a 4L container add 4L of milliQ water. Place the dialysis tubing containing the extracted LPS in 4L. The water should be change two times each day. The dialysis step should last for 4 days.

Lyophilization step:

1) The dialysate then is dry in a lyophilyzer (0.1mBarr and -55ºF) for 4-5 days. **NOTE:** A white-powder is formed.

2) The lyophilized material can be stored at -20ºC.

Esterification step:

1) The day before the esterification step the reflux condenser inner surface should be wash, rinse with acetone and dry.

2) Weight 0.100g of lyophilized material in a small round-bottom flask with stirrer.

3) Add 10mL of methanol (99% pure).

4) Add 5 drops of concentrated HCl and stir.

5) Open the water knob to circulate the water into the reflux condenser.

6) Attach the small round-bottom flask, labeled aqueous phase, and its lyophilized content to the bottom of the condenser. Cover the outside of the small round-bottom flask with cotton.

7) Heat the stirring solution at 50ºC for 2 hours.

8) Clean the extraction funnel and rinse it with ethyl acetate.

9) Decant the solution to the extraction funnel and add ethyl acetate.

10) Close the funnel's top holding the stopper. Holding the funnel horizontally displace the liquid by rotating the funnel horizontally, and open the valve to liberate the gas. Repeat about two times.

11) Mount the funnel above the round-bottom flask labeled aqueous phase, let the phases separate completely and open the valve to decant the aqueous phase, close the valve when the organic phase begins.

12) Put a new small round-bottom flask labeled organic phase. Decant the organic phase of the extraction funnel to this new labeled flask.

13) Again, put the aqueous phase in the extraction funnel, add ethyl acetate (step 10) and repeat the step 11 and 12 decanting the phases into their appropriate flasks.

14) Pour the organic phase into a wash, rinse with acetone and dried small Erlenmeyer flask and add sufficient Magnesium Sulfate to dry the sample.

15) Attach a dry funnel to the top of a new round-bottom flask and place a folder filter paper on it.

16) Wet the filter paper with ethyl acetate and pour the organic phase into the filter.

17) Wash the remaining contents of the organic phase flask with ethyl acetate and pour it on the filter.

18) Close the round-bottom flask and label accordingly.

Roto-evaporation step:

1) Turn on the roto-vap, pump and water bath.

2) Select the solvent from the roto-vap library and set the water bath to the temperature suggested in the library.

3) Fill the chilling containers with dry ice+acetone.

4) Let the cooling and heating baths reach the desired temp (32ºC).

5) Attach the tramp and secure with the clip included in the equipment.

6) Attach the round-bottom flask containing your sample to the end of the tramp using a clip.
7) Start the rotary function for the round bottom flask.

8) Press start to begin the vacuum and in turn the roto-evaporation.

9) Once there is only a drop left in your round-bottom flask press stop two times.

10) Wait for the **instrument** to return to atmospheric pressure.

11) Detach the round-bottom flask and the trap and turn off the water-bath, pump and roto-vap.

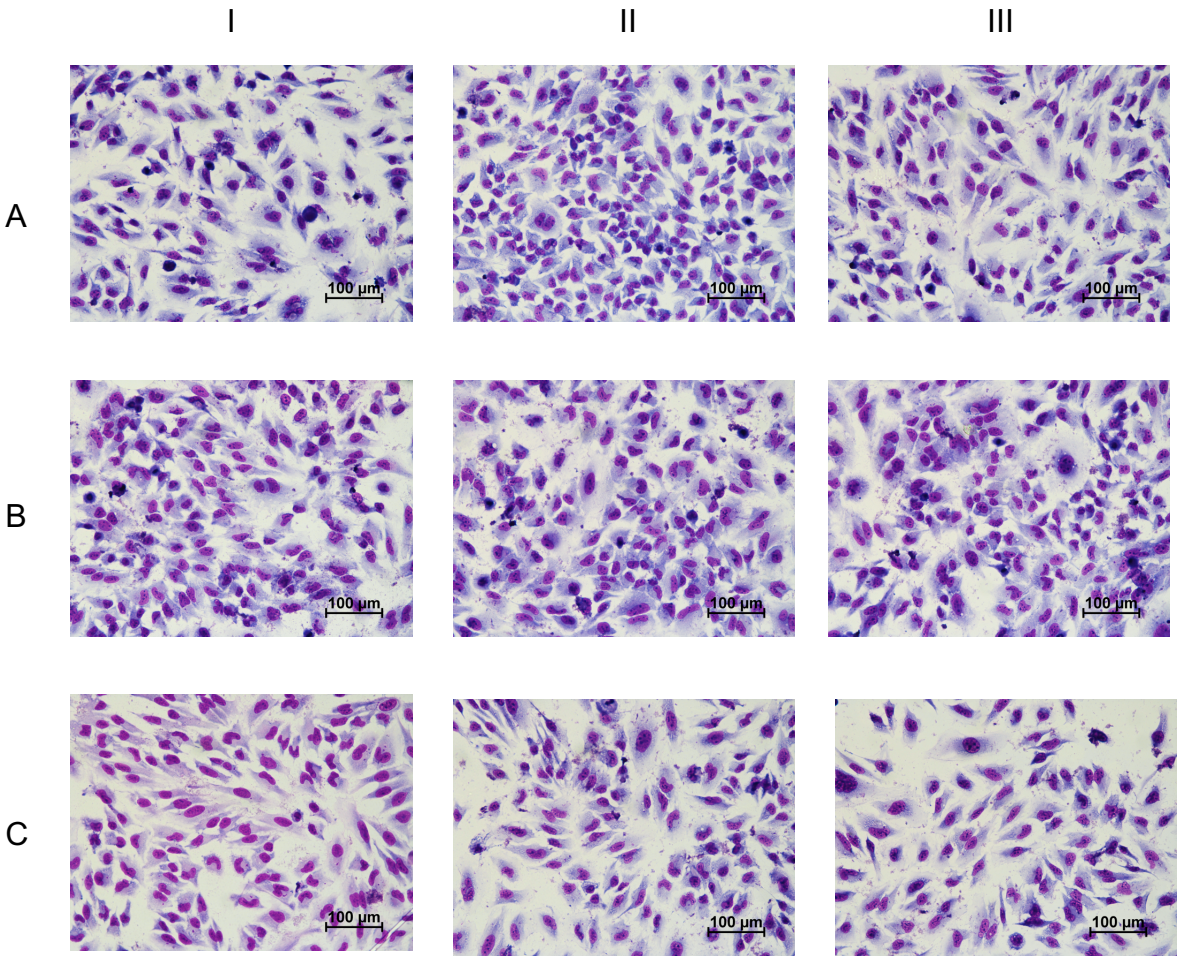

Figure S2.1a Giemsa staining of untreated HeLa cells. A, B, and C represent biological replicates. Three images of each sample were taken (represented by I, II, and III). Photos were taken after 72 hours post treatment at 40X of magnification.

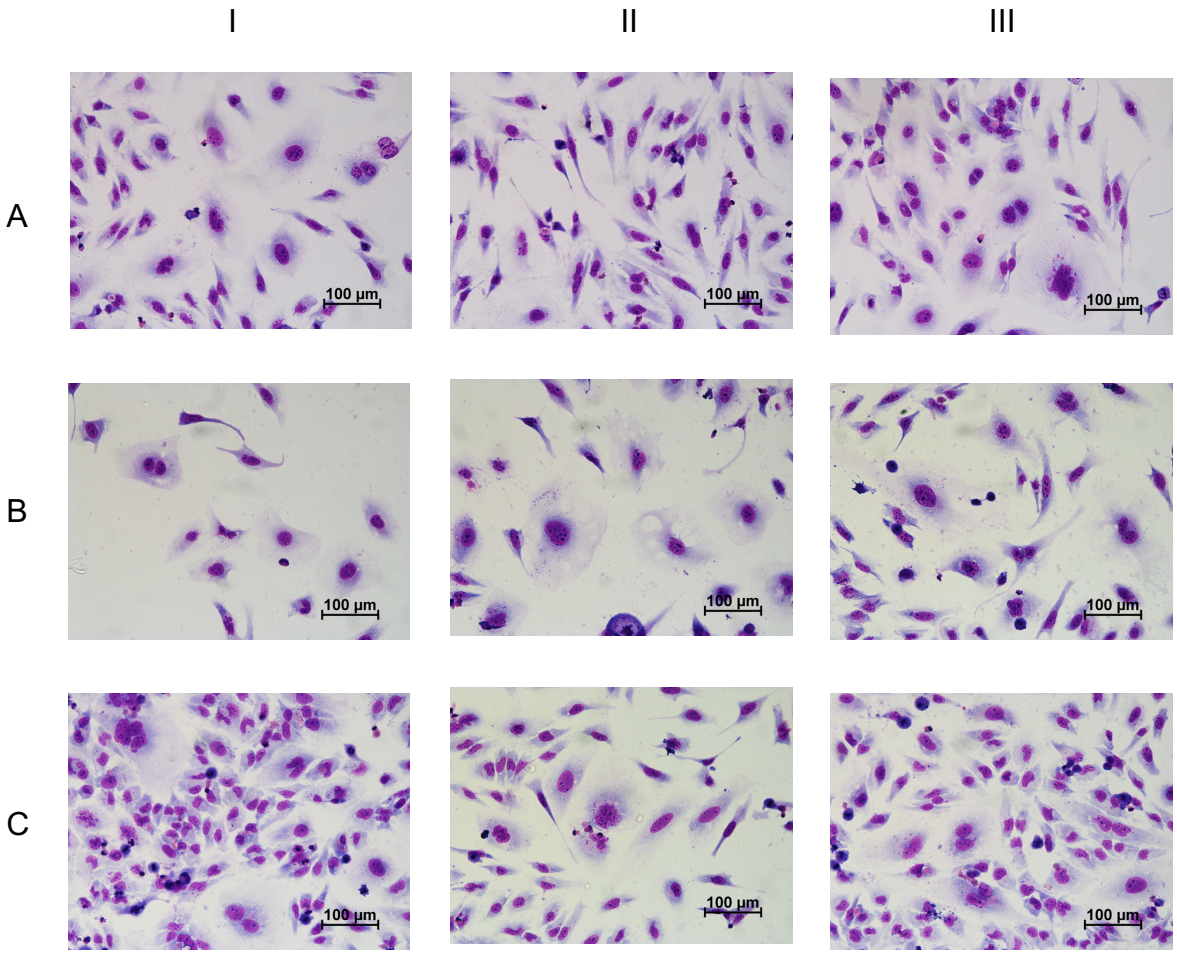

Figure S2.1b Giemsa staining of HeLa cells infected with *E. coli* IHE3034 (*pks* positive). A, B, and C represent biological replicates. Three images of each sample were taken (represented by I, II, and III). Photos were taken after 72 hours post infection time of 4 hrs at 40X of magnification. Cells were incubated at 37°C and 5 % CO_2.

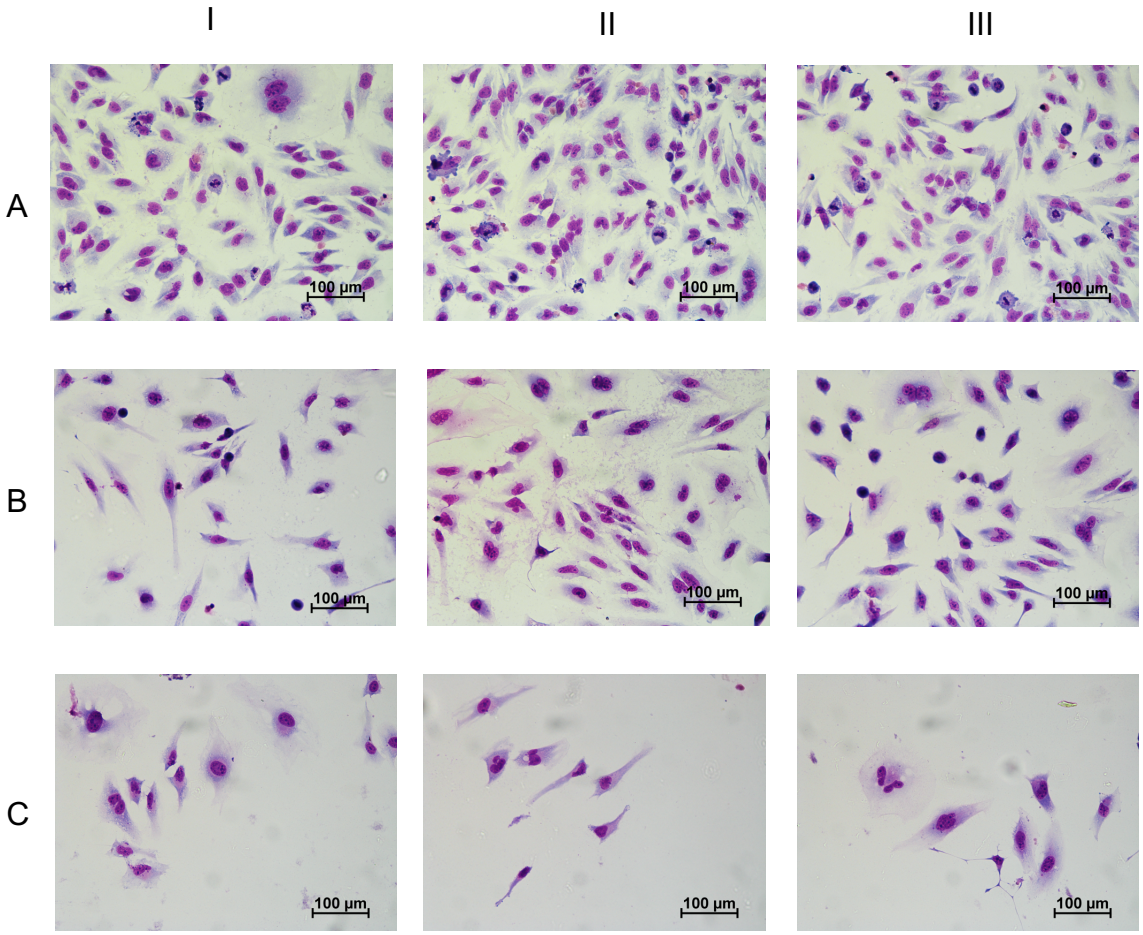

Figure S2.1c Giemsa staining of HeLa cells infected with *E. coli* IHE3034 Δ*clbP* (mutant). A, B, and C represent biological replicates. Three images of each sample were taken (represented by I, II, and III). Photos were taken after 72 hours post infection time of 4 hrs at 40X of magnification. Cells were incubated at 37°C and 5 % CO_2.

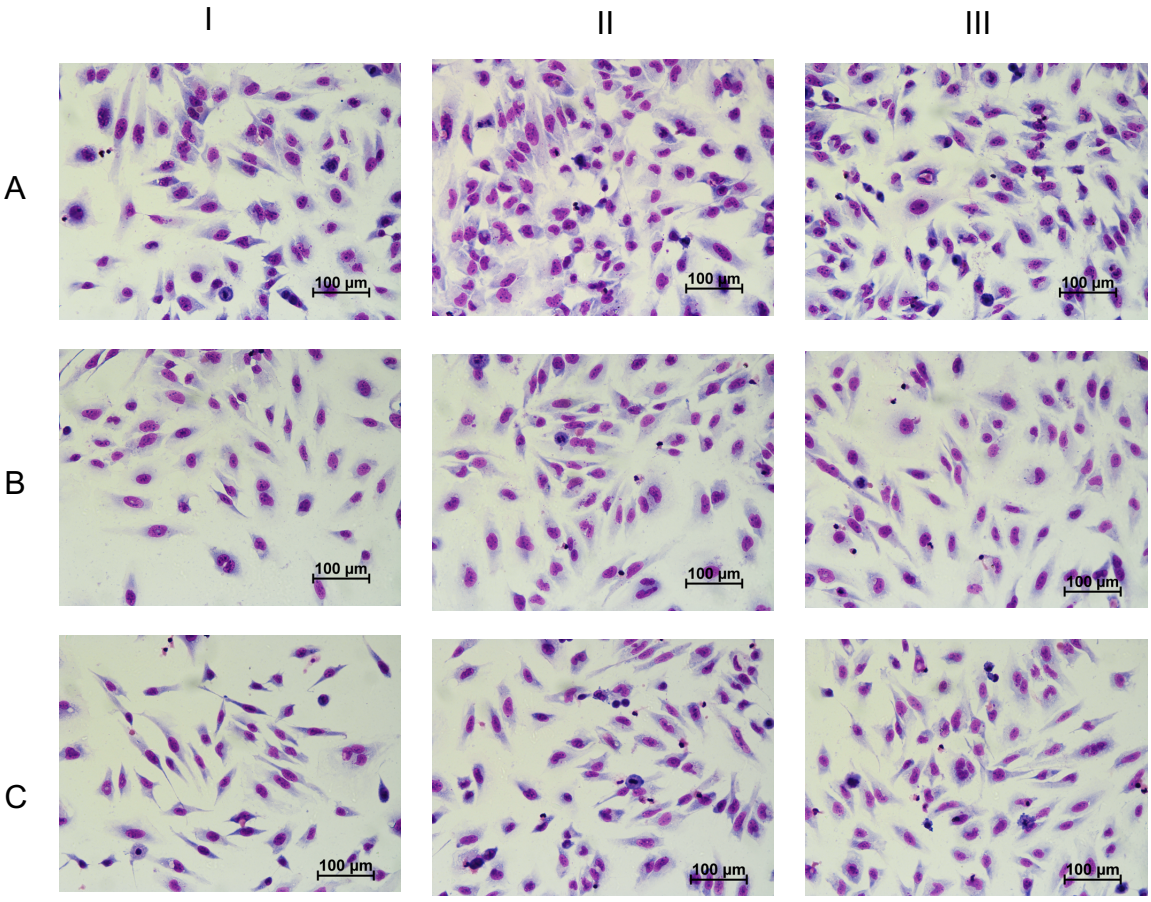

Figure S2.1d Giemsa staining of HeLa cells infected with *E. coli* DH10B (*pks* negative control). A, B, and C represent biological replicates. Three images of each sample were taken (represented by I, II, and III). Photos were taken after 72 hours post infection time of 4 hrs at 40X of magnification. Cells were incubated at 37°C and 5 % CO_2.

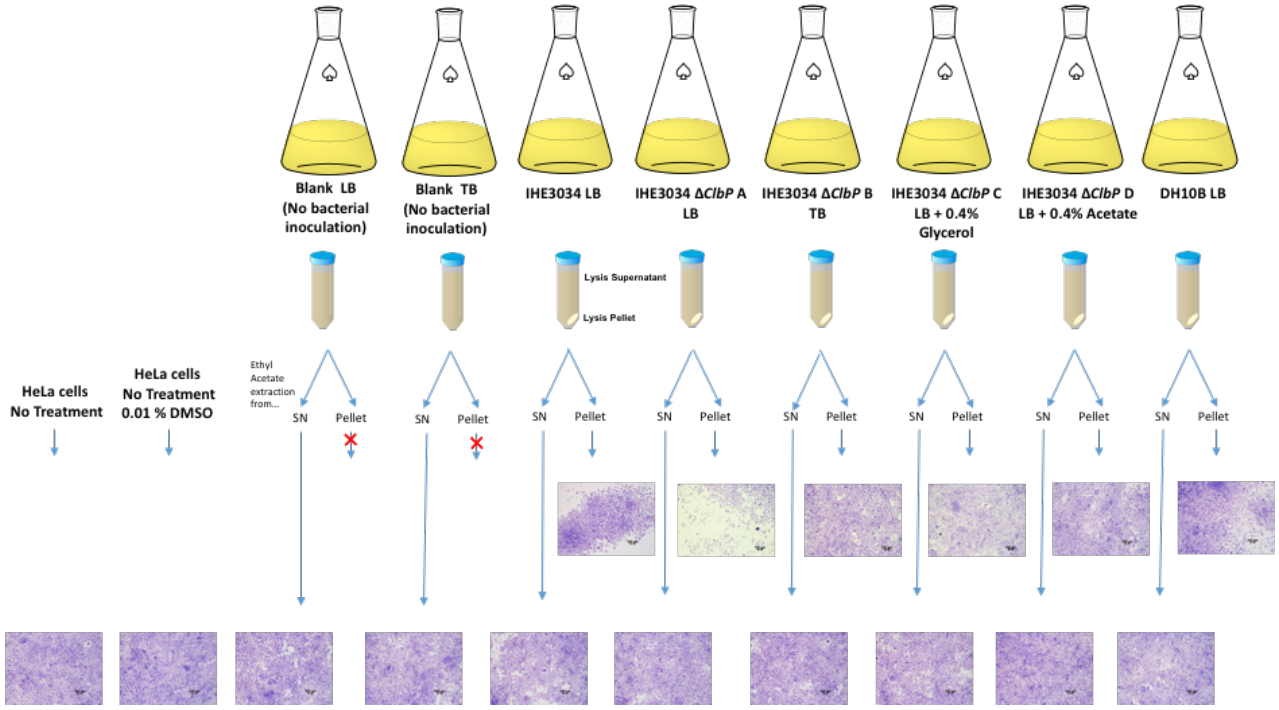

Figure S2.2 Giemsa staining of HeLa cells treated with organic extracts from *pks* positive and *pks* negatives *E. coli* strains. Experimental diagram of biological assay of ethyl acetate extract from *pks*+ and *pks*- *E. coli* strains on HeLa cells. Cells were treated with extract by a co-incubation of 4 hours at 37 ºC and 5 % CO_2. Photos were taken after 72 hours post treatment at 4X of magnification. Three images of each sample were taken, but just one representative image was used in this figure. All extracts were re-suspended in DMSO.

Chapter 3. Colibactin Does Not Affect the Bacterial Envelope of Its Producer Bacteria.

Abstract

The production of colibactin takes place in two stages: an inactive version of the compound is built in the cytoplasm and exported to the periplasmic space, where it is further matured by the ClbP peptidase. It has been shown that the deletion of *clbP* disrupts the maturation of colibactin, thus promoting the accumulation in the periplasmic space of numerous biosynthesis intermediates, some of which have been characterized chemically. To date, no one has reported the effect of such an accumulation of intermediates on the cellular morphology of the producing *E. coli* bacterium. In this work, we deleted *ClbP* expecting that an accumulation of compounds would cause a weakening of the bacterial envelope possibly manifested by morphological changes that could be readily detected by SEM. Here we present the first scanning electron microscopy images of a colibactin producer: the clinical strain *E. coli* IHE3034. The images of the colibactin producer were compared with those of a strain that cannot produce mature colibactin since it lacks ClbP. We show that the accumulation of colibactin intermediates does not have an effect on *E. coli* morphology or growth, indicating a quick metabolism of the incomplete toxin.

3.1 Introduction

The production of colibactin requires the group of enzymes encoded in the *pks* island which build the compound from acyl or amino-acyl units in successive Claisen-type condensation reactions[1]. The end-product of these reactions is the formation of the inactive compound known as pre-colibactin, which is readily exported into the periplasmic space by the transporter ClbM[2]. Once in the periplasmic space, the peptidase ClbP[3–6] hydrolyzes a portion of the inactive precursor to yield active colibactin.

It has been shown that the deletion of *clbP* results in the accumulation of colibactin intermediates[7]. In fact, the deletion of *clbP* has been used to increase the production and yield of intermediates for the elucidation of their structure. However, it is not known which effects, if any, this accumulation of colibactin precursors could have on the outer membrane of the producing bacteria.

Our laboratory has been interested in assessing the effects of colibactin on the producing bacteria, especially any effects on the integrity of the outer membrane. In this work, we compare SEM micrographs of various clinical isolates of *E. coli*, collected from Puerto Rico hospitals in order to compare membrane phenotypes between *pks*$^+$ and *pks*$^-$ isolates. We also performed the deletion of the *clbP* gene to induce the accumulation of colibactin precursors and to assess whether such accumulation would cause membrane disruptions. Our SEM images revealed the presence of membrane lesions, which seemed to be more frequent in *pks*$^+$ bacterial isolates. However, the

comparison between wild-type and Δ*clbP* variants revealed no membrane lesions, suggesting that the presence of membrane lesions in the clinical isolates is not related to colibactin production.

3.2 Materials and Methods

3.2.1 Strains. *E. coli* clinical isolates, both *pks*$^+$ and *pks*$^-$, were obtained as part of a carbapenem-resistance repository from hospitals in Puerto Rico [8]. *E. coli* IHE3034 *pks*$^+$ was kindly donated by Dr. Eric Oswald from the University of Toulouse, France. The *E. coli* DH10B *pks*$^-$ (non-genotoxic) was used in all the experiments as a control strain. All strains, including the Δ*clbP* mutant (detailed in chapter 2, section 2.2.1.2) were "re-animated" from cryogenic storage in lysogenic broth (LB) medium (Sigma-Aldrich) agar for 16-24 hours at 37 °C. Colonies were then selected and grown in LB. Culture conditions are specific according to the experiment or assay requirements.

3.2.2 Scanning electron microscopy (SEM). Samples for SEM analysis were prepared and processed as reported by Piroeva *et al*. Following is a brief description of each step.[9]

Bacterial growth. Exponential growth was achieved overnight in Luria-Bertani medium at 37 ^oC and 250 rpm. Bacterial samples were collected by centrifugation of the growth cultures at 3500 rpm for 5 min, followed by two pellet washes with ddH2O. Finally, 5–20 µL of sterile and filtered water were added and the pellet was carefully homogenized, thus ready for fixation for electron microscopy observation.

Sample fixation and dehydration. A coverslip (18 x 18 mm^2), sterilized by UV irradiation for 10 minutes, was used as a platform for bacterial fixation. The coverslip was dipped in 0.8 % agar solution and left horizontally, allowing the thin agar film to materialize for 30 minutes. Bacterial samples were carefully placed on the agar film and allowed to settle for 45 minutes. The samples were then dehydrated in an oven at 37 °C for 12 hours. Samples were processed by successive immersion in ethanol solutions from low to high concentrations (10, 25, 50, 75, 96, and 99 %). Samples were maintained in each ethanol solution for at least 30 minutes. Finally, samples were dried at 37 °C for about 1 hour.

Gold coating. Fixed and dehydrated samples are coated with a thin gold film (~10 nm) using a metal sputter system.

Scanning electron microscope (SEM) analysis. SEM analysis was performed with the high-resolution field emission scanning electron microscope (JEOL JSM-7500F SEM), using 2 kV (unless otherwise specified) acceleration voltage for a gentle electron beam. The sample (coverslip) was mounted on a double-coated conductive carbon tape that holds the sample firmly to the stage surface and a copper tape was placed as a ground strap from the sample surface to the SEM sample holder.

3.2.3 SEM micrograph analysis. The SEM images were analyzed in order to measure the area and length of *E. coli* cells, with the NIS-Element Advance Research Imaging Software (version 5.20) using the area defining line and the straight line tool

respectively, together with the manual measure function. Measurements were calibrated using the scale bars on the image and the scale function.

Values were reported as means ± standard error means of biological replicates unless otherwise specified. *P*-values were calculated using one-way analyses of variance (ANOVA) with the "Tukey's Multiple Comparison" test for multiple comparisons. All statistical analyses were conducted using Prism 6 software (GraphPad, La Jolla, CA, United States).

3.3 Results

3.3.1 SEM images of *pks*$^+$ and *pks*$^-$ clinical isolates.

We were initially driven to study the effect of colibactin production and accumulation on *E. coli* morphology, from examining the scanning electron micrographs (SEM) for several clinical isolates of *pks*$^+$ and *pks*$^-$ bacteria from a local strain repository at the University of Puerto Rico Medical School (Figure 3.1). From these electron microscopy images, it was easy to identify lesions on the surface of the *E. coli* bacteria which were detected almost exclusively in the *pks*$^+$ isolates but absent in the *pks*$^-$ isolates. The apparent damage observed on the *E. coli* envelope of *pks*$^+$ strains was not different from the damage caused by the application of an antimicrobial peptide or by membrane-disrupting quantum dots reported elsewhere[10].

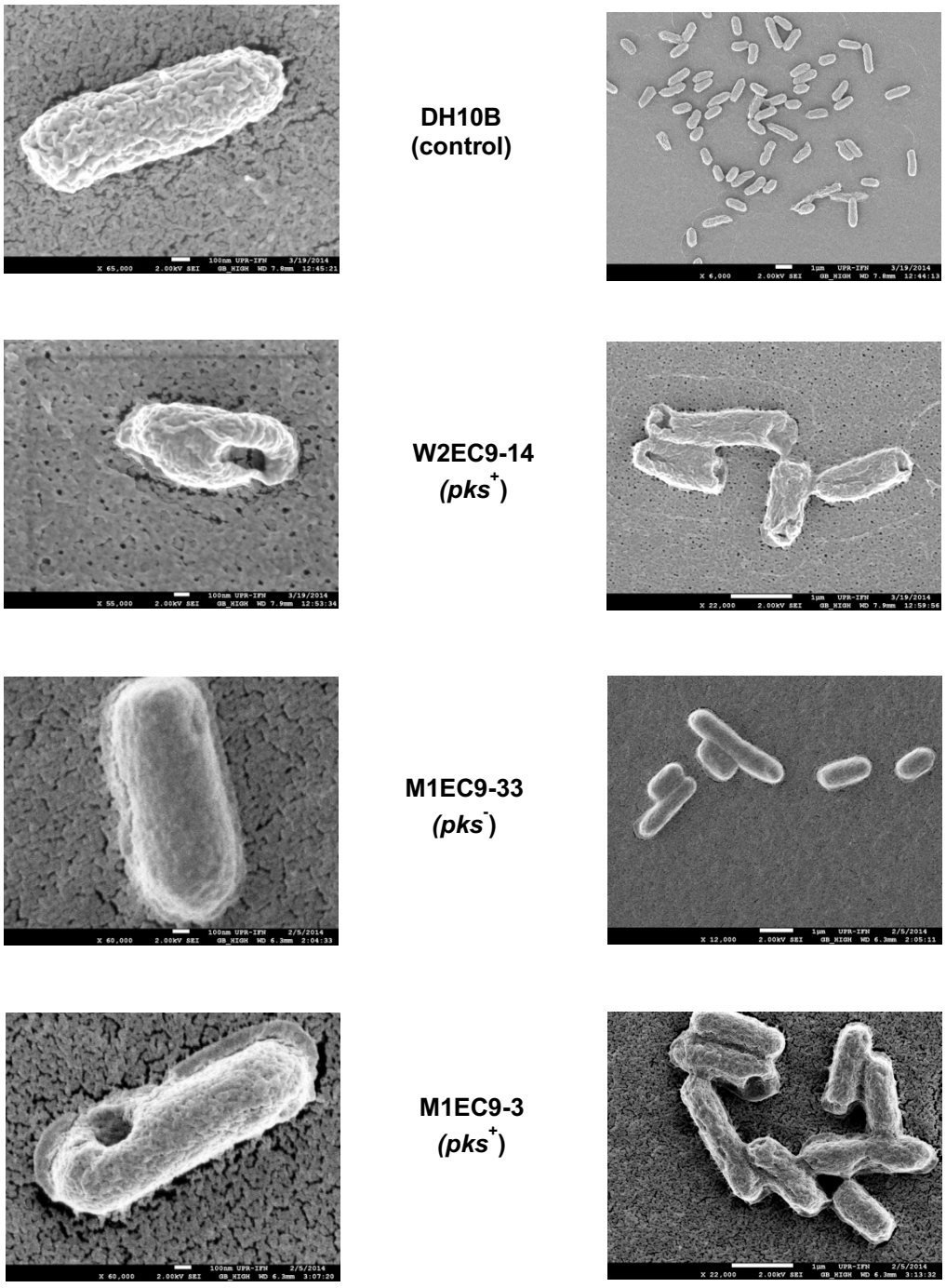

Figure 3.1: SEM images of *pks*- and *pks*+ clinical isolates obtained from a local pathogen surveillance repository. The cells were grown in LB medium at 37 ^{o}C, overnight. Fixation, dehydration, and gold coating of the samples were carried out on a glass surface coverslip. *Pks*+ *E. coli* clinical isolates show membrane surface imperfection in comparison with strains without *pks* genes.

3.3.2 SEM images of wild type IHE3034 and IHE3034 Δ*clbP E. coli.*

SEM images were collected for the IHE3034 wild-type and mutant strains to evaluate the effect of either colibactin production or accumulation on bacterial membrane following the same protocols employed for viewing the locally sourced strains. We expected that the deletion of the *clbP* gene would induce outer-membrane damage due to the accumulation of colibactin intermediates. To our surprise, the electron microscopy images of IHE3034 and IHE3034 Δ*clbP* revealed no morphological effect expected from the disruption of colibactin production. SEM micrographs shows heterogeneous (spherical and bacillus, Figure 3.2A-B) morphologies with a mean area of 0.68-0.80 μm^2 (Table 3.1) for both IHE3034 strains and the DH10B non-pathogenic strain without significant differences (*p*-value 0.0880; Figure 3.2C; Table 3.1). Bacterial length measurements also reveal no significant differences (*p*-value 0.711) between pathogenic strains (IHE3034) and the laboratory strain DH10B (Figure 3.2D, Table 3.1). Thus, neither the production of colibactin nor the accumulation of its intermediates affects the bacterial membrane integrity.

Table 3.1. Bacterial cell area and length for IHE3034, IHE3034 Δ*clbP* and, DH10B *E. coli* strains.

E. coli Strain		Cell Area				Cell Length			
		Mean Cell Area (μm^2)	Std Dev	Average Area (μm^2)	Std Dev	Mean Cell Length (μm)	Std Dev	Average Length (μm)	Std Dev
IHE3034	**A**	0.8	0.20	0.80	0.05	1.25	0.28	1.28	0.03
	B	0.85	0.21			1.31	0.31		
	C	0.75	0.18			1.27	0.31		
IHE3034 Δ*clbP*	**A**	0.82	0.22	0.78	0.06	1.25	0.33	1.24	0.03
	B	0.82	0.27			1.27	0.39		
	C	0.71	0.17			1.21	0.31		
DH10B	**A**	0.63	0.15	0.68	0.06	1.31	0.29	1.35	0.06
	B	0.68	0.21			1.31	0.35		
	C	0.74	0.23			1.42	0.37		

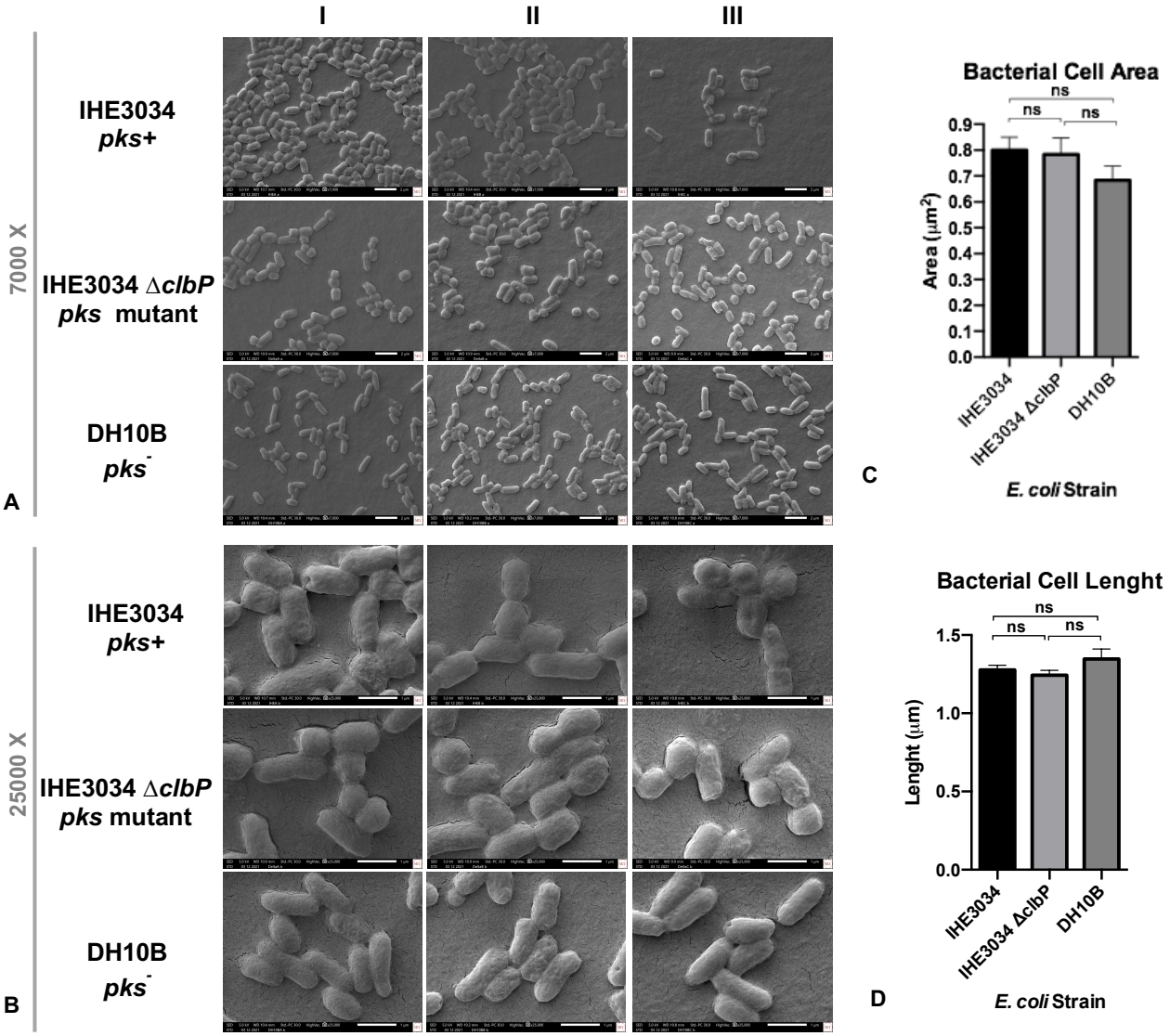

Figure 3.2: SEM images of IHE3034 *(pks⁺)* and its isogenic mutant strain Δ*clbP* vs DH10B (negative control), after 16 hours of incubation at 37 °C without antibiotic. Columns I, II and III are photos taken from biological replicates at A) 7000X and B) 25000X of magnification. Fixation, dehydration and gold coating of the samples were carried out on a glass surface coverslip. C) Area measurement analysis using micrograph taken at 7000X D) length measurement analysis using micrograph taken at 7000X. Both analysis were performed using NIS Element Software. Statistical analysis was performed using one-way ANOVA using GraphPad Prism (version 6.0) software.

3.4 Discussion

The genotoxic bacterial compound known as colibactin induces DNA damage[11,12], mutations[13] and promotes the development of tumors in mouse models[14,15], thus has been linked to colorectal cancer. Although the *pks* genes are more frequently found in individuals with colorectal cancer, the genes are also widely distributed in our population. Roughly 20 % of healthy individuals harbor the *pks* genes in their gut microbiota[16]. In a survey of bacteria isolated from infections acquired in Puerto Rico hospitals, our group found the *pks* island to be present in 10% of isolates (Baerga-Ortiz, personal communication). We now compare the SEM micrographs of these *pks*+ and *pks*- clinical strains isolated from Puerto Rico hospitals and report some variability with respect to membrane integrity in these samples. Initially, we observed the presence of membrane lesions that seemed to be only found in the *pks*+ isolates, thus raising the hypothesis of an association between colibactin production and membrane disruption.

If the instability of the outer membrane is related to the production of colibactin, then the deletion of the *clbP* gene should have resulted in clear membrane phenotypes. The deletion of *clbP* is known to cause the accumulation of colibactin intermediates while abolishing the production of mature active colibactin[17]. Our work attempted to document the effect of such accumulation of the polyketide/peptide intermediates of colibactin within the periplasmic space of the producing bacteria. However, the deletion of *clbP* did not induce the formation, nor any other morphological manifestation. Thus, the differences in membrane lesions observed in the clinical isolates cannot be attributed to

the presence or absence of the *pks* genes, since neither the wild type IHE3034 strain nor its *ΔclbP* mutant strain showed the expected morphological changes.

The hydrolase activity of clbP peptidase has been found to be highly variable even between *pks*$^{+}$ strains of *E. coli*. Hirayama *et. al.* recently reported that not all clbP peptidases have the same degree of enzymatic activity, with some variants being highly active and other variants on the verge of inactivity[18,19]. At present we have no evidence of how active the clbP peptidase is on our *E. coli* clinical isolates or in the IHE3034 strain that we used. However, this parameter could be critical in assessing the conversion of active colibactin and its possible interactions with the membrane.

3.5 References

(1) Li, Z.; Li, J.; Cai, W.; Lai, J. Y. H.; Mckinnie, S. M. K.; Zhang, P.; Moore, B. S.; Zhang, W.; Qian, P. Macrocyclic Colibactin Induces DNA Double-Strand Breaks via Copper-Mediated Oxidative Cleavage. *Nat. Chem.* **2019**, *11* (10), 880–889. https://doi.org/10.1038/s41557-019-0317-7.

(2) Mousa, J. J.; Yang, Y.; Tomkovich, S.; Shima, A.; Newsome, R. C.; Tripathi, P.; Oswald, E.; Bruner, S. D.; Jobin, C. MATE Transport of the E. Coli-Derived Genotoxin Colibactin. *Nat. Microbiol.* **2016**, *1* (1), 15009. https://doi.org/10.1038/nmicrobiol.2015.9.

(3) Dubois, D.; Baron, O.; Cougnoux, A.; Delmas, J.; Pradel, N.; Boury, M.; Bouchon, B.; Bringer, M. A.; Nougayrède, J. P.; Oswald, E.; Bonnet, R. ClbP Is a Prototype of a Peptidase Subgroup Involved in Biosynthesis of Nonribosomal Peptides. *J.*

Biol. Chem. **2011**, *286* (41), 35562–35570. https://doi.org/10.1074/jbc.M111.221960.

(4) Cougnoux, A.; Gibold, L.; Robin, F.; Dubois, D.; Pradel, N.; Darfeuille-Michaud, A.; Dalmasso, G.; Delmas, J.; Bonnet, R. Analysis of Structure-Function Relationships in the Colibactin-Maturating Enzyme ClbP. *J. Mol. Biol.* **2012**, *424* (3–4), 203–214. https://doi.org/10.1016/j.jmb.2012.09.017.

(5) Brotherton, C. A.; Balskus, E. P. A Prodrug Resistance Mechanism Is Involved in Colibactin. *J. Am. Chem. Sociaty* **2013**, *135*, 3359–3362. https://doi.org/10.1021/ja312154m.

(6) Bian, X.; Fu, J.; Plaza, A.; Herrmann, J.; Pistorius, D.; Stewart, A. F.; Zhang, Y.; Müller, R. In Vivo Evidence for a Prodrug Activation Mechanism during Colibactin Maturation. *ChemBioChem* **2013**, *14* (10), 1194–1197. https://doi.org/10.1002/cbic.201300208.

(7) Wernke, K. M.; Xue, M.; Tirla, A.; Kim, C. S.; Herzon, S. B.; Crawford, J. M. Structure and Bioactivity of Colibactin. *Bioorg. Med. Chem. Lett.* **2020**, *30* (15), 127280. https://doi.org/10.1016/j.bmcl.2020.127280.

(8) Robledo, I. E.; Aquino, E. E.; Vázquez, G. J. Detection of the KPC Gene in Escherichia Coli, Klebsiella Pneumoniae, Pseudomonas Aeruginosa, and Acinetobacter Baumannii during a PCR-Based Nosocomial Surveillance Study in Puerto Rico. *Antimicrob. Agents Chemother.* **2011**, *55* (6), 2968–2970. https://doi.org/10.1128/AAC.01633-10.

(9) Piroeva, I.; Atanassova-Vladimirova, S.; Dimowa, L.; Sbirkova, H.; Radoslavov, G.; Hristov, P.; Shivachev, B. L. A Simple and Rapid Scanning Electron

Microscope Preparative Technique for Observation of Biological Samples: Application on Bacteria and DNA Samples. *Bulg. Chem. Commun.* **2013**, *45* (4), 510–515. https://doi.org/10.1002/jemt.10184.

(10) Hartmann, M.; Berditsch, M.; Hawecker, J.; Ardakani, M. F.; Gerthsen, D.; Ulrich, A. S. Damage of the Bacterial Cell Envelope by Antimicrobial Peptides Gramicidin S and PGLa as Revealed by Transmission and Scanning Electron Microscopy. *Antimicrob. Agents Chemother.* **2010**, *54* (8), 3132–3142. https://doi.org/10.1128/AAC.00124-10.

(11) Cuevas-Ramos, G.; Petit, C. R.; Marcq, I.; Boury, M.; Oswald, E.; Nougayrède, J.-P. Escherichia Coli Induces DNA Damage in Vivo and Triggers Genomic Instability in Mammalian Cells. *Proc. Natl. Acad. Sci. U. S. A.* **2010**, *107* (25), 11537–11542. https://doi.org/10.1073/pnas.1001261107.

(12) Nougayrède, J.-P.; Homburg, S.; Taieb, F.; Boury, M.; Brzuszkiewicz, E.; Gottschalk, G.; Buchrieser, C.; Hacker, J.; Dobrindt, U.; Oswald, E. Escherichia Coli Induces DNA Double-Strand Breaks in Eukaryotic Cells. *Science.* **2006**, *313* (5788), 848–851. https://doi.org/10.1126/science.1127059.

(13) Pleguezuelos-Manzano, C.; Puschhof, J.; Rosendahl Huber, A.; van Hoeck, A.; Wood, H. M.; Nomburg, J.; Gurjao, C.; Manders, F.; Dalmasso, G.; Stege, P. B.; Paganelli, F. L.; Geurts, M. H.; Beumer, J.; Mizutani, T.; Miao, Y.; van der Linden, R.; van der Elst, S.; Ambrose, J. C.; Arumugam, P.; Baple, E. L.; Bleda, M.; Boardman-Pretty, F.; Boissiere, J. M.; Boustred, C. R.; Brittain, H.; Caulfield, M. J.; Chan, G. C.; Craig, C. E. H.; Daugherty, L. C.; de Burca, A.; Devereau, A.; Elgar, G.; Foulger, R. E.; Fowler, T.; Furió-Tarí, P.; Hackett, J. M.; Halai, D.;

Hamblin, A.; Henderson, S.; Holman, J. E.; Hubbard, T. J. P.; Ibáñez, K.; Jackson, R.; Jones, L. J.; Kasperaviciute, D.; Kayikci, M.; Lahnstein, L.; Lawson, L.; Leigh, S. E. A.; Leong, I. U. S.; Lopez, F. J.; Maleady-Crowe, F.; Mason, J.; McDonagh, E. M.; Moutsianas, L.; Mueller, M.; Murugaesu, N.; Need, A. C.; Odhams, C. A.; Patch, C.; Perez-Gil, D.; Polychronopoulos, D.; Pullinger, J.; Rahim, T.; Rendon, A.; Riesgo-Ferreiro, P.; Rogers, T.; Ryten, M.; Savage, K.; Sawant, K.; Scott, R. H.; Siddiq, A.; Sieghart, A.; Smedley, D.; Smith, K. R.; Sosinsky, A.; Spooner, W.; Stevens, H. E.; Stuckey, A.; Sultana, R.; Thomas, E. R. A.; Thompson, S. R.; Tregidgo, C.; Tucci, A.; Walsh, E.; Watters, S. A.; Welland, M. J.; Williams, E.; Witkowska, K.; Wood, S. M.; Zarowiecki, M.; Garcia, K. C.; Top, J.; Willems, R. J. L.; Giannakis, M.; Bonnet, R.; Quirke, P.; Meyerson, M.; Cuppen, E.; van Boxtel, R.; Clevers, H. Mutational Signature in Colorectal Cancer Caused by Genotoxic Pks + E. Coli. *Nature* **2020**, *580* (7802), 269–273. https://doi.org/10.1038/s41586-020-2080-8.

(14) Dalmasso, G.; Cougnoux, A.; Delmas, J.; Darfeuille-Michaud, A.; Bonnet, R. Bacterial Genotoxin Colibactin Promotes Colon Tumour Growth by Inducing a Senescence-Associated Secretory Phenotype. *Gut* **2014**, *5* (5), 675–680. https://doi.org/10.4161/19490976.2014.969989.

(15) Shimpoh, T.; Hirata, Y.; Ihara, S.; Suzuki, N.; Kinoshita, H.; Hayakawa, Y. Prevalence of Pks - Positive Escherichia Coli in Japanese Patients with or without Colorectal Cancer. *Gut Pathog.* **2017**, *9*. https://doi.org/10.1186/s13099-017-0185-x.

(16) Arthur, J. C.; Perez-Chanona, E.; Mühlbauer, M.; Tomkovich, S.; Uronis, J. M.;

Fan, T.; Campbell, B. J.; Abujamel, T.; Dogan, B.; Rogers, A. B.; Rhodes, J. M.; Stintzi, A.; Simpson, K. W.; Hansen, J. J.; Keku, T. O.; Fodor, A. A.; Jobin, C. Intestinal Inflammation Targets Cancer-Inducing Activity of the Microbiota. *Science.* **2012**, *338* (6103), 120–123. https://doi.org/10.1126/science.1224820.Intestinal.

(17) Vizcaino, M. I.; Engel, P.; Trautman, E.; Crawford, J. M. Comparative Metabolomics and Structural Characterizations Illuminate Colibactin Pathway-Dependent Small Molecules. *J. Am. Chem. Sociaty* **2014**, *136* (26), 9244–9247. https://doi.org/10.1021/ja503450q.

(18) Zhou, T.; Hirayama, Y.; Tsunematsu, Y.; Suzuki, N.; Tanaka, S.; Uchiyama, N.; Goda, Y.; Yoshikawa, Y.; Iwashita, Y.; Sato, M.; Miyoshi, N.; Mutoh, M.; Ishikawa, H.; Sugimura, H.; Wakabayashi, K.; Watanabe, K. Isolation of New Colibactin Metabolites from Wild-Type Escherichia Coli and in Situ Trapping of a Mature Colibactin Derivative. *J. Am. Chem. Soc.* **2021**, *143* (14), 5526–5533. https://doi.org/10.1021/jacs.1c01495.

(19) Hirayama, Y.; Tsunematsu, Y.; Yoshikawa, Y.; Tamafune, R.; Matsuzaki, N.; Iwashita, Y.; Ohnishi, I.; Tanioka, F.; Sato, M.; Miyoshi, N.; Mutoh, M.; Ishikawa, H.; Sugimura, H.; Wakabayashi, K.; Watanabe, K. Activity-Based Probe for Screening of High-Colibactin Producers from Clinical Samples. *Org. Lett.* **2019**, *21* (12), 4490–4494. https://doi.org/10.1021/acs.orglett.9b01345.

Chapter 4. Physicochemical Properties of Outer Membrane Vesicles from colibactin-producing *Escherichia coli*

Abstract

The *pks* genomic island is a set of genes that encode the production of colibactin in some strains of *E. coli* and other proteobacteria commonly found in the human gut. Colibactin is known for eliciting a variety of effects on the host cells that it contacts. It is synthetized in the bacterial cytosol and converted into its active version by the peptidase clbP, in the periplasmic space. Since the production of colibactin takes place in the space between the inner and outer membranes, we expected that the production of colibactin would affect the integrity of the bacterial envelope, causing a fundamental difference in the formation and composition of outer membrane vesicles (OMVs). Here we report the biophysical characterization of OMVs extracted from colibactin-producing *E. coli* strain IHE3034, by Dynamic Light Scattering (DLS) and by Scanning Electron Microscopy (SEM). The OMVs from IHE3034 strain were compared to the OMVs extracted from the deletion mutant, IHE3034 (Δ*clbP*), which does not produce active colibactin. We also compared the profiles of OMVs-derived proteins by SDS-PAGE and the lipid profiles by GC-MS. Our results suggest that colibactin production does not have any detectable effects on the chemical composition, size and amount of bacterial OMVs. We also checked for the presence of colibactin in OMVs by GC-MS, but we were unable to identify specific signals associated with colibactin. From this effort, we concluded that the production of colibactin does not have an effect on the production or on the properties of OMVs isolated from *E. coli*.

4.1 Introduction

Colibactin is a secondary metabolite produced by *E. coli* and other proteobacteria, including those residing in the human gut[1,2]. Bacteria that make colibactin can induce genotoxicity towards the host cells upon contact, and the presence of these bacterial strains in the human gut has been linked with colorectal carcinogenesis[3–5]. This genotoxin is made in the bacterial cytosol as a pre-colibactin precursor by a series of enzymes encoded in the *pks* genomic island and translocated to the periplasmic space through the transmembrane MATE transporter, clbM[6]. In this inter-membrane space, pre-colibactin is processed and activated by the peptidase clbP[7–10]. Exactly how colibactin is exported out of the bacteria after its activation, and which effects it may have on the bacterial envelope, remain unknown.

Bacteria have evolved various types of secretion mechanisms for the release of proteins, toxins, DNA, among other virulence and survival factors, in order to adapt to different enviroments[11]. These secretion systems are classified based on the mechanism of translocation across the membranes[11,12]. One of the mechanisms by which periplasmic content is released is by way of outer membrane vesicles (OMVs). OMVs are biological nanoparticles of 50 to 250 nm in diameter produced naturally by all gram-negative bacteria[13,14]. They are composed of proteins, phospholipids, and lipopolysaccharides (from the outer membrane of the producer bacteria) in a spherical arrangement[14,15]. These proteoliposomes provide the ideal environment to protect the encapsulated cargo from degradation until they reach their target[16,17]. OMVs are produced by both pathogenic and non-pathogenic bacteria[18,19]. However, OMVs have important biological roles in pathogenesis and intercellular interactions through the

transportation of virulence and pathogenic factors[20]. In fact, a correlation has been shown between OMV overproduction and bacterial pathogenicity[21,22].

Despite all the evidence regarding the colibactin biosynthetic route and its toxicity toward host cells, there is a lack of information on how colibactin is exported out of the bacterial cell. Since colibactin is made in the periplasmic space, it is possible that its export is guided by OMVs and linked with OMV production (Figure 4.1). With this in mind, in this chapter we report the production of OMVs in the clinical isolate *E. coli* IHE3034, a natural colibactin producer and compare it with the production of OMVs in a deletion mutant, IHE3034 (Δ*clbP*) which is incapable of producing active colibactin. We analyzed the amount, size, shape and lipid composition of OMVs, looking for differences attributable to colibactin production. Our data indicate that colibactin production does not have any effect on the production and composition of OMVs. We also attempted to find colibactin in isolated OMVs but found no signals consistent with the presence of active colibactin or pre-colibactin in OMVs.

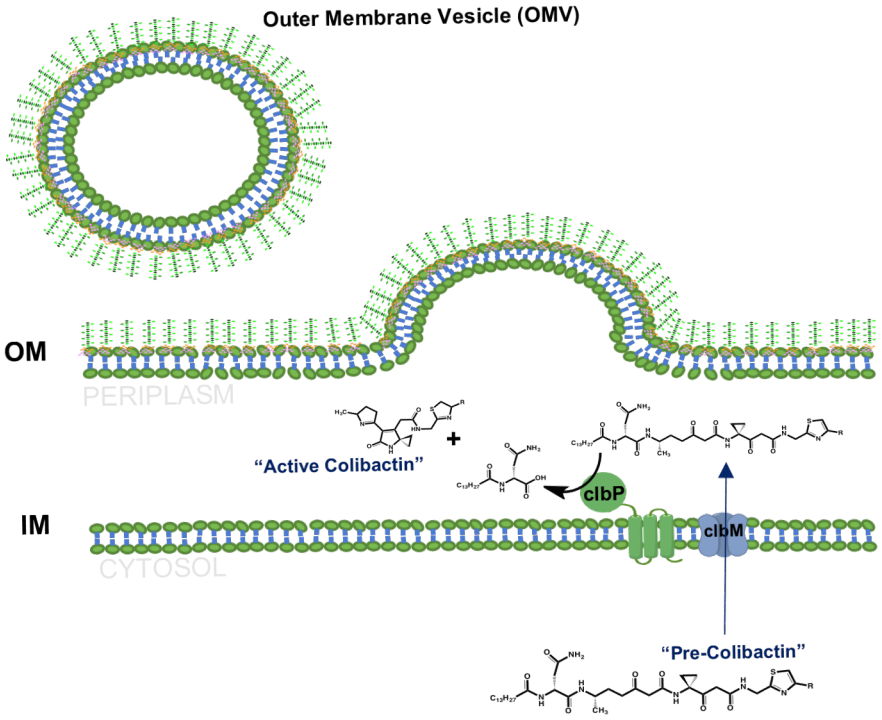

Figure 4.1. Schematic representation of the maturation of colibactin and its possible interaction with the OMVs of its producer bacteria. Colibactin is made in the bacterial cytoplasm as a precursor compound named pre-colibactin, which is translocated to the periplasmic space through the transporter protein clbM. Once in the periplasm, it is converted to active colibactin by the enzyme clbP.

4.2 Materials and Methods

4.2.1 Bacterial Strains. *E. coli* IHE3034 *pks*$^{+}$ was kindly donated by Dr. Eric Oswald from the University of Toulouse, France. The *E. coli* DH10B *pks*$^{-}$ (non-genotoxic) was used in all the experiments as a control strain. All strains, including the Δ*clbP* mutant (detailed in chapter 2, section 2.2.1.2) were "re-animated" from cryogenic storage in lysogenic broth (LB) medium (Sigma-Aldrich) agar for 16- 24 hours at 37 °C. Colonies were then selected and grown in liquid LB. Culture conditions are specific according to the experiment or assay requirements.

4.2.2 Isolation of OMVs. OMVs isolation methodology was adapted from Tyrer et al.[18] *E. coli* bacterial strains were grown in 250 mL of lysogenic broth medium (Sigma-Aldrich) pH 7.4 at 37 ^{o}C under constant rotation (120 rpm) for 18-20 hrs. The cultures were centrifuged at 4 ^{o}C, 5,000 rpm for 10 minutes. The resulting supernatants were collected and filtered by a 0.45 µm PVDF membrane (Stericup Durapore Cat. No. S2HVU02RE), and then ultra-centrifuged at 4 ^{o}C, 40,000 rpm for 3 hrs to obtain the OMV pellet (200 mL of culture OMV pellet). The resultant pellet was washed twice using TBS (TRIS-Saline Buffer; 50 mM TRIS, 150 mM NaCl, pH 8.4) and re-ultracentrifuge under the same conditions. OMV pellet was then re-suspended up to 1 mL of TBS and re-filter by a 0.45 µm PVDF membrane (SIGMA Cat. No. UFC30HV00). Samples were stored at 4 ^{o}C until further analysis.

4.2.3 OMV Production Quantification. The quantification of OMVs was performed by measuring its associated proteins[23–26]using the BCA Assay (Pierce BCA Protein Assay Kit, Prod. #23225) as described in the manufacturer's instructions. OMV isolates were

mixed with the bicinchoninic acid reagent and measured in a 96-well plate (UV Flat bottom Microtiter plates Cat No. 8404) using a photometric plate reader at 562 mm wavelength. A calibration curve using bovine serum albumin (BSA) was used.

4.2.4 Physicochemical characterization of OMVs by Dynamic Light Scattering (DLS). Malvern ZetaSizer Nano series ZS with 4 mW 632.8 nm laser was used to determine the average apparent hydrodynamic diameter of OMVs. Briefly, OMV isolates were diluted in a 1:10 ratio using 1X TBS (50 mM TRIS, 50 mM NaCl, pH 8.4). Then 1 mL of sample was added to a disposable plastic cuvette. The backscattering mode was used in triplicate for all the samples, and the z-average (i.e., hydrodynamic radius) and polydispersity index (PDI) were recorded.

4.2.5 Physicochemical characterization of OMVs by Scanning Electron Microscopy (SEM). The methodology used for OMV visualization by SEM was adapted from our previous study (See Chapter 3, section 3.1.2)[27]. Briefly, 5-10 µL of OMVs were resuspended in water and placed on the 0.8 % agar film and allowed to settle for 45 minutes. The film was then dehydrated in an oven at 37 ^{o}C for 12 hrs and immersed in ethanol solutions from low to high concentrations (10, 25, 50, 75, 96, and 99.99 %) and subsequently dried at 37 ^{o}C for 1 hour. The samples were then coated with a thin gold film (~10 nm) and analyzed in a JEOL 6480 LV scanning electron microscopy (SEM) using an ultra-high resolution field emission focused ion beam system, with 20 kV.

The SEM images were analyzed to determine the area and length of *E. coli* cells, with the NIS-Element Advance Research Imaging Software (version 5.20) using the area defining line and the straight line tool respectively, together with the manual measure

function. Measurements were calibrated using the scale bars on the image and the scale function. Values were reported as means ± standard error means (SEM) of biological replicates. *P*-values were calculated using one-way analyses of variance (ANOVA) with "Tukey's Multiple Comparison" test for multiple comparisons. All statistical analyses were conducted using Prism 6 software (GraphPad, La Jolla, CA, United States).

4.2.6 Fatty acid content of OMVs and bacterial cells. Acidic methanolysis was used to esterify fatty acids or other membrane-anchored compounds associated to *pks island* from the harvested OMVs and bacterial strains, followed by liquid-liquid extraction with ethyl acetate for further analysis by gas chromatography-mass spectrometry (GC-MS). Briefly, ~20 mg of lyophilized OMVs were incubated under reflux with 4 mL of methanol and 2 drops of HCl for 2 hrs at 50 °C. For bacterial cells, ~100 mg of lyophilized bacteria were put in reflux with 5 mL of methanol and 3 drops of HCl for 2 hrs at 50 °C. Liquid-liquid extraction was then performed with two steps of 10 mL of ethyl acetate. The enriched organic phase was dried with magnesium sulfate and the solvent was eliminated by evaporation with nitrogen (N_2 (gas)). Once dry, all samples were stored at -20 ^{o}C under a nitrogen atmosphere for fatty acid preservation until further analysis. For analysis by GC-MS (Bruker; DB-5 COLUMN), samples were re-suspended in 157.6 µL of ethyl acetate and transferred to glass vials. Then, 42.4 µL of methyl heneicosanoate 0.322 m*M* internal standard were added for a final volume of 200 µL.

The relative composition of fatty acids was calculated as follows: First, the millimoles of each fatty acid was determined using the formulas (1) and (2) where (A_{FA}/A_{IS}) is the ratio between the peak areas for each fatty acid and the peak area for the internal

standard obtained from the gas chromatogram, C_{IS} is the known concentration of the internal standard (in m*M*) and $\frac{Vol_{total\ dilution}}{Vol_{FA\ aliquot}}$ (sample dilution for GC analysis) is the dilution factor for the final sample (in μL). From here the millimoles of each fatty acid per gram of LPS extracted were calculated and graphed using equation (3).

$$C_{FA} = \left(\frac{A_{FA}}{A_{IS}}\right) C_{IS} \quad (1)$$

$$mmol_{FA} = \frac{C_{FA}\left(\frac{Vol_{total\ dilution}}{Vol_{FA\ aliquot}}\right)}{1000} \quad (2)$$

$$\frac{mmol_{FA}}{g_{extrated\ LPS}} \quad (3)$$

Values were reported as the means of three biological replicates and statistical significance was assessed by two-way analyses of variance (ANOVA) with "Tukey's Multiple Comparison" test for multiple comparisons. All statistical analyses were conducted using Prism 6 software (GraphPad, La Jolla, CA, United States).

4.2.7 OMV Protein Profile. OMV associated proteins were separated by SDS-polyacrylamide gel electrophoresis. Briefly, a ratio of 1:1 of OMV isolates with Laemmli Sample Buffer with 5 % β-mercaptoethanol was prepared and used to load a 4-20 % Polyacrylamide gel. Samples were then analyzed by SDS page electrophoresis at 100 V for 1.5 hrs. The gel was visualized using Silver staining following the manufacture's instruction.

4.3 Results

4.3.1 Quantification of OMVs isolated from *E. coli* strains

The production of OMVs is an indirect indicator of membrane stress in gram-negative bacteria[28]. The isolated OMVs were quantified by measuring their associated bacterial proteins by the BCA assay. We included a control sample consisting of neat LB media with no *E. coli* inoculation and subjected to the whole OMV isolation process (e.g. incubation, filtration, normal and ultra-centrifugation), which we called "Process Blank."

The OMVs isolated from IHE3034 and IHE3034 Δ*clbP* were at concentrations of 0.107 ± 0.008 and 0.16 ± 0.05 mg/(mL* OD) of total protein, respectively. Statistical analysis between WT and mutant strains show no significant difference in the production of OMVs (*p*-value 0.1875). By contrast, the OMVs isolated from the laboratory strain DH10B were at a concentration of 0.41 ± 0.01 mg/(mL* OD), which was statistically higher than the concentration of OMVs from the IHE3034 strains (Figure 4.2; Table 4.1). Altogether, these results suggest that the production of colibactin or the accumulation of colibactin intermediates does not affect the production or shedding of OMVs.

Table 4.1: OMV total proteins quantification.

Sample		OD 600	Ultra-centrifugated SN (mL)	Total Proteins Conc. (µg/uL)	Proteins/OD (µg/uL)*	Average (µg/uL)	Std. Dev (µg/uL)
IHE3034	A	1.003	200	0.108	0.108	0.107	0.008
	B	0.969		0.110	0.114		
	C	0.965		0.095	0.098		
IHE3034 ΔclbP	A	0.995		0.134	0.135	0.16	0.05
	B	0.97		0.126	0.130		
	C	0.985		0.223	0.226		
DH10B	A	0.827		0.335	0.405	0.41	0.01
	B	0.801		0.327	0.408		
	C	0.823		0.355	0.431		
Process Blank	A	0.095		0.002	N/A	N/A	N/A
	B	0.009		0.008	N/A		

*Proteins concentration were normalized by the amount of cultured bacteria using the optical density parameter which is proportional to the amount of bacteria in the culture.

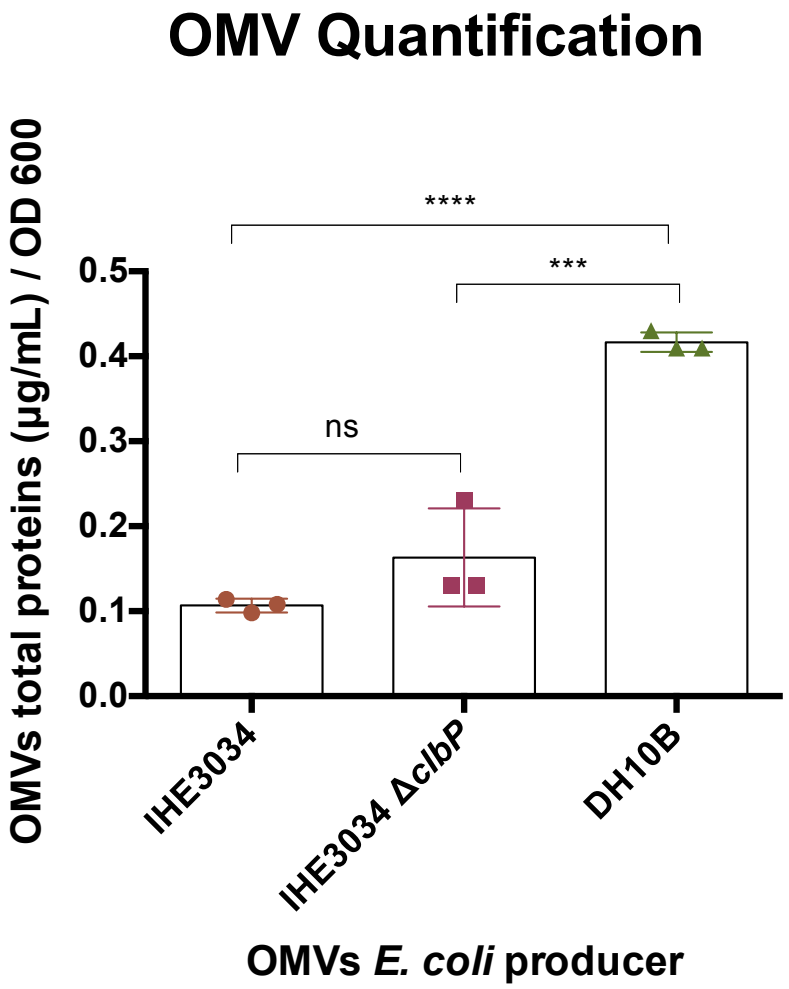

Figure 4.2. OMV quantification. Outer membrane vesicles were isolated and quantified from IHE3034, IHE3034 Δ*clbP* and DH10B *E. coli* cultures. The amount of OMVs was estimated from measurement of protein concentrations by the BCA assay (Pierce). No significant difference in OMV production was observed in IHE3034 as a result of the deletion of *clbP*. *p*-values: ns $p > 0.05$; * $p \leq 0.05$; ** $p \leq 0.01$; *** $p \leq 0.001$ and **** $p \leq 0.0001$

4.3.2 Characterization of OMV by Dynamic Light Scattering (DLS)

The presence of OMVs in the cell-free supernatants of IHE3034, IHE3034 Δ*clbP,* and DH10B *E. coli* strains was confirmed by dynamic light scattering (DLS). The DLS results showed that isolates from IHE3034, IHE3034 *ΔclbP*, and DH10B contain particles with a size distribution between 50 nm and 130 nm, within the expected range for OMVs[13,29,30]. The average hydrodynamic diameter (Z-average) of OMVs from IHE3034 and IHE3034 Δ*clbP* was 111 nm and 113 nm respectively and OMVs from DH10B laboratory strain showed a Z-average of 60 nm (Figure 4.3; Table 4.2 and 4.3).

While the distribution of OMV sizes in the IHE3034 clinical strains is homogeneous consisting of a single population, the OMVs isolated from the laboratory strain DH10B show two different populations with peaks at around 35 nm and 158 nm, revealing heterogenicity in particle sizes (Figure 4.3; Table 4.2). However, statistical analysis comparing Z-average show no significant differences (by one-way ANOVA) between OMVs from IHE3034 strains, and those from the DH10B laboratory strain (Figure 4.4). The Z-average for the process blank resulted in particle sizes of 227 nm which can only be an artifact of the DLS technique arising from buffer effects and salt content. Altogether, these results suggest that OMVs from both the IHE3034 and its isogenic *ΔclbP* mutant strains are larger on average than those isolated from the DH10B laboratory strain, and no effect on size was observed from the deletion of the *clbP* gene.

How similar or diverse are the particles in a sample can be determined by DLS measuring the polydispersity index (PDI). PDI < 0.4 implies narrow size distribution or more homogeneity and PDI > 0.4 implies broad distribution or more heterogeneity of

particles[31–33]. PDI of *E. coli* IHE3034 and its isogenic mutant isolates were low (< 0.4), indicating that particles in the solutions were homogenous in size (Table 4.3). The PDI values for the DH10B OMV and carrier control (Process Blank) were larger than 0.4, this confirming heterogeneity of particles in the samples (Table 4.3).

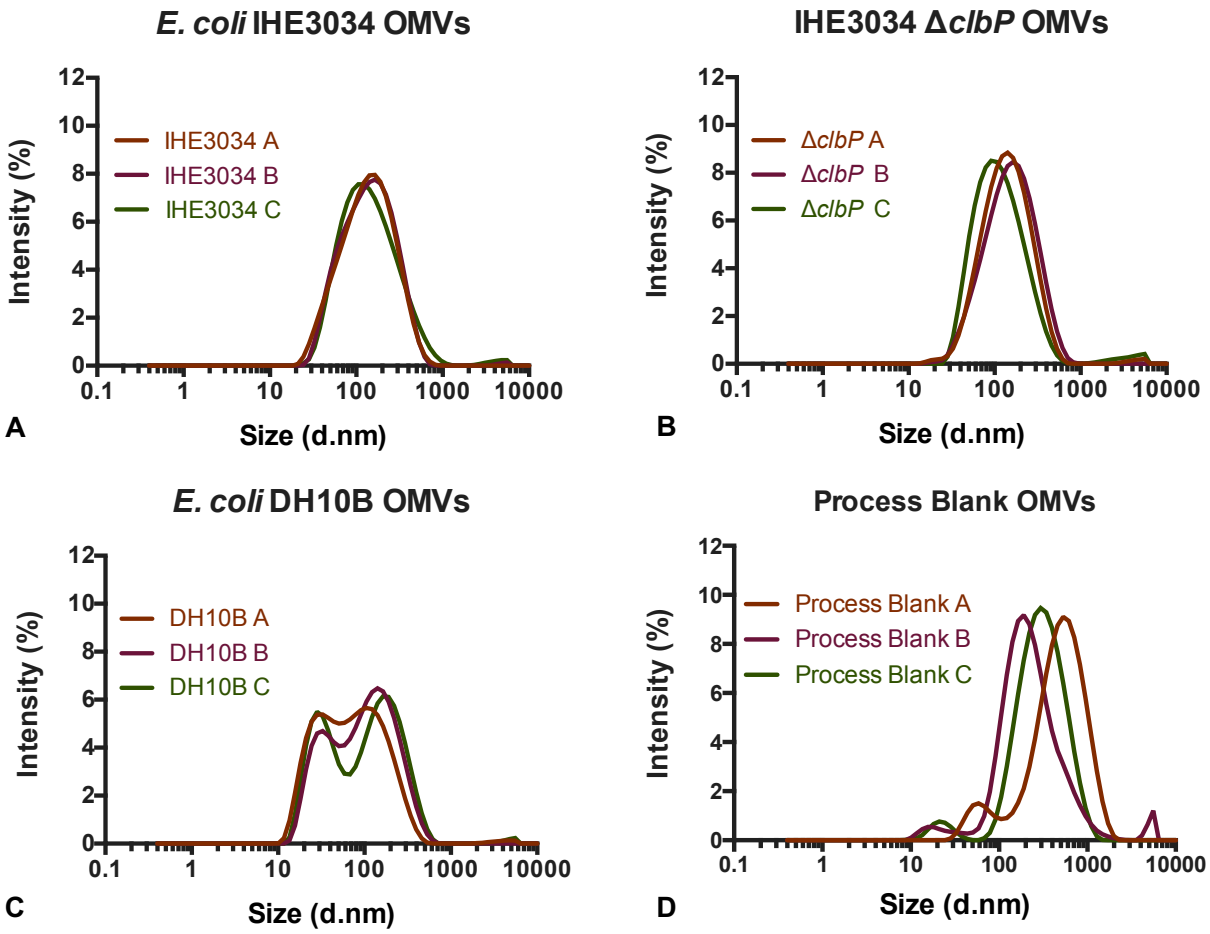

Figure 4.3 Hydrodynamic diameter size distribution of OMVs by DLS. After isolation, OMVs from (A) IHE3034, (B) IHE3034 Δ*clbP*, (C) laboratory strain DH10B and, (D) Process Blank carrier control were analyzed in a 1:10 dilution in a Marlvern Zetasizer Nano Series. Analysis were performed using biological replicates (n=3).

Table 4.2: OMV particle hydrodynamic diameter from DLS analysis. Three different biological replicates (A,B, and C) were measured three times each.

Sample	Z-Average (d.nm)	PdI	Mean Z-Average (d.nm)	Mean Z-Average StDev (d.nm)	Mean PdI	StDev PdI	Peak 1	Peak 2	Peak 3
IHE3034 OMV A	111.2	0.280	**109**	**2**	0.31	0.04	161.8	-	-
	107.9	0.353					175.2	-	-
	107.4	0.287					158.8	-	-
IHE3034 OMV B	115.0	0.281	**112**	**2**	0.30	0.03	171.3	-	-
	111.1	0.285					167.5	-	-
	110.6	0.338					162.6	4848	-
IHE3034 OMV C	111.2	0.344	**111.4**	**0.2**	0.35	0.01	178.5	4033	-
	111.6	0.350					177.6	4323	-
	111.5	0.357					178.0	-	-
IHE3034 Δ*clbP* OMV A	116.0	0.263	**115.0**	**0.9**	0.267	0.004	168.0	-	-
	114.6	0.267					151.5	4364	21.36
	114.3	0.271					165.4	-	-
IHE3034 Δ*clbP* OMV B	125.3	0.285	**125**	**2**	0.282	0.003	181.1	-	-
	126.9	0.280					183.8	-	-
	123.5	0.280					181.8	-	-
IHE3034 Δ*clbP* OMV C	99.18	0.278	**97**	**2**	0.275	0.003	139.3	5014	-
	96.89	0.276					117.7	3421	-
	96.30	0.272					142.4	-	-
DH10B OMV A	51.11	0.403	**51.3**	**0.3**	0.399	0.004	146.6	33.31	-
	51.17	0.398					146.7	34.26	-
	51.72	0.396					87.51	3980	-
DH10B OMV B	68.15	0.447	**66**	**2**	0.42	0.02	169.1	32.24	-
	64.15	0.402					115.9	-	-
	65.04	0.419					173.7	38.63	-
DH10B OMV C	61.17	0.494	**63**	**1**	0.48	0.01	172.3	32.12	-
	63.23	0.477					224.0	38.03	-
	63.41	0.482					188.1	36.31	4661
Process Blank A	259.5	0.63	**311**	**67**	0.5	0.1	549.4	73.91	-
	286.4	0.409					518.0	74.04	-
	386.6	0.528					702.2	49.77	-
Process Blank B	180.1	0.404	**166**	**14**	0.49	0.08	181.5	5186	-
	167.4	0.556					360.0	15.48	-
	151.7	0.523					300.8	28.59	-
Process Blank C	221.3	0.362	**204**	**21**	0.44	0.11	356.0	-	-
	209.3	0.400					370.5	22.13	-
	180.3	0.572					334.4	23.57	-
TBS Buffer	2617	**1**	**8528**	**5368**	1	0	2057	0.8842	-
	9868	**1**					2474	0.7026	-
	13100	**1**					2325	-	-

Table 4.3 Mean average hydrodynamic diameter and PdI (Polydispersity Index) comparison between OMV samples from *E. coli* IHE3034, *E. coli* IHE3034 Δ*clbP,* laboratory strain *E. coli* DH10B, and Process Blank control by DLS analysis. Mean average was calculated using Z-average values from biological and technical triplicates of each sample.

Sample	Z-Average (nm)*	Std. Dev. (nm)	PdI*	Std. Dev.
IHE3034 OMVs	111	2	0.32	0.03
IHE3034 Δ*clbP* OMVs	113	14	0.275	0.007
DH10B OMVs	60	8	0.44	0.04
Process Blank	227	75	0.49	0.04
TBS Buffer**	8528	5368	1	0

**TBS Buffer is the solution used for vesicles re-suspension
*Mean average was calculated using Z-average/PDI values from experimental triplicates for each sample.

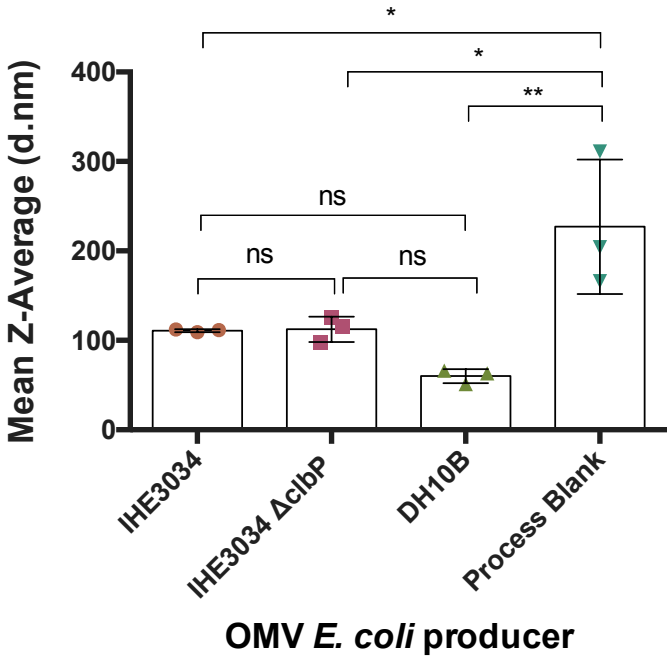

Figure 4.4 Mean average hydrodynamic diameter of OMVs samples from *E. coli* IHE3034, *E. coli* IHE3034 Δ*clbP,* laboratory strain *E. coli* DH10B and, Process Blank control by DLS analysis. Mean average was calculated using Z-average values from experimental triplicates of each sample. The statistical significance was assessed by one-way ANOVA. *p*-values: ns $p > 0.05$; * $p \leq 0.05$; ** $p \leq 0.01$; *** $p \leq 0.001$ and **** $p \leq 0.0001$.

4.3.3 Characterization of OMVs by Scanning Electron Microscopy (SEM)

The presence of OMVs in isolated samples was confirmed using SEM. The SEM micrographs confirm the presence of evenly spherical particles (Figure 4.5A; the rest of micrographs of OMVs analyzed are in section 4.6). Area measurements of vesicles isolates from *E. coli* IHE3034 and IHE3034 *ΔclbP* resulted in size distribution of 120 to 280 nm and of 100 to 260 nm respectively. Area measurements of vesicles isolated from the laboratory strain *E. coli* DH10B resulted in size distribution of 50 to 210 nm. These results reveal that the average sizes of OMVs seem similar to the results obtained from the DLS analysis. Also, the deletion of the *clbP* gene did not affect the average size or morphology of the OMVs. Interestingly, we also observed that OMVs from the IHE3034 clinical isolates (WT and mutant) were more abundant than the isolated vesicles sample from the laboratory strain DH10B. The “process blank” shows no spherical particles as expected.

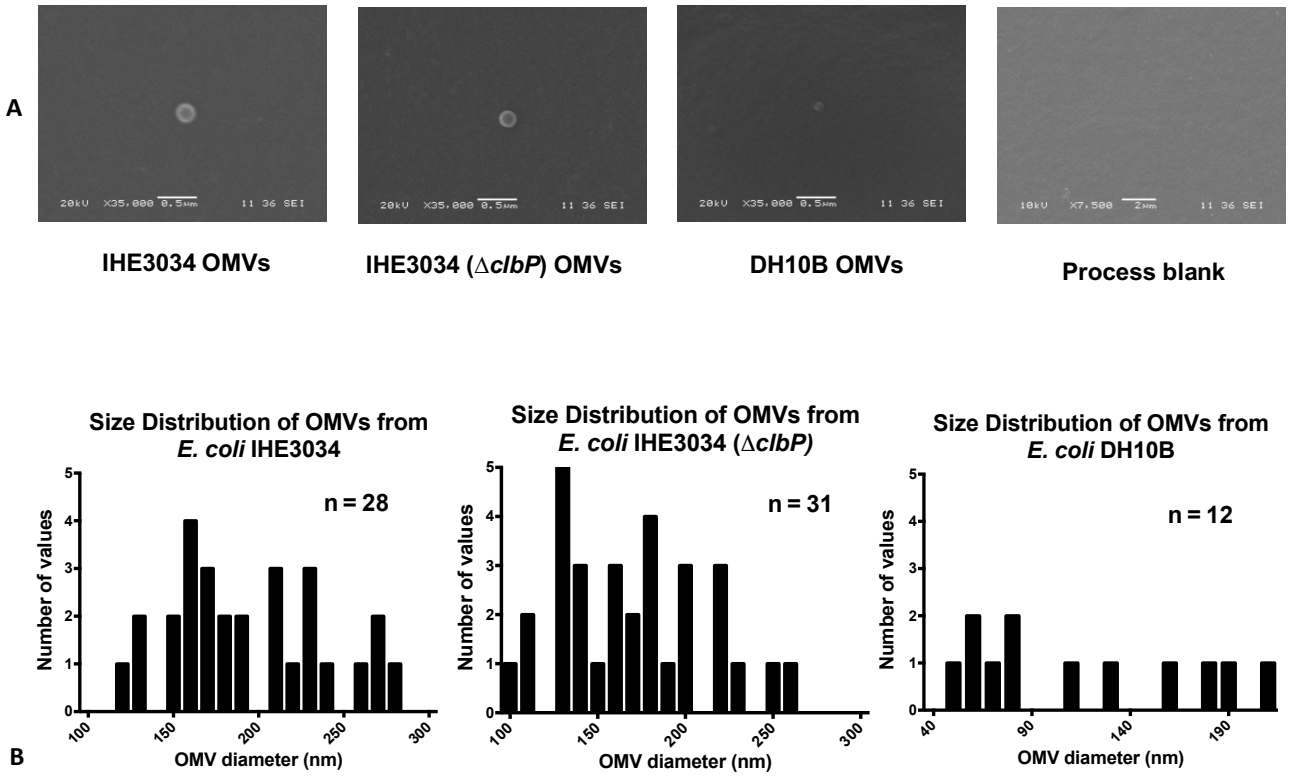

Figure 4.5. OMVs from *E. coli* IHE3034 clinical strains are larger than the laboratory strain lacking the *pks island E. coli* DH10B. A. Scanning electron microscope (SEM) micrograph of OMVs from IHE3034 (*pks*+), IHE3034 Δ*clbP* (Isogenic mutant), and DH10B (*pks*-) *E. coli* strains. **B**. Histograms of OMV diameter from *E. coli* IHE3034, IHE3034 Δ*clbP* and DH10B.

4.3.4 OMVs from *pks* positive *E. coli* IHE3034 analysis by GC-MS

Chemical analysis by GC/MS was carried out for both whole bacteria (IHE3034, IHE3034 Δ*clbP* and DH10B) and for their respective OMVs. Both, bacteria and OMVs were trans-esterified which resulted in the release of fatty acids and any membrane-anchored compound by a nucleophilic acyl substitution with a methyl group.

The possibility of finding colibactin intermediates anchored in the OMV membrane was evaluated using GC/MS. We searched for signals that were present in the GC/MS spectra of OMVs from the IHE3034 strains, but absent in the OMVs from the IHE3034 *ΔclbP* deletion mutant. We also searched for any GC/MS signals that did not find a match in the NIST standard database, indicating the presence of a novel compound. The GC/MS analysis of OMV samples revealed the presence of five signals when EI-MS (electro ionization mass spectrometry) spectra were evaluated against the NIST Standard reference database (Table 4.4). However, mass fragmentation of these unknown compounds were all typical of the fragmentation of fatty acids of unknown length or unsaturation. We also analyzed whole bacteria by this method and similar results were obtained: mostly fatty acids were found and quantified. Thus, no colibactin-related product was found or detectable in OMV samples or in its producer bacteria.

Table 4.4. List of unidentified signals from OMVs and its producer bacteria cell sample analyzed by GC/MS

Signal	Retention Time	IHE3034	IHE3034 *ΔclbP*	DH10B	NIST Database Match (%Probability)
UNK #1 *	21.4970	- ✓	- ✓	- ✓	C14:0 C16:0 C18:0 C11:1 (3-OH)
UNK #2	23.226	✓ ✓	✓ ✓	✓ ✓	C17:1 C17:1 (3-Cyclopropane)
UNK #3	24.332	✓ ✓	✓ ✓	✓ ✓	C17:1 C18:1
UNK #4	25.540	✓ ✓	✓ ✓	✓ ✓	C16:1 C19:1
UNK #5 *	27.095	- -	✓	- -	C12:0 Amide C18:1 Amide

*Only unknown in bacterial cell samples.

Green check marks denote the presence of the extracted compound in the cell pellet;

Black check marks denote the presence of the extracted compound in the isolated OMVs.

To determine whether colibactin production had any effect on the lipid composition of either OMVs and its producer bacteria, the fatty acid methyl esters (FAME) profile of IHE3034, IHE30304Δ*clbP,* and DH10B *E. coli* strains were also analyzed by GC/MS. We observed the dominant presence of 16:0 (palmitic acid), 12:0 (lauric acid), 14:0 (myristic acid) and, 16:1 (palmitoleic acid) fatty acids in all OMV samples, similar to the profile of other gram-negative bacteria[34]. No significant difference was observed in the FAME profiles of OMVs between the WT and the *clbP* mutant of IHE3034 nor in the non-pathogenic laboratory strain DH10B (Figure 4.6), indicating that colibactin production did not affect the lipid composition of OMVs.

The FAME profile of the whole live bacteria (from which the OMVs were isolated) was also evaluated. Results reveal the presence of 16:0 (palmitic acid) and UNK#2 (potentially 17:1 heptadecenoic acid) in a relative higher abundance (Figure 4.7). Although the fatty acid profile observed for all the samples was practically the same as expected for *E. coli* [35], interestingly, significant changes were detected in the relative amount of 16:0 between the IHE3034 wild-type and the clbP mutant strain.

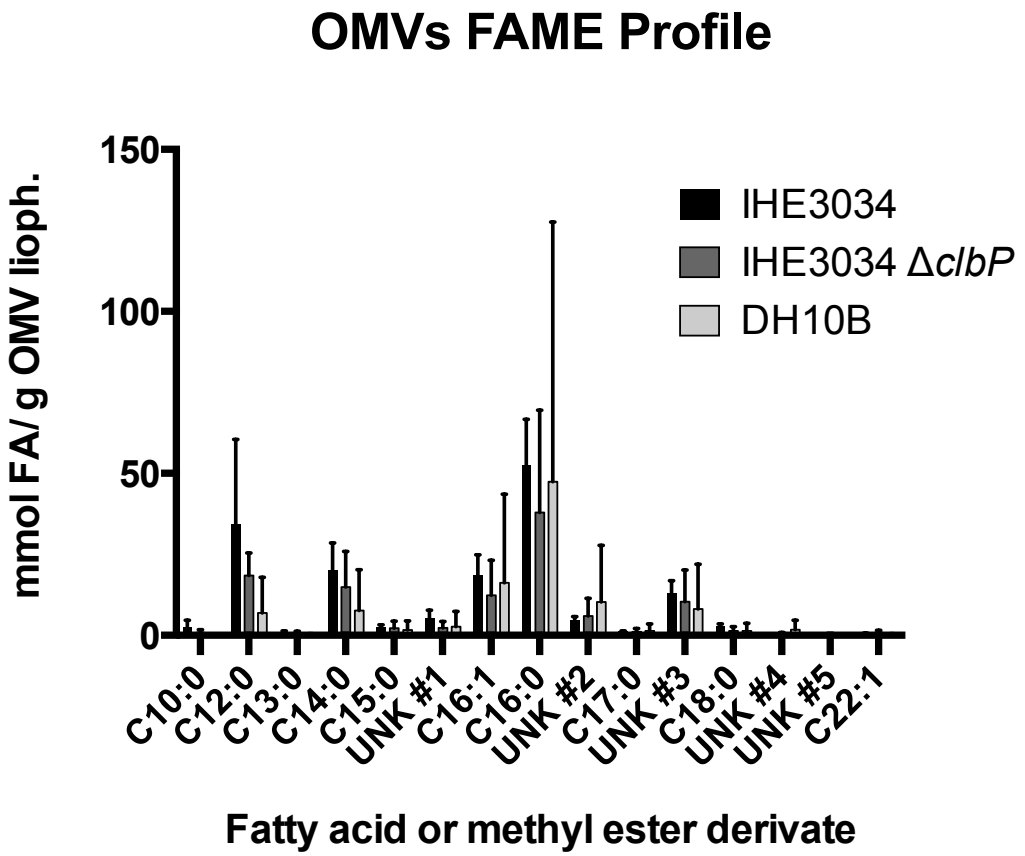

Figure 4.6. Fatty acids methyl ester (FAME) profile of isolated OMVs by GC Mass spectrometry. FAME profile of trans-esterified OMVs extracts for IHE3034 (WT, pks+), IHE3034 ∆clbP (isogenic mutant) and DH10B (negative control, pks-) *E. coli* strains. Possible identity of unknown compounds are described before in Table 4.4. The statistical significance was assessed by two-way ANOVA. *p*-values: *p*-values: ns (or not described) $p > 0.05$; * $p \leq 0.05$; ** $p \leq 0.01$; *** $p \leq 0.001$ and **** $p \leq 0.0001$.

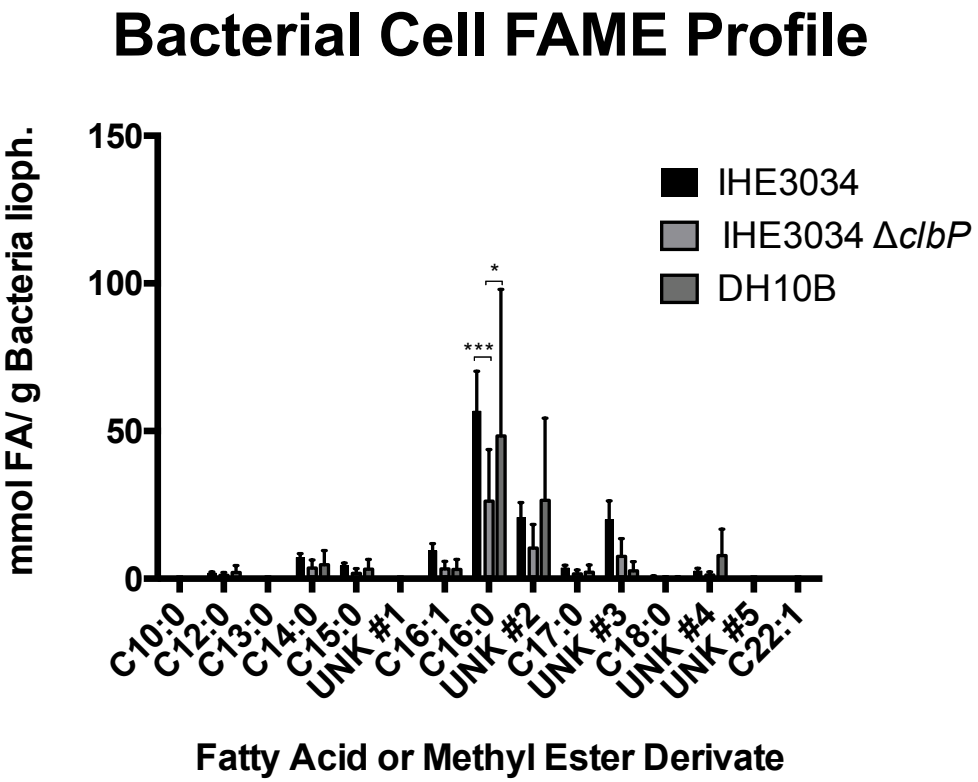

Figure 4.7. Fatty acids methyl ester (FAME) profile of the whole bacterial cell by GC-Mass spectrometry. FAME profile of bacterial cells trans-esterification extracts for IHE3034 (WT, *pks*+), IHE3034 Δ*clbP* (isogenic mutant) and DH10B (negative control, *pks*-) *E. coli* strains. Possible identity of unknown compounds are described before in Table 4.4.The statistical significance was assessed by two-way ANOVA. *p*-values: *p*-values: ns (or not described) $p > 0.05$; * $p \leq 0.05$; ** $p \leq 0.01$; *** $p \leq 0.001$ and **** $p \leq 0.0001$.

4.3.5 Protein content of OMVs by SDS/PAGE

The protein content of isolated OMVs from IHE3034, IHE30304Δ*clbP,* and DH10B *E. coli* strains was analyzed by SDS-PAGE. Results show the presence of approximately 11 major protein bands for both colibactin-producing WT strain and the clbP peptidase mutant strains, ranging in molecular weight (MW) from 10 to ~150 kDa (Figure 4.8). Proteins bands observed between IHE3034 strains were closely identical, thus, suggesting no detectable differences in OMV proteins associated with colibactin production. Protein analysis of the laboratory strain DH10B shows the presence of approximately 12 major proteins, ranging in MW from ~10 to 100 kDa (Figure 4.8). Carrier controls (process blank) did not show the presence of any protein band as expected. Differences in the protein bands pattern between OMVs from IHE3034 and DH10B strain were observed. We believe that this difference is attributable to the fact that they are different *E. coli* strains, but cannot be attributed to the production of colibactin since IHE3034 and its mutant presented the same protein profile that for the OMVs from the *clbP* mutant strain.

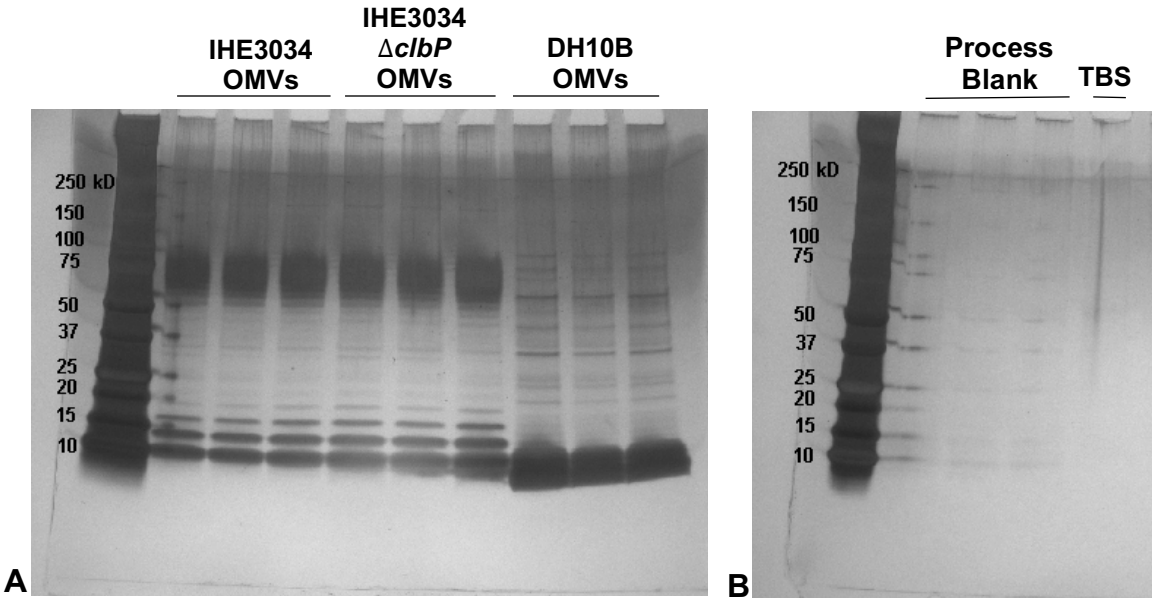

Figure 4.8 SDS-PAGE analysis of OMVs isolated from *E. coli* IHE3034, its isogenic mutant IHE3034 Δ*clbP* and the laboratory strain DH10B. Protein profiles of OMVs were evaluated from biological triplicates of (**A**) Isolated OMVs in biological replicates. (**B**) Isolated carrier control "Process Blank and the TBS Buffer used for vesicles re-suspension were also evaluated to rule out any contamination. Electrophoresis was carried out at 100 V for 1.5 hrs on a 4-20 % polyacrylamide gel, followed with silver-staining for visualization.

4.4 Discussion

Ever since the discovery of the *pks island*, there has been a fascination with the implications of colibactin (the toxin produced by the *pks island* encoded enzymes), in how it induces DNA damage and elicits malignant phenotypes[1,3]. The epidemiology for these genes seems to indicate that they are widely distributed in the population[36–38]. However, the evidence suggests that there is a higher prevalence of *pks island* genes among patients with colorectal cancer (CRC) and inflammatory bowel diseases (IBDs) [36,38,39]. Increasing evidence suggest that colibactin is probably playing an important role in tumorigenesis[40–44].

Despite the known toxicity of colibactin, there is a lack of research on how colibactin reaches host cells. Attempts to extract the active compound directly from its producer bacteria have been unsuccessful, and many of the isolated intermediates that have been reported do not induce the expected genotoxicity[1,45–47]. The difficulties in identifying how colibactin is translocated from the bacterial cell to the host cell, may be related to why its isolation has proven to be so difficult. Among all the known possible mechanisms that bacteria use to release or transport colibactin-like toxins, one that has generated much interest in our group and others [48], is the usage of OMVs.

The overall aim of this work was to characterize OMVs from a natural colibactin producer in order to evaluate whether a relationship exists between OMVs and the production of colibactin. To do so, we first confirmed the presence of OMVs in the cell-free supernatant of IHE3034, IHE3034 *ΔclbP,* and DH10B *E. coli* strains by DLS and SEM. Results from both techniques confirmed the presence of spherical particles with

diameters (~50 to ~280 nm interval diameter) which fall within the expected range of sizes[13,30,49]. The size of OMVs has shown to be an important factor in pathogenicity. A recent study revealed that larger OMVs (from pathogenic bacteria) cause a higher degree of double strands breaks and DNA damage on colonic epithelial cells[50] Also, in cancer-causing pathogen *H. pylori*, it has been shown that vesicle size plays a role in how OMVs enter epithelial cells, and cause damage[51]. Our results show that OMVs extracted from both clinical strains IHE3034 and IHE3034 Δ*clbP*, are larger in size that those extracted from the non-pathogenic DH10B, an observation that is consistent with size-dependent activity for OMVs. Interestingly, the differences in size between the OMVs from the pathogenic IHE3034 and the DH10B laboratory strain was not attributable to colibactin production since the Δ*clbP* mutant (which cannot produce active colibactin) also produced the larger OMVs.

Outer membrane vesicles are naturally produced by gram-negative bacteria either as defensive or offensive response to environmental conditions or as a response to membrane stress[52]. Although the role of OMVs as a mechanism of stress response has not been entirely delineated, OMVs are thought to mediate the export of virulence factors, unfolded proteins, or other enveloped stressors from the outer membrane or the periplasmic space[28]. We aimed to determine if the production of colibactin or its accumulation may act as a stressor to the bacterial membrane inducing the over production of vesicles. Since the colibactin biosynthetic pathway ends in the bacterial periplasm, we expected that a disruption in colibactin production (by the deletion of *clbP*) would induce changes in the release of OMVs. However, the production of OMVs

remained unaffected by the *clbP* deletion. Thus, our results contain no evidence of a colibactin-dependent release of OMVs.

Proteins play a fundamental role in the biogenesis of OMVs and in the cargo packing. OMV proteins not only mediate interactions with the host cells but also with the surroundings before reaching the target[20]. It has been shown that OMV proteins are involved in, and even determine, many of the activities and deleterious effects associated with OMVs[29,53]. Our results show that proteins band patterns of the OMVs from the *pks* positive IHE30434 and the Δ*clbP* mutant are nearly identical, indicating that colibactin production does not induce the expression or the recruitment of any new protein to the OMV. Differences in the protein content and production between OMVs from the IHE3034 clinical isolates and those from the DH10B laboratory strain were observed, but none that could be attributed to the production of colibactin. We attribute those differences more to the fact that they are different strains adapted to different conditions.

Fatty Acids Methyl Esters can be an indicator of physiological stress in certain bacterial species[54]. The fatty acid composition of bacteria has been shown to change in response to environmental effects[55]. While much is known about the fatty acid composition of the bacterial envelope as a whole, the precise lipid composition of OMVs is less well known. In this chapter, we attempted to shed light on (1) the fatty acid composition of OMVs and (2) the effect of colibactin production on the OMV lipid composition. The deletion of *clbP* did not induce major changes in the fatty acid composition of OMVs when compared to wild-type IHE3034, although a small but significant change in the composition of 16:0. Moreover, no significant difference was observed when the FAME

profile of the clinical strains was compared with the OMVs from the DH10B laboratory strain. These results indicate that neither colibactin production nor any other pathogenicity associated with the IHE3034 strains is causing changes in the lipids composition of OMVs.

The biogenesis of OMVs is not fully understood, but it is thought that the formation of bacterial vesicles involves the enrichment or exclusion of specific types of fatty acids, proteins, and other components according to the environment[30,56,57]. Under our specific culture conditions, the FAME GC/MS analysis of OMVs from IHE3034 *E. coli* strains and also for OMVs from the laboratory strain (non-pathogenic) reveals that the most predominant fatty acid in OMVs from *E. coli* was palmitic acid (16:0) which has also been reported to be the most abundant fatty acid in its outer membrane[58]. Our analyses also revealed that vesicles consisted of approximately 75% saturated fatty acids, while almost 99% of those were long-chain fatty acids (LCFA are fatty acids of 12 to 26 carbons length)[59]. With long and highly saturated fatty acids, the OMVs are predicted to be more rigid membranes than those typically found in *E. coli* as a whole, as has been describe elsewhere in the literature.

Our fatty acid analysis included a comparison between the FAME profile of OMVs and that of the whole bacteria. The lipid composition of the OMVs from IHE3034 *E. coli* strains was similar to that of the whole bacteria, but not identical. The whole bacteria produced predominantly 16:0, 17:1 and 18:1, with little contribution from shorter chain fatty acids, whereas the OMVs also contained 16:0, 17:1 and 18:1 but had a significant contribution from 12:0, 14:0 and 16:1 fatty acids. However, these results together indicate no direct alteration caused by the colibactin production since the OMVs from all

strains tested (both colibactin producers and non-producers) had similar fatty acid profiles. We also scrutinized the GC/MS data looking for colibactin or colibactin intermediates in the OMV samples, that could be detached by trans-esterification (as performed in Chapter 2 with LPS extract). Our intention was to detect any compound either bound or covalently attached to the bacterial outer membrane or to the OMVs. Nevertheless, colibactin was not found in OMVs nor the bacterial membrane of the IHE3034 *E.coli* strain.

In conclusion, we performed a complete physicochemical characterization of native OMVs from the clinical isolate *E. coli* IHE3034 which is a natural colibactin producer, originally isolated from a newborn with meningitis infection[60]. The OMV size distribution, lipid profile, and protein composition were determined for the *pks* positive IHE3034 *E. coli* strain and its Δ*clbP* mutant. However, taken together, these results show no effect of the *clbP* gene deletion on the physicochemical parameters of OMVs, suggesting the colibactin production does not affect the composition nor integrity of the outer membrane nor OMVs of the colibactin producer bacteria. Even so, OMVs could still employ a variety of mechanisms to mediate the effects of colibactin on the target cells. The next chapter will describe efforts to assess the biological activity of OMVs from a colibactin producer.

4.5 References

(1) Nougayrède, J.-P.; Homburg, S.; Taieb, F.; Boury, M.; Brzuszkiewicz, E.; Gottschalk, G.; Buchrieser, C.; Hacker, J.; Dobrindt, U.; Oswald, E. Escherichia Coli Induces DNA Double-Strand Breaks in Eukaryotic Cells. *Science.* **2006**, *313* (5788), 848–851. https://doi.org/10.1126/science.1127059.

(2) Putze, J.; Hennequin, C.; Nougayrède, J. P.; Zhang, W.; Homburg, S.; Karch, H.; Bringer, M. A.; Fayolle, C.; Carniel, E.; Rabsch, W.; Oelschlaeger, T. A.; Oswald, E.; Forestier, C.; Hacker, J.; Dobrindt, U. Genetic Structure and Distribution of the Colibactin Genomic Island among Members of the Family Enterobacteriaceae. *Infect. Immun.* **2009**, *77* (11), 4696–4703. https://doi.org/10.1128/IAI.00522-09.

(3) Cuevas-Ramos, G.; Petit, C. R.; Marcq, I.; Boury, M.; Oswald, E.; Nougayrède, J.-P. Escherichia Coli Induces DNA Damage in Vivo and Triggers Genomic Instability in Mammalian Cells. *Proc. Natl. Acad. Sci. U. S. A.* **2010**, *107* (25), 11537–11542. https://doi.org/10.1073/pnas.1001261107.

(4) Arthur, J. C.; Perez-Chanona, E.; Mühlbauer, M.; Tomkovich, S.; Uronis, J. M.; Fan, T.; Campbell, B. J.; Abujamel, T.; Dogan, B.; Rogers, A. B.; Rhodes, J. M.; Stintzi, A.; Simpson, K. W.; Hansen, J. J.; Keku, T. O.; Fodor, A. A.; Jobin, C. Intestinal Inflammation Targets Cancer-Inducing Activity of the Microbiota. *Science.* **2012**, *338* (6103), 120–123. https://doi.org/10.1126/science.1224820.Intestinal.

(5) Shimpoh, T.; Hirata, Y.; Ihara, S.; Suzuki, N.; Kinoshita, H.; Hayakawa, Y. Prevalence of Pks - Positive Escherichia Coli in Japanese Patients with or without Colorectal Cancer. *Gut Pathog.* **2017**, *9*. https://doi.org/10.1186/s13099-017-0185-x.

(6) Mousa, J. J.; Yang, Y.; Tomkovich, S.; Shima, A.; Newsome, R. C.; Tripathi, P.; Oswald, E.; Bruner, S. D.; Jobin, C. MATE Transport of the E. Coli-Derived Genotoxin Colibactin. *Nat. Microbiol.* **2016**, *1* (1), 15009. https://doi.org/10.1038/nmicrobiol.2015.9.

(7) Dubois, D.; Baron, O.; Cougnoux, A.; Delmas, J.; Pradel, N.; Boury, M.; Bouchon, B.; Bringer, M. A.; Nougayrède, J. P.; Oswald, E.; Bonnet, R. ClbP Is a Prototype of a Peptidase Subgroup Involved in Biosynthesis of Nonribosomal Peptides. *J. Biol. Chem.* **2011**, *286* (41), 35562–35570. https://doi.org/10.1074/jbc.M111.221960.

(8) Cougnoux, A.; Gibold, L.; Robin, F.; Dubois, D.; Pradel, N.; Darfeuille-Michaud, A.; Dalmasso, G.; Delmas, J.; Bonnet, R. Analysis of Structure-Function Relationships in the Colibactin-Maturating Enzyme ClbP. *J. Mol. Biol.* **2012**, *424* (3–4), 203–214. https://doi.org/10.1016/j.jmb.2012.09.017.

(9) Bian, X.; Fu, J.; Plaza, A.; Herrmann, J.; Pistorius, D.; Stewart, A. F.; Zhang, Y.; Müller, R. In Vivo Evidence for a Prodrug Activation Mechanism during Colibactin Maturation. *ChemBioChem* **2013**, *14* (10), 1194–1197.

https://doi.org/10.1002/cbic.201300208.

(10) Brotherton, C. A.; Balskus, E. P. A Prodrug Resistance Mechanism Is Involved in Colibactin. *J. Am. Chem. Sociaty* **2013**, *135*, 3359–3362. https://doi.org/10.1021/ja312154m.

(11) Costa, T. R. D.; Felisberto-Rodrigues, C.; Meir, A.; Prevost, M. S.; Redzej, A.; Trokter, M.; Waksman, G. Secretion Systems in Gram-Negative Bacteria: Structural and Mechanistic Insights. *Nat. Rev. Microbiol.* **2015**, *13* (6), 343–359. https://doi.org/10.1038/nrmicro3456.

(12) Guerrero-Mandujano, A.; Hernández-Cortez, C.; Ibarra, J. A.; Castro-Escarpulli, G. The Outer Membrane Vesicles: Secretion System Type Zero. *Traffic* **2017**, *18* (7), 425–432. https://doi.org/10.1111/tra.12488.

(13) Beveridge, T. J. Structures of Gram-Negative Cell Walls and Their Derived Membrane Vesicles. *J. Bacteriol.* **1999**, *181* (16), 4725–4733. https://doi.org/10.1128/jb.181.16.4725-4733.1999.

(14) Mayrand, D.; Grenier, D. Biological Activities of Outer Membrane Vesicles. *Can. J. Microbiol.* **1989**, *35* (6), 607–613. https://doi.org/10.1139/m89-097.

(15) Schwechheimer, C.; Kuehn, M. J. Outer-Membrane Vesicles from Gram-Negative Bacteria: Biogenesis and Functions. *Nat. Prod. Rep.* **2015**, *13* (10), 605–619. https://doi.org/10.1038/nrmicro3525.Outer-membrane.

(16) Berleman, J.; Auer, M. The Role of Bacterial Outer Membrane Vesicles for Intra- and Interspecies Delivery. *Environ. Microbiol.* **2013**, *15* (2), 347–354. https://doi.org/10.1111/1462-2920.12048.

(17) Kulkarni, H. M.; Jagannadham, M. V. Biogenesis and Multifaceted Roles of Outer Membrane Vesicles from Gram-Negative Bacteria. *Microbiol. (United Kingdom)* **2014**, *160*, 2109–2121. https://doi.org/10.1099/mic.0.079400-0.

(18) Tyrer, P. C.; Frizelle, F. A.; Keenan, J. I. Escherichia Coli-Derived Outer Membrane Vesicles Are Genotoxic to Human Enterocyte-like Cells. *Infect. Agent. Cancer* **2014**, *9* (1), 2. https://doi.org/10.1186/1750-9378-9-2.

(19) Chatterjee, D.; Chaudhuri, K. Association of Cholera Toxin with Vibrio Cholerae Outer Membrane Vesicles Which Are Internalized by Human Intestinal Epithelial Cells. *FEBS Lett.* **2011**, *585* (9), 1357–1362. https://doi.org/10.1016/j.febslet.2011.04.017.

(20) Kuehn, M. J.; Kesty, N. C. Bacterial Outer Membrane Vesicles and the Host-Pathogen Interaction. *Genes Dev.* **2005**, *19* (22), 2645–2655. https://doi.org/10.1101/gad.1299905.

(21) Ellis, T. N.; Kuehn, M. J. Virulence and Immunomodulatory Roles of Bacterial Outer Membrane Vesicles. *Microbiol. Mol. Biol. Rev.* **2010**, *74* (1), 81–94. https://doi.org/10.1128/mmbr.00031-09.

(22) Horstman, A. L.; Kuehn, M. J. Enterotoxigenic Escherichia Coli Secretes Active Heat-Labile Enterotoxin via Outer Membrane Vesicles. *J. Biol. Chem.* **2000**, *275* (17), 12489–12496.

(23) Klimentová, J.; Stulík, J. Methods of Isolation and Purification of Outer Membrane Vesicles from Gram-Negative Bacteria. *Microbiol. Res.* **2015**, *170*, 1–9. https://doi.org/10.1016/j.micres.2014.09.006.

(24) Eberlein, C.; Starke, S.; Doncel, Á. E.; Scarabotti, F.; Heipieper, H. J. Quantification of Outer Membrane Vesicles: A Potential Tool to Compare Response in Pseudomonas Putida KT2440 to Stress Caused by Alkanols. *Appl. Microbiol. Biotechnol.* **2019**, *103* (10), 4193–4201. https://doi.org/10.1007/s00253-019-09812-0.

(25) Meers, P. R.; Liu, C.; Chen, R.; Bartos, W.; Davis, J.; Dziedzic, N.; Orciuolo, J.; Kutyla, S.; Pozo, M. J.; Mithrananda, D.; Panzera, D.; Wang, S. Vesicular Delivery of the Antifungal Antibiotics of Lysobacter Enzymogenes C3. *Appl. Environ. Microbiol.* **2018**, *84* (20), 1–16. https://doi.org/10.1128/AEM.01353-18.

(26) Wagner, T.; Joshi, B.; Janice, J.; Askarian, F.; Škalko-Basnet, N.; Hagestad, O. C.; Mekhlif, A.; Wai, S. N.; Hegstad, K.; Johannessen, M. Enterococcus Faecium Produces Membrane Vesicles Containing Virulence Factors and Antimicrobial Resistance Related Proteins. *J. Proteomics* **2018**, *187*, 28–38. https://doi.org/10.1016/j.jprot.2018.05.017.

(27) Piroeva, I.; Atanassova-Vladimirova, S.; Dimowa, L.; Sbirkova, H.; Radoslavov, G.; Hristov, P.; Shivachev, B. L. A Simple and Rapid Scanning Electron Microscope Preparative Technique for Observation of Biological Samples: Application on Bacteria and DNA Samples. *Bulg. Chem. Commun.* **2013**, *45* (4), 510–515. https://doi.org/10.1002/jemt.10184.

(28) McBroom, A. J.; Kuehn, M. J. Release of Outer Membrane Vesicles by Gram-Negative Bacteria Is a Novel Envelope Stress Response. *Mol. Microbiol.* **2007**, *63* (2), 545–558. https://doi.org/10.1111/j.1365-2958.2006.05522.x.

(29) Bonnington, K. E.; Kuehn, M. J. Protein Selection and Export via Outer Membrane Vesicles. *Biochim. Biophys. Acta - Mol. Cell Res.* **2014**, *1843* (8), 1612–1619. https://doi.org/10.1016/j.bbamcr.2013.12.011.

(30) Kulp, A.; Kuehn, M. J. Biological Functions and Biogenesis of Secreted Bacterial Outer Membrane Vesicles. *Annu Rev Microbiol.* **2010**, *64*, 163–184. https://doi.org/10.1146/annurev.micro.091208.073413.Biological.

(31) Grande, R.; Celia, C.; Mincione, G.; Stringaro, A.; Di Marzio, L.; Colone, M.; Di Marcantonio, M. C.; Savino, L.; Puca, V.; Santoliquido, R.; Locatelli, M.; Muraro, R.; Hall-Stoodley, L.; Stoodley, P. Detection and Physicochemical Characterization of Membrane Vesicles (MVs) of Lactobacillus Reuteri DSM 17938. *Front. Microbiol.* **2017**, *8*, 1–10. https://doi.org/10.3389/fmicb.2017.01040.

(32) Paolino, D.; Cosco, D.; Celano, M.; Moretti, S.; Puxeddu, E.; Russo, D.; Fresta, M. Gemcitabine-Loaded Biocompatible Nanocapsules for the Effective Treatment of Human Cancer. *Nanomedicine* **2013**, *8* (2), 193–201. https://doi.org/10.2217/nnm.12.101.

(33) Cosco, D.; Paolino, D.; Cilurzo, F.; Casale, F.; Fresta, M. Gemcitabine and Tamoxifen-Loaded Liposomes as Multidrug Carriers for the Treatment of Breast Cancer Diseases. *Int. J. Pharm.* **2012**, *422*, 229–237. https://doi.org/10.1016/j.ijpharm.2011.10.056.

(34) Roier, S.; Zingl, F. G.; Cakar, F.; Durakovic, S.; Kohl, P.; Eichmann, T. O.; Klug, L.; Gadermaier, B.; Weinzerl, K.; Prassl, R.; Lass, A.; Daum, G.; Reidl, J.; Feldman, M. F.; Schild, S. A Novel Mechanism for the Biogenesis of Outer Membrane Vesicles in Gram-Negative Bacteria. *Nat. Commun.* **2016**, *7*, 10515. https://doi.org/10.1038/ncomms10515.

(35) Cho, K. Y.; Salton, M. R. J. Fatty Acid Composition of Bacterial Membrane and Wall Lipids. *Biochim. Biophys. Acta (BBA)/Lipids Lipid Metab.* **1966**, *116* (1), 73–79. https://doi.org/10.1016/0005-2760(66)90093-2.

(36) Gómez-Moreno, R.; Robledo, I. E.; Baerga-Ortiz, A. Direct Detection and Quantification of Bacterial Genes Associated with Inflammation in DNA Isolated from Stool. *Adv. Microbiol.* **2014**, *4* (15), 1065–1075. https://doi.org/10.4236/aim.2014.415117.

(37) Johnson, J. R.; Johnston, B.; Kuskowski, M. A.; Nougayrede, J. P.; Oswald, E. Molecular Epidemiology and Phylogenetic Distribution of the Escherichia Coli Pks Genomic Island. *J. Clin. Microbiol.* **2008**, *46* (12), 3906–3911. https://doi.org/10.1128/JCM.00949-08.

(38) Iyadorai, T.; Mariappan, V.; Vellasamy, K. M.; Wanyiri, J. W.; Roslani, A. C.; Lee, G. K.; Sears, C.; Vadivelu, J. Prevalence and Association of Pks+ Escherichia Coli with Colorectal Cancer in Patients at the University Malaya Medical Centre, Malaysia. *PLoS One* **2020**, *15* (1), 1–13. https://doi.org/https://doi.org/10.1371/journal.pone.0228217.

(39) Arthur, J. C.; Perez-Chanona, E.; Mühlbauer, M.; Tomkovich, S.; Uronis, J. M.; Fan, T.-J.; Campbell, B. J.; Abujamel, T.; Dogan, B.; Rogers, A. B.; Rhodes, J. M.; Stintzi, A.; Simpson, K. W.; Hansen, J. J.; Keku, T. O.; Fodor, A. A.; Jobin, C. Intestinal Inflammation Targets Cancer-Inducing Activity of the Microbiota. *Science.* **2012**, *338* (6103), 120–123. https://doi.org/10.1126/science.1224820.

(40) Arthur, J. C. Microbiota and Colorectal Cancer: Colibactin Makes Its Mark. *Nat. Rev. Gastroenterol. Hepatol.* **2020**, *17* (6), 317–318. https://doi.org/10.1038/s41575-020-0303-y.

(41) Tomkovich, S.; Yang, Y.; Winglee, K.; Gauthier, J.; Mühlbauer, M.; Sun, X.; Mohamadzadeh, M.; Liu, X.; Martin, P.; Wang, G. P.; Oswald, E.; Fodor, A. A.; Jobin, C. Locoregional Effects of Microbiota in a Preclinical Model of Colon

Carcinogenesis. *Cancer Res.* **2017**, *77* (10), 2620–2632. https://doi.org/10.1158/0008-5472.CAN-16-3472.

(42) Pleguezuelos-Manzano, C.; Puschhof, J.; Rosendahl Huber, A.; van Hoeck, A.; Wood, H. M.; Nomburg, J.; Gurjao, C.; Manders, F.; Dalmasso, G.; Stege, P. B.; Paganelli, F. L.; Geurts, M. H.; Beumer, J.; Mizutani, T.; Miao, Y.; van der Linden, R.; van der Elst, S.; Ambrose, J. C.; Arumugam, P.; Baple, E. L.; Bleda, M.; Boardman-Pretty, F.; Boissiere, J. M.; Boustred, C. R.; Brittain, H.; Caulfield, M. J.; Chan, G. C.; Craig, C. E. H.; Daugherty, L. C.; de Burca, A.; Devereau, A.; Elgar, G.; Foulger, R. E.; Fowler, T.; Furió-Tarí, P.; Hackett, J. M.; Halai, D.; Hamblin, A.; Henderson, S.; Holman, J. E.; Hubbard, T. J. P.; Ibáñez, K.; Jackson, R.; Jones, L. J.; Kasperaviciute, D.; Kayikci, M.; Lahnstein, L.; Lawson, L.; Leigh, S. E. A.; Leong, I. U. S.; Lopez, F. J.; Maleady-Crowe, F.; Mason, J.; McDonagh, E. M.; Moutsianas, L.; Mueller, M.; Murugaesu, N.; Need, A. C.; Odhams, C. A.; Patch, C.; Perez-Gil, D.; Polychronopoulos, D.; Pullinger, J.; Rahim, T.; Rendon, A.; Riesgo-Ferreiro, P.; Rogers, T.; Ryten, M.; Savage, K.; Sawant, K.; Scott, R. H.; Siddiq, A.; Sieghart, A.; Smedley, D.; Smith, K. R.; Sosinsky, A.; Spooner, W.; Stevens, H. E.; Stuckey, A.; Sultana, R.; Thomas, E. R. A.; Thompson, S. R.; Tregidgo, C.; Tucci, A.; Walsh, E.; Watters, S. A.; Welland, M. J.; Williams, E.; Witkowska, K.; Wood, S. M.; Zarowiecki, M.; Garcia, K. C.; Top, J.; Willems, R. J. L.; Giannakis, M.; Bonnet, R.; Quirke, P.; Meyerson, M.; Cuppen, E.; van Boxtel, R.; Clevers, H. Mutational Signature in Colorectal Cancer Caused by Genotoxic Pks + E. Coli. *Nature* **2020**, *580* (7802), 269–273. https://doi.org/10.1038/s41586-020-2080-8.

(43) Cougnoux, A.; Dalmasso, G.; Martinez, R.; Buc, E.; Delmas, J.; Gibold, L.; Sauvanet, P.; Darcha, C.; Déchelotte, P.; Bonnet, M.; Pezet, D.; Wodrich, H.; Darfeuille-Michaud, A.; Bonnet, R. Bacterial Genotoxin Colibactin Promotes Colon Tumour Growth by Inducing a Senescence-Associated Secretory Phenotype. *Gut* **2014**, *63* (12), 1932–1942. https://doi.org/10.1136/gutjnl-2013-305257.

(44) Dalmasso, G.; Cougnoux, A.; Delmas, J.; Darfeuille-Michaud, A.; Bonnet, R. Bacterial Genotoxin Colibactin Promotes Colon Tumour Growth by Inducing a Senescence-Associated Secretory Phenotype. *Gut* **2014**, *5* (5), 675–680. https://doi.org/10.4161/19490976.2014.969989.

(45) Vizcaino, M. I.; Engel, P.; Trautman, E.; Crawford, J. M. Comparative Metabolomics and Structural Characterizations Illuminate Colibactin Pathway-Dependent Small Molecules. *J. Am. Chem. Sociaty* **2014**, *136* (26), 9244–9247. https://doi.org/10.1021/ja503450q.

(46) Bian, X.; Plaza, A.; Zhang, Y.; Müller, R. Two More Pieces of the Colibactin Genotoxin Puzzle from Escherichia Coli Show Incorporation of an Unusual 1-Aminocyclopropanecarboxylic Acid Moiety. *Chem. Sci.* **2015**, *6* (5), 3154–3160. https://doi.org/10.1039/C5SC00101C.

(47) Wernke, K. M.; Xue, M.; Tirla, A.; Kim, C. S.; Herzon, S. B.; Crawford, J. M. Structure and Bioactivity of Colibactin. *Bioorg. Med. Chem. Lett.* **2020**, *30* (15),

127280. https://doi.org/10.1016/j.bmcl.2020.127280.

(48) Cañas, M.-A.; Giménez, R.; Fábrega, M.-J.; Toloza, L.; Baldomà, L.; Badia, J. Outer Membrane Vesicles from the Probiotic Escherichia Coli Nissle 1917 and the Commensal ECOR12 Enter Intestinal Epithelial Cells via Clathrin-Dependent Endocytosis and Elicit Differential Effects on DNA Damage. *PLoS One* **2016**, *11* (8), e0160374. https://doi.org/10.1371/journal.pone.0160374.

(49) Bonnington, K. E.; Kuehn, M. J. Protein Selection and Export via Outer Membrane Vesicles. *Biochim. Biophys. Acta* **2014**, *1843* (8), 1612–1619. https://doi.org/10.1016/j.bbamcr.2013.12.011.

(50) Ling, Z.; Dayong, C.; Denggao, Y.; Yiting, W.; Zhibiao, W. Escherichia Coli Outer Membrane Vesicles Induced DNA Double-Strand Breaks in Intestinal. **2019**, *25*, 45–52. https://doi.org/10.12659/MSMBR.913756.

(51) Turner, L.; Bitto, N. J.; Steer, D. L.; Lo, C.; D'Costa, K.; Ramm, G.; Shambrook, M.; Hill, A. F.; Ferrero, R. L.; Kaparakis-Liaskos, M. Helicobacter Pylori Outer Membrane Vesicle Size Determines Their Mechanisms of Host Cell Entry and Protein Content. *Front. Immunol.* **2018**, *9*. https://doi.org/10.3389/fimmu.2018.01466.

(52) MacDonald, I. A.; Kuehna, M. J. Stress-Induced Outer Membrane Vesicle Production by Pseudomonas Aeruginosa. *J. Bacteriol.* **2013**, *195* (13), 2971–2981. https://doi.org/10.1128/JB.02267-12.

(53) Jan, A. T. Outer Membrane Vesicles (OMVs) of Gram-Negative Bacteria: A Perspective Update. *Front. Microbiol.* **2017**, *8* (JUN), 1–11. https://doi.org/10.3389/fmicb.2017.01053.

(54) Mrozik, A.; Cycoń, M.; Piotrowska-Seget, Z. Changes of FAME Profiles as a Marker of Phenol Degradation in Different Soils Inoculated with Pseudomonas Sp. CF600. *Int. Biodeterior. Biodegrad.* **2010**, *64* (1), 86–96. https://doi.org/10.1016/j.ibiod.2009.11.002.

(55) Quezada, M.; Buitrón, G.; Moreno-Andrade, I.; Moreno, G.; López-Marín, L. M. The Use of Fatty Acid Methyl Esters as Biomarkers to Determine Aerobic, Facultatively Aerobic and Anaerobic Communities in Wastewater Treatment Systems. *FEMS Microbiol. Lett.* **2007**, *266* (1), 75–82. https://doi.org/10.1111/j.1574-6968.2006.00509.x.

(56) Schwechheimer, C.; Kuehn, M. J.; Rodriguez, D. L. Outer-Membrane Vesicles from Gram-Negative Bacteria: Biogenesis and Functions. *Nat. Rev. Microbiol.* **2015**, *13* (10), 605–619. https://doi.org/10.1038/nrmicro3525.Outer-membrane.

(57) Kato, S.; Kowashi, Y.; Demuth, D. R. Outer Membrane-like Vesicles Secreted by Actinobacillus Actinomycetemcomitans Are Enriched in Leukotoxin. *Microb. Pathog.* **2002**, *32*, 1–13. https://doi.org/10.1006/mpat.2001.0474.

(58) Hoekstra, D.; van der Laan, J. W.; de Leij, L.; Witholt, B. Release of Outer Membrane Fragments from Normally Growing Escherichia Coli. *BBA - Biomembr.* **1976**, *455* (3), 889–899. https://doi.org/10.1016/0005-2736(76)90058-4.

(59) Schönfeld, P.; Wojtczak, L. Short- and Medium-Chain Fatty Acids in Energy Metabolism: The Cellular Perspective. *J. Lipid Res.* **2016**, *57* (6), 943–954. https://doi.org/10.1194/jlr.R067629.

(60) Meier, C.; Oelschlaeger, T. A.; Merkert, H.; Korhonen, T. K.; Hacker, J. Ability of Escherichia Coli Isolates That Cause Meningitis in Newborns to Invade Epithelial and Endothelial Cells. *Infect. Immun.* **1996**, *64* (7), 2391–2399. https://doi.org/10.1128/iai.64.7.2391-2399.1996.

4.6 Supplemental Material

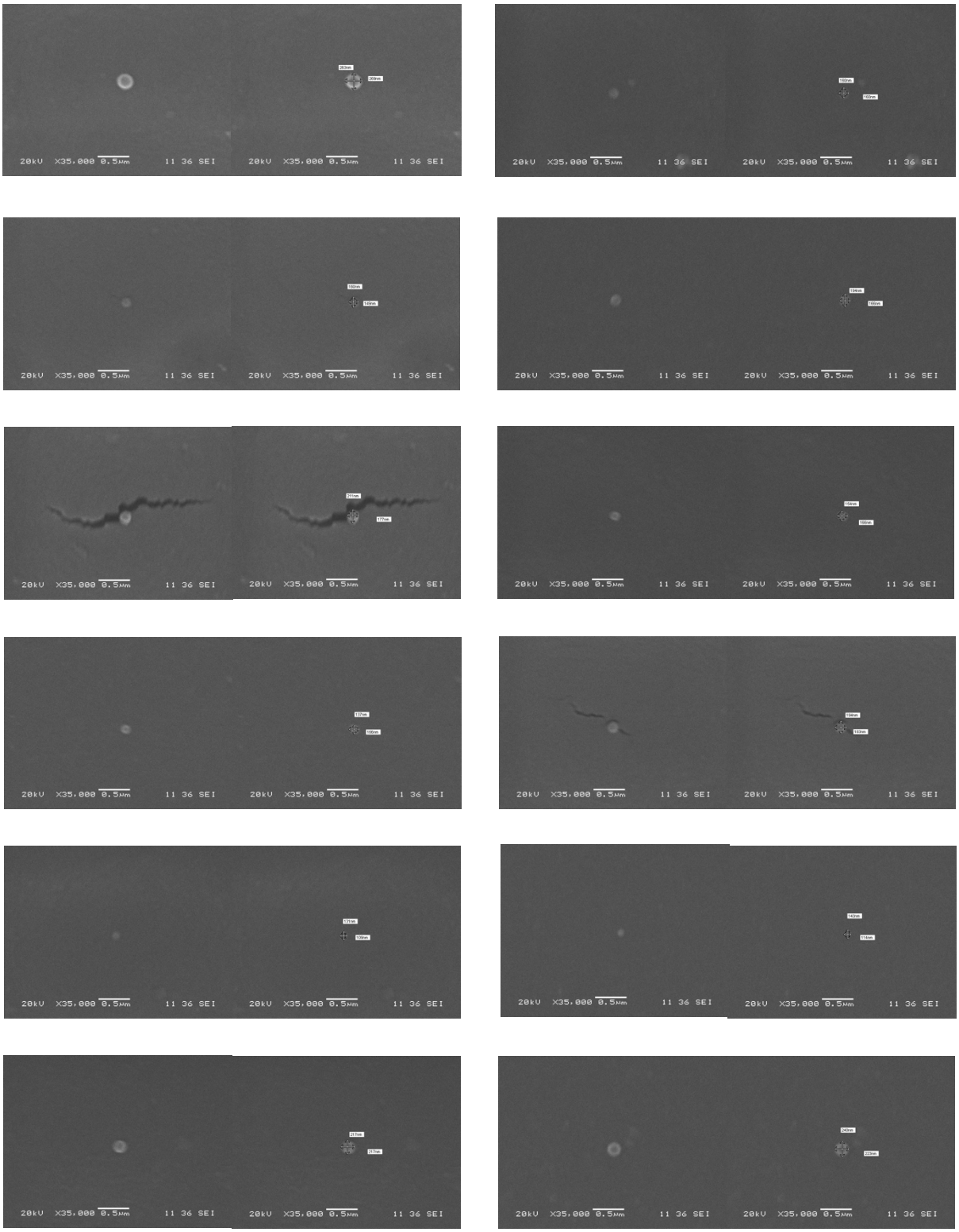

Figure S4.1. *E. coli* IHE3034 OMVs SEM micrographs (1/3).

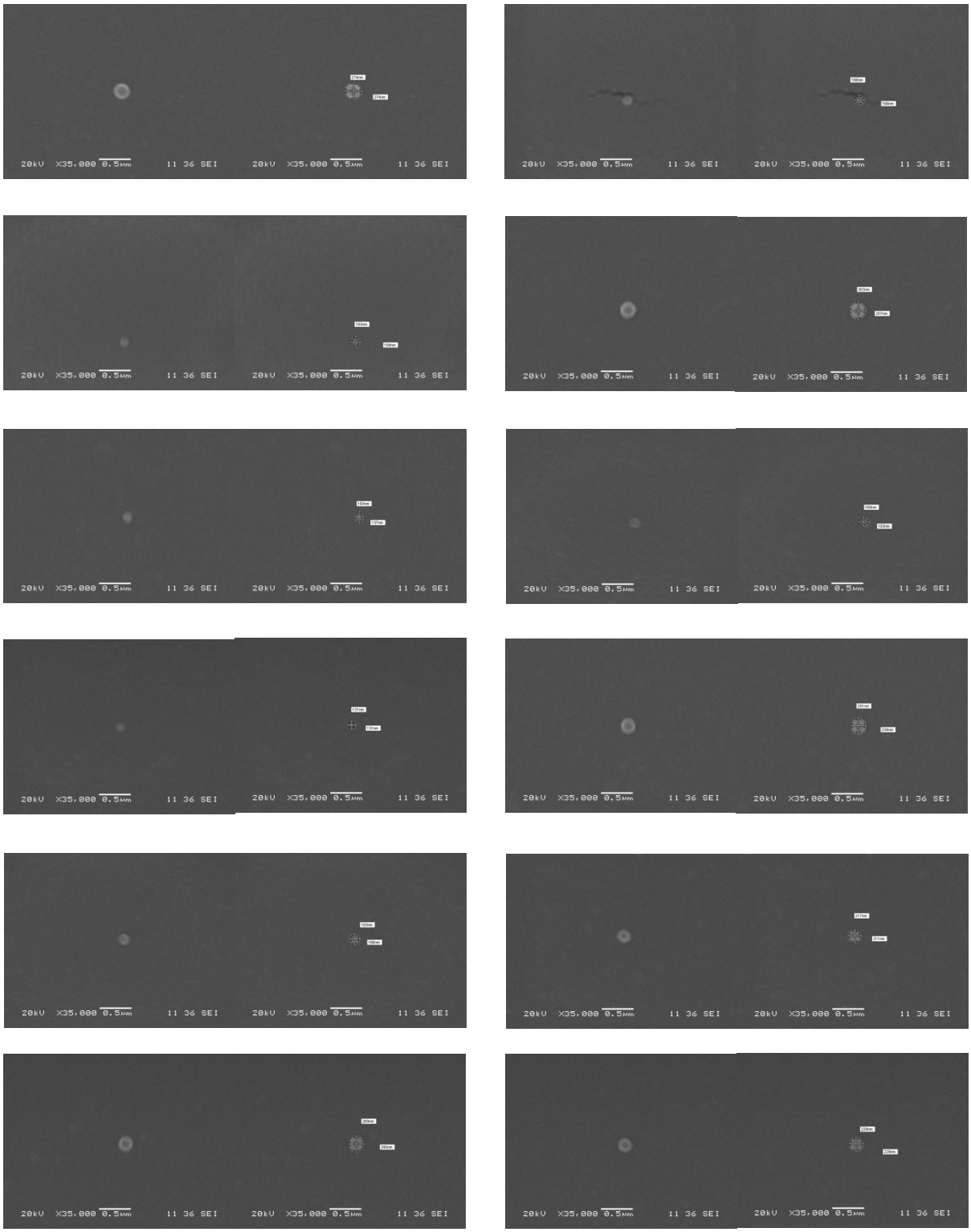

Figure S4.1. *E. coli* IHE3034 OMVs SEM micrographs (2/3).

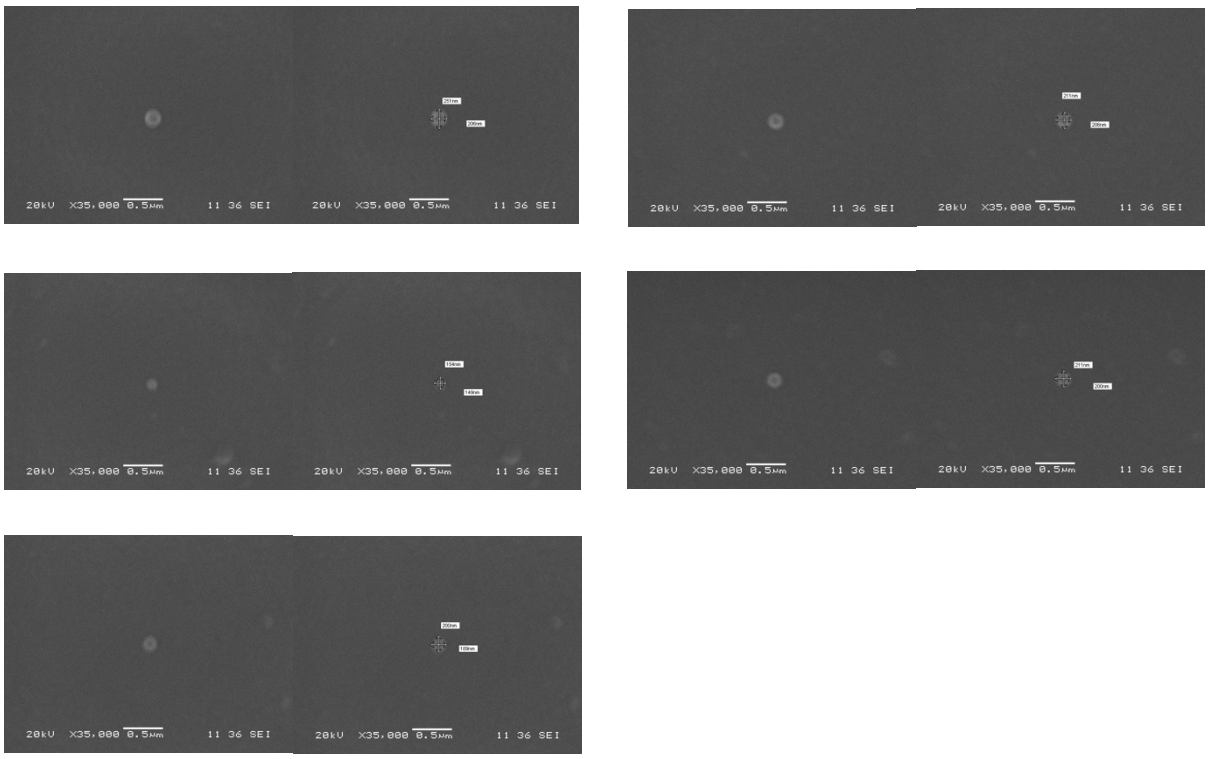

Figure S4.1. *E. coli* IHE3034 OMVs SEM micrographs (3/3).

Table S4.1. *E. coli* IHE3034 OMV approximate diameter by SEM.

***E. coli* IHE3034 OMV diameter by SEM (n=28)**		
Vertical (nm)	**Horizontal (nm)**	**Average**
131	109	120
143	114	129
131	131	131
137	166	152
154	149	152
160	149	155
160	160	160
154	166	160
183	137	160
166	166	166
183	154	169
160	183	172
183	166	175
194	166	180
194	183	189
211	177	194
211	200	206
211	206	209
217	211	214
217	217	217
251	206	229
229	229	229
240	223	232
251	234	243
269	240	255
263	269	266
274	274	274
303	257	280

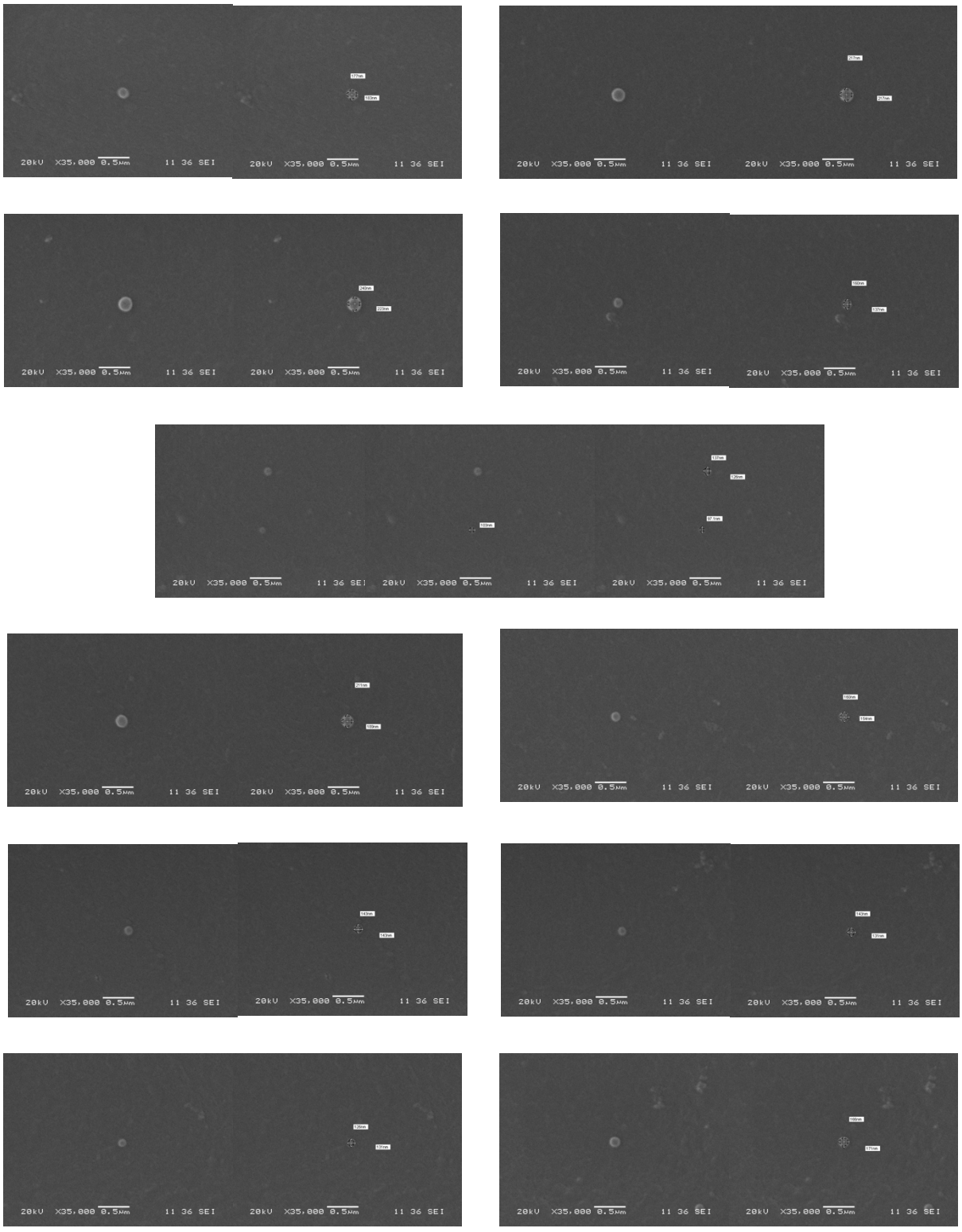

Figure S4.2 *E. coli* IHE3034 (Δ*clbP*) OMV SEM micrographs (1/3)

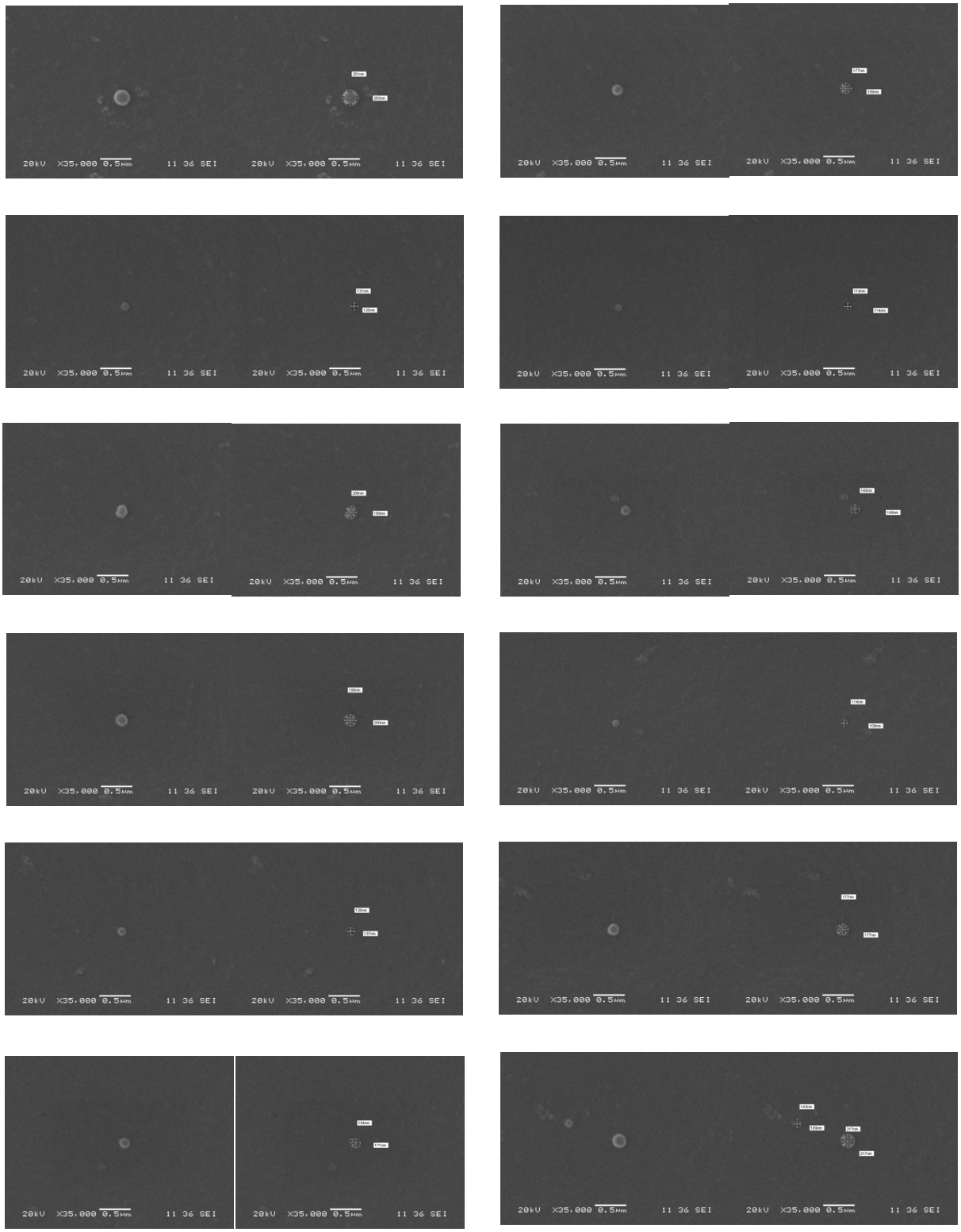

Figure S4.2 *E. coli* IHE3034 (Δ*clbP*) OMV SEM micrographs (2/3)

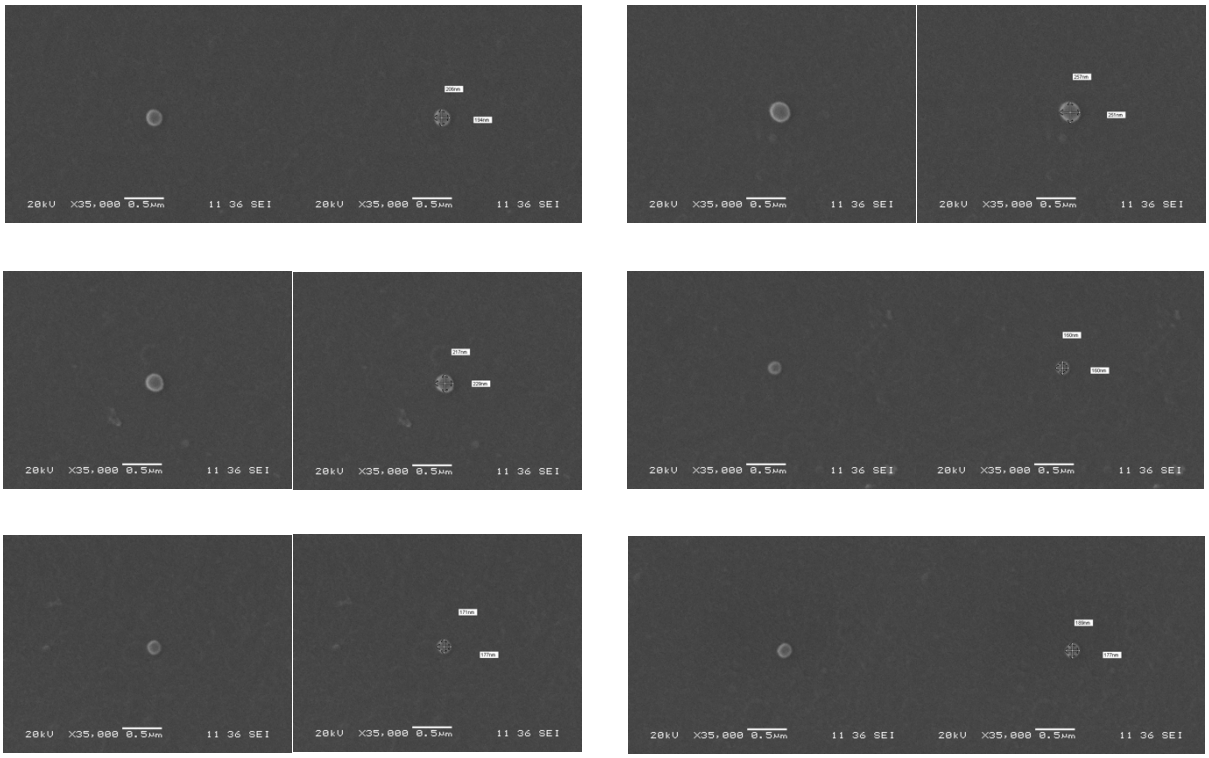

Figure S4.2 *E. coli* IHE3034 (Δ*clbP*) OMV SEM micrographs (3/3)

Table S4.2 *E. coli* IHE3034 (Δ*clbP*) OMV approximate diameter by SEM.

***E. coli* IHE3034 (Δ*clbP*) OMV diameter (n=31)**		
Vertical (nm)	**Horizontal (nm)**	**Average**
177	183	180
240	223	232
137	126	132
97	103	100
160	154	157
143	143	143
143	131	137
126	131	129
166	171	169
251	263	257
177	189	183
131	120	126
114	114	114
206	189	198
149	149	149
189	200	195
114	109	112
126	137	132
177	177	177
154	171	163
143	109	126
217	217	217
206	194	200
257	251	254
217	229	223
160	160	160
171	177	174
189	177	183
217	217	217
160	137	149
211	189	200

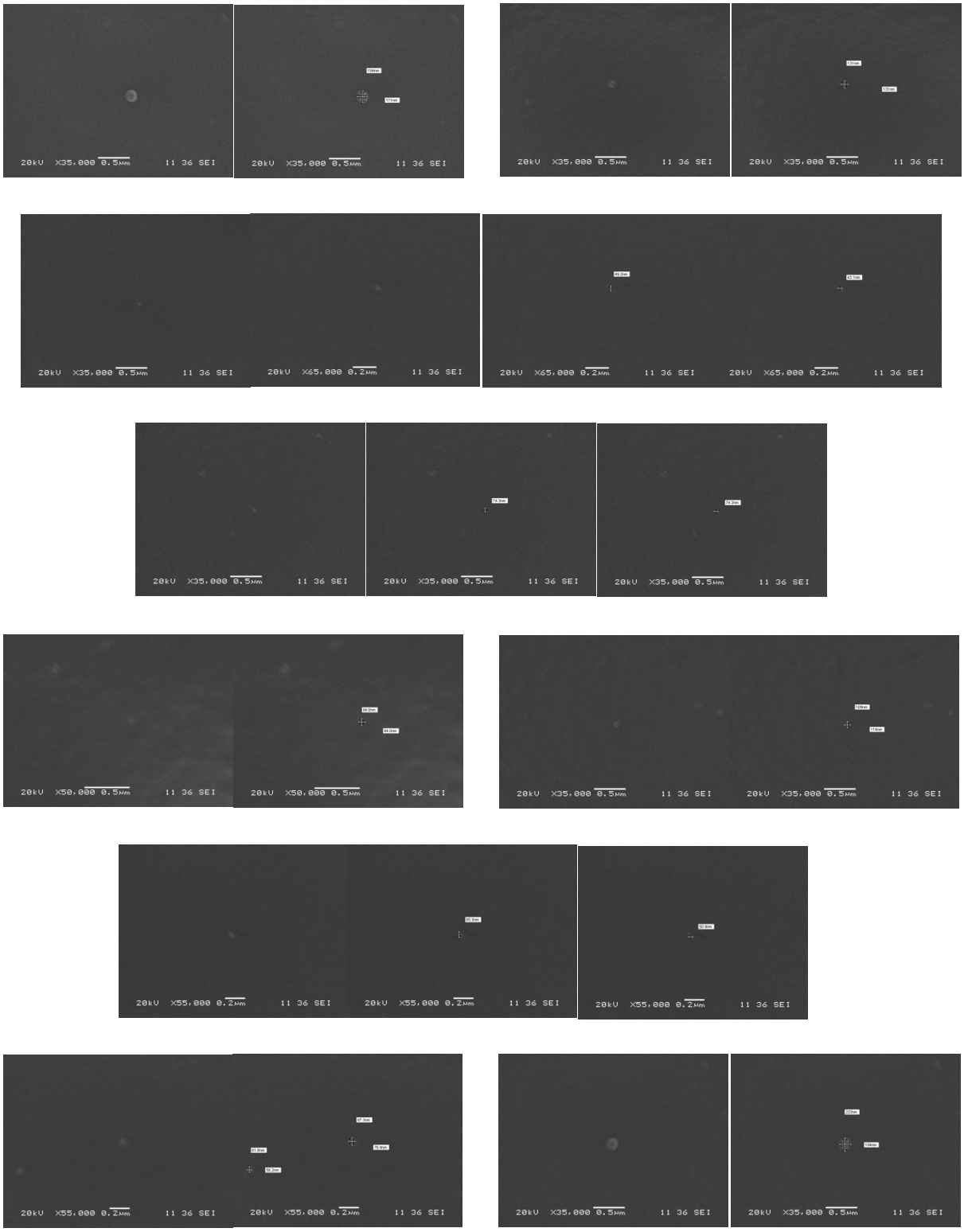

Figure S4.3. *E. coli* DH10B OMV SEM micrographs

Table S4.3. *E. coli* DH10B OMV approximate diameter by SEM**.**

***E. coli* DH10B OMV diameter (n=12)**				
Vertical (nm)	**Horizontal (nm)**	**Average (nm)**		
194	171	**183**	±	**16**
131	131	**131**	±	**0**
49.2	43.1	**46**	±	**4**
74.3	74.3	**74.3**	±	**0**
84	84	**84**	±	**0**
65.5	50.9	**58**	±	**10**
109	114	**111**	±	**4**
223	194	**209**	±	**21**
61.6	58.2	**60**	±	**2**
87.3	76.4	**82**	±	**8**
163	163	**163**	±	**0**
194	194	**194**	±	**0**

Table S4.4 OMV samples amount used for trans-esterification.

OMV Esterification				
Sample		Empty sample tube (g)	Sample tube + OMVs lyophilized(g)	OMV lyophilized (mg)
IHE3034	1	6.4225	6.4375	15.00
	2	6.4070	6.4235	16.50
	3	6.4313	6.4438	12.50
IHE3034Δ*clbP*	1	6.3945	6.4111	16.60
	2	6.4321	6.4608	28.70
	3	6.4123	6.4479	35.60
DH10B	1	6.3490	6.3696	20.60
	2	6.3945	6.4088	14.30
	3	6.4432	6.4661	22.90
Blank	1	6.3706	6.3716	1.00
	2	6.3107	6.3237	13.00
	3	6.4262	6.4559	29.70

*Esterif Rxn; 4 mL etanol/2 drops HCl

Table S4.5 Bacterial cell sample amount used for trans-esterification.

Cell Pellet Esterification				
Sample		Empty round flask(g)	Round flask + lyophilized cell pellet (g)	Lyophilized cell pellet esterified (mg)
IHE3034	1	27.7419	27.8694	127.50
	2	29.8928	29.9935	100.70
	3	25.9459	26.0532	107.30
IHE3034Δ*clbP*	1	27.7407	27.8444	103.70
	2	25.9458	26.0456	99.80
	3	29.8928	29.9974	104.60
DH10B	1	25.9450	26.0424	97.40
	2	29.5442	29.6426	98.40
	3	29.8935	29.9837	90.20
Blank	1	6.4567	6.4905	33.80
	2	6.4258	6.4520	26.20
	3	6.7420	6.7642	22.20

*Esterif Rxn; 5 mL etanol/3 drops HCl

Chapter 5. Outer Membrane Vesicles as Mediator of Colibactin Toxicity: Biological Activity and Internalization

Abstract

The *pks* genomic island is a gene cluster from certain strains of gram-negative bacteria that are implicated in the development of colorectal cancer (CRC) and inflammatory bowel diseases (IBD). Its genes encode the production of the natural product, colibactin, which is genotoxic to mammalian cells. Evidence about the mechanism by which colibactin is delivered to host cells is lacking. Since it has been proved that colibactin is not secreted into the bacterial environment nor is exported by the usual bacterial secretion system, we explored the involvement of bacterial outer membrane vesicles (OMVs) in colibactin toxicity. Here we report that exposing mammalian cells to OMV derived from IHE3034, an *E. coli* strain competent to make colibactin, which were sufficient to elicit the hallmarks of genotoxicity, including megalocytosis and the activation of the DNA repair machinery of the cell. Even so, we did not observed that OMVs from the *pks* positive strain causes interstrand crosslink as described for colibactin genotoxic mechanism. However, the observed cellular damage caused by the isolated vesicles resembled the damage caused by live *pks*+ *E. coli*, the secretion of OMVs could be someway linked with the colibactin toxic mechanism towards mammalian cells.

5.1 introduction

Colibactin is a non-ribosomal peptide/polyketide hybrid metabolite that is produced by enzymes encoded in the pks genomic island[1]. The presence of *pks* genes in the commensal microbiome has been implicated with sporadic CRC and IBD disease development[2–6]. It has been also demonstrated that biopsies from CRC patients have a higher prevalence of the pks genes when compared to biopsies from healthy patients[2,7]. In fact, bacteria harboring these genes induce tumor growth, both in chronic intestinal inflammation mouse models and in intestinal biopsies from CRC patients[4], further supporting the link between colibactin and carcinogenesis.

Strains of *E. coli* harboring the *pks* genes are capable to induce double-strand breaks (DSBs) and interstrand crosslinks (ICL) on DNA of mammalian cells upon contact[1,2,6]. Consequently, these types of damages on host cells, activate a DNA damage response (DDR), which triggers the activation of several kinases that will phosphorylate different factors in order to (1) sense the damage, (2) block cell division by the activation of checkpoint response; or by the (3) activation of DNA repair mechanisms. The DDR is a complex and multifactorial event (Figure 5.1)[8], but a common pathway is one that when, after a DNA DSBs insult, the protein kinase ATM and Histone γH_2AX are activated by its phosphorylation[9]. Histone γH_2AX serves as DSBs sensor and ATM, in turn, activates protein kinase CHK1 and/or CHK2 (mainly activated as DSBs response)[9,10]. Then, activated CHK1/CHK2 together with ATM and others kinases, activate a signaling cascade that includes the inhibition of cyclin-dependent kinases (CDK) activity[9]. Inhibition of CDK slows down or arrests the cell cycle in order to give the cell time to repair the

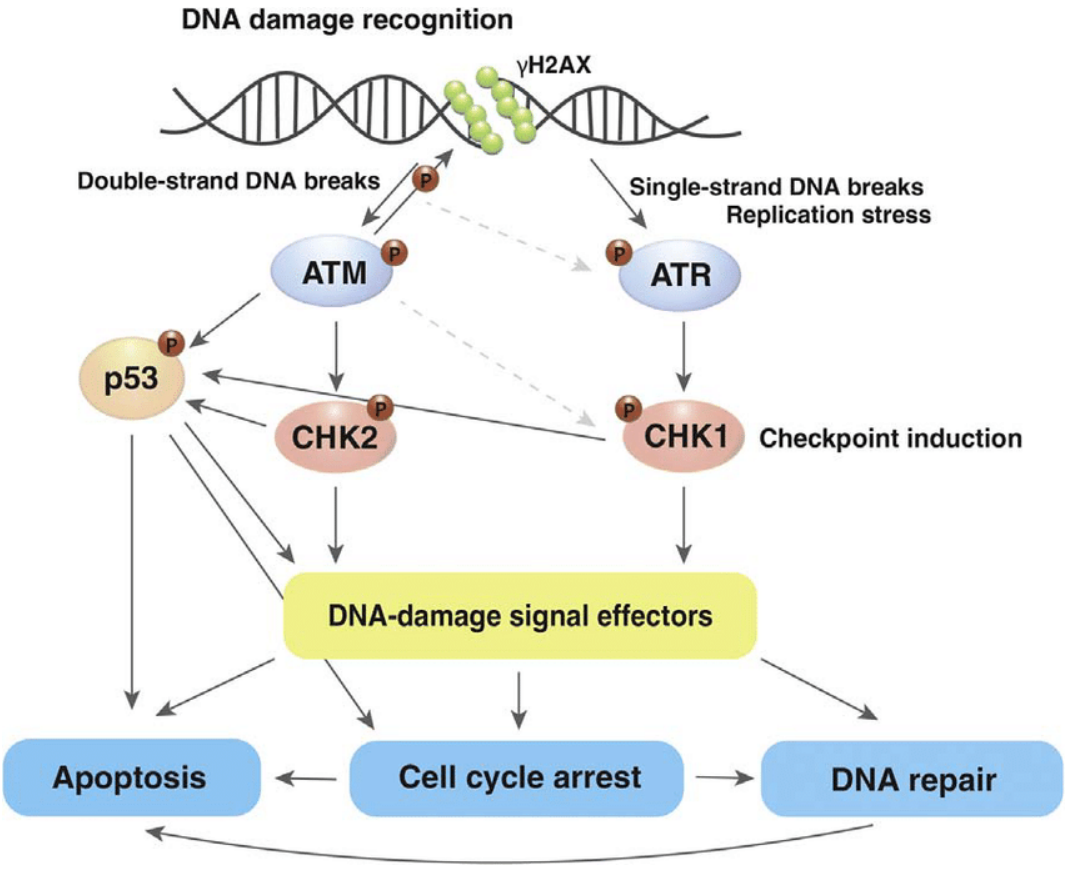

Figure 5.1. Simplified representation of the DNA damage response pathway. DNA damage and replication stress-induced double-strand and single-strand DNA breaks activate ATM and ATR kinases, respectively. ATM and ATR are key signal transducers of downstream DDR pathways. Once phosphorylated, they trigger the activation of downstream cell-cycle regulators CHK1 and CHK2, which in turn signal downstream checkpoints that stop cell-cycle progression and activate DNA damage repair and tolerance mechanisms. ATM also phosphorylates H2AX and amplifies DNA damage signal. In addition, DDR induces the activation critical sensors of DNA damage, which determines cell fate depending on the levels of DNA damage or DNA-repair efficiency. Image taken from Tšuiko *et al.* 2018

damages in DNA before continuing to mitosis and cell division[9]. Also, as part of the DDR, also is activated the production of effectors enzymes in charge to do the repairing work. When this damages sensing and repair repose fail, some cells are programed to apoptosis (programmed cell death) and others become senesce or aberrant[3,4] promoting the release of carcinogenic factors to nearby cells. This accumulation of unrepaired genetic alterations promotes carcinogenesis converting healthy cells into tumor cells.

To date, there is no described mechanism that directly addresses how colibactin interacts with the host cell to exert damages. Among the secretion pathways of bacteria, outer membrane vesicles (OMVs) figure as one of interest by their particular characteristics. OMV provide a secretion pathway for gram-negative bacteria and is responsible for the release of the outer membrane and periplasm content out of the cell.[11,12] Actually, OMVs of some bacterial strains has been found to promote aberrant growth in mammalian cells upon contact.[13] On the other hand, colibactin is presumably made within the bacterial cytosol and transported to the periplasmic space by a transporter protein where the genotoxin is processed and activated.[14,15] Once in the periplasmic space, OMVs could be playing a role in promoting the biogenesis of vesicles or using it as a vehicle to reach its target cells. Thus, OMVs could be a possible mechanism of transportation for the *pks* island biosynthetic product.

In this chapter, we report the involvement of bacterial OMVs in mediating the deleterious phenotypes attributed to colibactin. We isolated OMVs from both a colibactin-producing bacteria and its corresponding *clbP* gene deletion mutant, which cannot produce mature

colibactin, and tested them *in vitro* with mammalian cells. Our results show that OMVs derived from wild-type *pks*+ *E. coli* are, by themselves, able to induce megalocytosis and dsDNA damage in HeLa cells, thus demonstrating a link between OMVs and the genotoxic activity of colibactin.

5.2 Methods

5.2.1 Bacterial Strains. *E. coli* IHE3034 *pks*+ was kindly donated by Dr. Eric Oswald from the University of Toulouse, France. The *E. coli* DH10B pks- (non-genotoxic) was used in all the experiments as a control strain. All strains, including the Δ*clbP* mutant (detailed in chapter 2, section 2.2.1.2) were "re-animated" from cryogenic storage in lysogenic broth (LB) medium (Sigma-Aldrich) agar for 16- 24 hrs at 37 °C. Colonies were then selected and grown in liquid LB. Culture conditions are specific according to the experiment or assay requirements.

5.2.2 Isolation of OMVs. OMV isolation methodology was adapted from Tyrer et al.[13] *E. coli* bacterial strains were grown in 250 mL of LB medium (Sigma-Aldrich) pH 7.4 at 37 ^{o}C under constant rotation (120 rpm) for 18-20 hrs. The cultures were centrifuged at 4 ^{o}C, 5,000 rpm for 10 minutes. The resulting supernatants were collected and filtered by a 0.45 µm PVDF membrane (Stericup Durapore Cat. No. S2HVU02RE), and then ultra-centrifuged at 4 ^{o}C, 40,000 rpm for 3 hours to obtain the OMV pellet (200 mL of culture OMV pellet). The resultant pellet was washed twice using TBS (TRIS-Saline Buffer; 50 mM TRIS, 150 mM NaCl, pH 8.4) and re-ultracentrifuge under the same conditions. OMV pellet was then re-suspended up to 1 mL of TBS and re-filter by a 0.45 µm PVDF

membrane (SIGMA Cat. No. UFC30HV00). OMV enriched solutions were inoculated in LB agar plate to ensure no bacterial cells were present**.** Samples were stored at 4 ^{o}C until further analysis.

5.2.3 OMV Production Quantification. The OMV quantification was performed targeting OMV associated proteins[16–19]using the BCA Assay (Pierce BCA Protein Assay Kit, Prod. #23225) as described in the manufacturer's instructions. OMV isolates were measured in a 96-well plate (UV Flat bottom Microtiter plates Cat No. 8404) using a photometric plate reader at 562 mm wavelength. A calibration curve using bovine serum albumin (BSA) was used.

5.2.4 Cell growth and OMVs treatment. HeLa cells (ATCC CCL-2) were cultured in Dulbecco's Modified Eagle's Medium (DMEM, SIGMA Cat No. D5796) supplemented with 10 % fetal bovine serum (FBS, SIGMA Cat. No. F2442) and Penicillin/Streptomycin (100 U:100 µg/mL) (CORNING Cat. No. 30-002CI). The cells were incubated at 37 °C, in 5 % CO_2, and were maintained by serial passage every time they reached 85 – 90 % of confluence. For the experimental assays, the OMV dilution, after normalization by BCA Assay, was added to the HeLa cell culture at 50 % confluence and incubated for 4 or 72 hrs according to the particular experiment.

5.2.5 Labeling of OMVs. The labeling method used was adapted from *Tyrer et al.,* 2014[13]. OMVs were incubated with 1 % Vybrant™ DiO for 20 min. at 37 °C. Free dye was removed by performing three washes with 300,000 Da cutoff Vivaspin 500

ultrafiltration units. Briefly, OMVs were added to the ultrafiltration units with 500 µL of TBS and then centrifuged at 14,000 *g* for 25 minutes. The retentate (containing the OMVs) was diluted with 500 µL of TBS and the process was repeated two times.

5.2.6 OMV internalization by Confocal Microscopy. The visualization method to evaluate OMV internalization by HeLa cells was adapted from Tyrer et al., 2014[13]. HeLa cells were seeded (10,000 cells) in 8-wells tissue culture Chamber Slide (Lab-Tek II 154534) at 37 °C and 5 % CO_2 in DMEM (10 % FBS, Penicillin/Streptomycin (100 U:100 µg/mL), 25 mM HEPES) until 50 % of confluency was reached. Cells were then incubated with previously labeled OMVs (approx. 1.0 µg OMVs per well) for 0, 1, 2, 3, 4 and, 72 hours. The cells were washed two times with D-PBS and then fixed in 200 µL of neutral buffered PFA (4%, paraformaldehyde) for 10 minutes. Cells were then permeabilized with Triton X-100 (0.1 %) in D-PBS for 13 minutes. Then, cells were stained with TRITC-phalloidin (2 µg/uL, SIGMA) for 1 hour. The coverslips were then mounted in ProLong Diamond mounting medium with DAPI (Invitrogen P36971). The slides were imaged with a Nikon Eclipse Ti-E Inverted Fluorescence Microscope, with Plan Apo λ 20X (Aperture 0.75) and Plan Apo λ 100X Oil (Refractive Index 1.515; Numerical Aperture 1.45) objective of magnification, and Nikon A1plus camera. For 20X images, Image stacks were taken at 0.25 µm intervals (pinhole size 58.75 µm). Images were adjusted for presentation.

Confocal images were analyzed in order to evaluate the internalization of OMVs by HeLa cells and to measure the nuclear area of treated cells. Intensity analysis was performed using the NIS-Element Advance Research Imaging Software (version 5.20).

Values were reported as means ± standard error means of biological replicates. *p*-values were calculated using one-way analyses of variance (ANOVA) with the "Tukey's Multiple Comparison" test for multiple comparisons. All statistical analyses were conducted using Prism 6 software (GraphPad, La Jolla, CA, United States).

5.2.7 Phenotypic Analysis of HeLa cells treated with OMVs. HeLa cells were grown, using the same parameters as previously mentioned (section 5.2.4), in a 24 wells culture plate with a total volume of 1 mL and with a sterile round glass coverslip in each well. The OMVs, previously normalized to 20 μg/mL (0.02 μg/uL) by BCA Assay, were added to the HeLa cells and co-incubated for 4 hours. Then, the HeLa cells morphology was analyzed under a light microscope (Nikon ECLIPSE LV100N POL) using Giemsa staining, following the manufacturer's instructions (SIGMA Cat. No. GS500). Briefly, cells attached to the round coverslip were fixed using methanol, followed by three consecutive washes with ddH2O. Then, cells were incubated at room temperature with 1 mL of 1:20 solution of Giemsa stain:water for 30 minutes. Coverslips were transferred upside down in a microscope slide with a minimal amount of Xylene-based mounting media.

5.2.8 Detection of DNA damage markers in HeLa cells treated with OMVs: The OMVs, at a normalized final concentration of 8 μg/mL (40 μg OMVs/5 mL culture media) by BCA Assay, was added to the HeLa cells and co-incubated for 4 hours. Then, the cells were washed three times with D-PBS and scraped in 500 µL of 1X Laemmli Buffer (BIO-RAD Cat. No. 161-0737) with 5 % β-mercaptoethanol. The resulting cell solution was sonicated for 10 sec. to shear the DNA. 20 µL of each sample were heated for 10 minutes

at 95 °C and then centrifuged at 15,000 rpm for 5 minutes. The supernatant was collected and the extracted proteins were separated by 10% SDS-polyacrylamide gel electrophoresis and electro-transferred to a 0.22 μm nitrocellulose membrane for immunoblotting. Briefly, the protein transfer system iBlot2 ® was used to transfer protein from gels to nitrocellulose membranes using the P0 parameter. The iBind® Western Device was prepared by adding the primary and secondary antibody solutions and washes to the corresponding chambers. By following the manufacturer's protocol, dilutions of 1:1000 of the primary DNA Damage markers (anti-*p*ATM, anti-*p*Chk1, and anti-*p*Chk2), anti-GAPDH, and the secondary anti-rabbit HRP conjugated antibodies were prepared using the iBind® solutions. The membrane was removed from the iBind® system after 3.5 h and analyzed by chemiluminescent autoradiography for protein detection. Protein loading was normalized with anti-GADPH.

5.2.9 *In vitro* OMVs-DNA Crosslinks Assay. Isolated OMVs from *pks*+ IHE3034 (WT), its isogenic mutant IHE3034 Δ*clbP,* and DH10B *E. coli* strains were exposed to linearized pUC19 DNA plasmid following a methodology adapted from Bossuet-Grief et al. and Xue et al.[20,21]. Briefly, the pUC19 DNA plasmid was linearized with BAMHI (NEB) and purified using the QIAquick PCR kit (Qiagen). In a 96 wells plate 1 µg of OMVs were exposed to 500 ngs of DNA in 100 µl o total volume of DMEM-5 mM EDTA, 25 mM HEPES, 10% FBS, 1X Pens/Strep (100 U:100 µg/mL). Cisplatin 100 µM was used as a positive control. After incubation (4 and 24 hrs) at 37 ^{o}C and 5 % CO_2. DNA was purified using the QIAquick PCR kit.

To evaluate the respective OMVs producing bacteria, *pks*+ IHE3034 (WT), its isogenic mutant IHE3034 Δ*clbP* and DH10B *E. coli* strains were grown in LB media overnight at 37 ^{o}C and 200 rpms. Then, bacterial cells (approx. 5.98 x 10^5 cells) were exposed to DNA with DMEM- 5 mM EDTA, 25 mM HEPES, 10 % FBS, 1X Pens/Strep for 10 hrs of incubation at 37 ^{o}C and 5 % CO_2. In both cases (OMVs or bacteria) EDTA was be added to protect DNA from DNases degradation.

Treated DNA samples were analyzed by denaturing gel DNA electrophoresis. A volume of 5 μL of DNA samples were mixed with 15 μL of 0.4 % denaturing buffer (0.4% NaOH, 10% Glycerol, 0.013 % bromophenol blue). After 10 min. of incubation DNA samples were loaded in a 1 % agarose gel prepared in TBE (Tris-Borate-EDTA) Buffer. The samples were run in TBE Buffer for 1.5 hrs at 90 V. After electrophoresis, gel was soaked in 100 mL of TBE Buffer with GelRed Dye for 30 to 60 minutes.

5.3 Results

5.3.1 OMVs are bacterial-free.

To ensure that biological effects to be assayed are attributable just to the isolated OMVs without any contamination of bacteria carried through the isolation process, OMV enriched solutions were inoculated in LB bacterial culture media. As result, no growth were observed for any of the OMV isolates cultivated (Figure 5.2), confirming that OMV samples are sterile or live cell-free.

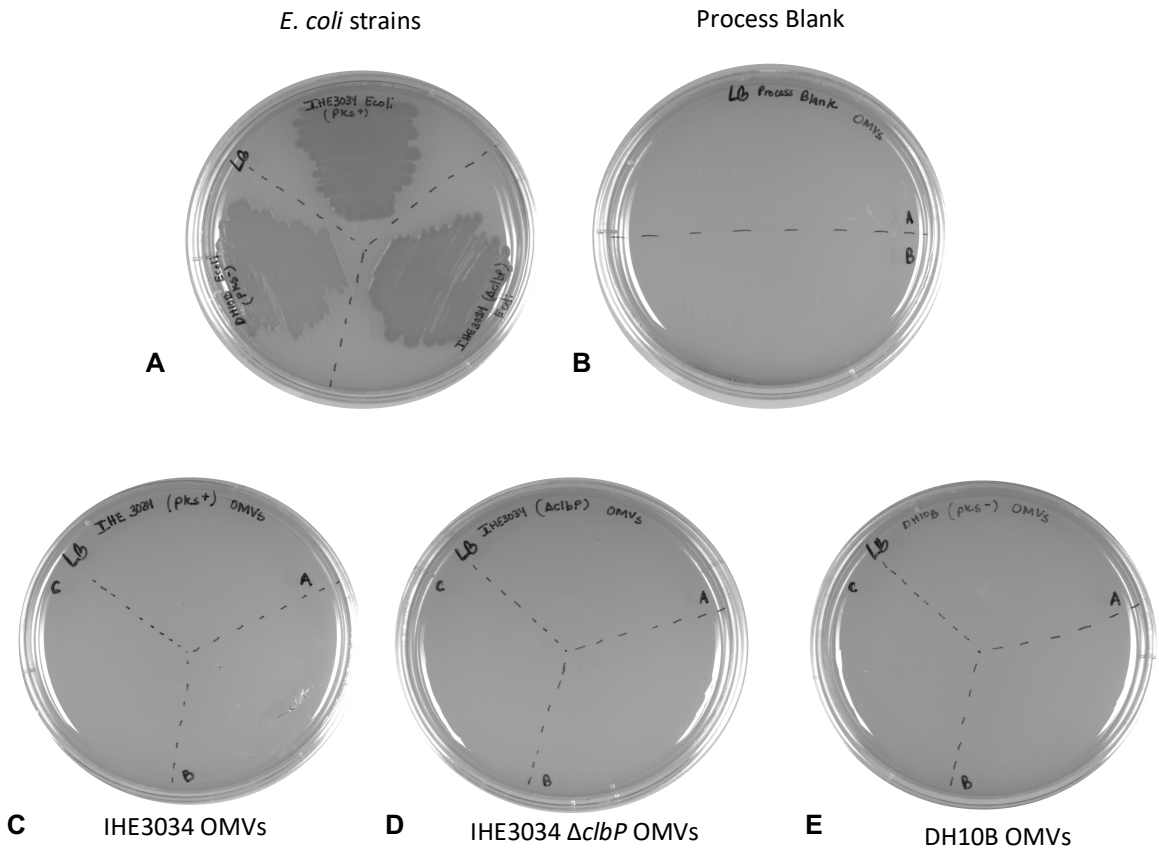

Figure 5.2. Bacterial-free OMV isolates. Isolated OMV samples streaked on LB Agar plates after 24 hrs of incubation at 37 °C. **A)** Bacteria used to isolate OMVs was used as positive control. **B-E)** No bacterial growth was observed in any of the OMV isolates (isolated from IHE3034, IHE3034 *⊿clbP*, and DH10B cultured *E . coli* strains) nor negative control "process blank". A, B, and C in each plate represent biological replicates.

5.3.2 OMV from *E. coli* IHE3034 cause megalocytosis in a human cell line.

The capacity of OMV isolated from an colibactin-producing *E. coli* strain to induce magalocytosis was assayed on HeLa cells in biological replicates. In effect, results show that bacterial OMVs from the *pks*+ strain *E. coli* IHE3034 induce megalocytosis on the cultured HeLa cells after 4 hrs of co-incubation (Figure 5.3 A; images of triplicates are in section 5.6, Figure S5.2 a, b, c, d, and e). Interestingly, we observed that OMVs from IHE3034 Δ*clbP* mutant strain, which we expected would abolish said phenotype, also caused megalocytosis when compared to the controls. The megalocytosis caused by the mutant strain is clearly equal or more than the effects of the OMVs from the WT strain *E. coli* IHE3034. OMVs from DH10B (our laboratory control strain) did not induced any change on the morphology of treated cells when compared with cells without treatment.

To quantitatively determine the degree of megalocytosis induced by OMVs, the nucleus area of treated cell was measured. Results reveal that OMVs from IHE3034 WT strain induce nuclear enlargement approximately 1.3 and 1.4 times bigger than the enlargement caused by OMVs from *E. coli* DH10B and cells without treatment respectively (Figure 5.3 B). Confirming the observed megalocytosis in the images of Figure 5.3, OMVs from the *E. coli* IHE3034 Δ*clbP* mutant strain cause 1.4 times more nuclear enlargement than the OMVs from wildtype strain on treated cells. Statistical analysis (one-way ANOVA) reveal that OMVs from Δ*clbP* mutant strain generate more nuclear enlargement than the OMVs from the WT strain (p-value < 0.0001). It should note that some megalocytic cells show to be multinucleated with several nucleus of small/normal sizes. Altogether, these results strongly suggest that the lack of clbP peptidase somehow promote more cellular enlargement, in other words more megalocytosis.

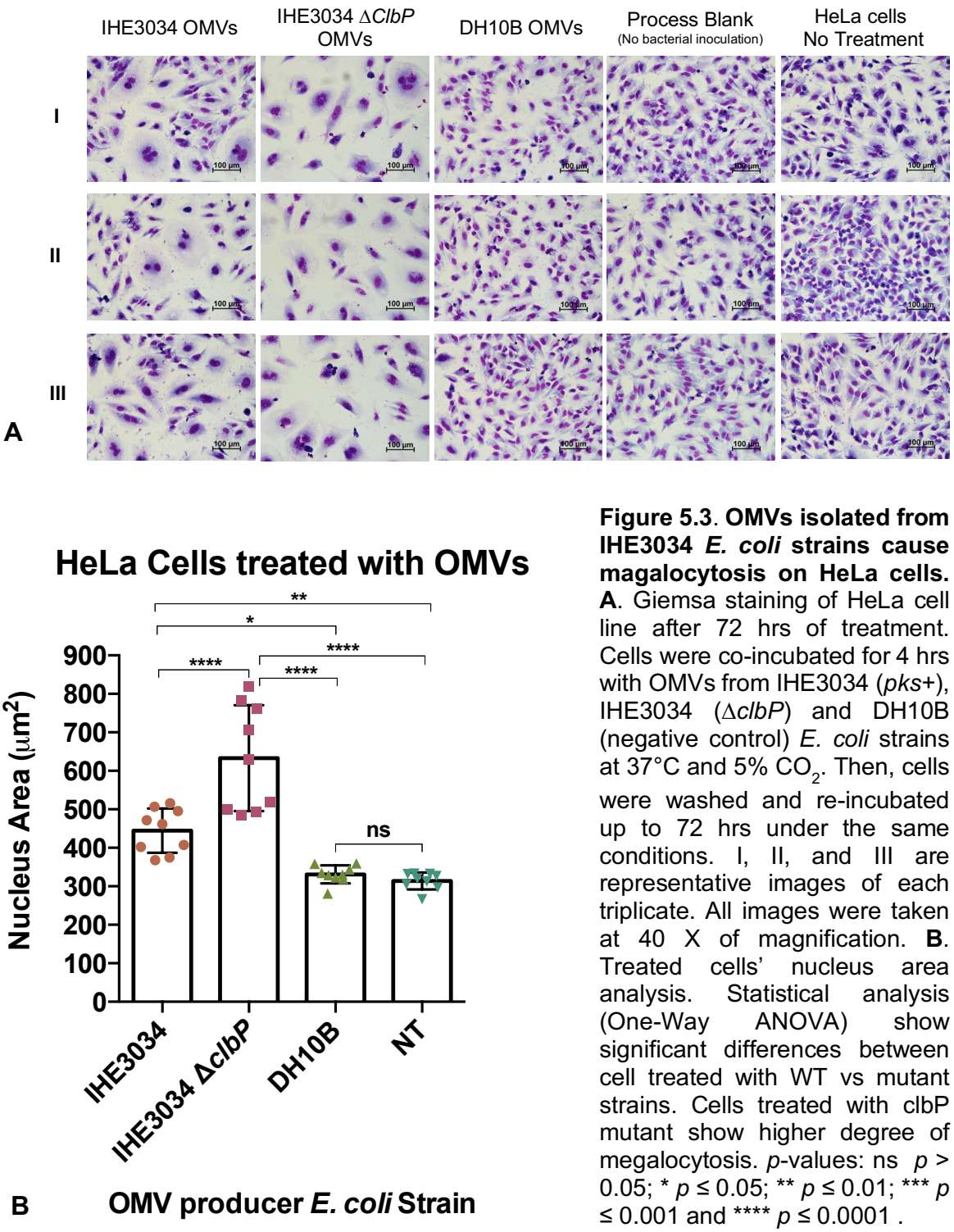

Figure 5.3. OMVs isolated from IHE3034 *E. coli* strains cause magalocytosis on HeLa cells. **A**. Giemsa staining of HeLa cell line after 72 hrs of treatment. Cells were co-incubated for 4 hrs with OMVs from IHE3034 (*pks*+), IHE3034 (Δ*clbP*) and DH10B (negative control) *E. coli* strains at 37°C and 5% CO_2. Then, cells were washed and re-incubated up to 72 hrs under the same conditions. I, II, and III are representative images of each triplicate. All images were taken at 40 X of magnification. **B**. Treated cells' nucleus area analysis. Statistical analysis (One-Way ANOVA) show significant differences between cell treated with WT vs mutant strains. Cells treated with clbP mutant show higher degree of megalocytosis. *p*-values: ns $p > 0.05$; * $p \leq 0.05$; ** $p \leq 0.01$; *** $p \leq 0.001$ and **** $p \leq 0.0001$.

Table 5.1 Nucleus area measurements of HeLa cells treated with OMVs.

Strain		Mean Area (μm^2)	St Dev. (μm^2)	Cell Nucleus Area Average (μm^2)	St Dev. (μm^2)	Average (μm^2)	St Dev. (μm^2)
OMV IHE3034 A	**1**	367.89	127.35	448	75	445	48
	2	461.58	345.21				
	3	515.54	295.31				
OMV IHE3035 B	**1**	495.64	308.68	491	18		
	2	471.9	248.31				
	3	506.88	122.67				
OMV IHE3036 C	**1**	402.59	226.22	395	18		
	2	374.63	244.48				
	3	407.44	226.48				
OMV IHE3034 Delta clbP A	**1**	783.05	332.41	688	148	633	122
	2	518.05	230.47				
	3	762.82	289.37				
OMV IHE3035 Delta clbP B	**1**	500.15	353.7	493	8		
	2	493.59	190.36				
	3	484.12	217.58				
OMV IHE3036 Delta clbP C	**1**	629.23	312.83	718	95		
	2	705.69	442.24				
	3	818.95	372.86				
OMV DH10B A	**1**	330.01	94.21	329	6	331	17
	2	334.51	101.29				
	3	322.87	103.57				
OMV DH10B B	**1**	319.09	105.66	315	31		
	2	281.11	99.01				
	3	343.6	114.92				
OMV DH10B C	**1**	329.31	105.72	349	17		
	2	359.51	90.92				
	3	358.26	140.78				
No Treatment A	**1**	312.93	102.54	300	29	314	16
	2	266.36	85.3				
	3	319.89	74.12				
No Treatment B	**1**	331.62	96.32	311	18		
	2	296.97	100.09				
	3	304.94	85.98				
No Treatment C	**1**	332.65	108.95	331	3		
	2	326.87	108.96				
	3	332.81	93.29				

5.3.3 OMVs from *E. coli* IHE3034 are internalized by HeLa cells.

Fluorescent microscopy was used to confirm that OMVs are internalized by HeLa Cells. By labeling OMVs with the fluorescent probe, membrane-intercalating dye 3,3′-dioctadecyloxacarbocya-nine perchlorate (DiO) we were able to show that vesicles entered into the cells. After co-incubation with labeled OMV (green), treated cells were stained with TRITC-Phalloidin and DAPI for cell body (red) and nucleus (blue) visualization respectively. As results, OMVs from IHE3034 strains, both WT and Δ*clbP* mutant, and from DH10B non-pathogenic strain are internalized by HeLa cells, since green label was localized inside of treated cells (red and blue areas Figure 5.4).

The entrance OMV to HeLa cells was monitored for 0, 1, 2, 3, 4, and 72 hrs (Figure 5.4, images of 0, 2, and 3 hours seems similar to 1 hour of treatment, thus not was included in this analysis). Resulted confocal images show that after 4 hours of direct exposition, cells treated OMVs from IHE3034 Δ*clbP* show greener intensity in cell areas but minimal green intensity was observed in cells treated with OMVs from IHE3034 WT, DH10B, and process blank solution. After 72 hrs, cells treated with either WT or mutant IHE3034 strains show higher green intensity in cell area than cells treated with OMVs from negative control DH10B (Figure 5.4). As expected, negative controls show minimal or no green intensity over the background levels in any of the time points evaluated. These results reveals that (1) the OMVs from all three strains were internalized by HeLa cells; (2) OMVs from the mutant strain deficient to produce active colibactin (Δ*clbP* mutant) is internalized faster than OMV from IHE3034 *WT* and DH10B negative control (non-pathogenic); (3) cells treated with OMVs from IHE3034 strains (either WT or Δ*clbP* mutant) for 72 hrs

show cell body a nucleus enlargement, but cells treated with OMVs from DH10B strain seem similar to negative control (process blank) and cells without treatment.

To quantitatively evaluate the internalization and localization of OMV on HeLa cells, the florescence intensity of labeled OMV (green, DiO fluorescent dye) was determined over cellular area (red, TRITC-Phalloidin fluorescent dye) and over nuclear area (blue, DAPI fluorescent dye). The intensity of green dye in the red labeled cells will give information about the internalization of OMV by the treated cell, whereas the intensity of green labeled vesicles in the blue stained nucleus will give information about their localization inside the nucleus of treated cells. Quantitative analysis reveal that OMVs from IHE3034 Δ*clbP* are localized in statistically significant higher amount inside of treated cells when compared with cells treated with OMVs from the wild-type strain IHE3034 (*p*-value 0.0076 for 4 hrs Figure S5.2 ; *p*-value 0.0406 for 72 hrs Figure 5.5). Also, results show that after 72 hrs OMVs from IHE3034 Δ*clbP* mutant are localized in statistically significant higher amount inside nucleus area nucleus of treated cells when compared with cells treated with OMVs from the wild-type strain (*p*-value 0.0285; Figure 5.6). These results suggest that OMV from mutant strain are more invasive to HeLa cells and have an easier access to nuclear region as consequence of clbP peptidase removal.

To quantitatively determinate whether OMVs causes megalocytosis in treated cells, the area of cell nucleus were measured using DAPI intensity (blue fluorescent dye) in confocal images. As results, data confirm (as observed in section 5.3.2) that OMVs from both IHE3034 and IHE3034 Δ*clbP* cause nucleus enlargement on HeLa cells by itself after 72 hrs of direct exposition when compared with cells treated with OMV from DH10B strain and with cells without treatment (Figure 5.7). Statistical analysis (one-way ANOVA)

resulted in no significant differences between IHE3034 and IHE3034 Δ*clbP* (*p*-value 0.3821). This suggest that OMVs from IHE3034 cause megalocytosis, but that effect is not reduced by the removal of clbP peptidase.

In order to visualize the localization of OMVs inside of treated cells, images were taken at 100X of magnification. Results reveals that OMVs from IHE3034 strains and from DH10B are internalized and localized in the perinuclear area. Interestingly, nucleus from cells treated with both IHE3034 strains are invaded by OMVs and seem larger and intoxicated when compared with cells treated with OMV from DH10B strain (Figure 5.8). Moreover, orthogonal views reconstructed from image slices 0.25 μm apart (pinhole size 58.75 μm), confirmed that the OMVs from the three strains were located in the perinuclear regions, but for OMVs from IHE3034 strain (WT and Δ*clbP* mutant) OMV invade nuclear envelope (Figure 5.9).

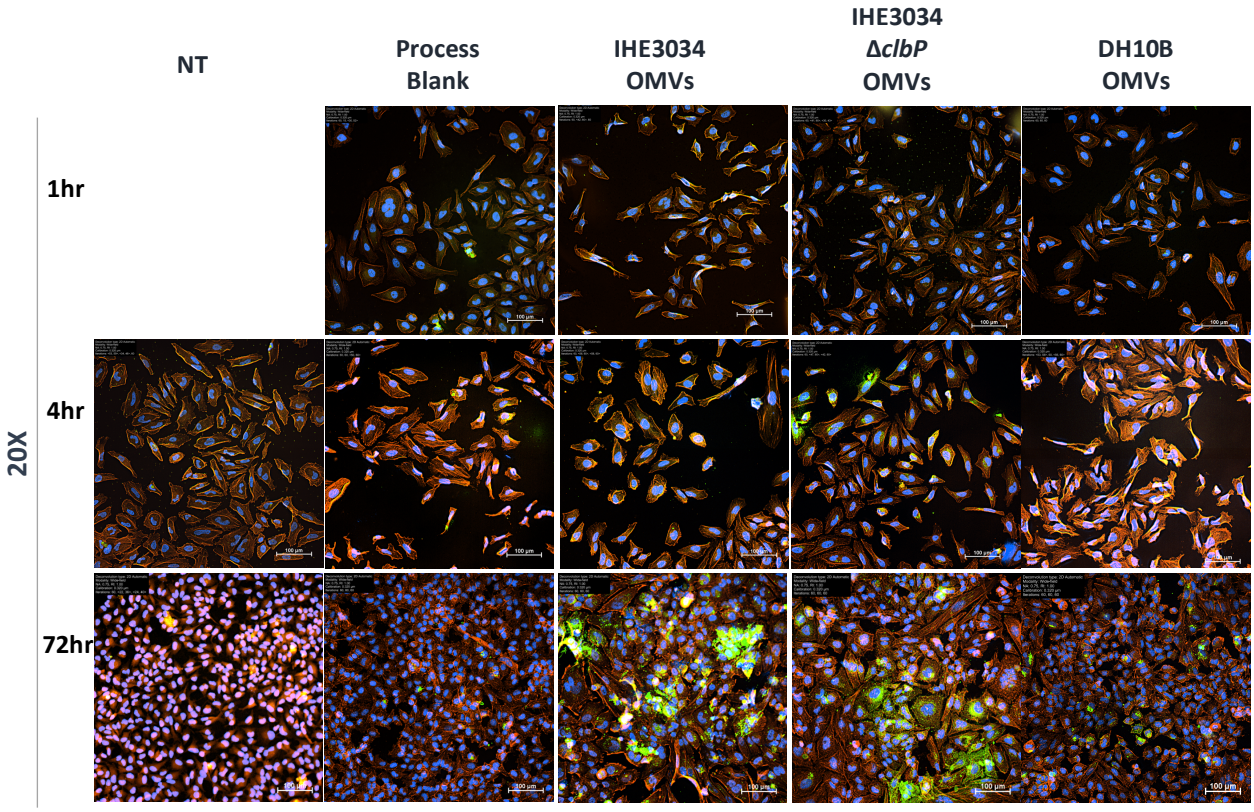

Figure 5.4 OMVs from IHE3034 *E. coli* are internalized by HeLa cells. Fluorescent DiO labelled OMVs (green) were added to HeLa cell for 1, 4, and 72 hrs before cells were stained for actin filaments (red, TRITC-Phalloidin dye) and nuclei (blue, DAPI dye). For 1 and 4 hrs of co-incubation, cells were stained for actin filaments (red) and nuclei (blue) after 72 hrs after treatment. For 72 hrs of co-incubation cells were stained right after treatment period.Note that at 72 hrs of direct exposition, cells treated with OMVs from IHE3034 strains show an enlarged cell body and nucleus when compare with cells treated with OMVs from DH10B laboratory *E. coli* strain. Magnification 100X, scale bar 100 μm.

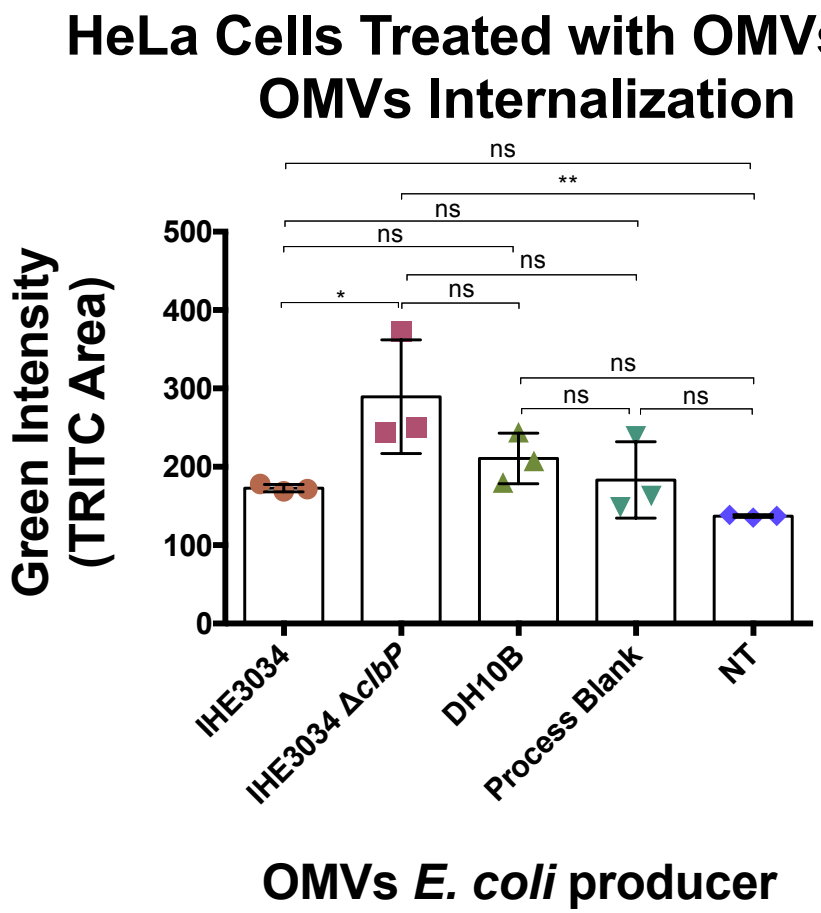

Figure 5.5 OMVs from IHE3034 Δ*clbP* mutant *E. coli* is internalized in significant higher amount than OMVs from WT strain by HeLa cells. Fluorescent DiO labelled OMVs were added to HeLa cell for 72 hrs before cells were stained for actin (TRITC-Phalloidin dye) filaments and nuclei. Three images at 20X of magnification were taken in randomly chosen areas of each sample to statistical analysis. Intensity of green (DiO dye) were measured in areas were cells were present (red, TRITC-Phalloidin dye) to determine the relative amount of OMV internalized by the treated cell. *P*-values: ns $P > 0.05$; * $P \leq 0.05$; ** $P \leq 0.01$; *** $P \leq 0.001$ and **** $P \leq 0.0001$

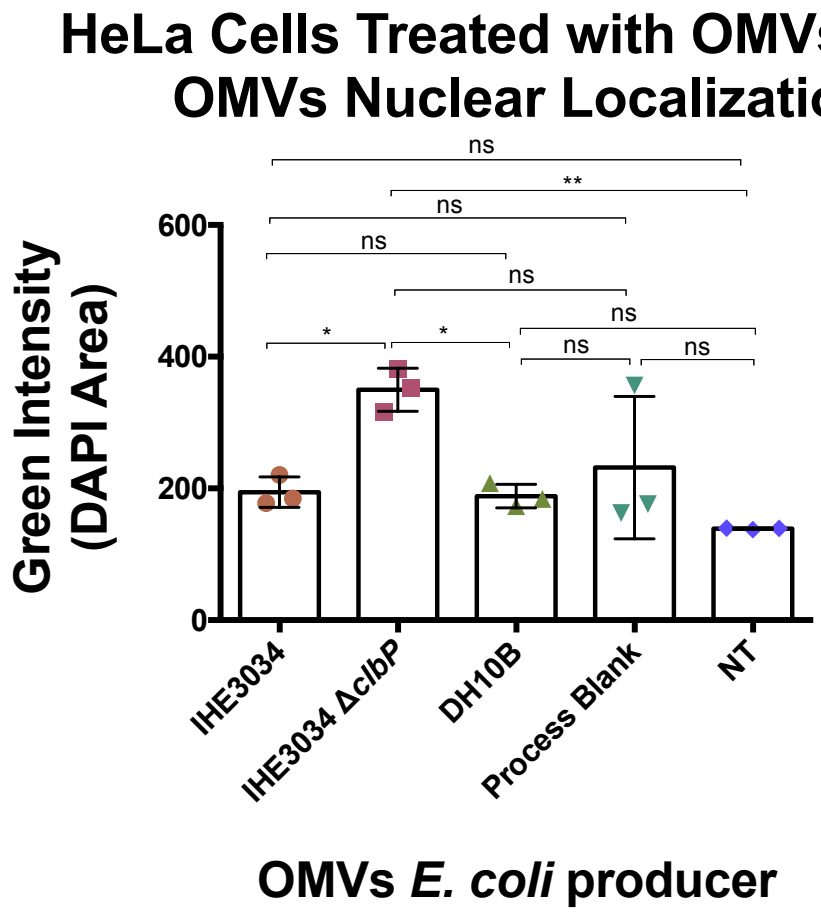

Figure 5.6 OMV from IHE3034 Δ*clbP* mutant *E. coli* are localized in the nucleus in significant higher amount than OMV from WT strain in HeLa cell after 72 hrs of treatment. Fluorescent DiO labelled OMVs were added to HeLa cell for 72 hrs before cells were stained for actin filaments and nuclei (DAPI). Three images at 20X of magnification were taken in randomly chosen areas of each sample to statistical analysis. Intensity of green (DiO dye) were measured in areas were cell's nucleus were present (blue, DAPI dye) to determine the relative amount of OMV localized in the nucleus of treated cell. *P*-values: ns $P > 0.05$; * $P \leq 0.05$; ** $P \leq 0.01$; *** $P \leq 0.001$ and **** $P \leq 0.0001$

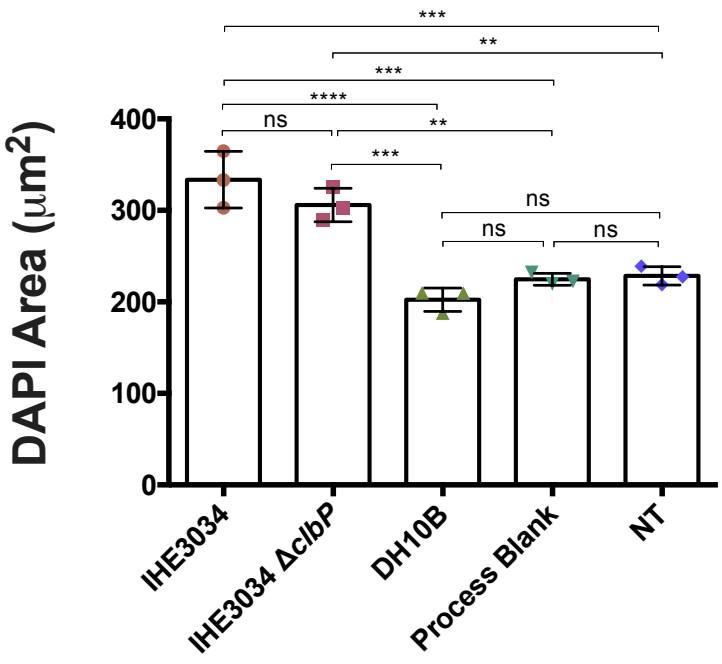

Figure 5.7. OMVs from IHE3034 and IHE3034 Δ*clbP* mutant *E. coli* causes megalocytosis on HeLa cells after 72 hrs of treatment. Fluorescent DiO labelled OMVs were added to HeLa cell for 72 hours before cells were stained for actin filaments and nuclei (DAPI). Three images at 20X of magnification were taken in randomly chosen areas of each sample to statistical analysis. One-way ANOVA statistical analysis show that IHE3034 strains both have similar capacity to induce megalocytosis (*p*-value 0.3821). *P*-values: ns $P > 0.05$; * $P \leq 0.05$; ** $P \leq 0.01$; *** $P \leq 0.001$ and **** $P \leq 0.0001$

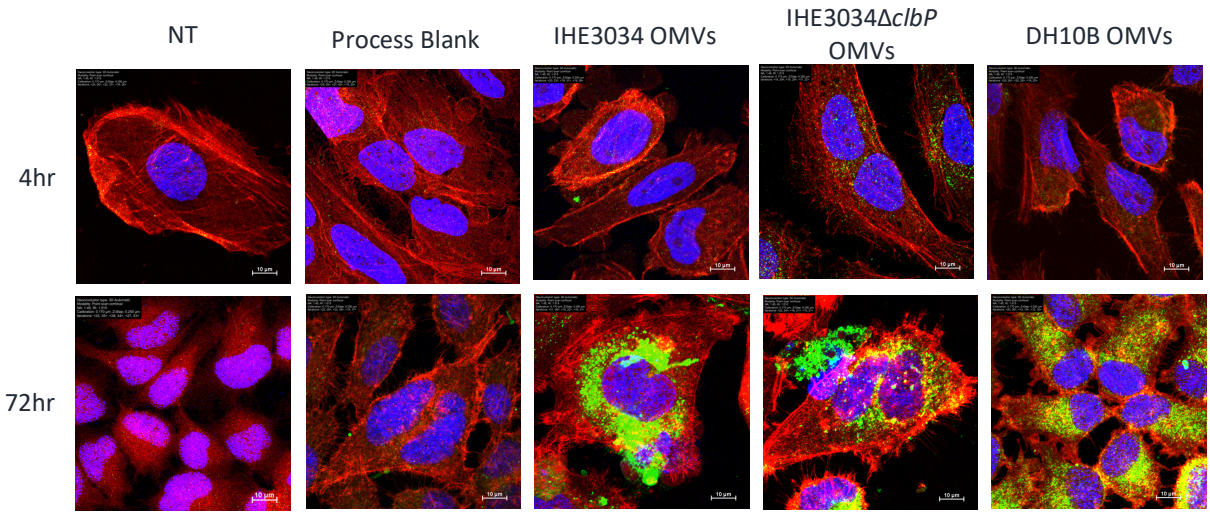

Figure 5.8 OMVs from IHE3034 *E. coli* localized in perinuclear region of HeLa cells. Fluorescent DiO labelled OMVs (green) were added to HeLa cell for 4 and 72 hrs. For 4 hrs of co-incubation, cells were stained for actin filaments (red) and nuclei (blue) after 72 hrs after treatment. For 72 hrs of co-incubation cells were stained right after treatment period. Note that cells treated with OMVs from IHE3034 strains show an enlarged, intoxicated multi-nucleus when compare with cells treated with OMVs from DH10B laboratory *E. coli* strain. Magnification 100X (oil immersed). Scale bar 10 μm.

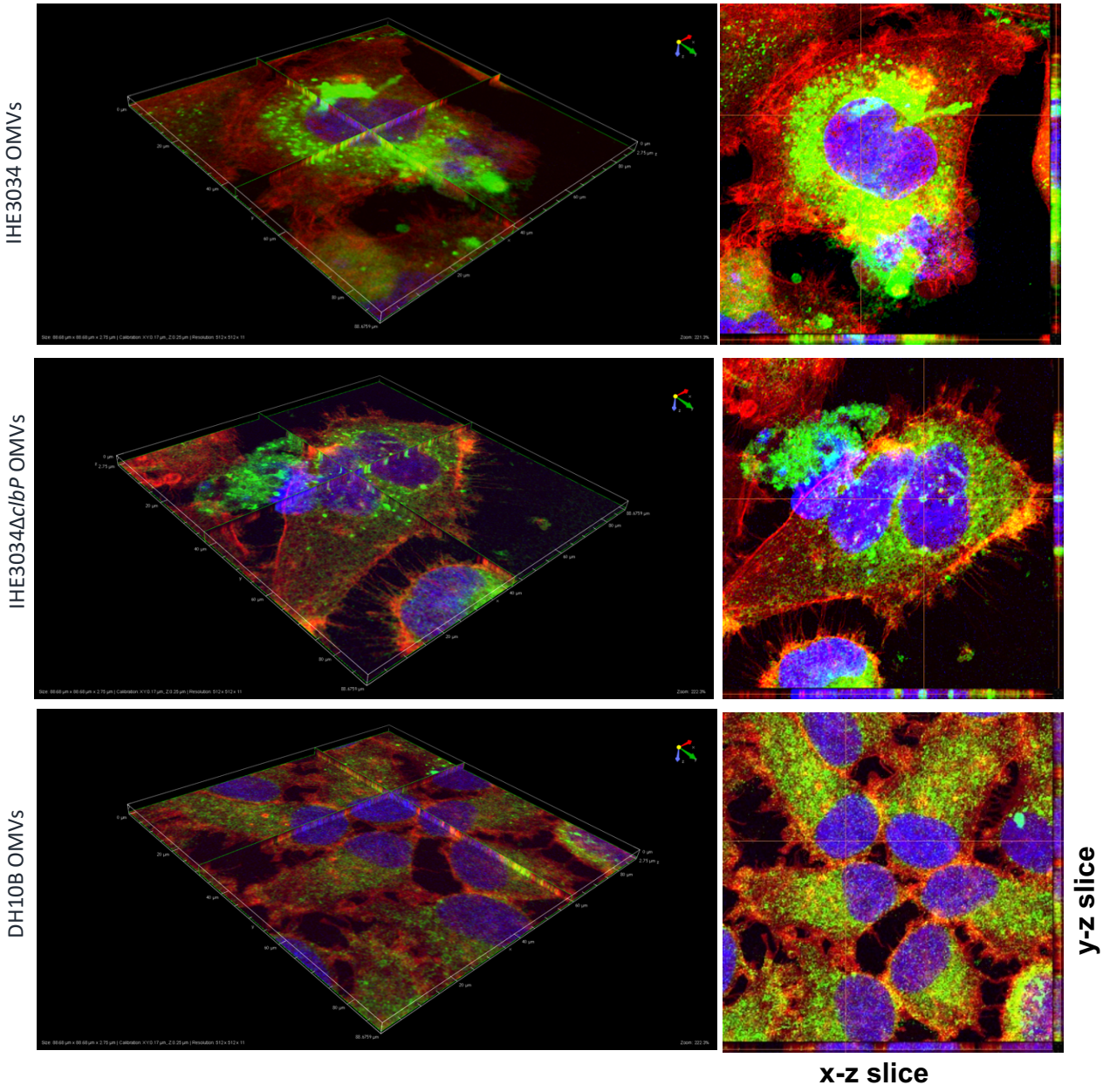

Figure 5.9. OMVs from IHE3034 and IHE3034 Δ*clbP* mutant *E. coli* strains penetrate the nuclear envelope of HeLa cells. Fluorescent DiO labelled OMVs (green) were added to HeLa cell. After 72 hrs of co-incubation cells were stained for actin filaments (red, TRITC-Phalloidin dye) and nuclei (blue, DAPI dye). Note that cells treated with OMVs from IHE3034 strains show an enlarged, intoxicated multi-nucleus when compare with cells treated with OMVs from DH10B laboratory *E. coli* strain. Images were taken at 100X of magnification.

5.3.4 OMVs from *E. coli* IHE3034 induce DNA Damage and double strand breaks in a human cell line.

The capacity of OMVs isolated from the colibactin-producing *E. coli* strain IHE3034 to induce DNA damage was assayed on HeLa cells. DNA damages was determined by the quantification of DNA Damages markers: histone γ-H_2AX, Chk1, and Chk2. The up-phosphorylation of the histone γ-H_2AX serves as a marker of specifically DNA double-stranded breaks, whereas Chk1 and Chk2 up-phosphorylation serve as markers of DNA damages in general.

OMVs were exposed to HeLa cell for 4 and 72 hrs to monitored the degree of damages as result of time exposition. First, the phosphorylation of the histone γ-H_2AX was determined on treated cells. At 4 hrs of co-incubation, cells treated with OMVs from both WT IHE3034 and Δ*clbP* mutant strains show 1.4 $\pm$ 0.1 times more *p*-H_2AX than cells without treatment. At 72 hrs of co-incubation, cells treated with OMVs from both WT IHE3034 and Δ*clbP* mutant strains show 6 $\pm$ 1 and 11 $\pm$ 1 times more *p*-H_2AX than cells without treatment. These result reveal that OMV from *pks* positive IHE3034 cause double-strand breaks (DSBs) on HeLa cells, but interestingly also reveal that after 72 hrs of exposition, OMVs from Δ*clbP* mutant cause the double of damages than OMV from the WT strain (*p*-value 0.0013). This suggest that the lack of clbP peptidase in the mutant strain generate OMVs more genotoxic than the OMV from the WT IHE3034 strain.

DNA Damage on treated cells were measured by the phosphorylation of markers Chk1 and Chk2. Cells treated with OMVs from the IHE3034 strains (WT and Δ*clbP* mutant) show a slightly increase in phosphorylation of Chk1 of < 0.5 times and < 1 time than cells without treatment after 4 and 72 hrs respectively (Figure 5.10 A) . In general, for Chk1

marker results were similar to the basal/background damages observed to negative controls with the exception of cells treated with OMVs from Δ*clbP* mutant after 72 hrs of co-incubation, however was not a huge increment relative to cells without treatment (Figure 5.10 A) On the other hand, for Chk2 markers a higher increase of its phosphorylation was observe on treated cells with OMVs from IHE3034 strains relative to cells without treatment. At 4 hrs of co-incubation, cells treated with OMVs from both WT IHE3034 and Δ*clbP* mutant strains show 2.6 $\pm$ 0.3 and 3.7 $\pm$ 0.2 times more *p*-Chk2 than cells without treatment respectively. At 72 hrs of co-incubation, cells treated with OMVs from both WT IHE3034 and Δ*clbP* mutant strains show 4.5 $\pm$ 0.7 and 3 $\pm$ 1 times more *p*-H_2AX than cells without treatment respectively. Altogether these results means that bacterial outer membrane vesicles from *E. coli* IHE3034, which harbor the *pks* genes, are able to induce double-stranded breaks and DNA damage in human cells. Also, as consistent with previous results, reveal the OMV from the mutant strain IHE3034 Δ*clbP* have a tendency to be more genotoxic than OMV from its WT strain.

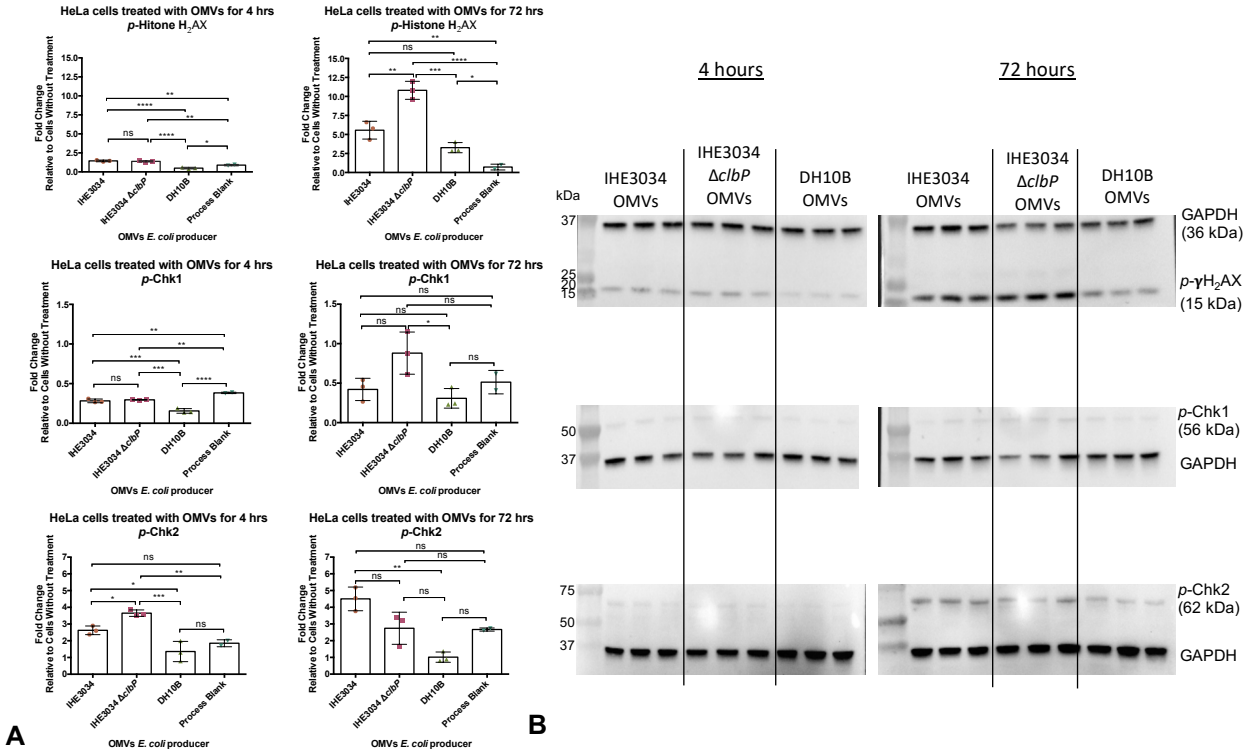

Figure 5.10 OMVs from *pks+ E. coli* IHE3034 strains cause DSBs and DNA Damage. A) Density analysis of immunoblotting to target the DNA Damage marker p-Histone γH_2AX, p-Chk2 and p-Chk1, all markers of DNA damage. Statistical analysis (one-way ANOVA) were made for three biological replicates. B) Inmmunoblotting image representation of DNA damage assay. OMVs from *E. coli* IHE3034 induces the up-phosphorilation of Histone γH_2AX, Chk1, and Chk2, all markers of DNA damage. Assay was performed on HeLa cells by 4 and 74 hrs of co-incubation at 37 ºC and 5 % CO_2. For cells treated by 4 hrs, cells were harvested after 72 hrs post treatment with OMV. *P*-values: ns $P > 0.05$; * $P \leq 0.05$; ** $P \leq 0.01$; *** $P \leq 0.001$ and **** $P \leq 0.0001$.

5.3.5 OMVs from IHE3034 does not cause DNA interstrand crosslinks.

To establish whether the OMVs genotoxic activity of IHE3034 strains is directly related to colibactin toxicity, the formation of interstrand crosslinks (ICL) was assayed by the direct exposition of OMVs to linear plasmid DNA (pUC-19). Results show that OMVs from neither IHE3434 nor DH10B *E. coli* strains cause ICL (Figure 5.11 A) in comparison with the positive control where the live bacteria *E. coli* IHE3034 and the positive control cisplatin which generated the ICL formation (Figure 5.11 B). These results confirm that OMVs genotoxicity is not directly related to colibactin's described genotoxic mechanism of action.

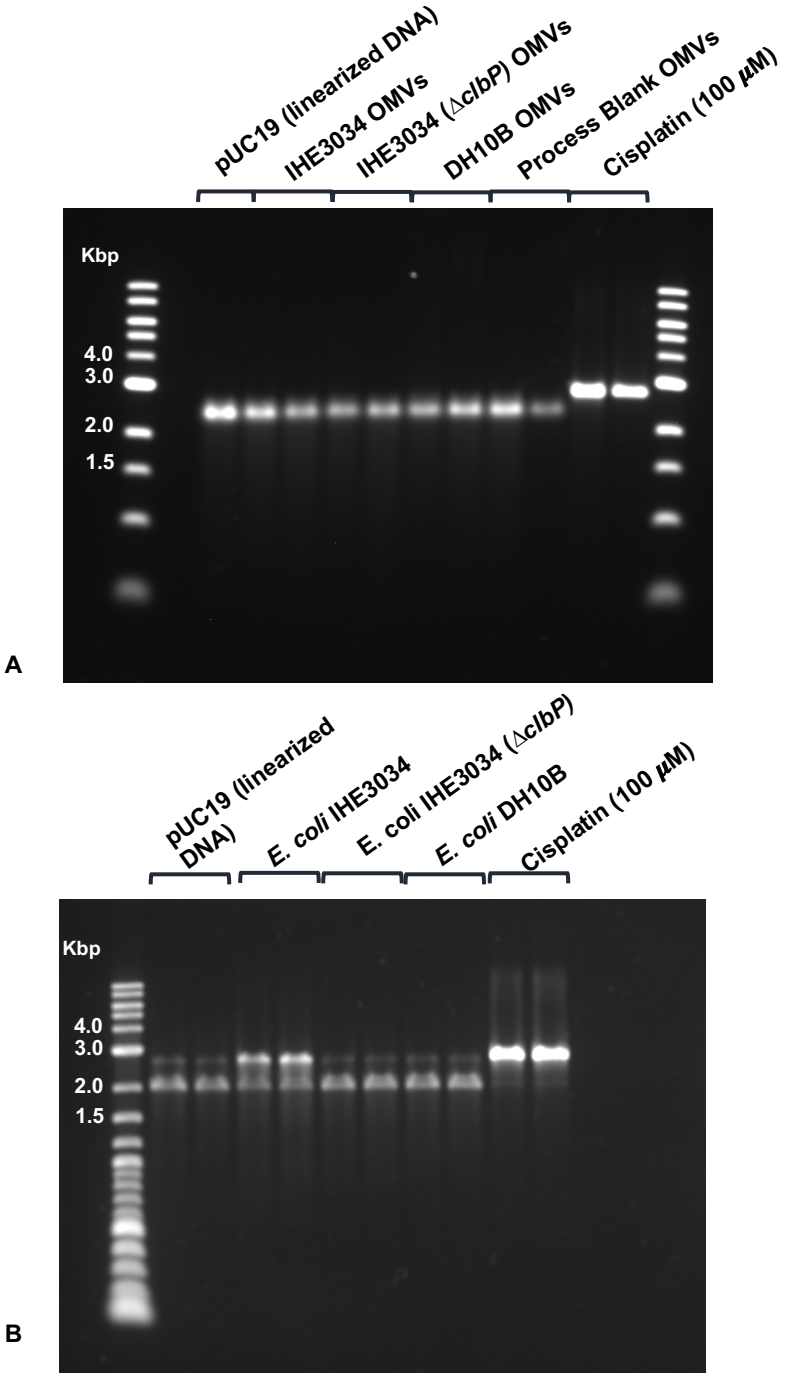

Figure 5.11 OMVs from *pks* positive IHE3034 *E. coli* strain does not cause DNA crosslinks as its producer bacteria does. Linearized plasmid double-strand DNA (300 ng) was incubated for 24 hrs with OMVs or its producer live bacteria or 100 **μ**M and then analyzed by denaturing gel electrophoresis. **A)** Agarose DNA electrophoresis of DNA exposed to OMVs from IHE3034 (*pks*+), IHE3034 (Δ*clbP*) and DH10B (negative control) *E. coli* strains. **B)** Agarose DNA electrophoresis of DNA exposed to IHE3034 (*pks*+), IHE3034 (Δ*clbP*) and DH10B (negative control) *E. coli* strains live bacteria. Assay was performed in biological duplicates.

5.4 Discussion

Colibactin in a natural product produced by *E. coli,* including strains that reside in the human gut. This secondary metabolite causes DNA double stranded breaks (DSBs) and DNA interstrand crosslinks (ICLs) in mammalian cells which lead to megalocytosis of infected cells. This megalocytosis most of the time is accompanied with nuclear enlargement and cell cycle arrest. The presence of *E. coli* capable to produce colibactin has been link with bacterial induced colorectal cancer in human[3,4,6,7,22,23]. Despite all the knowledge that have been gained in how colibactin affect the cells there is still questions about how colibactin is transported from the *E. coli* periplasm to the target cell. How colibactin interact with bacterial membrane before exportation? It is colibactin transported by means of vesicles.? Are OMVs mediating the colibactins toxic traits? Bacterial membranes play a key role in mediating cellular and extracellular activities between living cells and their environment, specifically the outer membrane. Outer membrane vesicles by themselves have been implicated in numerous biological processes[12], including virulence factors transportation, and genomic toxicity[24]. In this work we explore the route of OMV as a probable mediator of colibactin toxicity. To do so we isolated OMVs from *E. coli* which harbor or lacking the capacity to produce the active colibactin. We found for the first time that OMVs are sufficient for the elicitation of colibactin toxic phenotype. In other words OMVs causes megalocytosis, DNA Damage and DSBs.

Even though have been much work about the study of OMVs internalization and the fact that OMVs from is most of the time internalized by endocytosis. For instance OMVs from a *pks* positive *E. coli* to be internalized by OMVs clathrin dependant[25] but it was not

described how that OMV reached to the nucleus, an subsequently causes damages and megalocytosis[26]. Our confocal images reveals that our vesicles are localized on the perinuclear area of treated cells and some of them penetrate the nuclear envelope consistent with the enlargement of the nucleus observed. This was also observed in other works for other OMV from pathogenic bacteria[13,27].

The typical megalocytosis phenotype is accompanied with DNA Damages. Our OMV also show similar damages to colibactin's genotoxic described phenotypes by itself: (1) DSBs by the up-phosphorylation of the histones γH_2AX and DNA Damages by the up-phosphorylation of both Chk1 and Chk2 markers relative to cells without treatment. The OMVs from IHE3034 strains in general active more chk2 marker than the chk1 marker. The activation of chk2 marker have been associated with DSBs[28] which is consistent with the results of the activation of the histones γH_2AX.

A consistent finding in all of our results is that OMV from our clbP mutant which not produce the active colibactin show high toxicity. The OMVs from the mutant strains causes higher megalocytosis and DNA damages to cells than its WT version itself. At the present time we don't have a satisfactory explanation of why clbP mutant strain make OMV with high toxicity. However, there is some possible explanation for this: (1) colibactin is in effect not transported by means of OMVs and biological effect observed is because a different virulent factor. IHE3034 *E. coli* is a clinical isolate from a new born meningitis[29] which make other factors that can account to the toxicity of its OMV. One of them been the Cytolethal Distending Toxin (CDT) which this strain is known to harbor. CDT causes

also DNA damages and a similar morphological phenotype called cell distention. (2) clbP is playing a role in other virulence factor and its removal somehow evolve OMVs of IHE3034 more genotoxic; (3) the unmatured colibactin intermediate is incorporated in OMV as "waste material to be discarded" but is more toxic or equally toxic than colibactin but by other mechanism not discovered/studied yet. It is possible that the deletion of clbP was not enough to eliminate colibactin's toxicity completely or that the mutant was able to recover some of its function by means of another enzyme with similar activity found in this particular strain, hence making it difficult for us to make a cause and effect correlation. However, it is evident from our experiments that the presence of clbP or colibactin production is playing a role in OMV genotoxicity, suggesting an involvement of OMVs in pks-induced cellular phenotype.

The fact that OMV have all the hallmarks of colibactin toxicity suggested that OMVs also will show DNA interstrand cross links (ICL) activity. However we incubated purified DNA with OMVs and found no evidences of ICL. Yet the bacterial cell do prove that cause DNA crosslinks and was abolished in the clbP mutant which provided further evidence of a successfully clbP deletion.

Since OMVs are extracted from live bacterial cultures and even though there are validated protocols for bacterial OMV isolation, there was a real possibility that live bacteria, having survived the ultracentrifugation protocol, could still be present and competent to cause the observed megalocytosis phenotype. To rule out that possibility, we incubated in parallel the extracted OMVs in LB agar and saw no colony formation after 24 hrs,

indicating that our OMV preparations did not contain any live bacteria to account for the observed effects. This outcome indicates that both the observed megalocytosis as well as the up-phosphorylation of DNA damage markers were due to the exposition of the mammalian cells to OMVs; confirming the active participation of OMVs in the toxicity of the *pks*+ IHE3034 *E. coli* strain.

In conclusion the data presented in this study clearly indicate that OMV from a colibactin-producing *E. coli* causes DSBs and DNA Damages. Moreover, it was determined that, unexpectedly, OMV from the strain which we manually converted into a strain uncapable to make active colibactin are more toxic. Thus, raising more questions about whether there is an association between OMV from bacterial strains harboring the *pks* genes and the genotoxic hallmarks attributed to colibactin. Even though other groups have mentioned the possibility of colibactin being transported by OMVs[25], to our knowledge, this is the first study that establishes a direct correlation between OMV production and *pks* island genotoxic effects towards mammalian cells. However the lack of ability of our OMVs to induce interstrand crosslink (ICLs), our principal question of, How colibactin is transported from the bacteria to the target cell?, remain without a satisfactory answer.

5.5 References

(1) Nougayrède, J.-P.; Homburg, S.; Taieb, F.; Boury, M.; Brzuszkiewicz, E.; Gottschalk, G.; Buchrieser, C.; Hacker, J.; Dobrindt, U.; Oswald, E. Escherichia Coli Induces DNA Double-Strand Breaks in Eukaryotic Cells. *Science.* **2006**, *313* (5788), 848–851. https://doi.org/10.1126/science.1127059.

(2) Arthur, J. C.; Perez-Chanona, E.; Mühlbauer, M.; Tomkovich, S.; Uronis, J. M.; Fan, T.; Campbell, B. J.; Abujamel, T.; Dogan, B.; Rogers, A. B.; Rhodes, J. M.; Stintzi, A.; Simpson, K. W.; Hansen, J. J.; Keku, T. O.; Fodor, A. A.; Jobin, C. Intestinal Inflammation Targets Cancer-Inducing Activity of the Microbiota. *Science.* **2012**, *338* (6103), 120–123. https://doi.org/10.1126/science.1224820.Intestinal.

(3) Dalmasso, G.; Cougnoux, A.; Delmas, J.; Darfeuille-Michaud, A.; Bonnet, R. Bacterial Genotoxin Colibactin Promotes Colon Tumour Growth by Inducing a Senescence-Associated Secretory Phenotype. *Gut* **2014**, *5* (5), 675–680. https://doi.org/10.4161/19490976.2014.969989.

(4) Cougnoux, A.; Dalmasso, G.; Martinez, R.; Buc, E.; Delmas, J.; Gibold, L.; Sauvanet, P.; Darcha, C.; Déchelotte, P.; Bonnet, M.; Pezet, D.; Wodrich, H.; Darfeuille-Michaud, A.; Bonnet, R. Bacterial Genotoxin Colibactin Promotes Colon Tumour Growth by Inducing a Senescence-Associated Secretory Phenotype. *Gut* **2014**, *63* (12), 1932–1942. https://doi.org/10.1136/gutjnl-2013-305257.

(5) Tomkovich, S.; Yang, Y.; Winglee, K.; Gauthier, J.; Mühlbauer, M.; Sun, X.; Mohamadzadeh, M.; Liu, X.; Martin, P.; Wang, G. P.; Oswald, E.; Fodor, A. A.; Jobin, C. Locoregional Effects of Microbiota in a Preclinical Model of Colon Carcinogenesis. *Cancer Res.* **2017**, *77* (10), 2620–2632.

https://doi.org/10.1158/0008-5472.CAN-16-3472.

(6) Cuevas-Ramos, G.; Petit, C. R.; Marcq, I.; Boury, M.; Oswald, E.; Nougayrède, J.-P. Escherichia Coli Induces DNA Damage in Vivo and Triggers Genomic Instability in Mammalian Cells. *Proc. Natl. Acad. Sci. U. S. A.* **2010**, *107* (25), 11537–11542. https://doi.org/10.1073/pnas.1001261107.

(7) Shimpoh, T.; Hirata, Y.; Ihara, S.; Suzuki, N.; Kinoshita, H.; Hayakawa, Y. Prevalence of Pks - Positive Escherichia Coli in Japanese Patients with or without Colorectal Cancer. *Gut Pathog.* **2017**, *9*. https://doi.org/10.1186/s13099-017-0185-x.

(8) Tšuiko, O.; Jatsenko, T.; Parameswaran Grace, L. K.; Kurg, A.; Vermeesch, J. R.; Lanner, F.; Altmäe, S.; Salumets, A. A Speculative Outlook on Embryonic Aneuploidy: Can Molecular Pathways Be Involved? *Dev. Biol.* **2019**, *447* (1), 3–13. https://doi.org/10.1016/j.ydbio.2018.01.014.

(9) Jackson, S. P.; Bartek, J. The DNA-Damage Response in Human Biology and Disease. *Nature* **2009**, *461* (7267), 1071–1078. https://doi.org/10.1038/nature08467.

(10) Bartek, J.; Lukas, J. Chk1 and Chk2 Kinases in Checkpoint Control and Cancer. *Cancer Cell* **2003**, *3* (5), 421–429. https://doi.org/10.1016/S1535-6108(03)00110-7.

(11) Schwechheimer, C.; Kuehn, M. J.; Rodriguez, D. L. Outer-Membrane Vesicles from Gram-Negative Bacteria: Biogenesis and Functions. *Nat. Rev. Microbiol.* **2015**, *13* (10), 605–619. https://doi.org/10.1038/nrmicro3525.Outer-membrane.

(12) Kulp, A.; Kuehn, M. J. Biological Functions and Biogenesis of Secreted Bacterial

Outer Membrane Vesicles. *Annu Rev Microbiol.* **2010**, *64*, 163–184. https://doi.org/10.1146/annurev.micro.091208.073413.Biological.

(13) Tyrer, P. C.; Frizelle, F. A.; Keenan, J. I. Escherichia Coli-Derived Outer Membrane Vesicles Are Genotoxic to Human Enterocyte-like Cells. *Infect. Agent. Cancer* **2014**, *9* (1), 2. https://doi.org/10.1186/1750-9378-9-2.

(14) Mousa, J. J.; Yang, Y.; Tomkovich, S.; Shima, A.; Newsome, R. C.; Tripathi, P.; Oswald, E.; Bruner, S. D.; Jobin, C. MATE Transport of the E. Coli-Derived Genotoxin Colibactin. *Nat. Microbiol.* **2016**, *1* (1), 15009. https://doi.org/10.1038/nmicrobiol.2015.9.

(15) Brotherton, C. A.; Balskus, E. P. A Prodrug Resistance Mechanism Is Involved in Colibactin. *J. Am. Chem. Sociaty* **2013**, *135*, 3359–3362. https://doi.org/10.1021/ja312154m.

(16) Klimentová, J.; Stulík, J. Methods of Isolation and Purification of Outer Membrane Vesicles from Gram-Negative Bacteria. *Microbiol. Res.* **2015**, *170*, 1–9. https://doi.org/10.1016/j.micres.2014.09.006.

(17) Eberlein, C.; Starke, S.; Doncel, Á. E.; Scarabotti, F.; Heipieper, H. J. Quantification of Outer Membrane Vesicles: A Potential Tool to Compare Response in Pseudomonas Putida KT2440 to Stress Caused by Alkanols. *Appl. Microbiol. Biotechnol.* **2019**, *103* (10), 4193–4201. https://doi.org/10.1007/s00253-019-09812-0.

(18) Meers, P. R.; Liu, C.; Chen, R.; Bartos, W.; Davis, J.; Dziedzic, N.; Orciuolo, J.; Kutyla, S.; Pozo, M. J.; Mithrananda, D.; Panzera, D.; Wang, S. Vesicular Delivery of the Antifungal Antibiotics of Lysobacter Enzymogenes C3. *Appl. Environ.*

Microbiol. **2018**, *84* (20), 1–16. https://doi.org/10.1128/AEM.01353-18.

(19) Wagner, T.; Joshi, B.; Janice, J.; Askarian, F.; Škalko-Basnet, N.; Hagestad, O. C.; Mekhlif, A.; Wai, S. N.; Hegstad, K.; Johannessen, M. Enterococcus Faecium Produces Membrane Vesicles Containing Virulence Factors and Antimicrobial Resistance Related Proteins. *J. Proteomics* **2018**, *187*, 28–38. https://doi.org/10.1016/j.jprot.2018.05.017.

(20) Xue, M.; Kim, C. S.; Healy, A. R.; Wernke, K. M.; Wang, Z.; Frischling, M. C.; Shine, E. E.; Wang, W.; Herzon, S. B.; Crawford, J. M. Structure Elucidation of Colibactin and Its DNA Cross-Links. *Science.* **2019**, *365* (6457). https://doi.org/.1037//0033-2909.I26.1.78.

(21) Bossuet-greif, N.; Vignard, J.; Taieb, F.; Mirey, G.; Dubois, D.; Petit, C.; Oswald, E. The Colibactin Genotoxin Generates DNA Interstrand Cross- Links in Infected Cells. **2018**, *9* (2), 1–15.

(22) Arthur, J. C.; Perez-Chanona, E.; Mühlbauer, M.; Tomkovich, S.; Uronis, J. M.; Fan, T.-J.; Campbell, B. J.; Abujamel, T.; Dogan, B.; Rogers, A. B.; Rhodes, J. M.; Stintzi, A.; Simpson, K. W.; Hansen, J. J.; Keku, T. O.; Fodor, A. A.; Jobin, C. Intestinal Inflammation Targets Cancer-Inducing Activity of the Microbiota. *Science.* **2012**, *338* (6103), 120–123. https://doi.org/10.1126/science.1224820.

(23) Healy, A. R.; Herzon, S. B. Molecular Basis of Gut Microbiome-Associated Colorectal Cancer: A Synthetic Perspective. *J. Am. Chem. Soc.* **2017**, *139* (42), 14817–14824. https://doi.org/10.1021/jacs.7b07807.

(24) Ling, Z.; Dayong, C.; Denggao, Y.; Yiting, W.; Zhibiao, W. Escherichia Coli Outer Membrane Vesicles Induced DNA Double-Strand Breaks in Intestinal. **2019**, *25*,

45–52. https://doi.org/10.12659/MSMBR.913756.

(25) Cañas, M.-A.; Giménez, R.; Fábrega, M.-J.; Toloza, L.; Baldomà, L.; Badia, J. Outer Membrane Vesicles from the Probiotic Escherichia Coli Nissle 1917 and the Commensal ECOR12 Enter Intestinal Epithelial Cells via Clathrin-Dependent Endocytosis and Elicit Differential Effects on DNA Damage. *PLoS One* **2016**, *11* (8), e0160374. https://doi.org/10.1371/journal.pone.0160374.

(26) Bielaszewska, M.; Rüter, C.; Bauwens, A.; Greune, L.; Jarosch, K. A.; Steil, D.; Zhang, W.; He, X.; Lloubes, R.; Fruth, A.; Kim, K. S.; Schmidt, M. A.; Dobrindt, U.; Mellmann, A.; Karch, H. *Host Cell Interactions of Outer Membrane Vesicle-Associated Virulence Factors of Enterohemorrhagic Escherichia Coli O157: Intracellular Delivery, Trafficking and Mechanisms of Cell Injury*; 2017; Vol. 13. https://doi.org/10.1371/journal.ppat.1006159.

(27) Lindmark, B.; Rompikuntal, P. K.; Vaitkevicius, K.; Song, T.; Mizunoe, Y.; Uhlin, B. E.; Guerry, P.; Wai, S. N. Outer Membrane Vesicle-Mediated Release of Cytolethal Distending Toxin (CDT) from Campylobacter Jejuni. *BMC Microbiol.* **2009**, *9*, 1–10. https://doi.org/10.1186/1471-2180-9-220.

(28) Zannini, L.; Delia, D.; Buscemi, G. Review CHK 2 Kinase in the DNA Damage Response and Beyond. **2014**, *6*, 442–457.

(29) Berlanda Scorza, F.; Doro, F.; Rodríguez-Ortega, M. J.; Stella, M.; Liberatori, S.; Taddei, A. R.; Serino, L.; Gomes Moriel, D.; Nesta, B.; Fontana, M. R.; Spagnuolo, A.; Pizza, M.; Norais, N.; Grandi, G. Proteomics Characterization of Outer Membrane Vesicles from the Extraintestinal Pathogenic Escherichia Coli ΔtolR IHE3034 Mutant. *Mol. Cell. Proteomics* **2008**, *7* (3), 473–485.

https://doi.org/10.1074/mcp.M700295-MCP200.

5.6 Supplementary Material

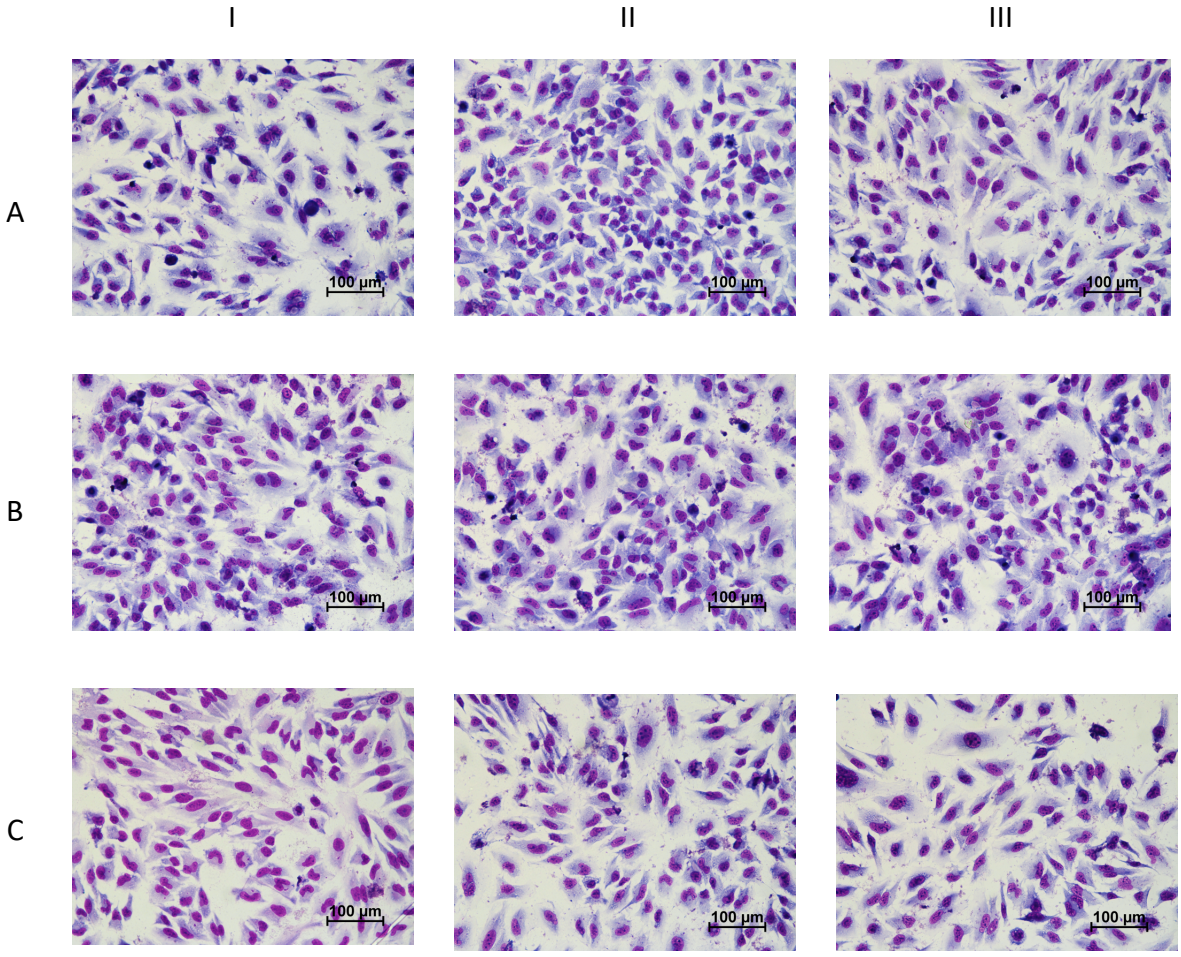

Figure S5.1a Giemsa staining of untreated HeLa cells. A, B, and C represent biological replicates. Three images of each sample were taken (represented by I, II, and III). Photos were taken after 72 hours post treatment at 40X of magnification.

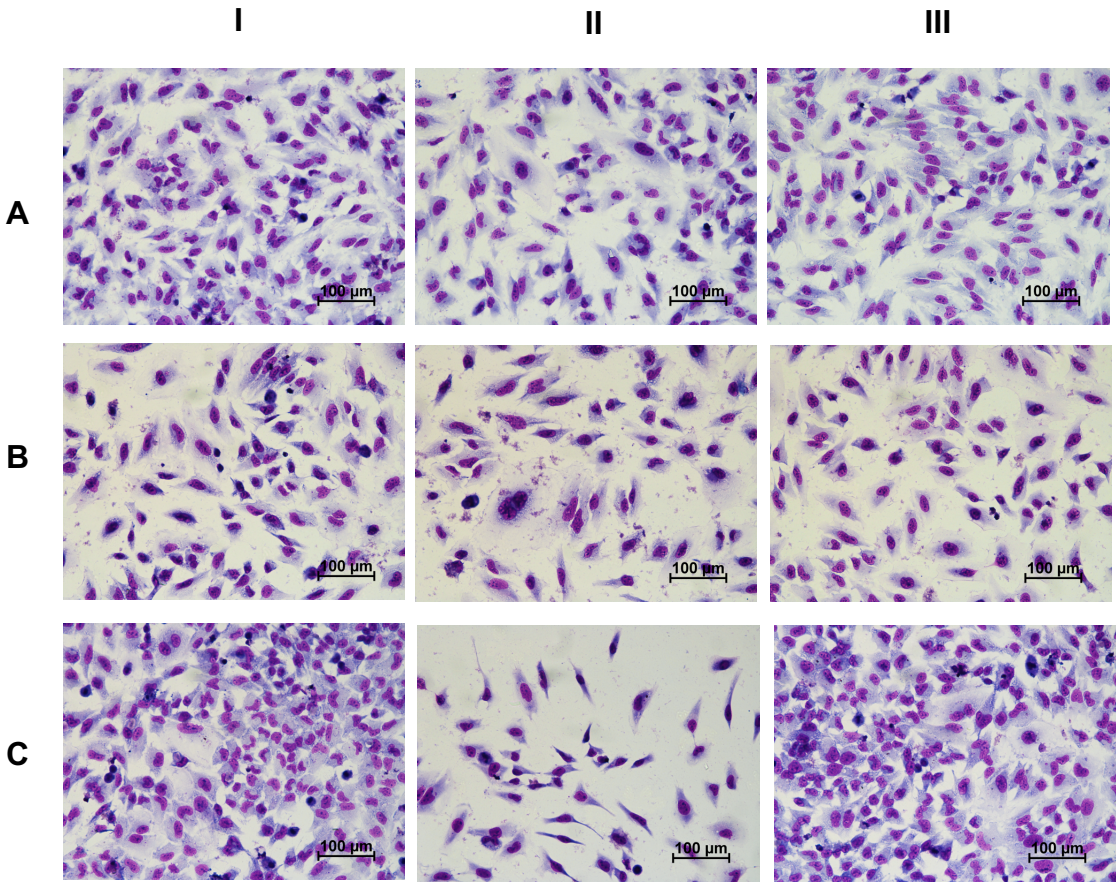

Figure S5.1b Giemsa staining of HeLa cells treated with OMV isolation "Process Blank". A, B, and C represent biological replicates. Three images of each sample were taken (represented by I, II, and III). Photos were taken after 72 hours post treatment at 40X of magnification.

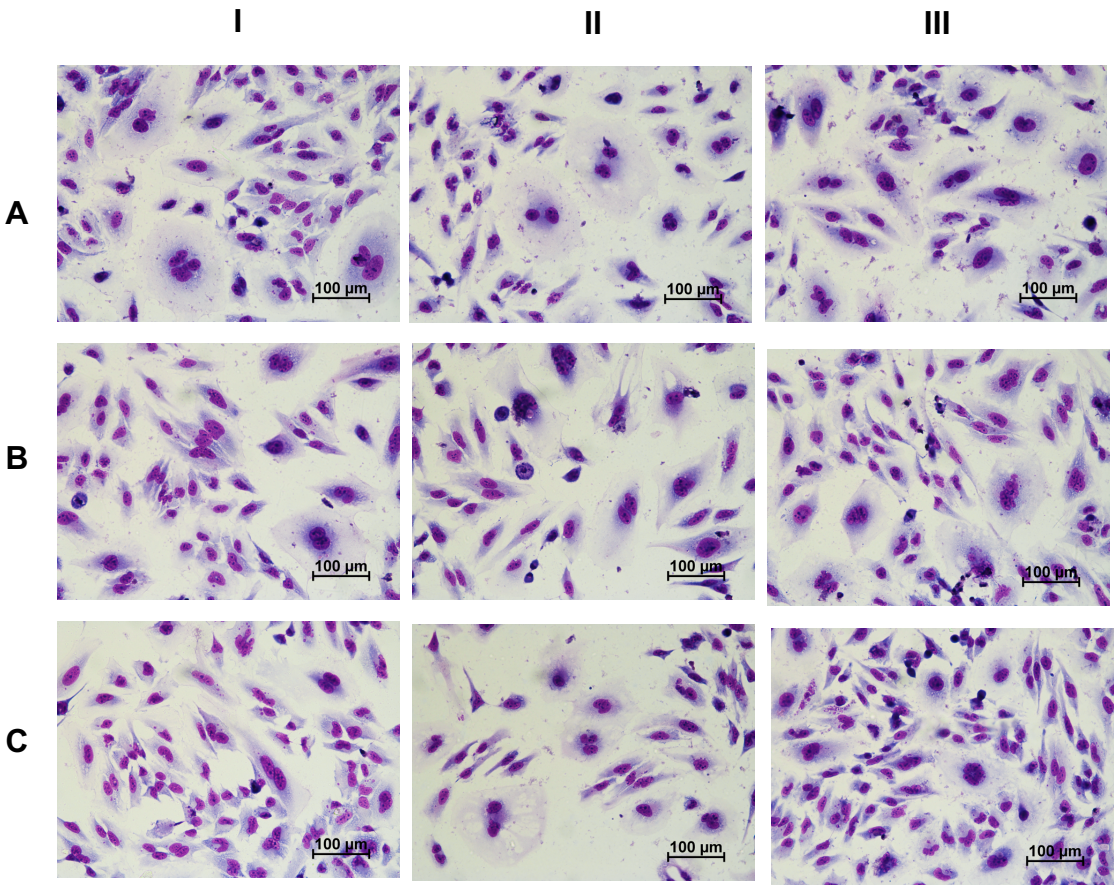

Figure S5.1c Giemsa staining of HeLa cells treated with OMVs isolated from *pks*$^{+}$ *E. coli* IHE3034 strain. A, B, and C represent biological replicates. Three images of each sample were taken (represented by I, II, and III). Photos were taken after 72 hours post treatment at 40X of magnification.

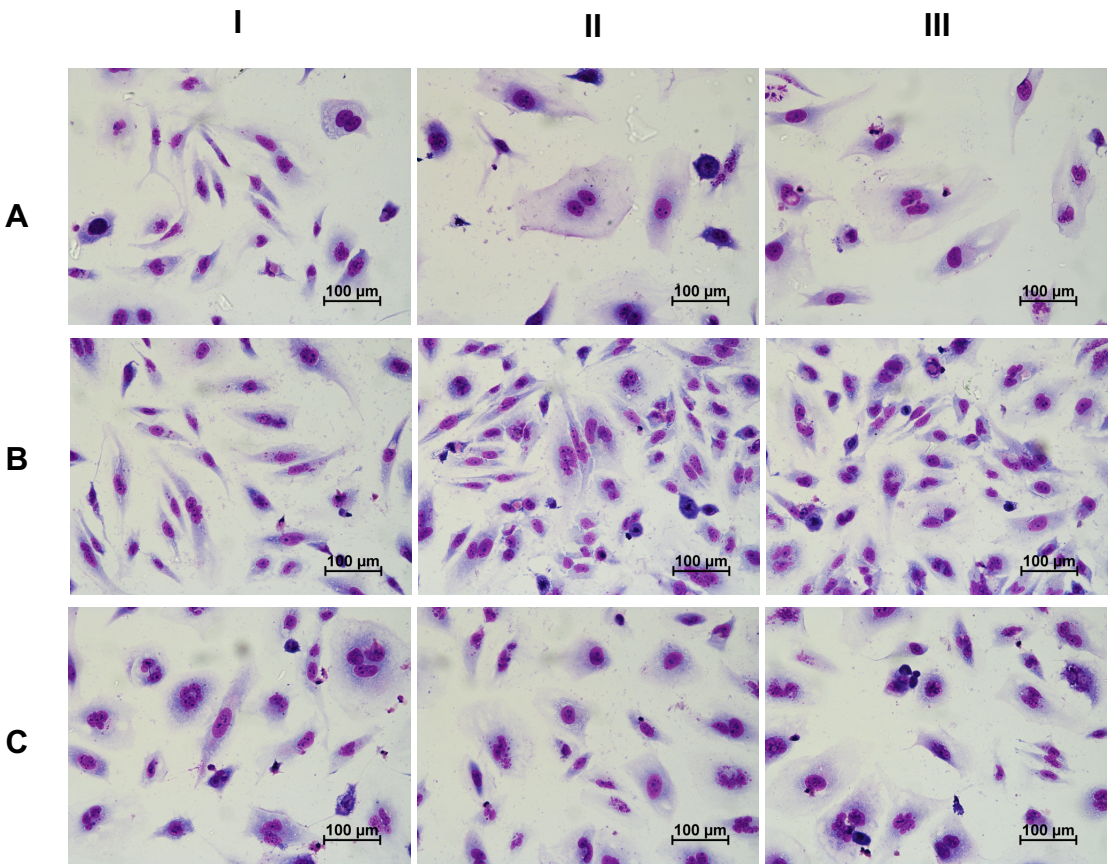

Figure S5.1d Giemsa staining of HeLa cells treated with OMVs isolated from *E. coli* IHE3034 Δ*clbP* mutant strain. A, B, and C represent biological replicates. Three images of each sample were taken (represented by I, II, and III). Photos were taken after 72 hours post treatment at 40X of magnification.

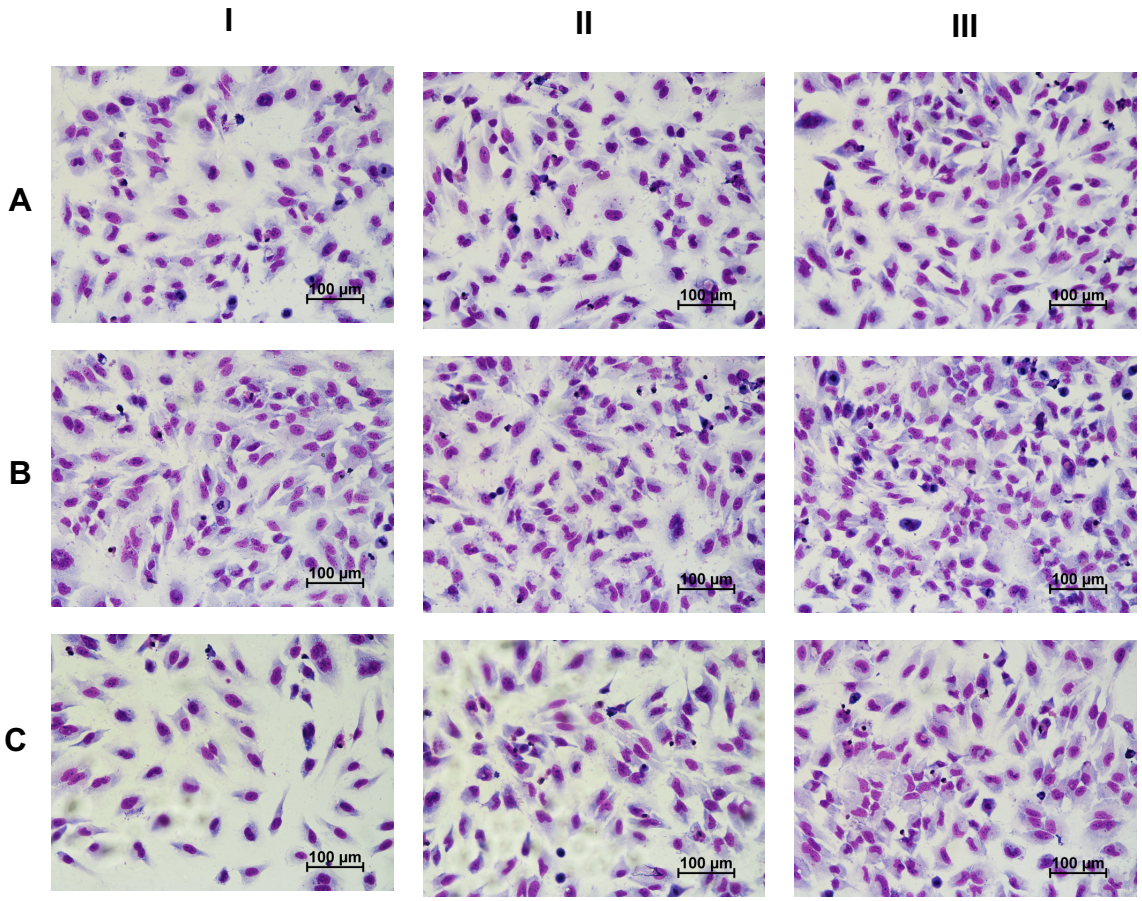

Figure S5.1e Giemsa staining of HeLa cells treated with OMVs isolated from *E. coli* DH10B control strain. A, B, and C represent biological replicates. Three images of each sample were taken (represented by I, II, and III). Photos were taken after 72 hours post treatment at 40X of magnification.

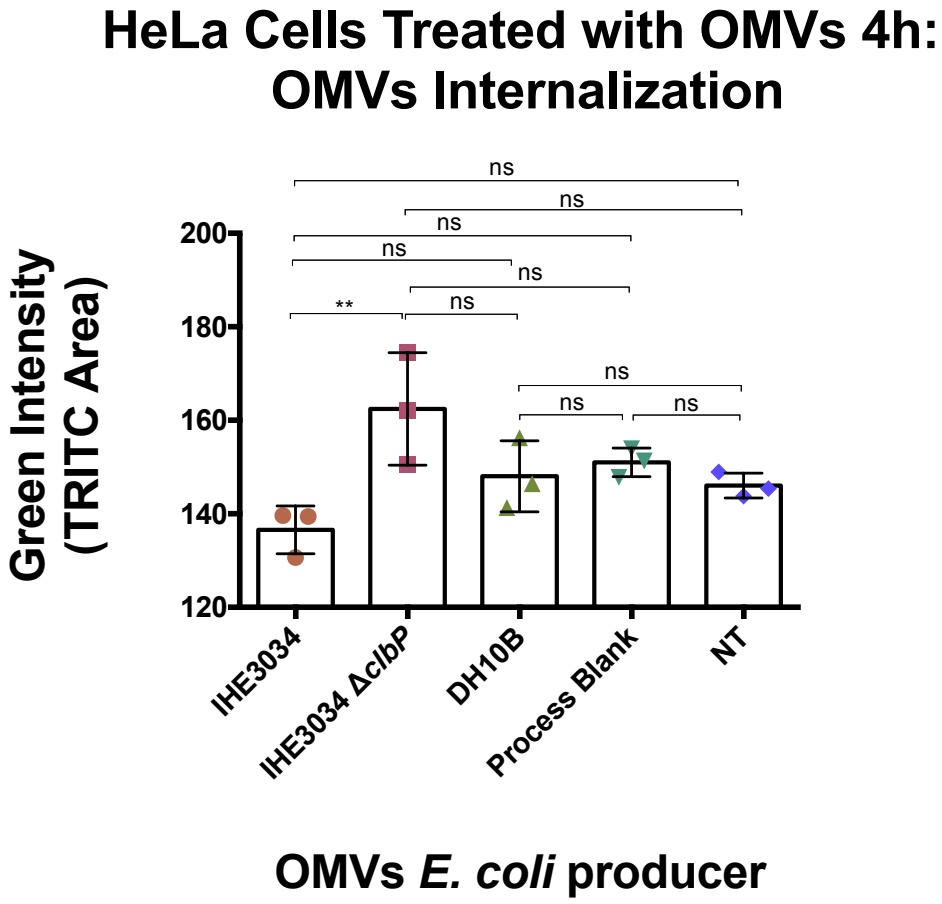

Figure S5.2 OMVs from IHE3034 Δ*clbP* mutant *E. coli* are internalized in significant higher amount than OMVs from WT strain by HeLa cells after 4 hrs of treatment. Fluorescent DiO labelled OMVs were added to HeLa cell for 4 hrs before cells were stained for actin (TRITC-Phalloidin dye) filaments and nuclei. Three images at 20X of magnification were taken in randomly chosen areas of each sample to statistical analysis. Intensity of green (DiO dye) were measured in areas were cells were present (red, TRITC-Phalloidin dye) to determine the relative amount of OMV internalized by the treated cell. *P*-values: ns $P > 0.05$; * $P \leq 0.05$; ** $P \leq 0.01$; *** $P \leq 0.001$ and **** $P \leq 0.0001$

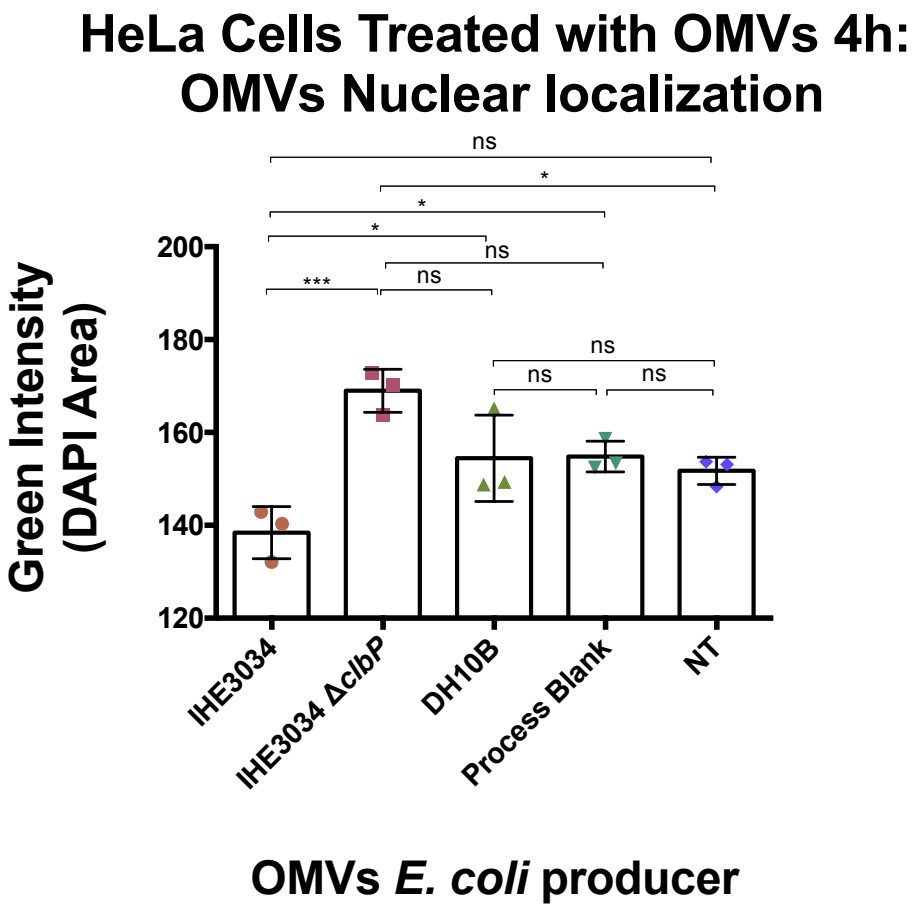

Figure S5.3 OMVs from IHE3034 Δ*clbP* mutant *E. coli* are localized in the nucleus in significant higher amount than OMVs from WT strain in HeLa cell after 4 hrs of treatment. Fluorescent DiO labelled OMVs were added to HeLa cell for 4 hrs before cells were stained for actin filaments and nuclei (DAPI). Three images at 20X of magnification were taken in randomly chosen areas of each sample to statistical analysis. Intensity of green (DiO dye) were measured in areas were cell's nucleus were present (blue, DAPI dye) to determine the relative amount of OMV localized in the nucleus of treated cell. *P*-values: ns $P > 0.05$; * $P \leq 0.05$; ** $P \leq 0.01$; *** $P \leq 0.001$ and **** $P \leq 0.0001$